The Role of HTLV-1 in Alteration of Immune Regulation Through Regulatory T Cell Dysfunction and Exosomal Manipulation

Monique Rochelle Anderson

Brooklyn, New York

Bachelor of Arts in Human Biology, June 2005
Stanford University, Stanford, CA

A Dissertation presented to the Graduate Faculty
of the University of Virginia in Candidacy for the Degree of
Doctor of Philosophy

Department of Pathology, Experimental Pathology Program, Molecular and Cellular Basis of Disease

University of Virginia
November 2017

Dedication and Acknowledgements

"None of us got where we are solely by pulling ourselves up by our bootstraps. We got here because somebody - a parent, a teacher, an Ivy League crony or a few nuns – bent down and helped us pick up our boots." – Thurgood Marshall

My journey to this point has been a living testament to how much can be accomplished with the love and support of those around you, so I want an acknowledgement committed for posterity of everyone who has been integral in the long process of completing this thesis. As might be clear from my unusual track, I initially matriculated to UVA as an MD, and after completing the HHMI-NIH Research Scholars Program, I decided to pursue a PhD. So firstly, I'd like to thank God, since there were many times I wanted to quit. I know I've been set on this path for a reason, and I can't thank Him enough. I'd also like to thank my parents, Nellie and Roy Anderson, for their unending patience with all of the twists and turns of the last several years. I know it was difficult for them to understand my desire to pursue a PhD when I was literally on the cusp of completing my MD, and I can only thank them for their understanding and then full support. They lent a willing ear when I called to cry my frustrations with particular experiments or life in general, and were always encouraging me with attestations to my abilities. From cat-sitting when I had to travel for research or spotting me cash when my budget became particularly tight, they have been pillars of strength even in the midst of my mother's cancer fight. I really can't say enough about them and am forever thankful that God saw fit to bless me with such parents who have reinforced my Faith and shepherded me to this point in my adulthood. As such, I dedicate this work to them.

Along with my parents, I'd also like to thank Louise and Simon Henry for their diligent support of myself and my parents. I've always felt that I was blessed with two sets of parents and that has never been more true than in the last 2 years. When my mom was initially diagnosed with breast cancer, I thought seriously about halting my studies, but the Henrys have often stepped in to accompany her to visits and help out at home, especially when I could not be there. Their presence has been a balm when anxiety for my mom's health has gotten overwhelming. So, I know that I would not be finishing at this point without their love and support.

In a similar vein, I would not be where I am without the group of cheerleaders in my life who have pushed me when I've faltered or wondered how I'd ever write this thesis: Christopher Sewell, Wanda Watson, Emily Leibovitch, Jeanne Billioux, Giovanna Manzano, Dexter Henry, Taurean Brown, Shelly Brown, Seyi Akanni, Nyater Ngouth, Shila Azodi, Tony Smalls and Tzu-Ying Chuang. They have each given me much needed pep talks along the way. I'd be remiss in not thanking Tzu-Ying for allowing me to crash on her couch, often at a moment's notice and without any expectation of payment as well as Emily for being a grad student mentor in the lab. I have mostly been trying to impersonate her path and results, with varying degrees of success. She just recently defended her dissertation and has been alternately encouraging and motivating me to get it done! Wanda, Chris, Taurean, and Seyi also deserve thanks in dealing with my often morose moods and taking the time to cheer me up through visits and planned activities. I'm sure I'm still managing to leave someone out, but I can't thank everyone enough.

In addition, the work presented here could not have been completed with many collaborations both within the Jacobson lab and beyond. So many thanks must go to my amazing lab members, past and present. Besides the amazing work going on in the lab, one of the reasons I joined was due to the group of people, and I haven't regretted that decision since. I couldn't ask for a better work environment, and I don't think I'll ever manage to duplicate this group anywhere. This includes: Kelsey Motanic, Giovanna Brunetto, Anna Abrams, Jaycob Herman, Breanna Caruso, Naomi Lee, Raya Massoud, Shila Azodi, Matt McCormick, Major Lin, Mike Moran, Luca Bartolini, Chiara Monaco, Alessandra de Paula Sousa Pohl, Jeanne Billioux, Nyater Ngouth, Oskari Virtanen, Melanie Delgado, Mary Alice Allnut, Will Leveque, Ashley Vellucci and Yoshimi Akahata. A special thanks to Yoshimi who has been an amazing staff scientist and has patiently helped me trouble shoot aspects of my experiments at every stage. She's the best!

In addition, much of the work presented here would not be possible without the help of close collaborators. I feel blessed to have had the opportunity to continue the work with Dr. Yoshihisa Yamano on regulatory T cells in HAM/TSP. The antibodies and assays of Dr. Yuetsu Tanaka have been invaluable in the detection of Tax protein in both of my projects. Dr. Fatah Kashanchi, as well as members of his laboratory including Michelle Pleet, Yao Akpamagbo and Alex, were instrumental in understanding how exosomes are involved in HAM/TSP and exosome isolation would not have occurred without their diligence. They patiently taught me how to work with nanotraps and analyze the exosome information. Similarly, Dr. Jennifer Jones taught me how to properly characterize exosomes, and she has continued to be a collaborator moving

forward. All of these relationships have shown me how essential and beneficial collaboration in science will be for me in my future career.

Finally, I feel it incumbent upon me to thank my research mentors. Research as a career path was not even on my radar until I volunteered on a project with Dr. Anne Gershon. Through working on VZV, I realized how much I enjoyed bench research and she has continued to be a mentor to me, even to this day. In the same vein, my former PI, Dr. Ai Yamamoto continues to be a mentor and guide for me. As she often likes to remind me, she initially wanted me to apply to an MD/PhD program when I was applying for med school. At that time, I told her that I didn't want to be in school for that long, which is the greatest irony considering how long I've been in school to this point.

And last, but certainly not least, I must thank Dr. Steven Jacobson. I initially joined Steve's lab as a medical student in the HHMI-NIH Research Scholars Program. While that program was formatted for one year, I enjoyed my research so much that a stayed a second year, which culminated in my first publication, included herein. Once it was time for me to return, I realized I had been well and truly "bit" by the research bug, and I wanted to pursue a PhD. Without blinking an eye, Steve said okay. Even while I've been at times frustrating in how slowly projects have been undertaken or brought to completion, he has been my biggest proponent. I feel that while I still have much growth to undergo before really seeing myself as a physician scientist, I have learned to approach scientific questions with the tools I've acquired while also being able to review and judge papers and projects with the experience I can now bring to bear. Dr. Jacobson has fostered an environment that is at once forward thinking and engaging, without the back-biting that can sometimes be found in labs. I can't thank him enough for all he has done

as my research mentor. I've made friends that will last a lifetime while I've been in his lab because of the collaborative environment he encourages in both the lab and branch. I'm really going to miss my time in the Jacobson lab and Neuroimmunology Branch. Now, I know what kind of PI I would like to be, should I ever have that opportunity.

In closing, I'd like to acknowledge my committee: Dr. Lou Hammarskjold, Dr. Kenneth Tung, Dr. Tom Bracciale (chair), Dr. Dean Kedes, Dr. Janet Cross, and Dr. Michael Brown. They have pushed me to see the bigger picture of my project, and I can only hope that the work documented here is a testament to the recommendations they've made throughout my tenure. Also, this work would not be possible without the clinical staff in the Neuroimmunology Branch (Irina Cortese, Joan Ohayon, Frances Andrada, Haneefa Muhammed, Chevaz Thomas, Dr. Jeanne Billioux, Dr. Shila Azodi), the patients who willingly donate samples, and our administrative staff (past and present), who have kept things running smoothly (Donna Thomas, Lisa Ingram, Iesha Baskins, Melissa Aery). Thank you for your patience and guidance.

Abstract

HTLV-1 is a human retrovirus that is associated with the neuroinflammatory disorder HTLV-1 associated myelopathy/ tropical spastic paraparesis (HAM/TSP). Much work has been undertaken to understand the mechanisms that lead to the development of this chronic progressive neuroinflammatory disorder in subsets of infected individuals. Similar to other inflammatory disorders, HAM/TSP appears to involve interaction between the immune system, viral/environmental triggers, and host genetics. When focusing on those individuals who develop HAM/TSP, certain factors are prominent. In particular, HTLV-1 is primarily found in the $CD4^+CD25^+$ T cell subset (Regulatory T cells: Tregs), which is responsible for peripheral immune tolerance and is known to be dysfunctional in HAM/TSP. This can be assessed in a number of ways. For example, recent evidence suggests that FoxP3, a lineage marker and master regulator of Tregs, expression and function is determined epigenetically through DNA demethylation in the Treg-specific demethylated region (TSDR). Additionally, Tregs have been shown to suppress activation through the production of microvesicles termed exosomes, which measure 30-150nm in size. Therefore, we analyzed the methylation state of the FoxP3 TSDR in peripheral blood mononuclear cells (PBMCs), $CD4^+$ T cells, and $CD4^+CD25^+$ T cells from normal healthy donors (NDs) and HAM/TSP patients. We demonstrated that there is decreased demethylation in analyzed PBMCs and $CD4^+CD25^+$ T cells from HAM/TSP patients as compared to NDs. Furthermore, decreased TSDR demethylation was associated with decreased functional suppression by Tregs and increased HTLV-1 Tax expression in HAM/TSP PBMC culture correlated with a concomitant decline in FoxP3 TSDR demethylation. Additionally, we assessed the content of exosomes

produced by ND and HAM/TSP patient PBMCs and found that HAM/TSP exosomes contained HTLV-1 Tax protein, *tax* mRNA, and HTLV-1 bZIP (HBZ) protein. Furthermore, Tax containing exosomes were present in cell-free, virus-free HAM/TSP patient cerebrospinal fluid (CSF) supernatant. Importantly, HAM/TSP patient derived exosomes were able to sensitize targets for Tax-specific cytotoxic T lymphocyte (CTL) lysis. We extended our studies into the potential consequences of Treg dysfunction into other immune subsets and found preliminary evidence to suggest that B cell receptors (BCRs) sequenced from HAM/TSP patient CSF recognize HTLV-1 specific antigens, which may potentially be present in isolated exosomes. Overall, we suggest that HTLV-1 infection leads to neuroinflammation in HAM/TSP through HTLV-1 mediated epigenetic modification leading to Treg dysfunction and through incorporation of HTLV-1 products in secreted exosomes, leading to antigen sensing and subsequent destruction of target cells by HTLV-1 specific CTLs and potentially HTLV-1 specific antibodies in the CNS. All of these factors may therefore contribute to HAM/TSP disease pathogenesis and warrant further investigation with the goal of developing clinical strategies that target these mechanisms.

Table of Contents

Dedication and Acknowledgements ii

Abstract vii

Table of Contents ix

List of Figures xiii

List of Tables xviii

List of Commonly Used Abbreviations xix

Chapter 1: General Introduction

- **HTLV-1** 2
- **HAM/TSP** 6
- **HAM/TSP Immunopathogenesis** 10
- **Project Rationale** 15

Chapter 2: Epigenetic Modification of the FoxP3 TSDR in HAM/TSP decreases functional suppression of Tregs

- **Regulatory T cells** 19
- **Tregs in HAM/TSP** 27
- **Results** 31
- **Methods** 54
  - **Storage of PMBCs and cell lines** 54
  - **Maintenance of cell lines** 54
  - **PBMC culture for Tax upregulation** 54
  - **Flow Cytometry** 55

DNA Isolation for TSDR methylation assessment 55

Bisulfite conversion 56

Quantitative PCR 56

tax & hbz mRNA quantification 57

Proviral load 58

$CD4^+CD25^+$ T cell enrichment 59

Suppression Assays 59

Lentiviral transgene construction 60

Purification of Lentiviral plasmids 61

Lentiviral packaging assay 62

Concentration of pseudovirus 63

Transduction of activated PBMCs 64

Transduction of cytokine primed PBMCs 65

Staining of transduced primary cells 65

Growth of TSDR plasmid 66

Transfection of TSDR with activation 67

Chapter 3: Functional Consequences of HTLV-1 medicated alterations in HAM/TSP patient exosomes

Introduction 69

Exosomes 69

Exosomes in Viral infection 73

Trafficking of antigens into exosomes 75

Viral Infection of Regulatory T cells 78

Results 81

Methods 111

Storage of PBMCs and cell lines 111

Maintenance of cell lines 111

Cell line culture for exosome cultivation 111

PBMC culture for exosomes cultivation 112

Exosome isolation 113

Western blotting 113

MESO ELISA 114

Acetylcholinesterase Enzyme Activity Assay 115

Exosomal RNA isolation and detection 115

CTL assay 116

T cell isolation 117

Statistical Analysis 118

Staining of T cells post-exosome exposure 118

PBMC treatment with exosomal inhibitors and/or activators 118

Listing and growth of HTLV-1 Tax, HBZ plasmids 119

Chapter 4: Consequences of HAM/TSP Treg dysfunction to non- T cells

Introduction 121

Results 123

Methods 130

Growth of Expi293F cells **130**

Transfection of Expi293F cells **130**

Purification of antibodies **132**

BCR antibody testing **132**

Anti-HTLV-1 protein verification **132**

Immunoprecipitation **133**

Immunoprecipitation with crosslinking **134**

Staining gels for band verification **135**

Chapter 5: Discussion **136**

Future Directions **152**

References **158**

Appendix I: Publications **182**

List of Figures

Chapter 1

Figure 1: HTLV-1 structure 3

Figure 2: Worldwide HTLV-1 prevalence 5

Figure 3: HAM/TSP categories 7

Figure 4: Model of HAM/TSP immunopathogenesis 11

Chapter 2

Figure 1: Regulatory B cells 20

Figure 2: TCR signal strength decides Treg fate 22

Figure 3: FoxP3 locus 24

Figure 4: Progressive demethylation of FoxP3 TSDR in development 26

Figure 5: FoxP3 TSDR demethylation is reduced in HAM/TSP 32

Figure 6: No correlation between the percent FoxP3+ cells and FoxP3 TSDR demethylation 34

Figure 7: Reduced FoxP3 TSDR demethylation correlates with reduced Treg suppression 35

Figure 8: HTLV-1 infected and HTLV-1 uninfected cell line profiles 37

Figure 9: Increased Tax expression correlates with reduced FoxP3 TSDR demethylation 39

Figure 10: Ctrl, Tax, and HBZ transduced HeLa cells 41

Figure 11: Concentration of pseudovirus using ultracentrifugation and PEG-it **42**

Figure 12: Flow cytometry demonstrated transduction of CD3 suspension activated ND PBMC **44**

Figure 13: Flow cytometry demonstrated transduction efficiency of ctrl-GFP and Tax-GFP psuedovirus in CD3-plate bound stimulated ND PBMCs **46**

Figure 14: Transduction efficiency of ctrl-GFP and Tax-GFP after short-term culture (3d) **48**

Figure 15: Transduction efficiency (%GFP) and TSDR demethylation in transduced ND (25611) PBMCs **50**

Figure 16: Transduced activated $CD4^+$ T cells **51**

Figure 17: Methylation of FoxP3 TSDR in transduced ND $CD4^+$ T cells **53**

Figure 18: Construction of pseudoviral particles **63**

Figure 19: Concentration of pseudoviral particles using PEG-it **64**

Chapter 3

Figure 1: Formation of exosomes from the endosomal compartment **70**

Figure 2: Protein contribution to exosome formation **77**

Figure 3: HTLV-1 actively infects regulatory T cells, allows for HTLV-1 protein expression and potential packaging into exosomes **79**

Figure 4: Nanotrapping exosomes from tissue culture supernatant **83**

Figure 5: HTLV-1 infected cell lines have exosomes containing HTLV-1 Tax protein **85**

Figure 6: Exosome production from cultured PBMCs **87**

Figure 7: Cultured HAM/TSP PBMCs produce exosomes containing HTLV-1 Tax **89**

Figure 8: Detection of exosomes containing HTLV-1 Tax in CSF of HAM/TSP patients **91**

Figure 9: HAM/TSP exosomes can sensitize targets to Ag-specific Responses **93**

Figure 10: HAM/TSP PBMCs shed exosomes containing HTLV-1 *tax* mRNA but do not carry HTLV-1 *hbz* mRNA **95**

Figure 11: $CD4^+CD25^+$ T cells diminish after exposure to HAM/TSP derived exosomes **97**

Figure 12: PD-1, FoxP3, and CTLA-1 expression in ND PBMCs after exposure to HAM/TSP derived exosomes **99**

Figure 13: Tax detection in exosomes isolated from AC PBMC culture **100**

Figure 14: HTLV-1 Tax detected in exosomes from AC & HAM/TSP CSF **101**

Figure 15: Hypothesized contribution of exosomes to HAM/TSP Pathogenesis **102**

Figure 16: Detection of HTLV-1 Tax in exosomes produced by HAM/TSP T cell subsets **103**

Figure 17: Detection of unmodified HTLV-1 Tax in HAM 17 along with ubiquitinated Tax (Tax Ub) in several HAM/TSP PBMC derived exosome samples **104**

Figure 18: CMV-Tax (Tax) and Tax mutants (Tax M22 and Tax M47) levels of ubiquitination **105**

Figure 19: HTLV-1 Tax and Tax monoubiquinated (Tax mono-Ub) after transfection with CMV-K88A, M33, M47, Tax and empty plasmids into HEK 293T cells **106**

Figure 20: Unmodified Tax detected in exosomes secreted by transfected 293T cells **107**

Figure 21: Lactacystin treatment of HTLV-1 Tax mutant transfected 293T cells **107**

Figure 22: Unmodified Tax was detected at higher levels in lactacystin treated exosomes **108**

Figure 23: Alix detection in exosomes post GW4869 treatment decreased at doses above 10μM **110**

Figure 24: Nanotrap particle technique for exosome isolation **112**

Chapter 4

Figure 1: Electrochemical ELISA of Abs generated from HAM/TSP CSF BCRs against Jurkat and MT2 lysates **124**

Figure 2: IgG Ab reactivity to cell lines **125**

Figure 3: Ab reactivity to HTLV-1 infected cell lines and HTLV-1 uninfected cell lines **126**

Figure 4: Reactivity to ND and HAM/TSP lysates using Abs generated from HAM/TSP CSF BCRs **127**

Figure 5: Western blots demonstrating reactivity of Abs generated from HAM/TSP BCRs against proteins expressed by Ju and MT2 **128**

Figure 6: Schematic of transfection of Expi293F cells for antibody production **132**

Chapter 5

Figure 1: Certain factors allow HTLV-1 infected Tregs to favor the development of ATLL or HAM/TSP **138**

Figure 2: HTLV-1 Tax interferes with transcriptional regulators or binds to methyltransferases to increase TSDR methylation **141**

Figure 3: Infected $CD4^+CD25^+$ T cells produce exosomes containing Tax **142**

Figure 4: Tax containing exosomes are activating in HAM/TSP, whereas exosomes produced by ND $CD4^+CD25^+$ Tregs are instead inhibiting **144**

Figure 5: How HTLV-1 Tax^+ exosomes may contribute to the immunopathogenesis of HAM/TSP in the CNS **147**

Figure 6: Dysfunctional Treg exosomes with HTLV-1 products, and HTLv-1 specfic CTLs create imbalanced immune responses that lead to HAM/TSP **150**

List of Tables

Chapter 1

Table 1: Comparisons between HAM/TSP and MS **9**

Chapter 2

Table 1: HTLV-1 disease associations **29**

List of Commonly Used Abbreviations

Ab	Antibody
AC	Asymptomatic Carrier
AchE	Acetylcholinesterase Enzyme
Ag	Antigen
APC	Antigen Presenting Cell
ASC	Antibody Secreting Cells
ATLL	Adult T cell Leukemia/ Lymphoma
BBB	Blood Brain Barrier
BCR	B Cell receptor
bZIP	Basic Leucine Zipper
C81	C8166 cell line
cAMP	Cyclic Adenosine Monophosphate
CBP	CREB Binding Protein
CMV	Cytomegalovirus
CNS	Central Nervous System
CpG	Cytosine followed by Guanine
CREB	cAMP Response Element Binding Protein
CSF	Cerebrospinal Fluid
CTL	Cytotoxic T lymphocyte
DNA	Deoxyribonucleic Acid

dsDNA	Double stranded Deoxyribonucleic Acid
EBV	Epstein Barr Virus
ELISA	Enzyme Linked Immunosorbent Assay
ESCRT	Endosomal Sorting Complexes Required for Transport
EV	Extracellular Vesicles
FoxP3	Forkhead Box P3 aka scurfin
GLUT1	Glucose Transporter 1
gRNA	genomic Ribonucleic Acid
HAART	Highly Active Anti-Retroviral Therapy
HAM/TSP	HTLV-1 Associated Myelopathy/ Tropical Spastic Paraparesis
HAND	HIV-Associated Neurocognitive Disorder
HBZ	HTLV-1 bZIP Factor
HHV	Human Herpes Virus
HSV	Herpes Simplex Virus
HLA	Human Leukocyte Antigen
hnRNP	Heterogeneous Nuclear Ribonucleoproteins
HT	HUT102 cell line
HTLV-1	Human T cell Lymphotropic Virus Type 1
IFN	Interferon
IL	Interleukin
ILV	Intraluminal vesicles
IN	Integrase
IP	Immunoprecipitation

JCV	John Cunningham Virus
Ju	Jurkat cell line
LTR	Long Terminal Repeat
MHC	Major Histocompatability Complex
miRNA	micro ribonucleic acid
MS	Multiple Sclerosis
MT	MT2 cell line
MV	Microvesicle
MVB	MultivesicularBody
ND	Normal Donor
NFAT	Nuclear Factor of Activated T cells
NK	Natural Killer cells
NT	Nanotrap particles
nTregs	Natural Regulatory T cells (thymus derived)
PBMC	Peripheral Blood Mononuclear Cell
PD-1	Programmed Cell Death Protein 1
PIAS1	Protein Inhibitor of Activated STAT1
PR	Protease
pTregs	Peripherally-induced Regulatory T cells
PVl	Proviral load
RNA	Ribonucleic Acid
RT	Real Time
RT	Retrotranscriptase

SLE	Systemic Lupus Erethematosus
TCR	T cell Receptor
Teff	Effector T cell
TL	TL-Om1 cell line
TNF	Tumor Necrosis Factor
Tr1	Type 1 Regulatory cell
Treg	Regulatory T cell (CD4)
TSDR	Treg Specific Demethylated Region
Ub	Ubiquitin
WB	Western Blot

Chapter 1

General Introduction

HTLV-1

The theory of viruses as agents of cancer or *oncornaviruses* (RNA tumor viruses) originated in the early 20th century through experiments conducted by Bang and Ellerman and later Rous, who demonstrated the transference of chicken tumors to other chicken with cell-free extracts(Weiss and Vogt, 2011). However, the discovery of human RNA viruses capable of causing cancer did not occur until 1980 when Human T cell Lymphotropic virus Type 1 (HTLV-1) was isolated from a patient with cutaneous T cell lymphoma by Gallo and Poiesz at the NIH and Yoshida and colleagues in Japan (Coffin, 2015; Gallo, 2005). HTLV-1 became not only the first human RNA oncovirus, but also the first exogenous human retrovirus discovered.

HTLV-1 belongs to the family *Retroviridae*, Genera *Orthoviridae*, and SubFamily *deltaretrovirus*. As a retrovirus, it has a general composition of 2 single-stranded genomic RNA (gRNA) strands within a capsid surrounded by an envelope. Most particles measure approximately 100nm in diameter and carry group-specific antigen (gag: capsid, nucleocapsid, matrix) as well as retrotranscriptase (RT), integrase (IN), and the viral protease (PR)(Kannian and Green, 2010) (**Fig. 1)**. Like other retroviruses, HTLV-1 attaches to the cell membrane via adhesion to a cellular receptor to viral env, followed by membrane fusion and viral entry (Kannian and Green, 2010). While the cellular receptors necessary for entry are still under investigation, prior research points to heparin sulfate proteoglycans (HSPGs), neuropillin-1 (Nrp1), and glucose transporter 1 (GLUT1) as necessary for entry of HTLV-1 into cells (Ghez et al., 2006; Hoshino, 2012; Tanaka et al., 2012). Upon entry, HTLV-1 reverse transcribes the gRNA to dsDNA and integrates into the host genome as a provirus within the nucleus.

While the study of HTLV-1 has not yielded any specific integration hotspots within the human genome, it does appear that integration into transcriptionally active sites is associated with progression toward disease (Meekings et al., 2008; Niederer et al., 2014).

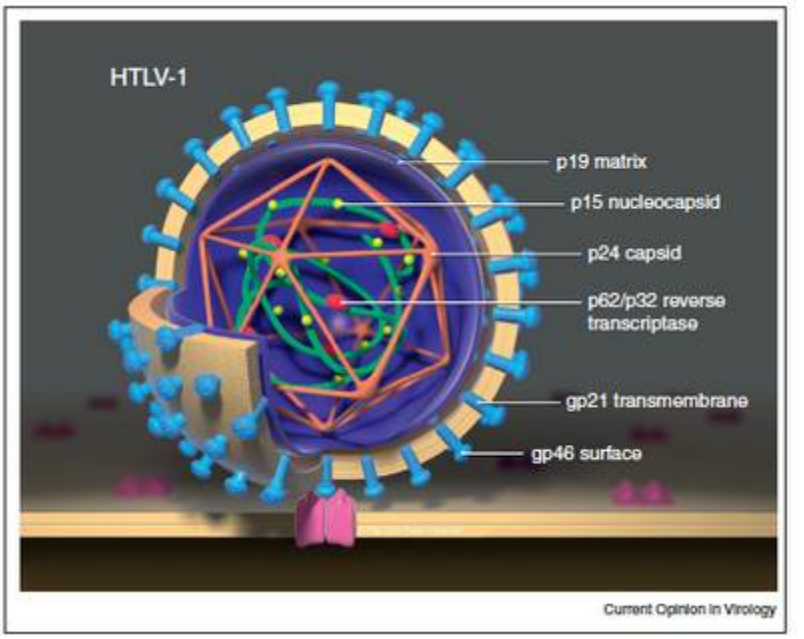

Figure 1: HTLV-1 structure (Lairmore et al., 2012)

Once integrated into the host genome, viral gene transcription can be initiated from the long terminal repeats (LTR) at either end of the provirus. Viral gene transcription is tightly controlled, both by the virus and the host. HTLV-1 Tax, a pleiotropic transactivating regulatory protein, is highly efficient at initiating viral transcription through the LTR by binding cyclic adenose monophosphate (cAMP) response element binding protein (CREB) and recruiting it to the LTR (Yin and Tully, 1996). HLTV-1 Tax additionally can bind several other cellular coactivators such as CREB and nuclear factor of activated T-cells (NFAT), resulting in increased cellular expression of the IL-2 receptor (CD25), increased interleukin production, chromatin remodeling, and distortion of the cell cycle (Boxus et al., 2008; Currer et al., 2012). Tax is instrumental in initiating spontaneous lymphoproliferation, in which infected peripheral blood mononuclear cells (PBMCs) are able to divide independently of IL-2 or other exogenous stimulation (Asquith et al., 2007) (Lairmore et al., 2012). Furthermore,

it can interfere with gene expression through binding to epigenetic modulators (Ego et al., 2005; Miyazato et al., 2016).

In addition to Tax, HTLV-1 also encodes Env, Rex, Gag and Pol proteins, as well as another regulatory protein called HTLV-1 bZIP factor (HBZ) (Li et al., 2009). HBZ is a basic leucine zipper protein encoded by the minus strand RNA of the HTLV-1 genome (Gaudray et al., 2002). Evidence supports a directly antagonistic effect of HBZ on Tax expression, though it also has growth stimulating effects (Sugata et al., 2016; Zhi et al., 2011). Although HBZ has not been directly implicated in altering DNA methylation, HBZ can bind and inhibit any transcription factor with a bZIP domain, including CREB and CREB binding protein (CBP)/ p300 (Lemasson et al., 2007; Matsuoka and Green, 2009).

The other major regulatory proteins encoded by the HTLV-1 genome, Rex, is a post-transcriptional regulator that facilitates transport of viral mRNA transcripts from the nucleus to the cytoplasm (Nakano and Watanabe, 2012). It specifically binds to the Rex-response element (RxRE) located at the 3' end of all HTLV-1 mRNA and has been shown to stabilize unspliced and singly-spliced mRNA (Nakano and Watanabe, 2012). It also binds to the cellular nuclear exporter chromosomal maintenance 1 (CRM1), forming a complex that can then exit the nucleus (Bai et al., 2012; Nakano and Watanabe, 2016).

HTLV-1 epidemiology

Currently, HTLV-1 infects approximately 10-20 million people worldwide (Gessain and Cassar, 2012). However, unlike HIV, the vast majority of infected individuals will remain asymptomatic carriers (ACs). The major diseases associated with

HTLV-1 infection are adult T cell leukemia/ lymphoma (ATLL; 1-5%), infective dermatitis, uveitis, pneumonitis, polymyositis, and HTLV-1 associated myelopathy/tropical spastic paraparesis (HAM/TSP; 0.25-4%) (Proietti et al., 2005) (Goncalves et al., 2010). The virus is endemic in areas of Japan, the Caribbean, South America, Western Africa, Melanesia, and the Middle East (**Fig. 2**) (Gessain and Cassar, 2012). Larger clinical studies have been unable to find significant viral genomic variations between endemic regions. Differences in disease rates could not be identified when comparing endemic areas, but there is anecdotal evidence suggesting a greater preponderance of HAM/TSP in the Caribbean (Nishimura et al., 1993) (Gessain and Cassar, 2012).

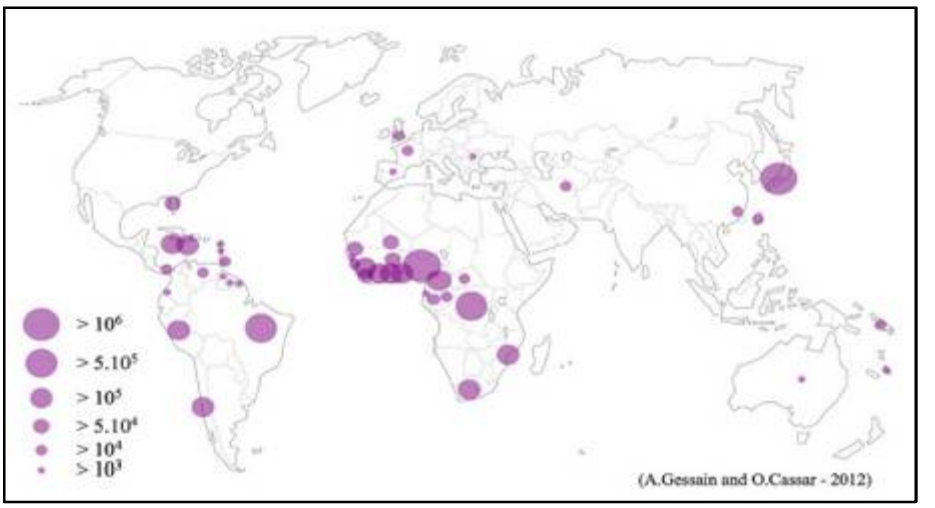

Figure 2: Worldwide HTLV-1 prevalence (Gessain and Cassar, 2012) HTLV-1 is endemic in certain regions of the world

HTLV-1 is transmitted sexually, parenterally, and vertically from mother-to-child through breastmilk (Goncalves et al., 2010). It primarily infects $CD4^+$ T cells, although instead of lysis, infection results in activation and proliferation as the virus primarily spreads in the host by clonal expansion (Carpentier et al., 2015). The virus is also capable of infecting,

$CD8^+$ T cells, plasmacytoid dendritic cells, B cells, and monocytes but establishes a reservoir in $CD4^+CD25^+$ T cells, a subset of which contains regulatory T cells (Tregs) (Grant et al., 2002; Gross and Thoma-Kress, 2016; Yamano et al., 2004). Individuals that progress to HAM/TSP typically have higher proviral loads and have often acquired the virus later in life through sexual transmission compared to ACs (Maloney et al., 1998; Matsuura et al., 2016; Nagai et al., 1998). Additionally, these patients often demonstrate an inflammatory immune infiltrate in the central nervous system (CNS) that characterizes the disease, resulting in a progressive demyelinating disorder targeting white matter tracts in the cervical and thoracic spinal cord (Izumo, 2010; Jacobson, 1996; Lepoutre et al., 2009). This progressive demyelination leads to symptoms of lower limb spasticity and ataxia, urinary and bowel retention, and paresthesias, usually beginning in the 4^{th} to 6^{th} decade of life (Matsuura et al., 2016; Romanelli et al., 2013).

HAM/TSP

The neuroinflammatory disorder caused by HTLV-1 occurs in approximately 0.25-4% of infected individuals (Proietti et al., 2005). As mentioned previously, while there is anecdotal evidence to support a greater prevalence of the disease in the Caribbean, there does not appear to be a genomic difference in the virus between regions to support this observation (Gessain and Cassar, 2012). After an incubation period of 6 months to 20 years in some cases, patients typically describe a clinical course where they initially experience leg weakness, stumbling episodes, and increased lower extremity spasticity (Shoeibi et al., 2013). As time progresses, many develop increasing difficulty walking which necessitates walkers and/ or wheelchairs. Urinary and bowel incontinence

typically manifests later in the disease course (Bangham et al., 2015; Martin et al., 2014). Other patient complaints include paresthesias, back pain, neuropathies, and erectile dysfunction (Evangelou et al., 2014). Each patient's clinical course differs, but can generally be divided into 4 categories as seen in **Fig. 3**: rapid progressors who progress to disability quickly (<1y) after initial symptoms, slow progressors who continue to demonstrate increasing disability throughout their lives, slow progressors who functionally decline for a number of years before then plateauing at a set level of disability and maintaining that level throughout their lives, or patients who follow a mild course of disease and never develop significant disability.

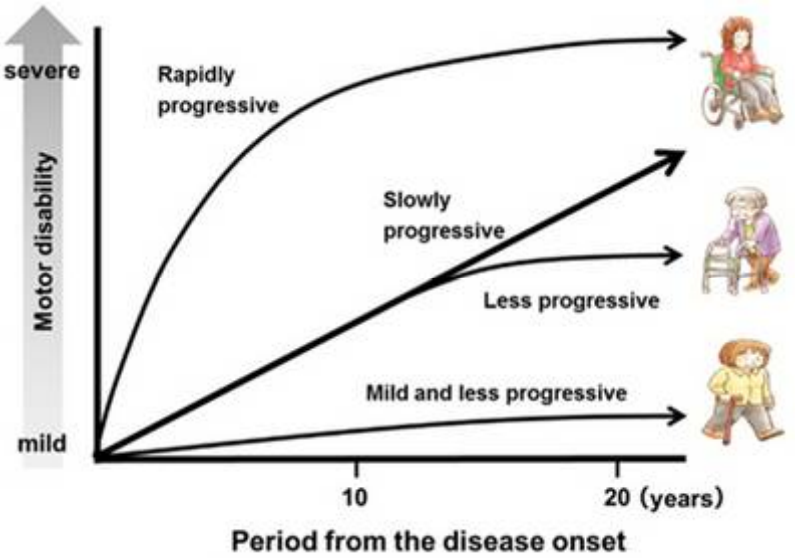

Figure 3: HAM/TSP categories (Yamano and Sato, 2012) Some HAM/TSP patients follow a mildly progressive course while others are slowly progressive and have more disability. Rapidly progressive patients represent a rare manifestation of the disease.

The subclassifications of the clinical course are quite similar to what is seen in another progressive neuroinflammtory disorder, multiple sclerosis (MS). Indeed, many HAM/TSP patients are misdiagnosed with primary progressive MS (Rocha et al., 2013), and while this occurs less frequently with increased awareness of the virus in areas of high endemicity, it still continues to be a problem even in places like Japan where HTLV-1 is well-known (Puccioni-Sohler et al., 2007).

Indeed, there are several characteristics shared between MS and HAM/TSP, including the presence of oligoclonal bands, demyelination, inflammation, and associations with certain human leukocyte antigens (HLAs) (**Table** 1). Additionally, similar to MS, HAM/TSP demonstrates perivascular and parenchymal infiltrates of lymphocytes in the CNS (Oh and Jacobson, 2008). Infiltrates of macrophages, astrocyte proliferation, and fibrillary gliosis can also be seen on histology (Iwasaki, 1990). Inflammatory lesions are typically localized to the thoracic and lumbar portions of the spinal cord (Jacobson, 1996). These lesions are symmetric and associated with demyelination and axonal degeneration in the lateral corticospinal and spinocerebellar tracts (Fuzii et al., 2014). Axonal loss manifests as a spinal cord atrophy, a histologic and radiographic feature found in HAM/TSP patients with long-term disease (Liu et al., 2014). Lesions in the white matter of the cerebrum are present in HAM/TSP, however unlike MS, they are typically not gadolinium enhancing lesions (Godoy et al., 1995; Puccioni-Sohler et al., 2012). Additionally, while the vast majority of patients with MS follow a relapsing-remitting course of neuroinflammatory events, a waxing and waning phenotype of HAM/TSP has not been reported (**Table 1**).

Though HAM/TSP has a preponderance for women similar to the skewed F:M ratio observed in autoimmune diseases like MS, HAM/TSP differs from other neuroinflammatory disorders because the disease has a known viral etiology (Gessain and Cassar, 2012). Neuromyelitis optica (NMO), acute disseminating encephalomyelitis (ADEM), transverse myelitis (TM), and MS similarly involve inflammatory infiltrates and demyelination, but are instead thought to be autoimmune in nature. It has been suggested that MS develops after an initial viral insult, which has been supported by

animal studies in which viral infection worsens the course of experimental autoimmune encephalomyelitis (EAE) (Kakalacheva et al., 2011; Leibovitch and Jacobson, 2014) (Leibovitch et al., 2013).

.Neuroinflammation is now thought to play a role in other neurodegenerative diseases and even psychiatric disorders, including Parkinson's disease, Alzheimer's

	HAM/TSP	Multiple Sclerosis
Clinical	Chronic progressive myelopathy	Relapsing remitting, primary progressive, or secondary progressive
Oligoclonal Bands	Yes	Yes,
MRI	Atrophy of spinal cord. Mimics CNS demyelination in brain similar to MS	Demyelinating lesions of CNS white matter
Disease duration	Life	Life
Etiological agent	HTLV-1	Unknown, but several viruses proposed
Demyelination	Yes	Yes
Inflammation	Yes	Yes
Lymphocytes in Lesions	Yes	Yes
Immune response	Yes	Yes
HLA association	Yes	Yes

Table 1: Comparisons between HAM/TSP and MS

disease, and depression (Chen et al., 2016; Wager-Smith and Markou, 2011). Understanding the role of neuroinflammation in central nervous system (CNS) disease progression therefore has potentially long ranging consequences to a number of diseases affecting millions of Americans. Thus, the study of the immunopathogenesis of HAM/TSP becomes a fruitful endeavor not only for those patients affected by the disease, but also for millions of other individuals suffering from the consequences of neuroinflammation.

HAM/TSP immunopathogenesis

There are several theories proposed to explain the immunopathogenesis of HAM/TSP. The damage that occurs in the CNS is believed to be due to a virally-mediated cytotoxic demyelinating inflammatory processes that begins with the entry of HTLV-1 infected lymphocytes from the periphery as illustrated in **Fig. 4** (Fuzii et al., 2014). Lymphocytes infiltrate the blood vessels of the leptomeninges and parenchyma, leading to an eventual opening of the blood brain barrier (BBB) (Jacobson, 2002). Indeed, as compared to healthy donors and asympomatic carriers (AC), HAM/TSP patients have increased adhesion molecules and HLA class I expression on the endothelium surrounding the spinal cord, as well as on infiltrating cells, perhaps explaining the entry of lymphocytes into this region that leads to damage (Curis et al., 2016; Osame, 2002; Umehara et al., 1996). Along with lymphocytes, foamy macrophagaes and proliferating astrocytes can be seen in the lesions of the spinal cord (Iwasaki, 1990; Yoshioka et al., 1993). Interestingly, these lesions also display increased MHC I expression (Jacobson, 2002). While $CD4^+$ T cells predominate the early CNS infiltrate of inflammatory cells, $CD8^+$ T cells infiltrate later in the disease process, and the pathology would indicate that most of the damage in the spinal cord is attributed to their presence (Lepoutre et al., 2009; Yamano and Sato, 2012). HTLV-1 specific cytotoxic T lymphocytes can be detected in both the active and chronic lesions that in HAM/TSP spinal cords, in close proximity to the increased expression of MHC I within these damaged areas (Jacobson, 2002). The majority of these lesions are restricted to cervical and thoracic cord. Recent radiologic studies of spinal cord atrophy support

initial damage occurring in the T-spine and progressing in an anteretrograde manner to the C-spine (Azodi et al, in press). This would support the observation that HAM/TSP patients present with almost exclusively lower extremity dysfunction.

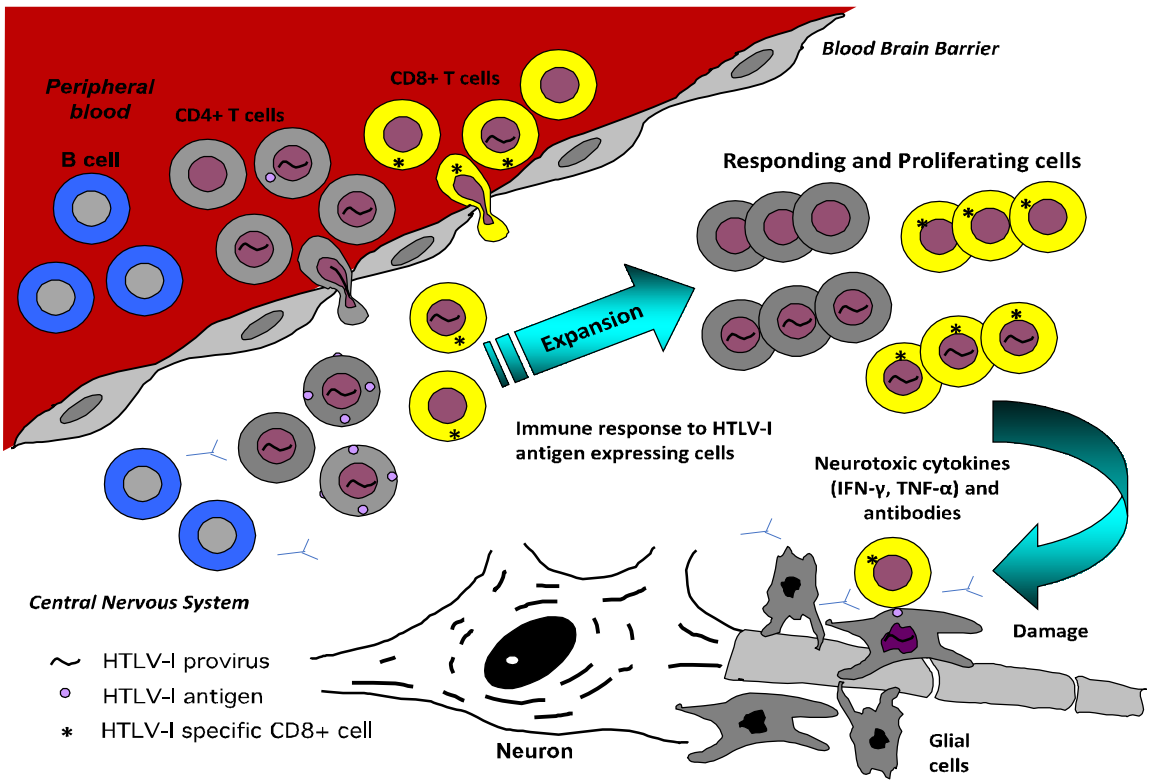

Figure 4: Model of HAM/TSP Immunopathogenesis. Infected $CD4^+$ and $CD8^+$ T cells cross the Blood Brain Barrier into the CNS where they can proliferate, producing potentially neurotoxic cytokines (bystander effect). HTLV-1 specific $CD8^+$ T cells and B cells may also directly target CNS resident cells (i.e. glia) that carry HTLV-1 antigens (direct CNS injury) or express antigens similar to HTLV-1 viral proteins (molecular mimicry)

Another leading theory that could explain contributions to CNS destruction in HAM/TSP involves a bystander effect (**Fig. 4**). This theory attributes the increased inflammatory cytokine production in the CNS as the root cause of damage to oligodendrocytes leading to demyelination (Osame, 2002). HAM/TSP patient cerebrospinal fluid (CSF) has been demonstrated to have increased inflammatory cytokine content such as IL-6 and interferon gamma (IFN-γ) as well as neopterin

(Nishimoto et al., 1990; Sato et al., 2013). Neopterin is produced by monocytes/ macrophages in response to IFN-γ, and is often used as a marker of immune activation (Murr et al., 2002). While the cytokines are not thought to do direct damage to CNS resident cells, except for IL-2 and tumor necrosis factor alpha (TNF-α) which can increase oligodendrocyte dysfunction, they are instrumental in the recruitment of immune cells that perpetuate the cycle of inflammation (Yamano and Sato, 2012). In particular, IL-6 and INF-γ increase the recruitment of microglia and aid in opening of the BBB and also increase adhesion molecules on the endothelium surrounding the BBB (Merrill and Benveniste, 1996). Furthermore, inflammatory cytokines like TNF-α can increase the production of free radicals, which are destructive to surrounding cells (Blais and Rivest, 2004; Fuzii et al., 2014).

A third prominent theory of HAM/TSP pathogenesis involves immune targeting and destruction of uninfected CNS resident cells through a process of molecular mimicry. Specifically, it is thought that immune responses directed against the virus cross-react with host-proteins that have similar structures to HTLV-1 antigens, thereby facilitating an autoimmune response that is actually due to viral specificity. HTLV-1 specific cytotoxic T Lymphocytes (CTLs) home to the thoracic spinal cord where HTLV-1 *gag, pX, and env* sequences have been localized, likely in association with infiltrating infected T cells (Jacobson, 1996). pX, is a gene that encodes the regulatory and accessory proteins of HTLV-1, including Tax, Rex, p12, p30, and HBZ (Aida et al., 2013; Kehn et al., 2004). As mentioned previously, both Tax and HBZ play important roles in the life cycle of HTLV-1. In addition to being involved in the increased inflammatory cytokine production of HAM/TSP, which includes increased IL-2, IFN-γ, and TNF-α, HTLV-1

Tax is also highly immunogenic (Melamed et al., 2015) (Cook et al., 2013). Indeed, HAM/TSP patients have been demonstrated to have a higher infiltrate of HTLV-1 Tax specific CTLs in both the peripheral blood, CSF, and CNS lesions as compared to ACs (Elovaara et al., 1993; Kubota et al., 2002; Matsuura et al., 2015). Interestingly, Tax has been reported to share structural homology with a host cellular protein called heterogeneous nuclear ribonuclear protein-A1(hnRNP-A1)(Lee et al., 2005). Antibodies from HAM/TSP patient CSF cross-reacted with this protein, which was also found to be expressed on the surface of neurons (Levin et al., 2002). Specifically, HTLV-1 Tax antibodies could also bind to hnRNP-A1. Immune responses to proteins in the hnRNP family are frequently associated with autoimmune diseases, including rheumatoid arthritis (Hassfeld et al., 1995; Jensen et al., 1988). Notably, hnRNP-A1 is more expressed on neurons than other cells of the CNS (Kamma et al., 1995). While this evidence points to the possibility of molecular mimicry, it is often difficult to unequivocally attribute a disease or pathogenesis exclusively to this process.

The aforementioned theories of immunopathogenesis in HAM/TSP all have one process in common; expression of HTLV-1 Tax is implicated in each mechanism, either by being a target of cytotoxic cells, enhancing inflammatory cytokine production, or serving as a mimic to a host autoantigen. Virtually all HAM/TSP patients express this protein, primarily in $CD4^{+}CD25^{+}$ T cells, although it has a dynamic expression profile (Yamano et al., 2004). When PBMCs are examined *ex vivo*, HTLV-1 Tax expression is difficult to detect (Gessain et al., 1991). Tax expression does not increase until after at least 18h of *ex vivo* culture, at which point it peaks and returns to a low expression level (Rende et al., 2011). This implies that the gene is tightly regulated, likely in part due to

its high immunogenicity. By contrast HTLV-1 HBZ, which is thought to have an antagonistic relationship to Tax, is expressed at much lower levels as compared to Tax, but can be detected in fresh PBMCs and maintains similar levels of expression throughout culture (Hilburn et al., 2011) (Cavallari et al., 2013). Interestingly, while HTLV-1 *tax* mRNA and Tax protein can be found equally in the cytoplasm and nucleus of infected cells, HTLV-1 HBZ protein is found almost exclusively in the cytoplasm of HAM/TSP patient PBMCs (Baratella et al., 2017). Conversely, *hbz* mRNA is largely sequestered in the nucleus, despite the necessity for cytoplasmic protein translation (Rende et al., 2011). This is partially due to the differential functional capacity of *hbz* mRNA, which has separate proliferative properties even without translation (Satou et al., 2006).

In addition to differential temporal expression and intracellular localization, HTLV-1 Tax and HBZ both contribute to the immune dysregulation of HAM/TSP. As has been observed in other inflammatory diseases, regulatory T cells (Tregs) dysfunction is implicated in HAM/TSP immune dysregulation and this dysfunction has been linked to both HTLV-1 *tax* and *hbz* regulatory genes. Treg dysfunction at both a molecular and functional level frame the aims of this thesis project and will be discussed separately in each of the following chapters, and outlined in the following Project Rationale. Namely, the contribution of HTLV-1 to Treg dysfunction at an epigenetic level will be introduced, supported, and discussed through experiments presented in **Chapter 2**. In **Chapter 3**, HTLV-1 contributions to Treg dysfunction in the production of microvesicles called exosomes will be discussed. Finally, since regulatory T cells are known to inhibit inflammation in other immune subsets, B cell receptor (BCRs) are examined and

assessed for changes in HAM/TSP patients in **Chapter 4**. **Chapter 5** will bring together these themes and summarize how each of these factors may contribute to HAM/SP immunopathogenesis. Cumulatively, these aims are proposed and formulated towards the goal of understanding how regulatory T cells contribute to HAM/TSP immunopathogenesis and what potential therapies can be elucidated from this understanding.

Project Rationale

The premise of viral alteration of host epigenetics is not novel (Paschos and Allday, 2010). Herpes viruses are well known for this phenomenon, gaining distinction as "histone hijackers" (Knipe et al., 2013; Zalckvar et al., 2013). However, the potential alteration of the FoxP3 Treg specific demethylated region (TSDR) by HTLV-1 would represent a novel viral target of the host epigenome. Prior research highlights that HTLV-1 has the capacity to modify the epigenome by upregulating DNA methyl transferases (DNMT)(Fang et al., 2001; Mikovits et al., 1998). HTLV-1 Tax, a pleiotropic regulatory protein, through its ability to bind to several host transcription factors and proteins, distinguishes itself as a primary suspect in alterations to FoxP3 protein levels. Indeed, prior work from the Jacobson lab demonstrated reduced FoxP3 protein levels after introduction of Tax into $CD4^+CD25^+$ T cells (Yamano et al., 2005). Furthermore, transduction of Tax into $CD4^+CD25^+$ T cells resulted in reduced suppression of proliferating allogeneic effector T cells (Teffs) (Araya et al., 2014). We propose that infection of Tregs by HTLV-1 and the expression of HTLV-1 protein, specifically HTLV-1 Tax, causes reduced Treg suppression of inflammatory immune

responses due to 1) Tax-induced reduction in FoxP3 TSDR demethylation and 2) the introduction of Tax and other HTLV-1 products in exosomal cargo, altering the function of exosomes from non-inflammatory to inflammatory. Combined, HTLV-1 dysregulates Treg function at a genetic and molecular level. Therefore, we suggest experiments that aim to analyze the methylation state of the FoxP3 TSDR in HAM/TSP patients as compared to NDs (**Chapter 2**). We also propose experiments that compare the state of the TSDR in HAM/TSP Tregs compared to ND Tregs and correlate this to Treg suppressive capacity in proliferation assays, as well as HTLV-1 protein expression levels.

Next, due to the role of exosomes in aiding Treg suppression, we aim to investigate the presence of HTLV-1 Tax and HBZ protein and mRNA in exosomes captured from HAM/TSP patient PBMC cultures as compared to ND PBMC cultures (**Chapter 3**). A novel nanotrap technology developed by Ceres Nanosciences (Manassas, VA) utilizes size and hydrophobic interactions to specifically trap exosomes onto a sieving shell that surrounds aromatic baits (Tamburro et al., 2011). This allows isolation of concentrated exosomes from as little as 250μL of human biological fluid (Jaworski et al., 2014b). Small volume isolation is especially important when working with cerebrospinal fluid (CSF), which is usually a limited resource. We will use these Nanotrap particle ® for exosome isolation from tissue culture supernatant and from patient material. Furthermore, we will analyze exosome content from HAM/TSP patient CSF as compared to exosomes isolated from HTLV-1 negative CSF samples. We will then assess the function of isolated exosomes in antigen-specific responses and immune cell alterations. Finally, since regulatory T cells are known to inhibit inflammation in other immune subsets, B cell receptor (BCRs) are examined and assessed for changes in

HAM/TSP patients in **Chapter 4**. In **Chapter 5**, we will bring together all of the data presented in this thesis to demonstrate that the demyelination and neuronal loss observed in HAM/TSP likely result from uncontrolled immune activation due to reduced TSDR demethylation and uptake of Tax-containing exosomes by CNS resident cells, allowing for cell lysis of these targets by HTLV-1 specific CTLs. These observations will hopefully lend to future therapies targeting Treg function both by altering the methylation state of the TSDR and exosome composition. More importantly, exosomes have shown promise as biomarkers in cancer, and applied to HTLV-1 infection, could serve as a predictor of future neurologic decline in previously asymptomatic individuals. In addition, the changes in BCR composition in HAM/TSP could represent yet another target for interventions. Collectively, the experiments described in this thesis add to our understanding of HAM/TSP immunopathogenesis, and could present new avenues for diagnosis and therapeutics for HAM/TSP patients.

Chapter 2

Epigenetic modification of the FoxP3 TSDR in HAM/TSP decreases functional suppression of Tregs

Portions taken from "**Epigenetic modification of the FoxP3 TSDR in HAM/TSP decreases the functional suppression of Tregs**" (Anderson et al JNIP 2014)

Introduction

Regulatory T cells

Tregs or "suppressor T cells" are an arm of the immune system responsible for the down-regulation of inflammatory immune responses to both self and foreign antigen (Belkaid, 2007; Sakaguchi, 2005). They play an integral role in autoimmune disease, allergy, transplant, cancer, and infectious disease (McHugh and Shevach, 2002). Their importance was first noted in mice studies where removal of a specific T cell subset resulted in large-scale fatal autoimmunity (Gershon and Kondo, 1970; Gershon and Kondo, 1971; Sakaguchi et al., 1985). In humans, Immunodysregulation Polyendocrinopathy Enteropathy X-linked syndrome (IPEX)-- an autoimmune disease that results in system-wide inflammation especially of the intestine, skin and endocrine organs-- was found to be due to a defect in the Treg subset (Bennett et al., 2001; Brunkow et al., 2001; Wildin et al., 2001). The disease is often fatal without a bone marrow transplant (Rao et al., 2007). Further investigation found that this defect was attributed to a mutation in the Forkhead box P3 (FoxP3) transcription factor, the lineage specific marker and master regulator of Tregs (Fontenot et al., 2003; Hori et al., 2003; Yagi et al., 2004).

Traditionally, the term Tregs refers to a subset of $CD4^+$ T cells that express CD25 (Ng et al., 2001). By some estimates, they comprise 5-10% of $CD4^+$T cells and up to 1-2% of PBMCs (Baecher-Allan et al., 2001). However, only those $CD4^+$T cells with the highest level of CD25 are thought to be functionally suppressive (Baecher-Allan et al., 2004); specifically, they are able to decrease the proliferation or activity of T cells, B cells, antigen presenting cells (APCs) and natural killer (NK) cells (Delgoffe et al., 2013;

Gasteiger et al., 2013). It is thought that heightened expression of the IL-2 receptor (CD25) allows them to restrict IL-2 availability to other immune cells (Thornton and Shevach, 1998; Vignali et al., 2008).

There are also other regulatory cells of the immune system, termed type 1 (Tr1) regulatory cells, regulatory $CD8^+$ T cells, and regulatory B cells. While neither is thought to play as large a role as Tregs in maintaining immune homeostasis, their function synergizes with that of more traditional Tregs. Regulatory $CD8^+$ T cells, which express the Qa-1 peptide complex, inhibit activated and memory T cells that also express this peptide complex (Long et al., 2017). Regulatory CD8 T cells appear to be restricted to the gut, but do seem to play a role in autoimmune responses in other locations (Fleissner et al., 2010; Wang and Alexander, 2009). They occur at much lower frequencies than standard Tregs, making their study difficult(Gol-Ara et al., 2012) . Similar to Tregs, regulatory CD8 T cells also express CD25 and FoxP3 (Churlaud et al., 2015). This is in contrast to the subset of regulatory B cells (Bregs) and Trl cells which do not express

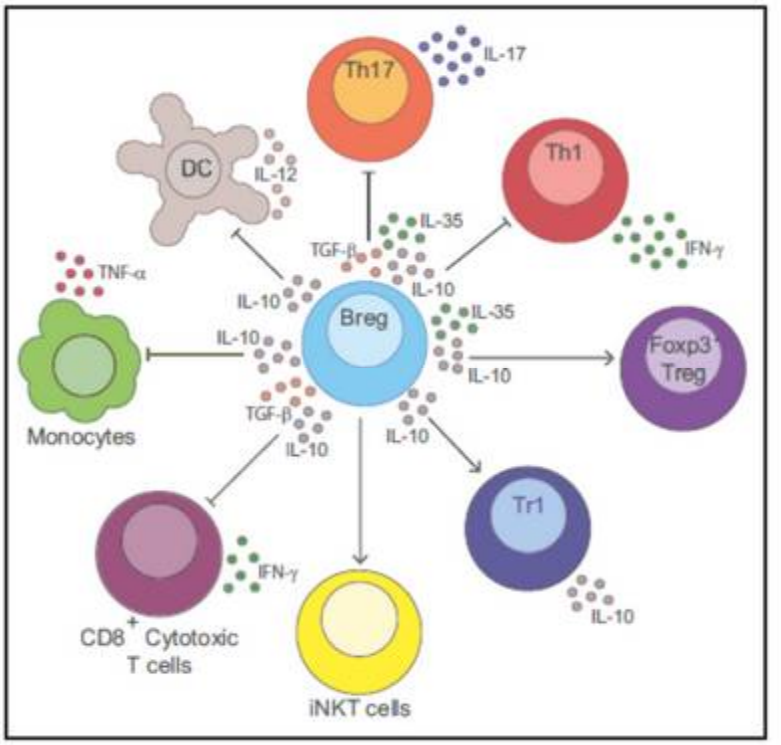

Figure 1: Regulatory B cells (Rosser and Mauri, 2015)

FoxP3 or CD25. While Bregs are thought to help maintain both Tregs and Trl cells through the production of IL-10 and transforming growth factor beta (TGF-β) (**Fig. 1)**, there has not been a lineage specific marker found to differentiate them from other B cells (Rosser and Mauri, 2015). Thus, it is postulated that they develop in response to certain stimuli and are not a distinct lineage in B cell development (Yang et al., 2013). Similarly, Tr1 cells are distinguished from other $CD4^+$ T cells by their production of IL-10 and TGF-β (Groux et al., 1997). They can express FoxP3 upon activation, but do not depend on FoxP3 for suppressive function and thus can develop from naïve T cells isolated from immune dysregulated, polyendocrinopathy, enteropathy, X-linked syndrome (IPEX) patients (Gol-Ara et al., 2012; Vieira et al., 2004).

Due to the difficulties in isolating and characterizing these other regulatory cells, much of what is known in immune dysfunction has focused on standard $CD4^+CD25^+$ Tregs. Therefore, the regulatory dysregulation in HAM/TSP explored in this thesis will focus on the understanding of how standard Tregs contribute to altered suppression.

In humans, Tregs are a defined T cell lineage that forms in the thymus early during development and later on in the periphery. The two origins of Treg development differentiate natural Tregs (nTregs; thymus derived) from peripheral Tregs (pTregs or iTregs; peripherally induced) (Josefowicz et al., 2012). When T cells develop in the thymus, certain mechanisms are in place to remove T cells that can recognize antigen, therefore decreasing the likelihood of resulting autoimmunity. After development of the T cell receptor (TCR) repertoire through VDJ rearrangement and somatic hypermutation, resulting T cells first are selected by positive selection to select TCRs capable of recognizing MHC and then go through negative selection to remove

TCRs that bind too tightly to MHC: self-peptide **(Fig. 2)**(Josefowicz et al., 2012). This process is aided by expression of the AIRE gene (autoimmune regulator) by APCs of the thymic medullary stroma, which allows for expression of antigens from almost every organ. However, during the process of selection, some T cells become anergic rather than undergoing apoptosis and cell death upon a intermediate TCR stimulus (Josefowicz et al., 2012). It is postulated that this allows for the selection of nTreg populations that recognize self.

Though nTreg selection principally occurs in the thymus, nTregs are capable of inhibiting T cell responses to both self and foreign antigens (Belkaid, 2007). Recent sequencing of nTreg TCR repertoires yielded a polyclonal population similar to that of conventional T cells, with no preference for recognition of self-peptides (Pacholczyk et al., 2007). Therefore, nTreg development likely also occurs to some extent in the periphery and throughout the lifetime of an individual, but these mechanisms are still poorly understood. Indeed, recent reports implicate IL-2 not only in the maintenance of nTregs but also as being required in the early stages of nTreg development (Bayer et al., 2005).

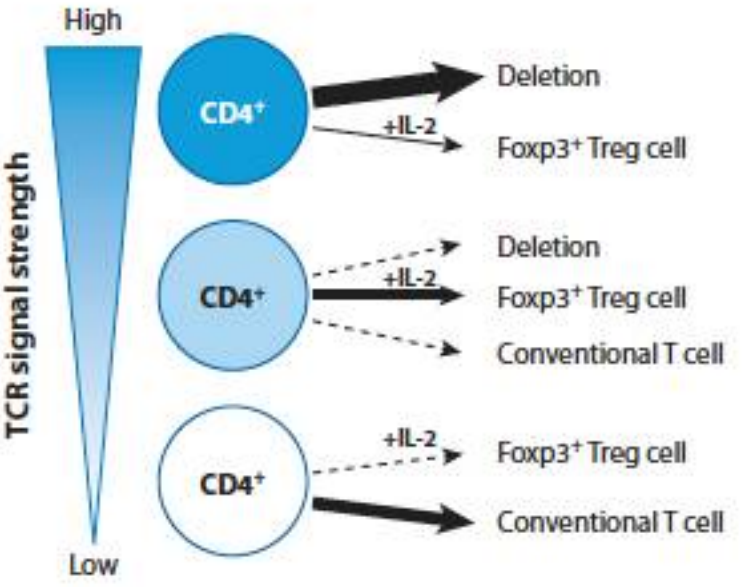

Figure 2: TCR signal strength decides Treg fate (Josefowicz et al., 2012)

Peripherally induced Tregs (pTregs) develop from naïve conventional T cells under certain environmental conditions. Historically, this is described as sub-stimulatory engagement of the TCR receptor in the presence of foreign antigen in lymphopenic environments (Yadav et al., 2013). This is best understood through pTreg development in the gut where they comprise almost 30% of gut T cells (Tanoue et al., 2016). TGF-β and retinoic acid are crucial for this process of T cell to pTreg transformation (Fu et al., 2004; Tanoue et al., 2016). Initially, pTregs were thought to be less stable than nTregs in terms of functional stability and cell marker characterization (Sawant and Vignali, 2014). However, it is now understood that both are quite stable and have similar cell surface markers (Tanoue et al., 2016). Indeed, it is now well accepted that human Tregs, both nTregs and pTregs, can be characterized as $CD3^{+}CD4^{+}CD25^{+}CD39^{+}PD\text{-}1^{+}CD127^{-}FoxP3^{+}$ T cells. They can be differentiated by the expression of neuropillin-1 (Nrp-1), which is present on nTregs but not expressed on pTregs (Yadav et al., 2012). Each also expresses the intracellular markers cytotoxic T-lymphocyte-associated antigen 4 (CTLA-4) and glucocorticoid-induced TNFR family related gene (GITR) (Lin et al., 2013). Helios, another Treg marker, also appears to differentiate the subsets as gut pTregs do not express Helios, although there are differing accounts in the literature (Elkord, 2016; Szurek et al., 2015; Thornton et al., 2010).

All Treg subsets are important for maintaining immune tolerance, and both nTregs and pTregs have been shown to be essential in preventing neuroinflammation (Jones and Hawiger, 2017; Koutrolos et al., 2014). Indeed, this ability to suppress in inflammatory environments is borne from stability in FoxP3 expression. As mentioned, FoxP3 is the master regulator and lineage marker of regulatory T cells. Pioneering

research in the field demonstrated that Foxp3 is under epigenetic regulation, maintenance of protein expression is dictated by the epigenetic state of the gene (Floess et al., 2007). Epigenetic modification represents another level of gene regulation through DNA methylation and histone acetylation (Begin and Nadeau, 2014), affecting gene transcription through accessibility of DNA to transcription factors (Huehn et al., 2009). There are three separate non-coding regions within the FoxP3 locus for which epigenetic regulation is apparent in Tregs: the FoxP3 promoter, TGF-β-sensor (CNS 1 enhancer), and Treg-specific demethylated region (TSDR) (CNS2) (**Fig. 3**) (Huehn et al., 2009; Lal and Bromberg, 2009; Toker and Huehn, 2011).

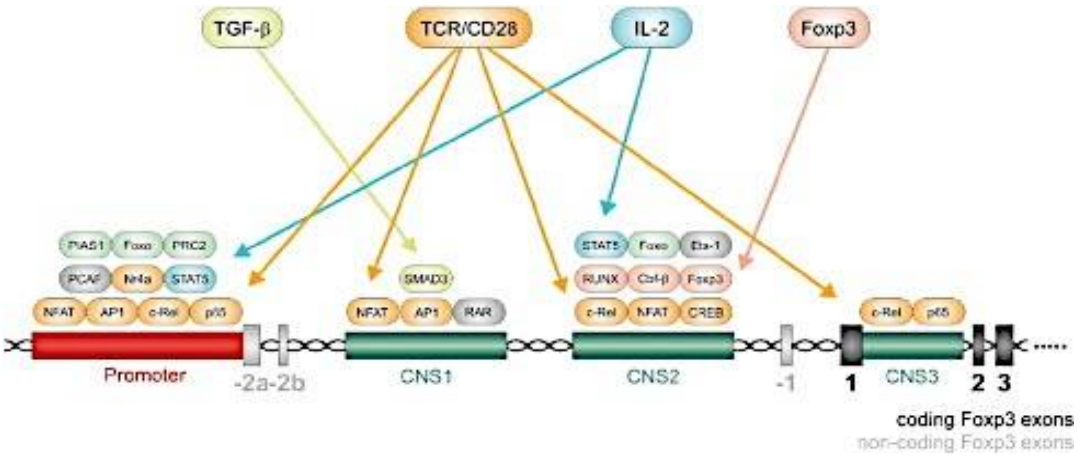

Figure 3: FoxP3 locus (Huehn and Beyer, 2015). FoxP3 locus is separated into Promoter, CNS1, CNS2 (TSDR) and CNS3 coding exons

Within each of these coding exons, there are clustered CpG islands that have cytosines that can have methyl groups attached to them (Lal and Bromberg, 2009). The greater the number of cytosines without methyl groups (demethylated), the more open the region is to transcription factors, allowing for stable and consistent expression of Foxp3 (Huehn et al., 2009). Interestingly, FoxP3 protein expression is decoupled from TSDR demethylation as it has been shown that activated T cells can have transient opening of

the FoxP3 promoter despite a methylated TSDR (Huehn et al., 2009; Mantel et al., 2006). Therefore, TSDR demethylation does not determine if FoxP3 will be expressed but rather the stability of that expression (Floess et al., 2007; Huehn et al., 2009), and this stable expression has been shown to be necessary for Treg suppressive function (Polansky et al., 2010).

The greatest difference in the methylation state in the FoxP3 locus occurs in the TSDR (CNS2), which is almost completely demethylated in both nTregs and pTregs (**Fig. 4**) whereas *in vitro* induced Tregs and activated T cells display a methylated TSDR (Miyao et al., 2012; Tanoue et al., 2016). As shown in the **Fig. 4**, whereas the TSDR becomes demethylated in nTregs through the process of nTreg development in the thymus and periphery, CNS1 demethylation and engagement of SMAD3 through TGF-β signaling must occur prior to CNS2 demethylation (Tanoue et al 2016, Okhura et al 2012) in pTregs. Therefore, while both nTregs and pTregs will show dementhylation in the TSDR, only pTregs will also show demethylation in the CNS1, which experimentally was shown to be dispensable for nTreg development (Tanoue et al., 2016; Zheng et al., 2010). Currently, all of the processes involved in progressive TSDR demethylation have are not completely outlined. It is thought that loss of binding to PIAS1 in the FoxP3 promoter, followed by demethylation of the promoter, allows binding of NFAT1 and STAT5. Through several other events not currently understood, progressive demethylation of the TSDR occurs (Toker and Huehn, 2011). Ets1 and CREB, as well as other transcription factors, can then bind to the TSDR and stabilize FoxP3 expression (Tanoue et al., 2016). Therefore, binding of the transcription factors, in particular, to

CNS2 confers the transcriptional enhancer activity to the TSDR (Toker and Huehn, 2011).

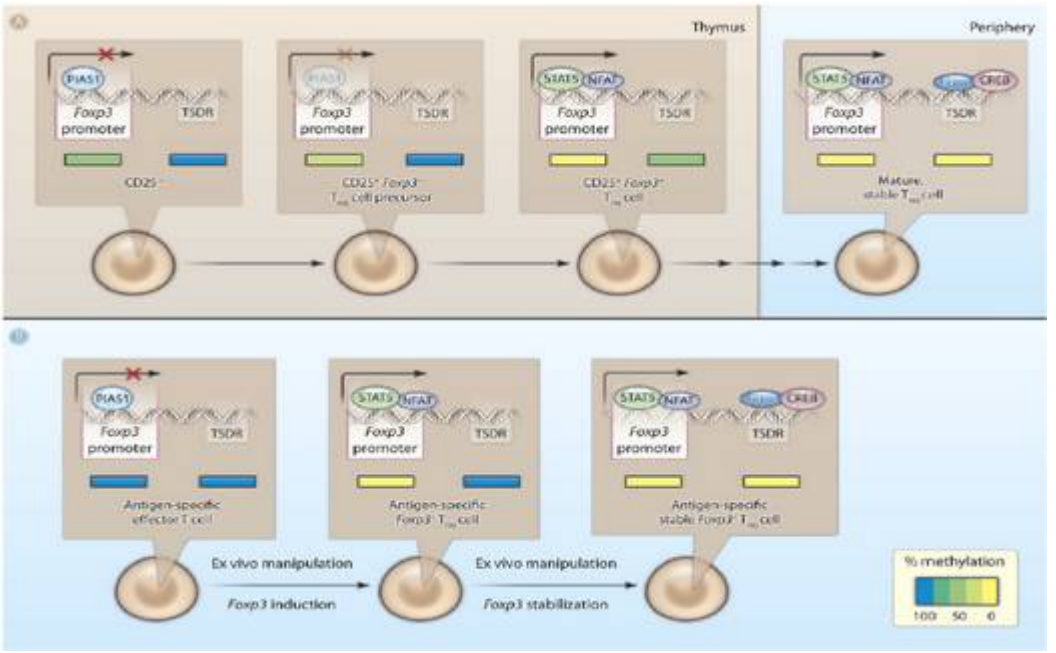

Figure 4: Progressive demethylation of FoxP3 TSDR in development (Toker and Huehn, 2011)

Stability of FoxP3 expression dictates suppressive function of Tregs, especially in regions of inflammation (Barbi et al., 2014). Tregs hone to areas of inflammation induced by effector functions to both self and foreign antigen (Belkaid and Tarbell, 2009). It is imperative that (1) infiltrating Tregs maintain suppressive function and (2) that there is a balance that allows for effector cells to clear foreign antigen without interference. Unstable regulatory cells, such as certain subsets of pTregs that have incomplete TSDR demethylation, or Tr1 regulatory cells which are completely lacking in TSDR demethylation, can enter sites of inflammation and convert to a more effector phenotype in which they begin to produce inflammatory cytokines (Yadav et al., 2013). This has been observed after the transference of *in* vitro TGF-β- induced Tregs and

pTregs into experimental autoimmune encephalomyelitis (EAE), an animal model of multiple sclerosis, but seems to be dependent on the environment into which they enter (Yadav et al JEM 2012). Other studies found that can conversion to pro-inflammatory phenotypes mainly occurred upon conversion of FoxP3^{lo} non-suppressive T cells that lacked demethylation in CNS2 (Miyao et al., 2012; Miyara et al., 2009).

It is clear that Tregs are capable of maintaining immune homeostasis in the vast majority of healthy individuals, as their absence can lead to catastrophic consequences. Reduced or dysfunctional Tregs are implicated in type 1 diabetes, IPEX, graft vs. host disease, psoriasis, rheumatoid arthritis (RA), SLE, and relapsing-remitting multiple sclerosis (RRMS) (Long and Buckner, 2011). While Tregs must infiltrate and suppress aberrant inflammatory conditions in autoimmune disease, the role of Tregs in infection is complicated. Indeed, in some cases normal Treg function can be detrimental to the clearance of pathogens (Belkaid, 2007). However, Tregs are also necessary to tamp down on the effector immune response and there are several cases where inefficient Treg control of immune responses to foreign antigen (Ag) leads to inflammatory disease. For example, while Tregs can hamper the response to herpes simplex virus (HSV), they are necessary to limit immunopathology to HSV in the eye (Belkaid and Rouse, 2005) (Suvas et al., 2004). HAM/TSP likewise represents an imbalance in the immune response to HTLV-1 and in the ability to limit immunopathology to HTLV-1. Similar to the viral and autoimmune diseases described above, Treg dysfunction may also contribute to the imbalance in displayed in HAM/TSP.

Tregs in HAM/TSP

As mentioned, HAM/TSP is characterized by an inflammatory immune infiltrate in the CNS that leads to progressive demyelination and lower limb motor dysfunction. Interestingly, while ATLL and HAM/TSP are the best known and characterized consequences of HTLV-1 infection, there are several inflammatory disorders that are also associated with HTLV-1 infection. These include Sjögrens syndrome, infective keratitis, pneumonitis, uveitis, polymyositis, and arthritis amongst others (**Table 1**). Of note, while there are no animal models that accurately reflect HAM/TSP, there are several animal models that demonstrate widespread inflammatory infiltrates. A transgenic mouse model expressing HTLV-1 Tax results in arthritis and reduced regulatory T cell populations (Ohsugi and Kumasaka, 2011) while transgenic rats expressing the LTR-env-pX region of HTLV-1 develop vasculitis, polymyositis, arthropathies and Sjögrens' syndrome (Nakamaru et al., 2001), similar to the diseases associated with HTLV-1 infection in humans. This suggests that the systemic and local inflammation seen in these HTLV-1 associated diseases are possibly due to a lack of immune suppression related to HTLV-1 infection, and support the argument that Treg dysfunction may be associated with HTLV-1 infection. While Treg function has not been fully explored in the other HTLV-1 inflammatory diseases, it has well been well established that Tregs in HAM/TSP are dysfunctional (Grant et al., 2008; Yamano et al., 2005). Indeed, the $CD4^{+}CD25^{+}$ subset, in which Tregs reside, serves as the dominant reservoir for HTLV-1 in HAM/TSP patients (Yamano et al., 2009; Yamano et al., 2004). The Tregs isolated from HAM/TSP patients are less able to reduce proliferation of allogeneic ND Teffs cells (Araya et al., 2014; Yamano et al., 2005). Moreover, HAM/TSP Tregs were more prone to production

of interferon (IFN)- λ, a key feature of Tregs with incomplete demethylation of the TSDR and therefore unstable suppressive function in inflammatory environments (Araya et al., 2014) (Yadav et al., 2013). This observation may explain the inability of Tregs present in HAM/TSP to halt the neuroinflammation.

Disease associated with HTLV-1 infection	
Adult disease	***Association***
Adult T-cell leukemia (ATL)	++++
HTLV-1-associated myelopathy/tropical spastic paraparesis (HAM/TSP)	++++
Uveitis (frequent in Japan)	++++
Infective dermatitis (rare)	+++
Polymyositis, inclusion body myositis	++
HTLV-1-associated arthritis	++
Pulmonary infiltrative pneumonitis	++
Sjögren's syndrome	+
Childhood disease	***Association***
Infective dermatitis (frequent in Jamaica)	++++
Tropical spastic paraparesis/HTLV-1-associated myelopathy (rare)	++++
Adult T-cell leukemia/lymphoma (very rare)	++++
Persistent lymphadenopathy	+

++++ proven association; +++ probable association; ++ likely association; + possible association

Adapted from Mahieux R & Gessain A, 2003

Table 1: HTLV-1 disease associations
http://www.mpbio.com/images/htlv/original/Disease%20association%20table.jpg

The observed changes in Treg function in HAM/TSP have been linked to HTLV-1 gene expression. Specifically, HTLV-1 Tax expression has been demonstrated to reduce FoxP3 expression and participate in the reduced function of Tregs (Oh et al., 2006) (Yamano et al., 2005). Interestingly, Tax has been shown to interfere with gene expression through binding to epigenetic modulators and binding directly to promoters (Bogenberger and Laybourn, 2008; Cheng et al., 2007; Ego et al., 2005). It can bind to MBD2, a methyl-CpG- binding domain protein thought to bind to methylated CpGs and recruit chromatin remodeling complexes (Ego et al., 2005). Importantly, a lack of MBD2

was associated with complete methylation of the TSDR (Wang et al., 2013). It remains to be seen whether Tax binding increases or prevents the function of MBD2 in the capacity of TSDR demethylation. Additionally, Tax participates in silencing of the SHP-1 promoter in a process termed Tax-induced promoter silencing (TIPS) by complexing with HDAC, a histone deacetylase, and leading to increased methylation (Cheng et al., 2007; Nakase et al., 2009). Of note, Tax expression is low to absent in PBMCs from patients with ATLL, which are characterized by high FoxP3 expression, hypomethylation of the TSDR, and Treg-like suppressive abilities (Araya et al., 2011; Shimazu et al., 2016; Yano et al., 2007). HTLV-1 Tax has multiple binding factors, including CREB, CBP/p300, and Ets1, all of which are implicated in maintenance of Foxp3 expression (Boxus et al., 2008). Alternatively, HTLV-1 HBZ has also been associated with observed Treg dysfunction of HAM/TSP through the generation of unstable Tregs (Zhao et al., 2011). Indeed, there is evidence that HBZ can directly increase FoxP3 expression through increased formation of pTregs, although there was no change in TSDR demethylation (Yamamoto-Taguchi et al., 2013).

The experiments presented here investigate the role of HTLV-1 Tax principally, and HBZ to a lesser extent, in the observed Treg dysfunction at an epigenetic level and demonstrate that HTLV-1 Tax is associated with altered methylation in the FoxP3 TSDR. The TSDR changes in HAM/TSP correlated with reduced Treg suppressive capacity. Furthermore, initial transduction experiments suggest that HTLV-1 Tax specifically reduces TSDR demethylation.

Results

FoxP3 TSDR demethylation in HAM/TSP patients

To examine TSDR demethylation in HAM/TSP primary T cells, DNA from whole PBMCs, $CD4^+$ T cells, and $CD4^+CD25^+$T cells was isolated and compared to NDs for FoxP3 TSDR methylation status. TSDR demethylation was calculated as the percentage of DNA in FoxP3 intron 1 that amplified with primers directed against demethylated CpG islands in FoxP3 Intron 1 versus DNA that amplified with primers against methylated CpG islands in FoxP3 Intron 1 (Materials and Methods; (Sahin et al., 2013; Toker and Huehn, 2011). In NDs, 2.066% (s.d.+/- 0.154%) of FoxP3 TSDR demethylation was detected in whole PBMCs (**Fig. 5A**). A significant increase in demethylation was detected in the total $CD4^+$ T cell (8.097%) population and even higher in the isolated $CD4^+$ $CD25^+$ T cell subset (60.15%) compared to whole PBMCS ($p=0.0004$ and $p< 0.0001$, respectively; **Fig. 5B**). Similar to ND, whole HAM/TSP PBMCs showed 3.022% (s.d.+/- 0.552) of FoxP3 TSDR demethylation with a statistically significant increase in demethylation in $CD4^+$ T cell (10.11%) and $CD4^+$ $CD25^+$ T cell subsets (48.43%) compared to whole PBMCs ($p=0.0018$ and $p<0.0001$, respectively; **Fig. 5B**). Thus, the enrichment of $CD4^+CD25^+$ T cells from whole PBMC significantly increases the percentage of FoxP3 TSDR demethylation and is consistent with previous studies (Liu et al., 2010).

The frequency of $CD4^+CD25^+$ T cells is known to be elevated in HAM/TSP patients compared to NDs (Mukae et al., 1994), and therefore must be considered when measuring FoxP3 TSDR methylation. As shown in **Fig. 5C**, indeed the frequency of

$CD4^+CD25^+$ T cells was significantly higher in HAM/TSP patients than NDs (p=0.0164). There was no significant difference in the percentage of $CD4^+$ T cells between the two groups (unpublished observations). Therefore, after normalization to the frequency of $CD4^+CD25^+$ T cells, HAM/TSP patients were found to have a statistically significant decreased demethylated percentage in isolated $CD4^+$ $CD25^+$ T cells as compared to NDs (p=0.0339; **Fig. 5D**). A similar trend was also observed in whole PBMCs although this relationship did not reach statistical significance (p=0.1659; **Fig.5E**) probably due to the low numbers of $CD4^+CD25^+$ cells in PBMC (**Fig. 5C**).

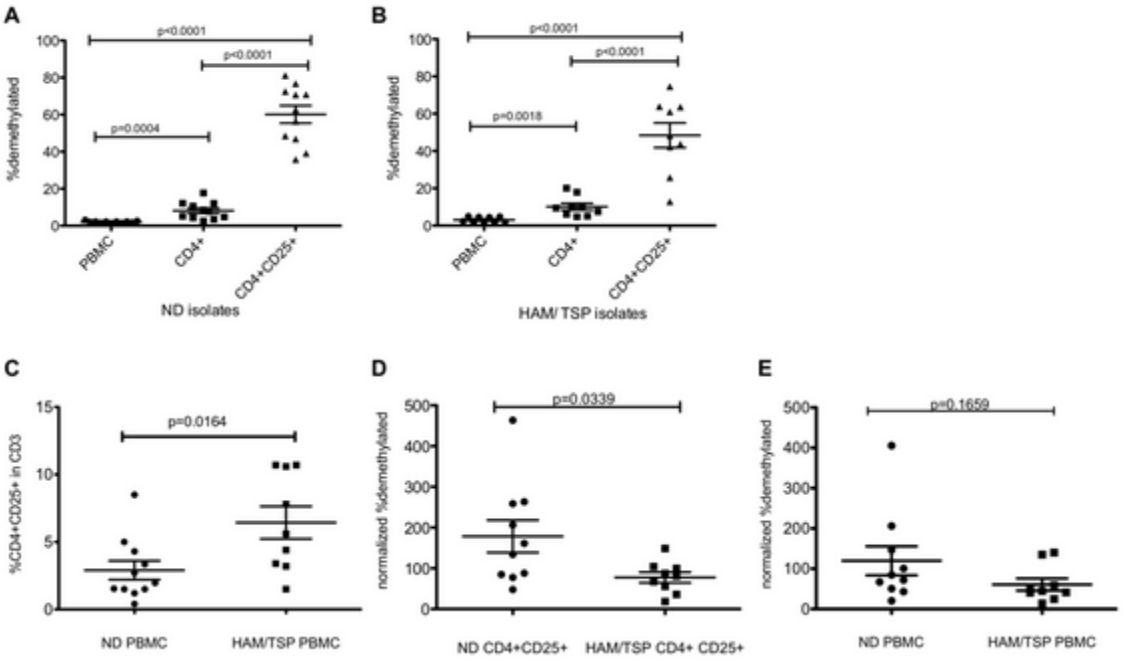

Figure 5. FoxP3 TSDR demethylation is reduced in HAM/TSP. (A) % FoxP3 TSDR demethylation in ND PBMC (n=10), isolated $CD4^+$ T cells, and isolated $CD4^+CD25^+$ T cells. (B) % FoxP3 TSDR demethylation in HAM/TSP PBMC (n=9), isolated $CD4^+$ T cells, and isolated $CD4^+CD25^+$ T cells. The long horizontal bars represent the mean for each group while the shorter bars represent the standard deviation. (C) A comparison of the %$CD4^+CD25^+$ in $CD3^+$ T cells of ND and HAM/TSP PBMC. (D) Normalized % FoxP3 TSDR demethylation in isolated $CD4^+CD25^+$ T cells of ND and HAM/TSP patients. % FoxP3 TSDR demethylation was normalized

to the % $CD4^+CD25^+$. (E) Normalized % FoxP3 TSDR demethylation in PBMC of ND and HAM/TSP patients. % FoxP3 TSDR demethylation was normalized to the % $CD4^+CD25^+$.

No correlation between the percent FoxP3+ cells and FoxP3 TSDR demethylation

Many investigators have relied upon FoxP3 by flow cytometry for characterization of Tregs (Miyara et al., 2009). Although in NDs it appears to be a reliable marker, FoxP3 can also be increased upon T cell activation (Wang et al., 2007). FoxP3 mRNA and protein has been demonstrated to be decreased in HAM/TSP patients, although this was demonstrated in isolated T cell subsets (Oh et al., 2006). Interestingly, when the percentage of $FoxP3^+$ cells in HAM/TSP PBMCs were compared by flow cytometry, $CD4^+CD25^+$ cells were shown to have equivalent FoxP3 percentage compared to NDs ($p=0.4676$; **Fig. 6A**). In particular, the percent $FoxP3^+$ cells in PBMCs and the level of FoxP3 TSDR demethylation did not correlate ($p= 0.2765$, $r^2= 0.0692$; **Fig. 6B**). These results are likely due to transient expression of FoxP3 in activated T cells, which are increased in HAM/TSP patients compared to NDs (Yamano et al., 2009). Therefore, the percent of $FoxP3^+$ cells by flow analysis poorly correlates with FoxP3 TSDR demethylation in human PBMCs and may not be a good surrogate marker of Treg function.

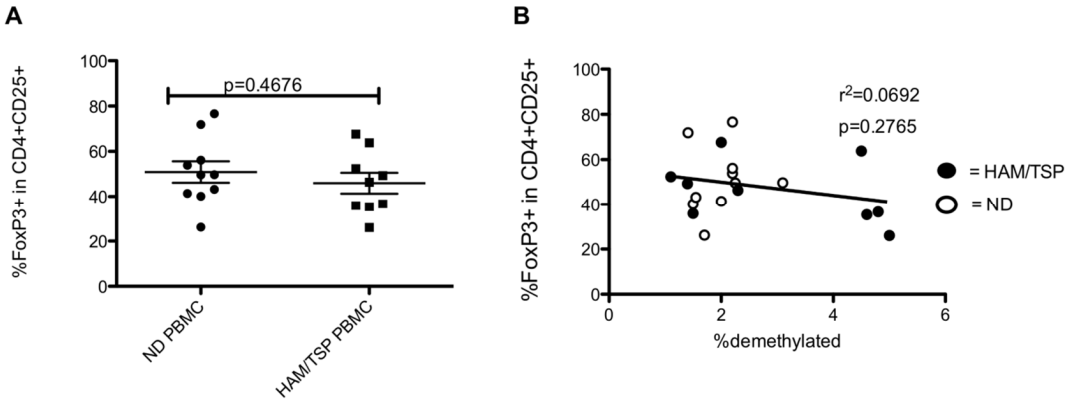

Figure 6. No correlation between the percent FoxP3+ cells and FoxP3 TSDR demethylation (A) % FoxP3$^+$ cells in CD4$^+$CD25$^+$ T cells of ND and HAM/TSP patients. The long horizontal bars represent the mean for each group while the shorter bars represent the standard deviation. (B) No correlation of the %FoxP3 TSDR demethylation in PBMCs with the % FoxP3+ cells in CD4$^+$CD25$^+$ T cells of ND (opened circles) and HAM/TSP patients (closed circles).

Correlation of FoxP3 TSDR demethylation with Treg suppressive function

The level of FoxP3 TSDR demethylation in isolated CD4$^+$CD25$^+$ T cells varied widely between the HAM/TSP patients included in our study. To determine if there was a correlation between methylation status of the FoxP3 TSDR and functional suppression of isolated CD4$^+$CD25$^+$ T cells, allogeneic Treg suppression assays were performed. NDs with previously confirmed demethylated TSDRs were compared with HAM/TSP patients with confirmed methylated TSDRs. As a control, ND CD4$^+$CD25$^+$ T cells were able to suppress allogeneic activated ND CD4$^+$CD25$^-$ T cells (Teffs) and this suppressive capacity increased depending on Treg:Teff ratio (**Fig. 7A-C**). In contrast, HAM/TSP patients CD4$^+$ CD25$^+$ T cells suppressed to a significantly lesser extent, especially at high Treg:Teff (1:1) (p= 0.0041;**Fig. 7C**). A two-way ANOVA analysis demonstrated a

significant difference in suppression between HAM/TSP and ND and Treg:Teff ratio. In addition, there was a trend (with 2 normal donors and 2 HAM/TSP patients) for the level of demethylation in the FoxP3 TSDR to correlate with the level of suppression. These results demonstrated that the decrease of Treg suppressive function in HAM/TSP patients may be associated with the demethylation status of FoxP3 TSDR.

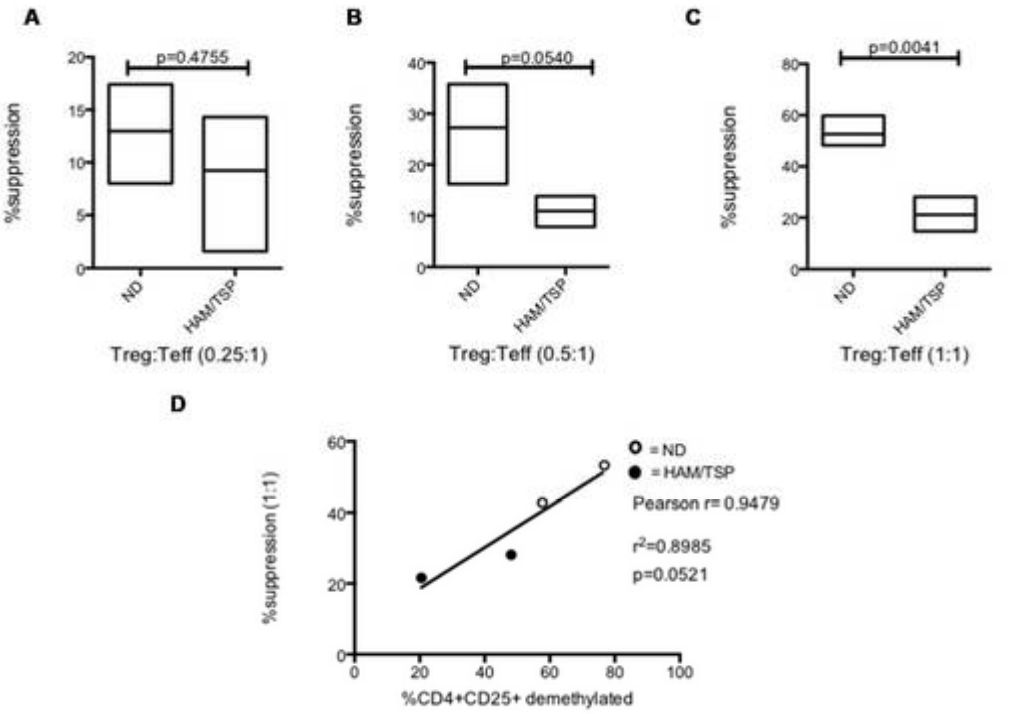

Figure 7. Reduced FoxP3 TSDR demethylation correlates with reduced Treg suppression. Lymphoproliferation suppression assays were set up and ND (n=3) or HAM/TSP (n=2) $CD4^+CD25^+$ T cells were added at different ratios of Treg:Teff = 0.25:1 (A), 0.5:1 (B) and 1:1 (C). The % suppressions of Treg were normalized to Teff proliferation without Treg.
(D) Correlation between $CD4^+CD25^+$ TSDR % demethylation and suppressive capacity as determined in lymphoproliferation suppression assays at Treg:Teff ratio of 1:1.

FoxP3 demethylation in HTLV-1 CD4$^+$ T cell lines

Due to the observation of altered TSDR methylation status in HAM/TSP PBMCs and reduced Treg suppression in HAM/TSP Tregs, it was of interest to determine if HTLV-1 infected T cell lines also demonstrated TSDR alterations. Initially, HTLV-1-infected and uninfected cell lines were characterized for expression of virus specific gene products, Treg markers (CD25 and FoxP3) and the demethylation levels of the FoxP3 TSDR.

Both HTLV-1-infected cell lines MT2 and HUT102 express CD25 (95.7%, 96.5% respectively) (**Fig. 8A**) while the HTLV-1-uninfected cell lines Jurkat and MOLT-3 were CD25 negative (**Fig. 8A**). Only MT2 expressed a high percentage of FoxP3 in the CD25$^+$ T cell population (97.6%) (**Fig. 8A**). In contrast, HUT102 had very few CD25$^+$ FoxP3$^+$cells (1.3%) (**Fig. 4A**). The two uninfected CD25$^-$ T cell lines had low levels of FoxP3 positivity (**Fig. 8A**) consistent with previous reports (Yagi et al., 2004).

Given the variation of CD25 and the percent FoxP3 positivity in these cell lines, the level of FoxP3 TSDR demethylation was determined. The MT2 cell line, which had the highest percentage of FoxP3 by flow cytometry, had a FoxP3 TSDR that was completely demethylated, displaying similar levels of demethylation to that reported in natural thymus-derived Tregs from healthy donors (95-99.98%) (**Fig. 8B**) (Janson et al., 2008). By contrast, HUT102 was completely methylated (**Fig. 8B**). Similarly, the two uninfected T cell lines that had low FoxP3 positivity by flow cytometry also displayed complete methylation.

Since HTLV-1 gene products including Tax and HTLV-1 basic leucine zipper factor (HBZ) have previously been suggested to interact with FoxP3 (Grant et al., 2008;

Satou et al., 2011), we determined if FoxP3 methylation status was associated with expression of these viral proteins. Since MT-2 expressed both *tax* and *HBZ* mRNA, all the data was normalized to *tax* and *HBZ* mRNA expressions in MT-2 as 1.00. When compared to MT-2, HUT102 expressed more *tax* mRNA (12.24 times) but had lower *HBZ* mRNA levels (**Fig. 8C and 8D**), as previously reported (Satou et al., 2006). As expected, *tax* and *HBZ* mRNA were not detected in Jurkat and MOLT3, the two HTLV-1-uninfected cell lines. Thus, *tax* mRNA expression levels were elevated in the HTLV-1-infected cell line that had complete FoxP3 TSDR methylation (HUT 102, **Fig. 8B**). By contrast, the MT2 cell line which had lower levels of *tax* expression had a completely demethylated FoxP3 TSDR. Since both HTLV-1 infected T cell lines expressed HTLV-1 *HBZ*, there appeared to be no relationship with FoxP3 TSDR methylation.

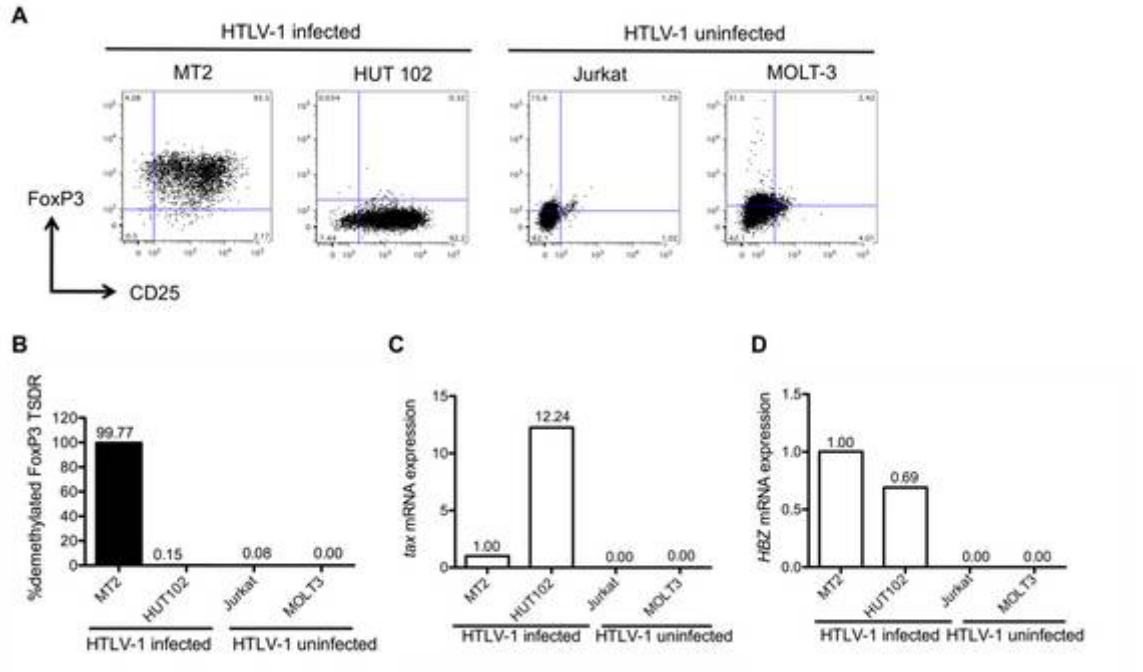

Figure 8. HTLV-1-infected and HTLV-1-uninfected cell line profiles. (A) Flow cytometry profiles of HTLV-1-infected and HTLV-1-uninfected cell lines. The x-axis

denotes CD25 expression and the y-axis denotes FoxP3 expression. (B) FoxP3 TSDR demethylation analysis of HTLV-1-infected and HTLV-1-uninfected cell lines. (C) *tax* mRNA expression in the cell lines by RT-PCR. The data were calculated as relative amount to MT2 (1.00). (D) *HBZ* mRNA expression in the cell lines by RT-PCR. The data were calculated as relative amount to MT2 (1.00).

Correlation of FoxP3 TSDR demethylation with HTLV-1 Tax expression

HTLV-1 Tax is a pleiotropic viral protein that transactivates a number of cellular pathways, directly regulates interleukin production, promotes IL-2 independent growth in infected T cells, and impacts gene expression through chromatin remodeling (Currer et al., 2012). HAM/TSP patients are known to express more of this viral gene than asymptomatic carriers (AC) (Nagai et al., 1998). Moreover, Tax has previously been shown to decrease FoxP3 levels after transfection into ND $CD4^+CD25^+$ T cells (Yamano et al., 2005). We therefore asked if there was also a correlation with increased HTLV-1 Tax expression in HAM/TSP $CD4^+CD25^+$ T cells and decreased FoxP3 TSDR demethylation.

Freshly thawed PBMCs do not express HTLV-1 Tax at baseline (0 hours) by flow cytometry (**Fig. 9A**), however, after short-term culture (24 hours), variable levels of Tax expression were observed, particularly in the $CD4^+CD25^+$ T cell subset (**Fig. 9A**). Increasing levels of HTLV-1 Tax in $CD4^+CD25^+$ HAM/TSP T cells had a strong linear correlation (Coefficient of determination $r^2= 0.7736$, $p=0.0145$; **Fig. 9B**) with a decline in the FoxP3 TSDR demethylation from HAM/TSP PBMC. This decreased FoxP3 TSDR demethylation in HAM/TSP also correlated with the levels of HTLV-1 *tax* mRNA expression in PBMC after 24-hour culture (unpublished observations). As controls, there were no changes in FoxP3 TSDR demethylation in short-term cultures of ND PBMCs that were HTLV-1 Tax negative (**Fig. 9B**, circled points). To determine if the decline in FoxP3 TSDR

demethylation may be attributed to Treg death via $CD8^+$ cytotoxic T lymphocyte (CTL) killing, two HAM/TSP patient samples were depleted of $CD8^+$ T cells by bead isolation. As shown in **Fig. 9C**, in the absence of $CD8^+$ T cells, both patients still demonstrated a large decline in FoxP3 TSDR demethylation post-culture that mirrored a concomitant increase in *tax* mRNA expression (**Fig. 9D**). This result suggests that the observed decrease in TSDR demethylation during *ex vivo* culture can be attributed to increased expression of HTLV-1 genes, more specifically HTLV-1 Tax.

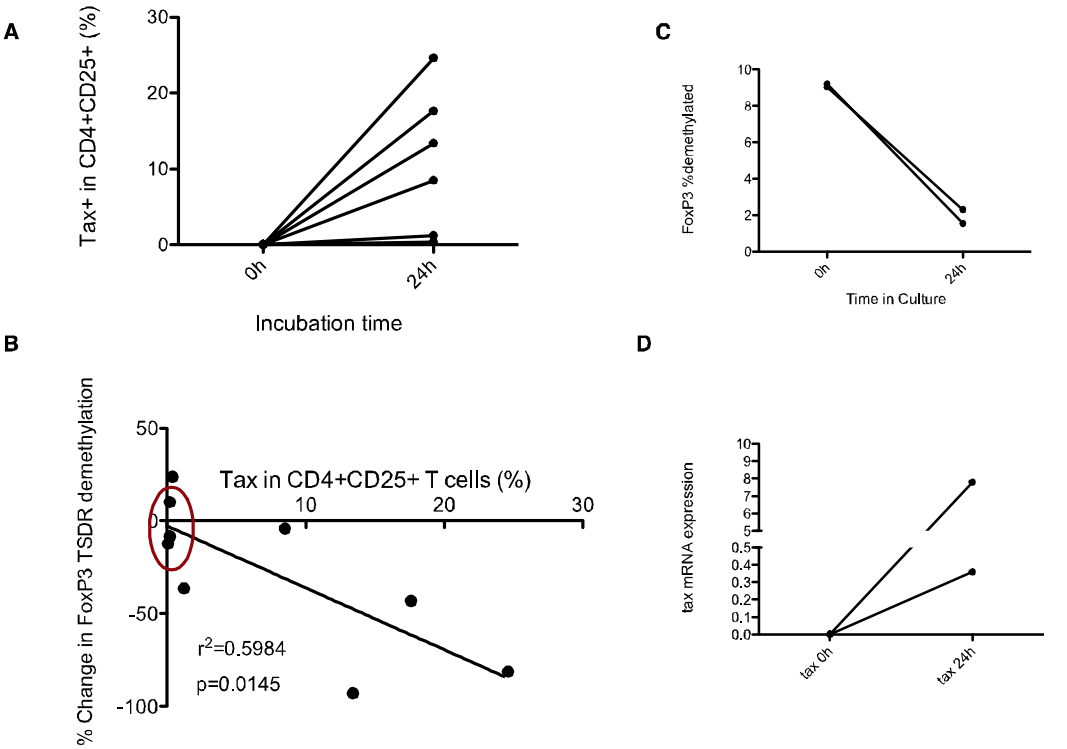

Figure 9. Increased Tax expression correlates with reduced FoxP3 TSDR demethylation. (A) Tax protein expression in $CD4^+CD25^+$ T cells of HAM/TSP patients before and after culture. PBMCs of HAM^{55}/TSP patients (n=6) were cultured for 24 hours. (B) Correlation of the Tax protein expression in $CD4^+CD25^+$ T cells of HAM/TSP patients with the change in FoxP3 TSDR demethylation before and after culture for 24 hours. ND samples are circled in red. Coefficient of determination r^2= 0. 7736 (C) %FoxP3 TSDR demethylation in isolated HAM/TSP

$CD4^+$ T cells *ex vivo*. (D) *tax* mRNA expression in isolated HAM/TSP $CD4^+$ T cells *ex vivo*

Transduced HTLV-1 genes are differentially expressed

Another approach to understanding how expression of HTLV-1 proteins alters Treg function is to transduce ND Tregs with HTLV-1 Tax and/or HBZ and assess Treg function. Previous work in the Jacobson lab demonstrated that transfection of $CD4^+CD25^+$T cells with HTLV-1 Tax reduced the amount of FoxP3 that was expressed (Yamano et al., 2005). Yamano and colleagues further elaborated on this by demonstrating decreased Treg suppression with expression of HTLV-1 Tax in $CD4^+CD25^+$ T cells (Araya et al., 2014). As noted earlier in this work, increased expression of HTLV-1 Tax in culture decreased FoxP3 TSDR demethylation. Again, while decreased TSDR demethylation correlated with decreased functional suppression (**Fig. 7D**), a direct causation could not be established at that time. Therefore, it was proposed that HTLV-1 genes be placed into lentiviral vectors and introduced individually into ND Tregs followed by assessment of: (1) TSDR demethylation (2) Treg suppressive function (3) exosome content.

HTLV-1 Tax-GFP was acquired from Dr. Hua Cheng from the University of Maryland (UMD), and modified by excising Tax and inserting HTLV-1 HBZ (unspliced). In addition, a control (ctrl-GFP) plasmid was generated that did not have either transgene. Production of the pseudovirus in HEK 293T cells with appropriate ratios of gag-pol, rev, and VSV-G (env) plasmids for each GFP plasmid was demonstrated. Initial transductions of Tax, HBZ, and ctrl psuedovirus into HeLa cells showed high transduction efficiency, although differential localization of the transduced

transgenes. While GFP from the control plasmid was expressed at higher levels throughout the cell **(Fig. 10A**), the Tax and HBZ fusion proteins appeared to cluster and localize to the nucleus (**Fig. 10B, 10C)**. While it has been demonstrated that HBZ protein preferentially localizes to the cytoplasm, it is unclear if similar molecular checkpoints are involved in the determination of localization in the expressed fusion transgenes.

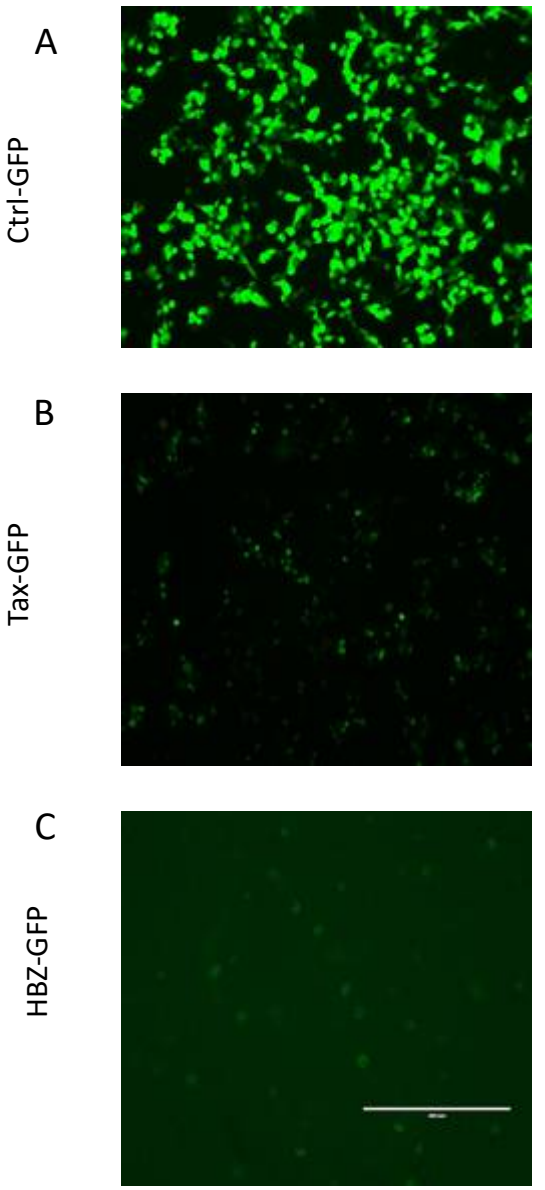

Figure 10: Ctrl, Tax, and HBZ Transduced HeLa cells. (A) HeLa cell transduced with Ctrl-GFP pseudovirus and imaged 3d post-transduction express GFP at high levels and throughout the cytoplasm and nucleus. (B) HeLa cells transduced with Tax-GFP express GFP at much lower levels signifying Tax expression in a punctate distribution similar to nuclear expression profile (C) HBZ-GFP psuedovirus transdueced HeLa cells have a similar distribution of GFP expression to those cells transduced with Tax-GFP

Indeed, while some of the decreased GFP intensity could be explained by cellular localization, it also appeared that after transfection into 293T for packaging, each pseudovirus also yielded different titers. Testing of several different ratios for the packaging of Tax and HBZ yielded

consistently lower titers (50-75%) lower than the ctrl-GFP pseudovirus (**Fig. 11**). Lower pseudovirus titers could be explained by toxicity of the HTLV-1 transgenes such that 293Ts are not able to form as many viral particles when these genes are expressed. Due to the low viral titer (~6x10^6) in viral supernatants and the variability in the titer of each HTLV-1 transgene, we aimed to increase viral titers. This was accomplished through low-speed ultracentrifugation (25Krpm) or PEG-it solution. PEG-it is a virus precipitation solution composed of polyethylene glycol, which is optimized for the capture of lentiviral based particles.

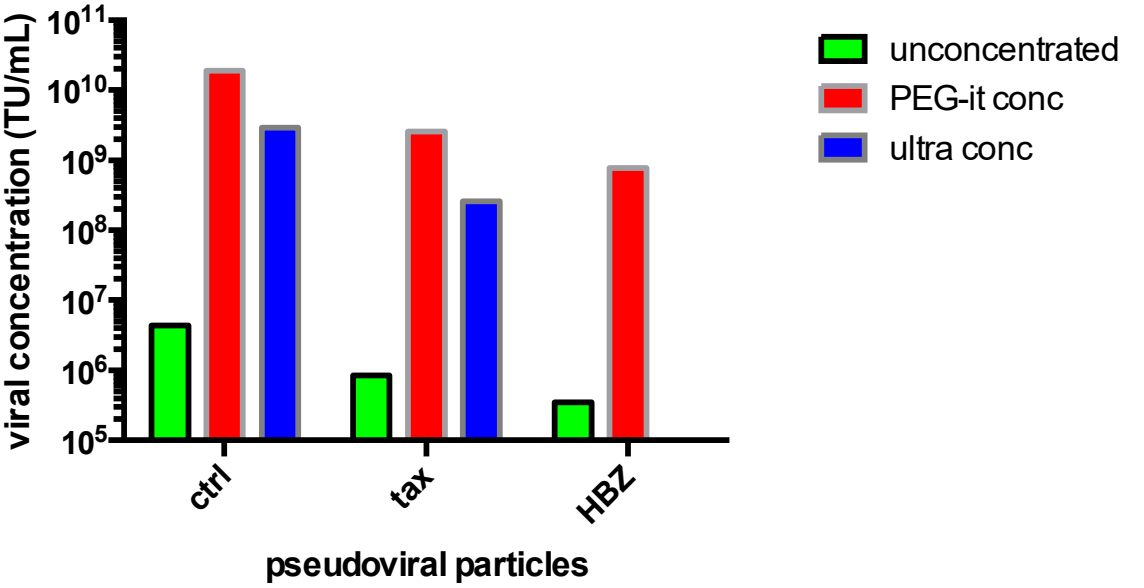

Figure 11: Concentration of pseudovirus using ultracentrifugation and PEG-it Ctrl-GFP, Tax-GFP, and HBZ-GFP psuedovirus particles were collected from 293T supernatants and applied to HeLa cells for determination of viral titers. Some supernatants were spun down at 25K x g (blue) or precipitated with PEG-it solution (red). Initial viral titers for Tax-GFP and HBZ-GFP ranged from 5x10^5-1 x 10^6/mL, whereas Ctrl-GFP titers were usually 6 x10^6/mL in unconcentrated fractions. Ultracentrifugation or PEG-it concentration brought titers up to 10^9-10^{10} particles/mL

As can be seen in **Fig. 11**, both ultracentrifugation (ultra conc) and PEG-it concentration increased viral titers by up to 4 logs.

ND PBMCs can be transduced upon activation

Several working conditions were used for transduction of primary cells. As mentioned previously, transduction of primary T cells is difficult, especially if they are unstimulated (Bilal et al., 2015). As such, transduction of primary PBMCs with prior cytokine incubation and CD3-activated PBMCs was assessed for cell viability post-transduction, expression of GFP, and expression of CD3, CD4, CD8, and CD25. Either plate-bound CD3 or suspension CD3 was used to activate whole PBMCs for 48h. After stimulation with 50ng of CD3 in suspension, PBMCs were transduced with 500μL of ctrl-GFP or tax-GFP viral supernatant (unconcentrated). After transduction, cells were maintained in 300IU/mL recombinant human (rh) IL-2 for 1 week to allow for recovery. In a representative experiment, cell viability was approximately 50% as measured by FSC vs SSC (**Fig. 12A,** 47.6%) or live/dead stain (**Fig. 12B,** 51.2%**)** for ND PBMCs transduced with ctrl-GFP pseudovirus. Pre-activation with CD3 in suspension followed by transduction with the ctrl pseudovirus resulted in a 12.4% $CD4^+CD25^+$ population (**Fig. 12 C,** 29.5% of total $CD4^+$ T cell population expressed CD25).

As can be seen in **Fig. 12D**, 34.8% (63. 6% of total $CD4^+$ T cells) express CD4 and GFP after maintenance in 300IU/mL rh IL-2 for 7 days. This corresponds to 43.8% of $CD4^+CD25^+$ T cells expressing ctrl-GFP (**Fig. 12E**). In comparison, transduction with the tax-GFP pseudovirus was far less efficient. While tax-GFP transduction resulted in similar levels of cell viability, as measured by FSC vs. SSC (**Fig. 12F,** 56.7%) or live/dead stain (**Fig. 12G**, 59.7%), the levels of activation after transduction with HTLV-1 Tax-GFP were increased to 19.9% $CD4^+CD25^+$T cells (40.9% of total $CD4^+$ T cell population expressed CD25). While this might suggest increased activation resulting

from Tax-transduction, the levels of GFP expression were reduced to only 1.02% of $CD4^+$ (**Fig. 12I) (**2.1% of total $CD4^+$**)** and 2.24% of $CD4^+CD25^+$ T cells (**Fig 12J)** express Tax-GFP.

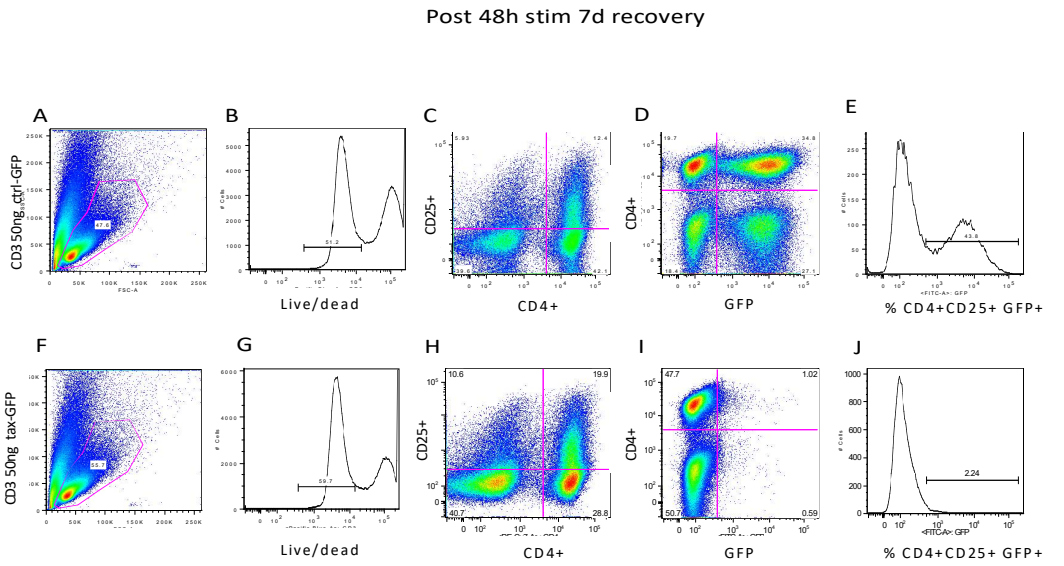

Figure 12: Flow cytometry demonstrated transduction of CD3 suspension activated ND PBMCs
(A-E) Flow cytometry results of ctrl-GFP transduced ND PBMCs after activation with 50ng of CD3 in suspension for 48h (F-J) Flow cytometry results of tax-GFP transduced ND PBMCs after activation with 50ng of CD3 in suspension for 48h. (A) FSC vs SSC of ctrl-GFP transduced PBMC(B) Live/Dead cell plot of ctrl-GFP transduced PBMCs (C) CD4 vs CD25 plot of ctrl-GFP transduced PBMCs (D) CD4 vs GFP plot of ctrl-GFP transduced PBMCs (E) $CD4^+CD25^+$T cells express ctrl-GFP transgene (F) Cell viability following tax-GFP transduction shown with FSC vs. SSC (G) Cell viability following tax-GFP transduction shown with live/dead stain (H) CD4 vs CD25 plot of tax-GFP transduced PBMCs (I) CD4 vs GFP plot of ctrl-GFP transduced PBMCs (J) $CD4^+CD25^+$T cells express tax-GFP transgene

While activation with CD3 in suspension may be sufficient for transduction with the ctrl pseudovirus, it was suggested that this method may be inefficient for expression of the HTLV-1 transgenes. Therefore, $2x10^6$ PBMC were added to 2.5µg of plate-bound CD3 and stimulated for 48h in the presence of 100IU/mL rhIL-2. As shown in **Fig 13A**,

pre-activation with plate bound CD3 followed by transduction with ctrl-GFP resulted in 66.8% viability by FSC vs. SSC as compared to 47.6% (**Fig. 12A**). Viability as demonstrated by a live/dead stain was 67.6% using plate bound CD3, an improvement over viability with pre-activation with anti-CD3 in suspension (**Fig. 12B**). The $CD4^+CD25^+$ T cell population following ctrl-GFP transduction was 16.9% (**Fig. 13C**) (26.2% of the total $CD4^+$ T cell population express CD25), which demonstrates a slightly increased activated $CD4^+$ population compared to pre-activation with anti-CD3 in suspension. Transduction efficiency is slightly increased when using plate-bound CD3 pre-activation as compared to anti-CD3 in suspension which is demonstrated in **Fig. 13D**, where 47.5% are $CD4^+GFP^+$ (68.8% of total $CD4^+$ T cells) and 52.2% of $CD4^+CD25^+$ T cells are GFP^+ (**Fig. 13E**) after transduction with 500μL of ctrl-GFP viral supernatant (~3 x 10^6 viral particles). This increased to 73.5% of total $CD4^+$ T cells when 1mL of ctrl-viral supernatant was used (~ $6x10^6$ viral particles, data not shown), indicating that a higher multiplicity of infection (MOI) used for transduction of $5x10^5$ PBMCs may improve transduction efficiency further. Transduction with Tax-GFP after plate bound pre-activation also demonstrated increased viability in both the FSC vs. SSC plot (**Fig 13F, 75.2%)** and live/dead plot (**Fig. 13G,** 80.0%**),** accompanied by a similar increase in the $CD4^+CD25^+$ T cell population (**Fig. 13H**, 36.5%) (66.5% of total $CD4^+$T cells express CD25). However, it should be noted that while the brightness and definition of the $CD4^+GFP^+$ population (**Fig 13I**, 1.17%) (2.1% of total $CD4^+$ T cell population) following activation with plate bound anti-CD3 compared to suspension (**Fig. 12I**), the efficiency in GFP expression in $CD4^+CD25^+$ T cells did not change with alteration of stimulation method (**Fig. 13J,** 1.61% vs **Fig.** 12J, 2.2%). There was a significant improvement in

live cells when stimulated with plate bound CD3 (59.7% vs. 80%), which may indicate that this condition is more tolerable to thawed PBMCs than CD3 in suspension.

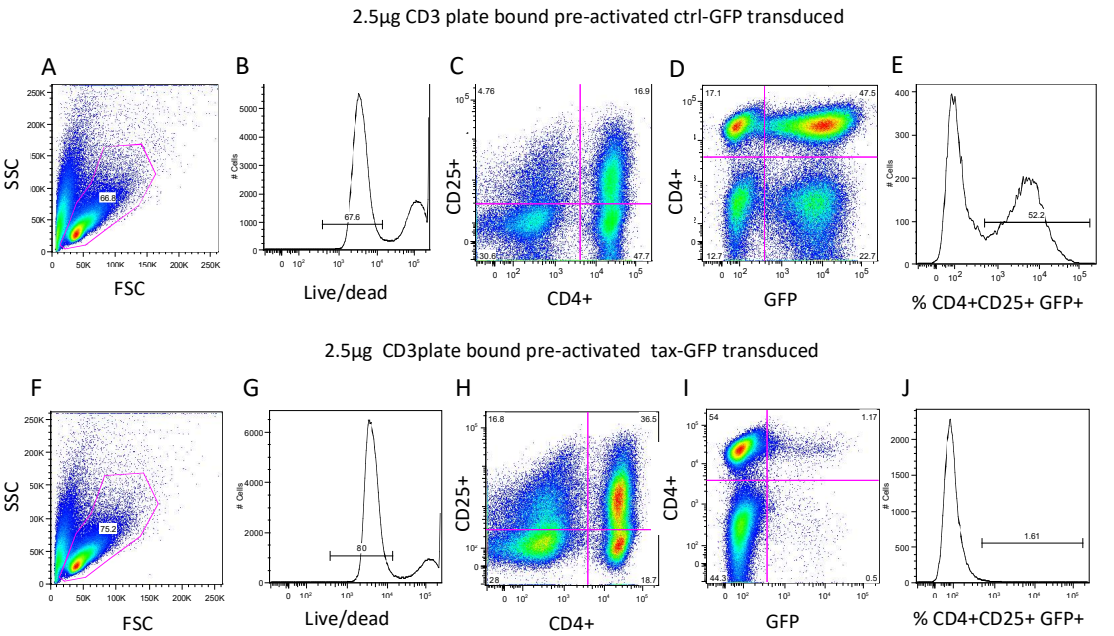

Figure 13: Flow cytometry demonstrated transduction efficiency of ctrl-GFP and Tax-GFP pseudovirus in CD3-plate bound stimulated ND PBMCs (A-E) Flow cytometry results of ctrl-GFP transduced ND PBMCs after activation with 2.5µg of plate bound CD3 for 48h (F-J) Flow cytometry results of Tax-GFP transduced ND PBMCs after activation with 2.5µg of plate bound CD3 for 48h. (A) FSC vs SSC (B) Live/Dead cell plot of transduced cells (C) $CD4^+CD25^+$ plot of live ctrl-GFP transduced cells (D) CD4 vs. GFP plot of live ctrl-GFP transduced cells (F) Cell viability following Tax-GFP transduction shown with FSC vs. SSC (G) Cell viability following Tax-GFP transduction shown with live/dead stain (H) $CD4^+CD25^+$ plot of live Tax-GFP transduced cells (I) CD4 vs. GFP plot of live tax-GFP transduced cells (J) $CD4^+CD25^+$T cells express Tax-GFP transgene

However, there was no observable improvement in the efficiency of tax-GFP transduction. This may suggest that GFP expression in tax-GFP transduced cultures is not sustainable in a 7d culture although in Cheng et al, Tax-GFP clones were maintained for up to 2 weeks (Ren et al., 2015).

Reduced incubation period post-transduction increases Tax-GFP expression

Given that CD3 stimulation with plate-bound antibody or antibody in suspension appeared to be similarly effective in priming PBMCs for transduction, we continued with CD3 stimulation using antibody in suspension for future experiments. It was suggested that Tax-GFP may be toxic compared to ctrl-GFP, and therefore while increased time in culture may allow the cells to recover from transduction, it may also allow a selective disadvantage to the Tax-GFP$^+$ cells (ie. they grow slower or die off). The Tax-GFP and HBZ-GFP pseudoviruses do not appear to be defective as they were shown to transduce cell lines at high levels, therefore the experimental conditions were further adjusted. ND PBMCs were activated for 48h with 50ng/mL CD3 and 300IU/mL rhIL-2 followed by transduction with 1mL-3mL of viral supernatant applied to $5x10^5$ cells for 2h at 1000 x g at 32^0C. Cell surface markers, cell viability and GFP expression was assessed 3d post transduction after recovery in 20%FBS CRPMI supplemented with 300IU/mL rhIL-2.

As can be seen in **Fig. 14 A, B**, cell recovery is not complete 3d post-transduction of ctrl-GFP. Cell viability is <40% as assessed by FSC vs. SSC (**Fig 14A,** 32.8%**)** live/dead stain (**Fig. 14B,** 39.1%). Interestingly, the levels of activation are increased 3d post-transduction, demonstrated by a larger CD4$^+$CD25$^+$ T cell population (**Fig. 14C**, 33.2% or 65.3% of CD4$^+$ population are CD4$^+$CD25$^+$). Shorter culture post-transduction did not overly reduce transduction efficiency of the ctrl-GFP pseudovirus (**Fig. 14D**, 29% CD4$^+$ GFP$^+$ or 52.1% of CD4$^+$ T cells are CD4$^+$GFP$^+$). As shown in **Fig. 14E,** 47.8% of CD4$^+$CD25$^+$ T cells express GFP. Similar to ctrl-GFP, Tax-GFP transduced PBMCs have not quite recovered cell viability as shown by FSC vs. SSC (**Fig, 14F,** 30.7%) and live/dead stain (**Fig. 14G,** 35.9%). Increased CD4$^+$ T cell activation was also noted (**Fig.**

14H, 39.6% $CD4^+CD25^+$ or 84% of $CD4^+$ T cells are $CD4^+CD25^+$).

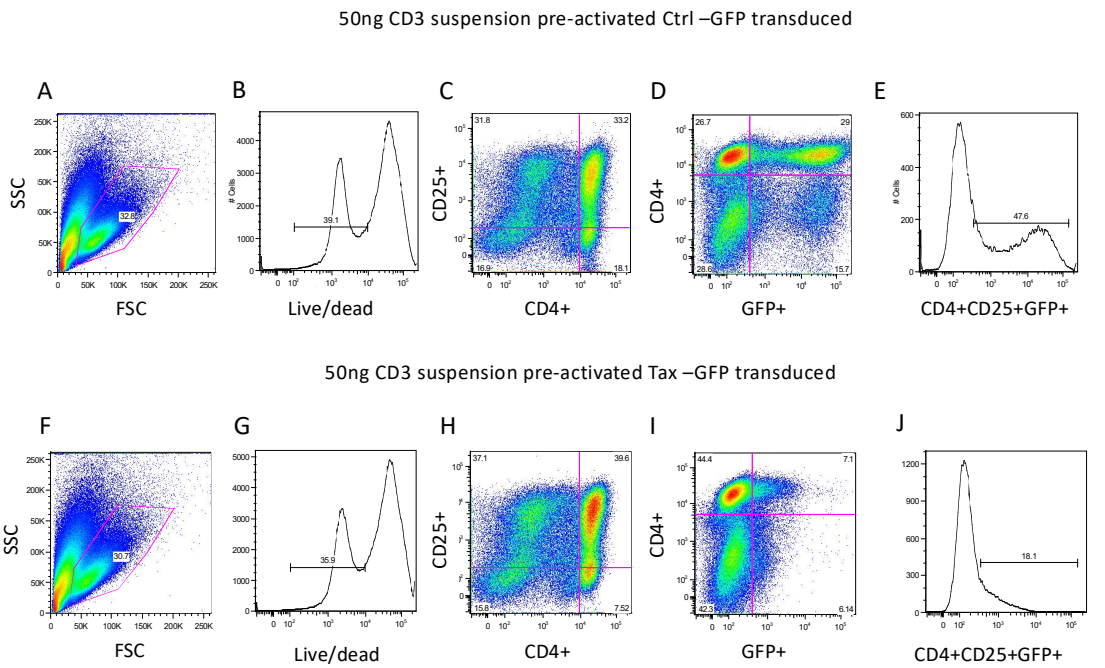

Figure 14: Transduction efficiency of ctrl-GFP and Tax-GFP after short-term culture (3d)
(A) FSC vs SSC of ctrl-GFP transduced PBMCs (B) Live/Dead cell plot of ctrl-GFP transduced cells (C) CD4 vs CD25 of ctrl-GFP transduced PBMCs demonstrating activation (D) CD4 vs. GFP of live ctrl-GFP transduced PBMCs demonstrating transgene expression (E) $CD4^+CD25^+$T cells express ctrl-GFP transgene (F) FSC vs. SSC of Tax-GFP transduced PBMCs (G) Live/dead stain following Tax-GFP transduction demonstrating cell viability (H) CD4 vs CD25 of Tax-GFP transduced PBMCs demonstrating activation (I) CD4 vs. GFP of live Tax-GFP transduced PBMCs demonstrating transgene expression (J) $CD4^+CD25^+$T cells express Tax-GFP transgene

However, the Tax-GFP^+ cells have increased in the $CD4^+$ T cell population (**Fig. 14I,** 7.1% or 13.8% of $CD4^+$ are $CD4^+GFP^+$ vs **Fig. 12I,** 1.02% or 2.1% of $CD4^+$are $CD4^+GFP^+$ at 7d). In the $CD4^+CD25^+$ T cell population 18.1% express GFP at 3d post-transduction (**Fig. 14J**) vs. 1.81% at 7d (**Fig. 12J**). This data suggests that Tax-GFP^+ T cells are not long-lived after transduction and should be assessed earlier, despite

incomplete recovery of cell-viability. Due to these constraints, FoxP3 TSDR demethylation was assessed on transduced PBMCs after 2-3d in culture.

Variable transduction efficiencies between different pseudovirus transgenes

As can be seen in **Fig. 15 (left panel)**, transduction efficiency between different pseudoviruses was still unequal. While differences in TSDR demethylation could be observed after transduction, especially in Tax-GFP transduced PBMCs, the pattern also appeared to mirror the transduction efficiency. For example, HBZ-GFP did not transduce well and shows comparable TSDR demethylation to PBMCs transduced with a pseudovirus that does not carry a transgene or GFP (blank) (**Fig. 15 (right panel))**. Contrastingly, HTLV-1 Tax transduced at higher efficiency at shown by a larger GFP^+ % in $CD4^+CD25^+$ T cells and had a low TSDR demethylation as compared to PBMC transduced by blank pseudovirus. Ctrl pseudovirus and ctrl pseudovirus concentrated with PEG-it (ctrl peg) transduced 25% and 15% of $CD4^+CD25^+$ T cells but yielded similar levels of TSDR demethylation. Additionally, as was noted in **Fig. 5C**, the TSDR demethylation of PBMCs is much lower than what is found in purified $CD4^+CD25^+$ T cells. This is likely a dilutional effect as Tregs comprise about 2% of circulating PBMCs and up to 10% of $CD4^+$ T cells (Baecher-Allan et al., 2001).

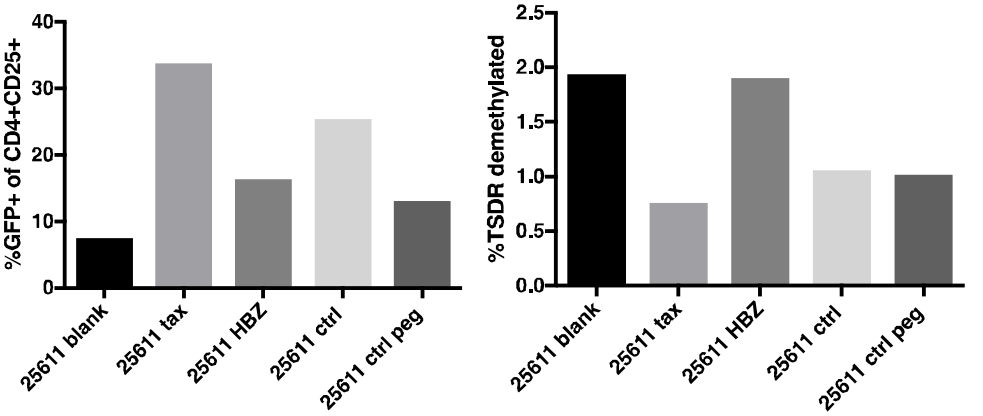

Figure 15: Transduction efficiency (%GFP) and %TSDR demethylation in transduced ND (25611) PBMCs. Blank corresponds to empty pseudovirus particles. Tax, HBZ and ctrl denote corresponding GFP expressing pseudovirus. Peg refers to PEG-it concentration.

Transduction of $CD4^+$ T cells results in reduced TSDR demethylation

Given that PBMCs do not yield a high percentage of FoxP3 TSDR demethylation, resulting changes due to expression of HTLV-1 genes will be difficult to observe. Therefore, we aimed to transduce $CD4^+CD25^+$ T cells, but started with $CD4^+$ T cells. Some protocols for lentiviral transduction of T cells suggest activation of whole PBMCs followed by sorting and then transduction of T cells while others call for activation of sorted T cells followed by transduction. We compared both strategies for T cell transduction efficiency and where possible, resulting TSDR demethylation status.

$CD4^+$ T cells were isolated with either MACS bead isolation or FACS sorting. Initially, $5x10^5$ cells were stimulated in a 96-well plate with 5µg/mL of plate-bound CD3 and 1µg/mL of CD28 for 24h followed by transduction of ctrl-GFP (20µL), Tax-GFP (50µL), and HBZ-GFP (50µL) ultraconcentrated pseudoviruses. Of note, while ctrl-GFP also transduced approximately 19.4% of activated $CD4^+$ T cells as shown by $\%GFP^+$

cells in the small gate (**Fig. 16D)**, no corresponding Tax (Lt4) staining was detected (**Fig. 16E).**

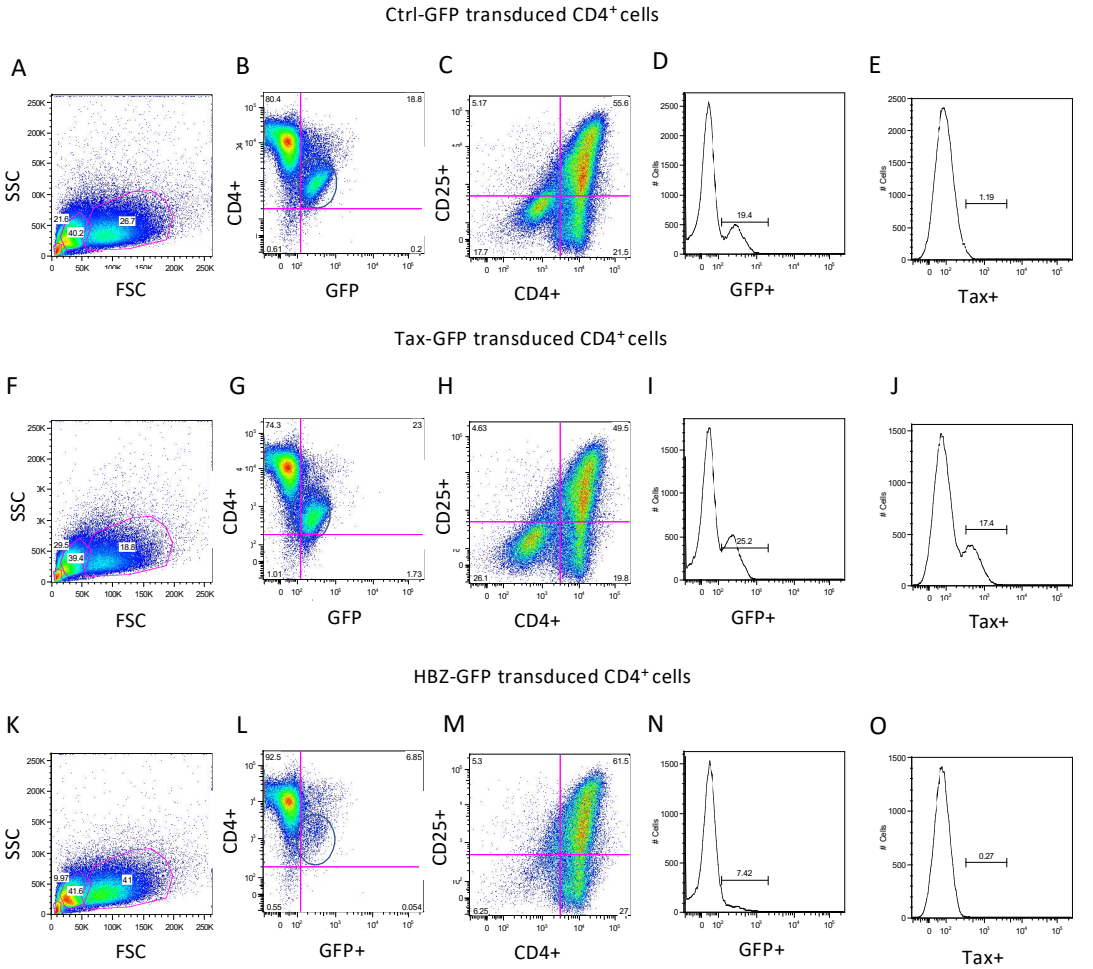

Figure 16: Transduced activated CD4$^+$ T cells. (A) FSC vs. SSC of ctrl-GFP transduced CD4$^+$ T cells (B)CD4 vs. GFP of ctrl-GFP transduced CD4$^+$ T cells (C) CD4 vs. CD25 of ctrl-GFP transduced CD4$^+$ T cells (D) GFP histogram of CD4$^+$CD25$^+$ in small gate of ctrl-GFP transduced CD4$^+$ T cells (E) Tax (Lt4) of CD4$^+$CD25$^+$ demonstrating Tax staining in ctrl-GFP transduced CD4$^+$ T cells in small gate (F) FSC vs. SSC of Tax-GFP transduced CD4$^+$ T cells (G)CD4 vs. GFP of Tax-GFP transduced CD4$^+$ T cells (H) CD4 vs. CD25 of Tax-GFP transduced CD4$^+$ T cells (I) GFP histogram of CD4$^+$CD25$^+$ in small gate of Tax-GFP transduced CD4$^+$ T cells (J) Tax (Lt4) of CD4$^+$CD25$^+$ demonstrating Tax staining in tax-GFP transduced CD4$^+$ T cells in small gate (K) FSC vs. SSC of ctrl-GFP transduced CD4$^+$ T cells (L) CD4 vs. GFP of HBZ-GFP transduced CD4$^+$ T cells (M) CD4 vs. CD25 of HBZ-GFP transduced CD4$^+$ T cells (N) GFP histogram of CD4$^+$CD25$^+$ in small gate of HBZ-GFP transduced CD4$^+$ T cells (O) Tax (Lt4) of CD4$^+$CD25$^+$ demonstrating Tax staining in HBZ-GFP transduced CD4$^+$ T cells in

As can be seen in **Fig. 16I**, the Tax-GFP pseudovirus is transduced at an efficiency of about 25% in activated $CD4^+$ T cells. As expected, the GFP fluorescence expressed by $CD4^+CD25^+Tax^+$ corresponds to wildtype Tax protein as shown by staining with the Tax (Lt4) antibody at nearly equivalent expression levels (17.4%). HBZ-GFP transduced at much lower efficiencies (**Fig. 16C**, <10% GFP^+), which was expected due to the lower viral titer of an earlier viral stock. HBZ-GFP transduced T cells did not stain for Tax (Lt4) (**Fig. 16C, column 5**). One interesting observation is that the GFP expressing cells in all of the transductions appear to have diminished CD4 staining (**Fig. 16, column 2**). This could be a consequence of successful lentiviral transduction. It is well known that infection with HIV causes subsequent downregulation of CD4, one of the receptors for the virus (Lundquist et al., 2002). It is unclear from the literature if this is also observed after transduction with lentiviral pseudoparticles, since they lack HIV Nef.

While $CD4^+$ T cells have higher levels of TSDR demethylation in FoxP3 than PBMCs, it typically is around 10% (**Fig. 5A**). We thought that transduction of $CD4^+$ T cells would better demonstrate that transduction with HTLV-1 Tax, and or HBZ, alters the epigenetic state of the FoxP3 TSDR. Initial results from one ND (23296) showed definite reductions in TSDR demsethylation in both the Tax and HBZ (HBZ naught) transduced $CD4^+$ T cells as compared to cell that were not transduced (no xduction where cells were only subjected to polybrene and spinoculation) (**Fig. 17**). Unfortunately, TSDR demethylation could not be calculated for blank pseudovirus transduced and ctrl-GFP (ctrl) pseudovirus transduced ND 23296 $CD4^+$ T cells.

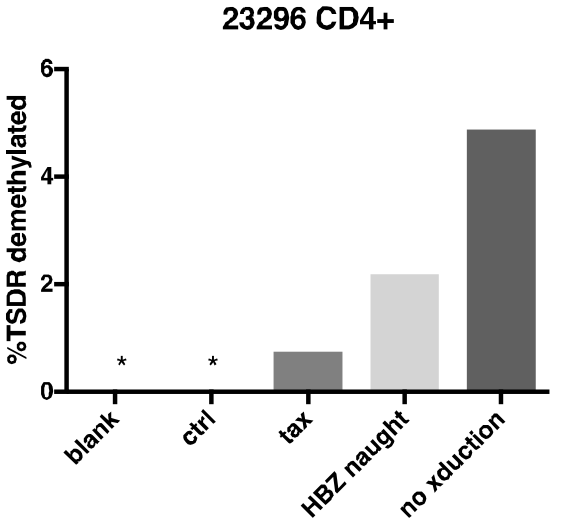

Figure 17: **Methylation of FoxP3 TSDR of transduced ND CD4$^+$ T cells. Cells were transduced with blank (no transgene or GFP) pseudovirus, ctrl (GFP only), Tax (Tax-GFP), HBZ naught (HBZ-GFP), or no xduction (addition of polybrene only).**

Given these results, it appears that transduction of HTLV-1 transgenes can result in reduced demethylation of the FoxP3 TSDR. This would indicate that both Tax and HBZ could alter Treg suppression capacity through this mechanism. After showing that transduction of sorted CD4$^+$ T cells requires CD3/CD28 and a slightly longer period of activation as compared with whole PBMCs which can be activated for 24-48h with anti-CD3, future experiments will focus on the activation of CD4$^+$CD25$^+$ T cells followed by HTLV-1 viral gene transductions to assess the TSDR methylation state.

Although we have only investigated HTLV-1, altered TSDR demethylation by viral genes could be a more common phenomenon. More specifically, viral infection may alter the methylation of other host genes. The FoxP3 TSDR is under investigation due to the close correlation of its epigenetic changes and Treg function as well as observed correlations to HTLV-1 gene expression. It would therefore be of interest to assess the changes in TSDR methylation in other virally-infected Tregs. For example, a common ubiquitous herpesvirus, HHV-6, has also been reported to infect Tregs (Li et al., 2008).

Methods:

Storage of PBMCs and cell lines:

PBMCs were isolated by Ficoll-Hypaque (Lonza, Walkersville, MD) centrifugation, and were cryopreserved in liquid nitrogen prior to use. All NDs were noted to be healthy and HTLV-1 negative. HTLV-1 infected cell lines TL-Om1, HUT102, MT2 and C8166 and the uninfected cell lined Jurkat and MOLT3 were also cryopreserved prior to use.

Maintenance of cell lines:

For maintenance in cell culture, cell lines were slowly thawed with the addition of C-RPMI (RPMI 1640 supplemented with 10% FBS, 100U/mL penicillin, 100μg/ml streptomycin sulfate, and 2mM L-glutamine) and maintained in this media with weekly splitting.

PBMC culture for Tax upregulation:

PBMC were cultured at 5 x 10^6 cells/ well in a 6 well plate for 18-24h for HTLV-1 Tax expression. 6 HAM/TSP and 3 ND PBMCs were incubated at 37ºC in RPMI 10%FBS for 24h to allow for peak expression of HTLV-1 Tax (Rende et al., 2011). Cells were then stained with CD3-Pacific Blue, CD4-PECy7, CD25-PE, CD8-PerCp5.5 (BD Biosciences, San Jose, CA) for cell surface staining. FoxP3-APC (eBioscience, San Diego, CA), and Lt-4-Alexa Flour® 488 (kindly provided by Dr. Tanaka) were added for intracellular staining according to the manufacturer's protocol. Cells were also stained with monoclonal isotype control Abs as negative controls and analyzed on LSRII for staining intensity. PBMCs were then isolated and DNA extraction was performed using DNEasy

Blood & Tissue Kit (Qiagen, Germantown, MD) and then processed with bisulfite conversion for analysis of FoxP3 TSDR demethylation state.

Flow cytometry

For analysis of $CD4^+$ T cell population, cells were stained with 1μL each of CD3-APC-Cy7, CD4-PE-Cy7, and CD25-PE (BD Bioscience) and then fixed with Fixation Buffer (eBioscience) following their supplied protocol. After washing the cells with 200μL of Fix/perm buffer (eBioscience), 5μL of FoxP3 antibody (236A/E7; eBioscience) was added to cells for the intracellular staining. To account for staining in a 96 well plate, the plate was spun at 1300rpm for 5min after which fix/perm buffer was removed. The cells were then washed twice with 200μL of 1X permiabilization buffer (eBiosciences), after which FoxP3 was added. Monoclonal isotype controls were used for each Ab and set as the negative control. Flow cytometric analysis was performed using a LSRII (BD Biosciences). All data were analyzed using FlowJo software (Tree Star, San Carlos, CA).

DNA Isolation for TSDR methylation assessment

Total DNA was isolated from cell lines or cells obtained from NDs and HAM/TSP patients using the DNEasy Blood and Tissue Kit. All samples were incubated with RNAse at 37C for > 30 min to ensure removal of all RNA (max of 1h). Briefly, after cells were spun at 1300rpm for 5 min, the cell pellet was resuspended in 200μL of PBS and 20μL of Proteinase K. 4μL of RNAse A was added and incubated at 37ºC for >30min (maximum of 1h) for the complete removal of DNA. Samples were then processed

according to the Qiagen protocol for DNA isolation from the DNEasy Blood & Tissue kit.

Bisulfite Conversion

Initial bisulfite conversions for TSDR analysis prior to 3/2017 was performed with a minimum of 1μg of DNA, due to harshness of the reaction. Bisulfite conversions were completed using the Cells-to-CpG kit (Thermo Fisher Scientific, Waltham, MA) following initial digestion with EcoRI and PCR cleanup. Subsequent bisulfite conversions on TSDR transfected cell lines, transduced TL-Om1 cells, and transduced ND PBMCs were performed on a maximum of 1μg (250ng-1μg) using the EZ DNA Methylation-Lightning Kit (Zymo Research, Irvine, CA) following EcoRI digestion and PCR cleanup.

Quantitative PCR

Bisulfite converted DNA was amplified in two separate reactions on a ViiA7 thermocycler (Thermo Fisher Scientific). One reaction amplified demethylated FoxP3 and the other amplified methylated FoxP3 using primers and probes directed against FoxP3 intron 1 (Stockis et al., 2009). The primers and probes are as follows: umethylated FoxP3 F (sense) TCTACCCTCTTCTCTTCCTCCA, unmethylated FoxP3 R (antisense) GATTTTTTTGTTATTGATGTTATGGT, unmethylated FoxP3 probe FAM AAACCCAACACATCCAACCA MGBNFQ, methylated FoxP3 F (sense) CTCTTCTCTTCCTCCGTAATATCG, methylated FoxP3 R (antisense) GTTATTGACGTTATGGCGGTC, methylated FoxP3 probe FAM

AAACCCGACGCATCCGAC MGBNFQ. The reactions occurred in a total volume of 20µL with 5µL of bisulfite converted DNA (~125ng total) in triplicate. The thermocycler conditions were as follows: 50ºC for 2 min, 95ºC for 10 min, 20 cycles at 95ºC for 15s (denaturation) and 60ºC for 1 min (annealing and extension), and 25ºC for 2 min. The level of demethylation was calculated as published previously (Stockis et al., 2009) and values from female patients were doubled to account for the 2X chromosomes: % unmethylated=$2^{\Delta Ct}/(1+2^{\Delta Ct})$, where ΔCt=(Ct with methylated primers)-(Ct with unmethylated primers)

tax and _hbz_ mRNA quantification

Total RNA was extracted from PBMCs using RNeasy Mini Kit (Qiagen) according to the manufacturer's instructions. 85 ng of total RNA was converted into cDNA and amplified in a one-step reaction using TaqMan® RNA-to-Ct TM 1-Step Kit (Thermo Fisher Scientific) according to the manufacturer's instructions. *tax* primer and probe sequences (Oh et al 2006) (Oh et al., 2005) 5' -GGCCCTTCTCCAGGACAGA-3' and 5' -GCTGATCATGGCTGGGTTGT-3' , and the probe was 5' -FAM-ACTTCATGCATCAGCTCTCCACTGTGGATTAMRA-3' or *hbz* primer and probe (Enose-Akahata et al., 2013) forward 5′-AGAACGCGACTCAACCGG-3′, (reverse) 5′-TGACACAGGCAAGCATCGA-3′ and (probe) 5′-TGGATGGCGGCCTCAGGGCT-3′. were combined with HPRT primer and probe (TaqMan Gene Expression assay Hs02800695_m1, ThermoFisher Scientific) and added to mRNA samples and amplified on a Viia7 (Thermo Fisher Scientific) thermocycler as follows: 48°C for 15 min, 95°C for 10min, and 45 cycles at 95°C for 15 s and 60°C for 1 min. MT2 was used as a calibrator

sample and the level of *tax* and *HBZ* mRNA expression was then calculated using the comparative CT method on ViiA 7 software.

Proviral load

Proviral load was determined from DNA using the same *tax* primers and probes mentioned previously (Nagai et al 2001) (Oh et al., 2005) and amplified as a standard curve against TARL2 DNA standards. Tax primers are as follows: 5' -ACAAAGTTAACCATGCTTATTATCAGC-3' positioned at nt 7276–7302 and 50 -ACACGTAGACTGGGTATCCGAA-30 positioned at nt 7355–7334 in the pX region of HTLV-1 as detailed in the Genbank database. The TaqMan fluorescent probe was 5' -TTCCCAGGGTTTGGACAGAGTCTTCT-3' positioned at nt 7307–7332 for HTLV-I pX region. The primer set for β-actin was 5' -CACACTGTGCCCATCTACGA-3' positioned at nt 2146–2165 and 5' -CTCAGTGAGGATCTTCATGAGGTAGT-3' positioned at nt 2250–2225 while the probe was 5' -ATGCCCTCCCCCATGCCATCCTGCGT-3' positioned at nt 2171–2196. DNA standards were extracted from HTLV-I–negative PBMC for β-actin and TARL-2 [25] for pX to make a standard curve. All samples were performed in triplicate. Relative proviral load was determined against *actin* quantity in the samples and run on a ViiA7 thermocycler as noted for quantitative PCR. The thermal cycler conditions were as follows: 50º C for 2 min (for the activation of uracil-N-glycosylase [UNG]), 95º C for 10 min (for the inactivation of UNG and the activation of Taq polymerase), and 45 cycles at 95º C for 15 s (denaturation) and 60º C for 1 min (annealing and extension). The amount

of HTLV-I proviral DNA was calculated as copy number of HTLV-I (pX) per 100 number PBMC = [(copy number of pX)/ (copy number of β-actin/2)] x 100.

$CD4^+CD25^+$ T cell enrichment

For TSDR analysis, PBMCs were thawed and then enriched for $CD4^+$ T cells using $CD4^+CD25^+$ Treg isolation kit (Miltenyi Biotec, Bergisch Gladback, Germany). $CD4^+$ T cells were then labeled with CD25-biotin beads and separated on a column for isolation of $CD4^+CD25^+$ and $CD4^+CD25^-$ T cells. Purity was assessed by flow cytometry using a CD25- PE antibody (BD Biosciences clone (M-A251). The results for levels of FoxP3 TSDR demethylation were adjusted to the purity of $CD4^+CD25^+$ T cell isolation from each patient (that ranged from 50.7 to 90.6% mean=65.5 in HAM/TSP and 22.7-80.1% mean 53.03 in ND, p=NS)

Suppression Assays

Suppressive function of Tregs in ND and HAM/TSP patients was assessed by inhibitor effects of allogeneic cell proliferation. Briefly, magnetically isolated $CD4^+CD25^+$ T cells from 3 ND and 2 HAM/TSP patients were placed in wells with T_{effs} ($CD4^+CD25^-$) previously integrated with 2.5μM CFSE (Thermo Fisher Scientific, Carlsbad, CA). T_{effs} were added at 2 x 10^4 cells in 96 U-bottom microplates containing varying amounts of irradiated Tregs for final ration of Treg: Teff of 0.25:1 to 1:1, 500ng/mL anti-CD3 HIT3a (BD Biosciences) and 5x10^4 cells of autologous irradiated ND PBMCs (used as feeder cells) in 5 % Human AB serum in RPMI 1640 with 100 U/mL penicillin, 100μg/mL streptomycin sulfate, and 2mM L-glutamine. PBMCs and Tregs were gamma irradiated

to 3000 rad using a Cs irradiation source. After culture for 3 days, cells were stained with CD3-APC, CD4- Alexa700, and CD-25 PE (BD Biosciences) and then analyzed on an LSRII for proliferation. Cells stained with monoclonal isotype antibodies were used as negative controls.

Lentiviral transgene construction

Tax1-GFP cloned in pLCEF8, a modified vector of pLL3.7 in which human elongation factor α (hEF1α) has replaced the U6 promoter, was obtained from Dr. Hua Cheng (UMD). To create a control plasmid lacking the transgene but still expressing GFP, Tax1 was excised from pLCEF8 by restriction digest using BamH1 and EcoRI. Digested plasmids were run in 1.2% agarose gel, cut, and purified with the Qiagen Gel Exraction kit. The cut fragment was blunted following the Quick Blunting kit protocol (New England Biolabs, Ipswich, MA) and re-run on an agarose gel to verify proper sizing. Ligation occurred at 14ºC O/N with T4 ligase (Thermo Fisher Scientific). Tax1 excision from religated control (ctrl-GFP) plasmid was confirmed with MacVector analysis of Genewiz sequencing. Ctrl-GFP was transformed into DH5α e.coli (Thermo Fisher Scientific) and later grown in standard LB broth at 37ºC in ampicillin (50μg/mL). For insertion of HBZ into pCEF8, Tax-1 was excised with EcoRI and BamHI as detailed above. In addition, PCR primers were designed to add EcoRI and BamHI restriction sites to the tail of HBZ cloned out of HBZ-AU1 plasmid (luciferase vector): HBZ pLCEF8F 5' GAGGAATTCATGGCGGCCTCAGGGCTGTTTCGAT3', HBZ pLCEF8 5'CTCGGATCCTTGCAACCACATCGCCTCCAG 3'. HBZ with new restriction sites was amplified from HBZ-AU1 plasmid using Platinum PCR supermix (Thermo Fisher

Scientific) following the following PCR protocol: 94ºC for 2' for 1 cycle, followed by 94ºC for 30", 55ºC for 30", and 68ºC for 1 min for 30 cycles, 68ºC for 7' for 1 cycle, and hold at 4º C. The HBZ PCR product was run on a 0.8%Agarose gel and subsequently excised and gel purified following the Qiagen Gel Purification kit protocol. This gel product was double digested with EcoRI and BamHI and run on a 0.8%Agarose gel with the double digested Tax1-GFP plasmid described above. Both were excised, gel purified, and then ligated with T4 ligase at a 3:1 vector: insert molar ratio (pLCEF8 ~10kb, HBZ ~600bp): 4µL 5X ligation buffer, 54.9ng empty pLCEF8, 100.5ng HBZ, 2µL T4 ligase. Ligation occurred at 14ºC water bath O/N. HBZ insertion was confirmed after EcoRI/ BamHI digestion and visualization of a HBZ fragment on gel. Resulting HBZ-GFP plasmid was transformed in DH5α e. coli and grown in standard LB with ampicillin (50µg/mL).

Purification of lentiviral plasmids

Tax-GFP, HBZ-GFP, and Ctrl-GFP plasmids were amplified in 150-250mL of LB with ampicillin (50µg/mL) at 37ºC with shaking at 225rpm O/N. Bacterial cultures were spun at 600 x g for 15-20min at 4ºC. Qiafilter Plasmid Maxi or Qiagen Plasmid Maxi kits were used for plasmid purification. Pellets were resuspended in 10mL Buffer P1 followed by addition of 10mL of Buffer P2. Lysates were then incubated for 5min at room temperature. Prechilled Buffer P3 was added to lysates after which tubes were inverted 4-6x. Lysates were then either spun at > 20K x g for 30min at 4ºC followed by a respin of supernatant at 20K x g for 15min, or placed in a QIAfilter cartridge for 10min at room temperature. The resulting supernatant was applied to an equilibrated QIAGEN Tip and

allowed to elute via gravity flow, followed by 2 washes with 30mL of Buffer QC. Elution of DNA occurred with 15mL of Buffer QF followed by precipitation of eluate with 10.5mL of Isopropranol. This was then spun at 15K x g for 30 min followed by a wash with 5mL of 70% ethanol and a respin at 15K x g for 10min at 4ºC. Plasmid DNA pellets were rehydrated in 1M Tris-EDTA pH 8.0.

Lentiviral packaging assay

HEK 293T cells were split at 3 x10^6 cells per 10cm plate 24h prior to transfection. Transgene and packaging plasmids were added as follows, illustrated in **Fig. 18**: Ctrl-GFP transfections used 150µg of ctrl-GFP plasmid, 37.5µg of pCMV-VZV-G(VSV-G) plasmid, 57µg of pRSV-Rev (Rev) plasmid, and 57µg of pMDLg-pRRE (Gag-pol) plasmid (all obtained from Addgene) in 14mL OptiMEM with Xtreme Gene HP (3µL per 1µg, Roche, Basel, Switzerland) for 15 10cm plates. Tax-GFP transfections used 120µg of Tax-GFP, 45µg of VSV-G, 120µg of Rev, and 60µg of Gag-pol. Alternatively, plasmid ratios equivalent to those used for ctrl-GFP were also used. HBZ-GFP transfections used 120µg of HBZ-GFP plasmid, 30µg of VSV-G, 30µg of Rev, and 60µg of Gag-pol. Media was changed 24h after transfection and replaced with CRPMI supplemented with 5% FBS, 1mM Sodium Butyrate, 100U/mL penicillin, 100µg/ml streptomycin sulfate, and 2mM L-glutamine. Culture supernatants were collected after another 24h and spun at 1300rpm for 10min to remove cells. Cell-free supernatants were then filtered through a 0.45µm filter (EMD Millipore) to exclude non-pseudoviruses. Supernatants were replaced with 5% CRPMI (w/o Sodium butyrate) and collected after

another 24h. This 72h post-transfection supernatant was spun for removal of cell debris, filtered and concentrated with PEG-it (Systems Biosciences (SBI), Palo Alto, CA).

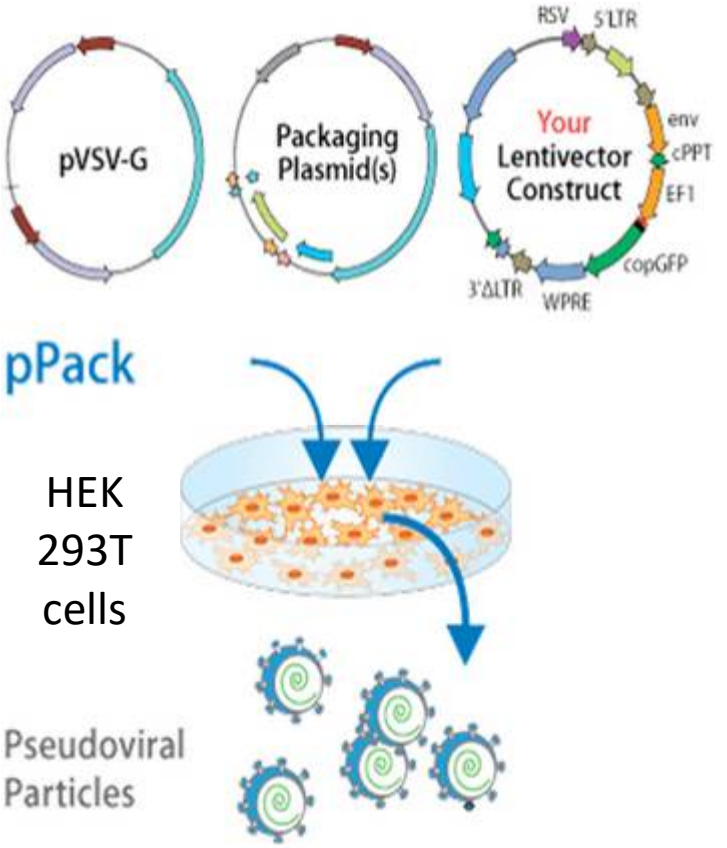

Figure 18: construction of pseudoviral particles (Image taken from SBI webpage https://www.systembio.com/downloads/Manual_LentivectorExpressionSystem_5_070613_web.pdf)

Concentration of pseudoviruses

Pseudoviruses were concentrated from some 293T cell supernatants following filtration. Filtered supernatants were either spun at 25K x g for 1h30min followed by reconstitution in 1-2mL of 5% CRPMI (w/o sodium butyrate). Or filtered supernatants were concentrated with PEG-it solution. Briefly, 5X PEG-it was added to filtered supernatant for final 1X concentration (e.g. 25mL for 100mL supernatant) followed by refrigeration for >12h but no more than 5d as shown in **Fig. 29**. Pegylated viral solutions were then

spun at 1500 x g for 30 min at 4ºC, and respin of supernatant at 1500 x g for 5min. The resulting white pellet was resuspended in 1-2mL of 5% CRPMI (w/o sodium butyrate).

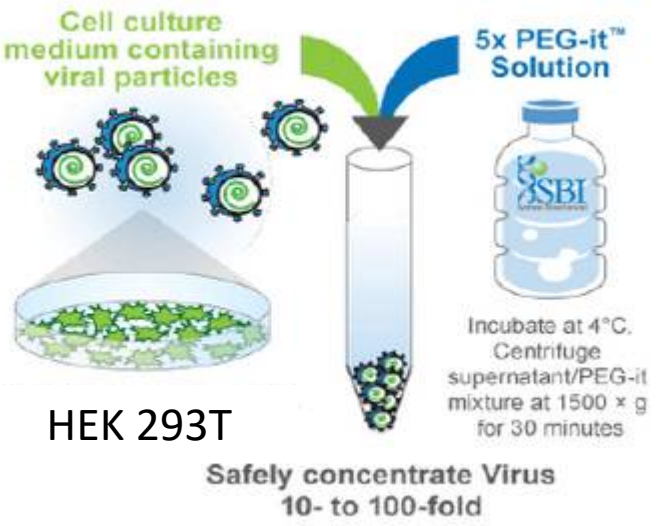

Figure 19: Concentration of pseudovirus particles using PEG-it (from SBI protocol https://www.systembio.com/downloads/Manual_PEG-it_web_021312.pdf)

Transduction of activated PBMCs

$3x10^6$ PBMCs/ well were activated for 48h on 2.5µg/mL pre-coated CD3 (HIT3a, Invitrogen) in a 12 well-plate with supplemented with 100IU/mL hrIL-2 in RPMI or AIM-V, 10% FBS, 100U/mL penicillin, 100µg/ml streptomycin sulfate, and 2mM L-glutamine. $5x10^5$ cells were transduced with 1-3mL of unconcentrated viral supernatant (1-6 x 10^6 viral particles) or 50-125µL of concentrated virus in a 12-well or 24-well plate supplemented with 8µg/mL polybrene (EMD Millipore) and 50IU/mL hrIL-2. Cells were then spun at 1000 x g for 2h at 32ºC and incubated at 37ºC O/N. Media was replaced with RPMI or AIM-V, 20% FBS supplemented with 300IU/mL IL-2, 100U/mL penicillin, 100µg/ml streptomycin sulfate, and 2mM L-glutamine (post-transduction

media). Cells were maintained in this post-transduction media for 2-6d, with the media changed every 3d.

Transduction of cytokine primed PBMCs

1 x 10^6 PMBCs/ well were maintained in CRPMI, 10%FBS, 100U/mL penicillin, 100µg/ml streptomycin sulfate, and 2mM L-glutamine supplemented with 300IU/mL rhIL-2 for 48h. Transduction occurred with ctrl-GFP, Tax-GFP, HBZ-GFP, or blank pseudovirus as stated above. Post-transduction media is described as above but with an addition of 50ng/mL CD3 added in suspension for cell expansion.

Transduction of activated T cells

5 x 10^5 $CD4^+$ or $CD4^+CD25^+$ T cells were activated with 5µg of plate-bound CD3 and 2µg of CD28 for 48h-72h. Transduction with 5mL of viral supes supplemented with 100µL of PEG-it concentrated pseudovirus occurred as described earlier. Cells were placed in post-transduction media supplemented with 50ng/mL CD3 and 300IU/mL hrIL-2. Otherwise, 2 x 10^6 irradiated (5000 rad) PBMCs were added to cultures as feeder cells

Staining of transduced primary cells

For analysis of transduction efficiency in different T cell subsets, PBMCs were stained for surface markers with CD3- Pacific BlueCD4-PE-Cy7, CD8-PerCp-Cy5.5, CD25 PE, CD14 APC-Cy7. Additional Live/Dead-Violet was added for some samples; these were not stained with CD3-Pacific Blue. The protocol for live/dead staining is as follows: After surface staining, cells were washed with 200µL 1X PBS per well in 96-well plate.

Live/dead-Violet was added at 1μL/1mL PBS per $1x10^6$ cells and incubated at 4ºC for 30min. Cells were spun at 1300rpm for 5min and washed with 200μL of PBS. If not intracellular staining was needed, cells were respun and resuspended in 1%paraformaldehyde (PFA), PBS. For intracellular staining, cells were processed immediately following surface staining (w/o Live/Dead stain) or immediately following Live/Dead stain. Intracellular staining protocol is as follows: To account for staining in a 96 well plate, the plate was spun at 1300rpm for 5min after which cell were resuspended in 200μL of Fix/perm buffer (eBioscience). The cells were then washed twice with 200μL of 1X permiabilization buffer (eBiosciences) x2. After washing the cells with, 5μL of FoxP3 antibody (236A/E7; eBioscience) or 1μL of Tax-FITC or 1μL Tax-Alexa 647 was added to cells for the intracellular staining. Cells were resuspended in 200μL of FACS-B (1X PBS, 1%FBS, 0.01% NaN_3) prior to analysis on BD LSR II.

Growth of TSDR plasmid

The FoxP3 TSDR was cloned into pCpGL as described previously (Polansky et al., 2010)and obtained from the authors. This plasmid has a zeocin (ThermoFisher Scientific) resistance element and cannot transform into e. coli containing the Tn5 transposable element (i.e. DH5αF´IQ, SURE, SURE2) as these will confer resistance separate from the plasmid. pCpGL-TSDR was transformed into TOP10 e. coli and placed onto zeocin plates made in low Na LB-Agar :7.5g of BactoAgar (BD) added to 500mL of Lennox Broth (5g/L NaCl, 10g/L Tryptone, 5g/L yeast extract; Quality Biological, Gaitherburg, MD) supplemented with 25μg/mL zeocin. Transformed e. coli were grown

at 32ºC. Large preps for plasmid amplification were grown in Lennox Broth with 25μg/mL zeocin at 32ºC.

Transfection of TSDR with activation

HEK 293T and HeLa cells were spit at 2 x 10^5 cells per well in 6-well plate. 2μg of pCpGL-TSDR was transfected with XtremeGene HP (Roche) 24h after plating. 24h following transfection, media was replaced with DMEM supplemented with 10% FBS, 100U/mL penicillin, 100μg/ml streptomycin sulfate, and 2mM L-glutamine. Each well received 100IU/mL of hrIL-2, 1μg/mL PHA, 10μg/mL IFN-α, 10ng/mL phorbol 12-myristate 13-acetate (PMA) 0.5ng/mL ionomycin, or no additional treatment. Cells with treated with 0.25% trypsin and collected 18h post-stimulation for TSDR analysis as described earlier.

Chapter 3

Functional consequences of HTLV-1 mediated alteration in HAM/TSP patient exosomes

Portions taken from "**Viral Antigens Detectable in CSF Exosomes from Patients with Retrovirus Associated Neurologic Disease: Functional Role of Exosomes"** (Anderson et al 2017 submitted for consideration in Proceedings of the National Academy of Sciences (PNAS))

Introduction

In addition to potential alterations in the methylation state of the TSDR in HAM/TSP Tregs, reduced Treg suppression could be quantified in a number of additional ways. Tregs are typically tested for suppressive function in proliferation assays in which Teffs are assessed for proliferation after the addition of these Tregs (Collison and Vignali, 2011). However, our understanding of how Tregs suppress is expanding such that such assays may not accurately represent how these cells function *in vivo.* While proliferation assays allow for contact dependent suppression through binding of CTLA-4, PD-1 and Nrp-1 to their cognate receptors, Tregs also release cytokines and other molecules that are important in their ability to suppress effector functions. Indeed, Tregs can release granzymes, TGF-β, IL-10, and IL-35 amongst others to inhibit, metabolically disrupt and kill effector cells (Sojka et al., 2008) (Vignali et al., 2008). Included in the released contents of Tregs for suppression is a form of microvesicle called exosomes. In mouse studies, exosomes containing suppressive miRNAs were released from regulatory T cells and contributed greatly to their ability to suppress effector functions (Okoye et al., 2014). Furthermore, disruption of exosome release reduced Treg suppression. Recent studies also suggest that exosome release by Tregs and other immune cells play a strong role in immune suppression (Greening et al., 2015; Whiteside, 2016).

Exosomes

Extracellular vesicles (EVs) are vesicles released by cells into the extracellular space. They comprise both microvesicles (MVs) which originate from the plasma membrane and range from 100nm-1000nm, apoptotic bodies which are the result of

dying cells blebbing and compartmentalizing (1μm-5μm), and exosomes which range from 30nm-100 or 150nm (Helwa et al., 2017; Zeringer et al., 2015). Exosomes are intraluminal vesicles (ILVs) that formed in the endosomal compartment and are released into the extracellular space after fusion of multivesicular bodies (MVBs) with the plasma membrane instead of fusion with lysosomes for degradation (**Fig. 1**) (Bissig and Gruenberg, 2014; Robbins and Morelli, 2014). In a process called "back fusion", ILVs deliver plasma membrane invaginations (through clathrin-mediated and clathrin-independent endocytosis) to the endosomal network, making them (and therefore exosomes) capable of carrying both intracellular and extracellular products (Alenquer and Amorim, 2015; Nour and Modis, 2014).

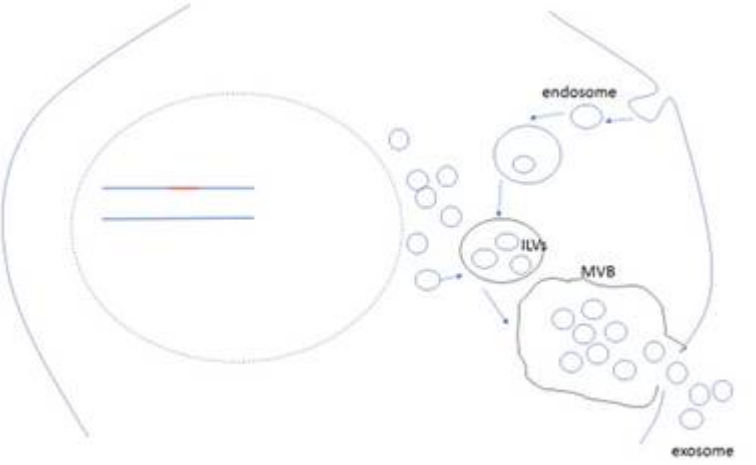

Figure 1: Formation of exosomes from the endosomal compartment. Endosomes form and collect in vesicles, becoming intraluminal vesicles (ILVs). ILVs collect in multivesicular bodies (MVBs) prior to fusing with the plasma membrane and entering the extracellular space, at which point ILVs are called exosomes

The exact intracellular signals that direct ILVs to the plasma membrane for release are still under investigation. Endosomal sorting complexes required for transport (ESCRT) machinery has been studied in its role for directing ubiquitin-labeled proteins

into endosomes for delivery into MVBs, and, as such, ESCRT proteins, like Alix and TSG101, are enriched in exosomes (Matsuo et al., 2004). Lipid raft-associated proteins such as transferrin and caveolins, and other proteins involved in membrane trafficking, like the tetraspanins CD9, CD63, and CD81, which have been shown to bind to ESCRT machinery, are also enriched in exosomes (Meckes and Raab-Traub, 2011; Sampey et al., 2014).

However, ESCRT is not the only method by which exosome formation can occur as there are also ESCRT independent methods by which proteins, lipids, and RNA can enter the endosomal pathway. For example, oligodendrocytes direct exosome formation via the ceramide pathway (Trajkovic et al., 2008), while other cell types rely on oligomerization of tetraspanin complexes (Perez-Hernandez et al., 2013; van Niel et al., 2011). Furthermore, while knockdown of some ESCRT components may abrogate exosome production, it does not completely knock it out (Stuffers et al., 2009; Tamai et al., 2010). Indeed, Rab GTPases, a known family of conserved proteins that regulate vesicular trafficking and membrane fusion events, are also involved in exosome formation as denoted by their high abundance in isolated exosomes (Schorey et al., 2015; Tamai et al., 2010). Several are implicated in the release of exosomes, including Rab11, Rab27, Rab5, Rab35, and Rab7, depending on cell type (Alenquer and Amorim, 2015; Schorey et al., 2015). Rab 27a, in particular, regulates the fusion of MVBs at the plasma membrane to release ILVs (Ostrowski et al., 2010; Schorey et al., 2015). Knockdown of Rab 27a inhibits exosome secretion from tumor cell lines (Ostrowski et al., 2010; Robbins and Morelli, 2014). There are several other Rabs that have also proven essential through a diminution in exosome levels after their knockdown, including Rab 2B, Rab9A, Rab5A, and Rab27b (Robbins and Morelli, 2014). Being GTPases, the activation of each Rab is

dependent on an influx of calcium, as is the case for Rab 11 in the K562 cell line, which may involve SNARE complexes (Colombo et al., 2014; Fader et al., 2009; Savina et al., 2005). Altogether, there are clearly several players within the cell that contribute to the endosomal compartment and, ultimately, to the release of exosomes, further emphasizing the importance of this pathway in normal biology.

As mentioned, the content of exosomes can lead to immunosuppressive effects, as is exemplified by exosomes produced by regulatory T cells which carry immunosuppressive miRNAs (Okoye et al., 2014). In addition to miRNAs, exosomes can carry proteins, mRNAs, enzymes, lipids, and carbohydrates. The cargo of exosomes differs based on the cell releasing them and therefore the contents of exosomes released by regulatory T cells will necessarily differ from the exosomes released by dendritic cells or activated T cells. Almost every cell investigated has been found to be capable of producing exosomes. Indeed, while immunosuppressive exosomes have largely been attributed to the Tregs, other cells can produce exosomes that help reduce inflammation. There are even cells that release exosomes that help promote and maintain regulatory T cells (Mrizak et al., 2015; Pashoutan Sarvar et al., 2016; Wang et al., 2008). Exomes isolated from milk have been shown to promote induction of regulatory T cells in culture and have further been shown to promote nTreg formation in the thymus (Admyre et al., 2007; Melnik et al., 2014). Exosomes have even been found to induce the release of immunosuppressive compounds by Tregs (Schuler et al., 2014).

Given their important role in intracellular communication, methods of exosome isolation have been heavily investigated. Their microscopic size and potential overlap with other microscopic organisms has necessitated careful isolation methods.

Traditionally, serial steps of ultracentrifugation have been favored for the removal of these vesicles from fluid preparations. However, this method is time consuming, volume limiting, wasteful, and can often result in exosomes that are altered/ damaged (Lamparski et al., 2002; Zeringer et al., 2015). As such other technologies have been employed that utilize size, charge, and chemical means for isolation of exosomes. For example, there are certain products, like ExoQuik, which allow for polymer-based exosomal precipitation while other technologies allow for bead-based immunonologic separation of exosomes based on tetraspanin expression. Still other technologies, such as qEV columns, separate exosomes based on chromatography and filtration. Each method has its advantages and disadvantages in the ability to specifically isolate exosomes separately from other microvesicles. Presented here, another method utilizing synthetic hydrogel nanoparticles called Nanotrap particles ® has demonstrated specific isolation of exosomes. The method of isolation requires size and charge exclusion as well as binding to sugars on tetraspanins (unpublished), which may explain the increased specificity of the technology.

Exosomes in viral infection

Considering that the function of released exosomes is dependent on the cargo and receptors on the exosomes, it follows that any alteration in the cell contents of the exosome-producing cell would alter the function of released exosomes. Indeed, infected cells have been shown to vastly alter exosomal contents. Hepatitis C Virus (HCV) infection represents a well-documented case of viral coopting of exosomal communication for the delivery of viral components (Anderson et al., 2014). It is well

known that the HCV viral genome can remain in ILVs and be secreted within exosomes, where they can operate as infectious particles (Longatti et al., 2015; Ramakrishnaiah et al., 2013). By using a transwell assay, Longatti et al. showed that they were able to infect Hu7 cells after exposure to these shed exosomes without the need for direct cell–cell contact. Further, this infection was inhibited by blocking exosomal release with a sphingomyelinase inhibitor. Other pathogens are closely associated with the Rab GTPases and other components of the ESCRT pathway which allows for incorporation of viral components into developing exosomes. For example, HIV Gag has been shown to interact with tetraspanins, especially CD63 and CD81, to aid in virion egress (Madison and Okeoma, 2015). Human herpes virus (HHV)-6 virions have been visualized by electron microscopy in MVBs and egress by the exosomal release pathway (Mori et al., 2008). Herpes viruses, like herpes simplex I (HSV1) and Epstein Barr virus (EBV or HHV-8) each can incorporate cellular components into exosomes that alter the immune response upon release. HSV-1 infection is associated with increased stimulator of IFN genes (STING) protein export in exosomes, which is postulated to increase survival in uninfected cells (Kalamvoki and Roizman, 2014). EBV, in addition to the incorporation of viral LMP1, also promotes the incorporation of galectin-9, which induces apoptosis of EBV-specific T cells upon release (Flanagan et al., 2003; Klibi et al., 2009). Another retrovirus, HIV, was found to package Nef in released exosomes that could render uninfected T cells more susceptible to infection after exposure to these exosomes (Arenaccio et al., 2014; Campbell et al., 2008). Compounded with data indicating the presence of exosomes containing HIV proteins in the serum of HIV patients undergoing highly active antiretroviral therapy (HAART), it becomes apparent that incorporation of

viral components into released exosomes plays a role in HIV infection and may aid the viral persistence (Jaworski et al., 2014b). Indeed, the ability to detect viral antigens in exosomes even in the absence of viral detection has yielded increased interest in exosomal detection in HIV associated neurologic disorders (HAND), as well as in other disorders in which immune responses to a pathogen are apparent but where the pathogen is difficult to detect. Autoimmune diseases are often hypothesized to be initiated by viral infection and this theory appeared to gain support through the sensing of EBV antigens in exosomes isolated from cells in proximity of system lupus erythematous (SLE) cutaneous lesions (Baglio et al., 2016). There are many other examples to be found in the literature demonstrating the vast and varied methods by which viral infection can alter exosome content and thereby alter host immune responses. None thus far has focused on potential consequences to exosomal content and function upon infection of regulatory T cells.

Trafficking of antigens into exosomes

The mechanisms involved in the formation of exosomes and the steps leading to their release into the extracellular space is still under investigation. While the ESCRT pathway has been implicated, there are several ESCRT-independent pathways that are also utilized in exosome formation. To understand how proteins could preferentially sort into exosomes requires an understanding of each of these mechanisms.

Further elaborating on the ESCRT pathway, the endosomal sorting complexes required for transport (ESCRT) is actually composed of four sets of machinery referred to as ESCRT 0, I, ESCRT II, and ESCRT III (Urbanelli et al., 2013). ESCRT 0 recognizes ubiquinated proteins and recruits them for endosomal sorting through interaction of its

ubiquitin-binding Hrs FYVE domain with phosphatidyl inositol 3-phosphate (PI3P) (Henne et al., 2011). ESCRT 1 is then recruited through tumor susceptibility gene 101(TSG101) interaction with the hepatocyte growth factor-regulated tyrosine kinase substrate (Hrs) PSAP of ESCRT 0 (Schmidt and Teis, 2012). ESCRT 1 then recruits ESCRT II proteins which then recruit ESCRT III, which is stabilized by the recruitment of Alix (ALG-2 interacting protein X) (Villarroya-Beltri et al., 2014). For the complex to dissociate from the plasma membrane requires energy in the form of ATP. This is provided by the ATPase VsP4 (Henne et al., 2011).

While ubiquitination is a tool for protein sorting into ESCRT-dependent exosomes, there are other mechanisms as well. Syndecans, which are a main source of heparin sulfate in the cell membrane, bind to syntenin which can interact with CD63 and Alix (**Fig. 2**) (Villarroya-Beltri et al., 2014). Syndecans possess lateral heparin sulfate polysacharide chains which can be cleaved into shorter chains by heparanse activity in the endosomes (Roucourt et al., 2015). Shorter heparain sulfate chains condense and cluster leading to syndecan oligermerization, which appears to allow for syntenin binding in a cargo-dependent manner (Stoorvogel, 2015). This ultimately allows for sorting into endosomes. Indeed, silencing of either syntenin or syndecans reduced exosome production (Baietti et al., 2012). Therefore, any protein that can bind to syndecans can also sort to exosomes. This suggest that ubiquitination, which is usually the first step in the ESCRT pathway, is not strictly necessary for sorting of cellular proteins into exosome.

In addition to ESCRT dependent pathways, exosomes are also known to form through ceramide oligomerization. Ceramide can cause spontaneous bending and coalescence of microdomains in endosomal membranes (Trajkovic et al., 2008). Furthermore, T cell $CD63^+$ exosome shuttling to APCs involved ceramide synthesis (Mittelbrunn et al., 2011). Tetraspanin clustering in tetraspanin-enriched domains (TEMs) also appears to be involved in exosome formation and protein sorting. In particular, there are a number of viral proteins known to preferentially sort to exosomes through interactions with tetraspanins. In particular, EBV LMP1 binds to CD63 and sorts to exosomes (Verweij et al., 2011). Separately, CD81 plays an important role in exosome composition through interactions of its cytoplasmic domain (Andreu and Yanez-Mo, 2014). Another cited mechanism for protein sorting into exosomes is through oligomerization. However, this mechanism was shown to be important in protein sorting to shedding vesicles from the plasma membrane, although the authors noted that it is often difficult to differentiate these from endosomally derived

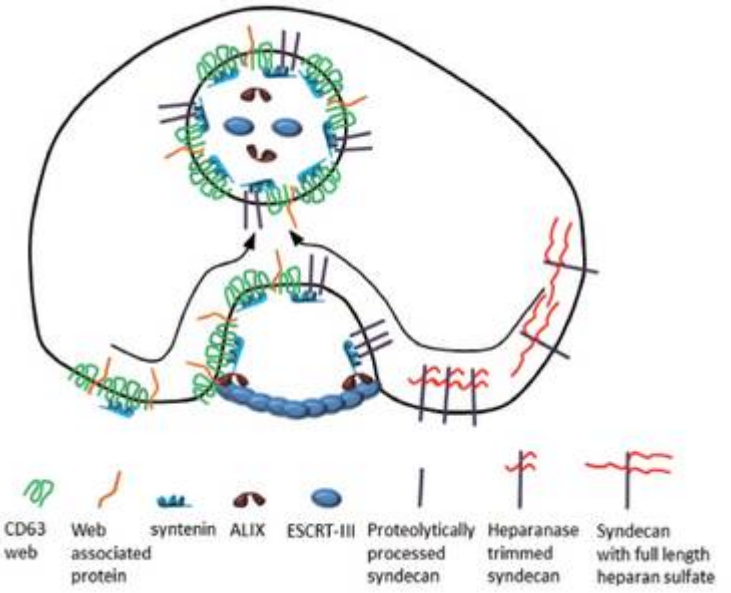

Figure 2: Protein contribution to exosome formation (Stoorvogel, 2015)

vesicles (Shen et al., 2011). Additionally, it has been shown that acylation serves as another method of protein tagging for export in microvesicles (Fang et al., 2007).

RNA localization to exosomes involves additional mechanisms. It has been observed that miRNAs carry specific EXOmotifs that allow for preferential packaging into exosomes, as enrichment of specific miRNAs in exosomes has been observed in human studies (Villarroya-Beltri et al., 2013). These motifs facilitate binding to heterogeneous ribonucleoprotein A2B1 (hnRNPA2b1), which is preferentially sumoylated in exosomes (Villarroya-Beltri et al., 2013). It is an RNA binding and transport protein known to be particularly important in RNA trafficking in neurons (Han et al., 2010). Additionally, Annexin-2 may also play a role in RNA sorting into exosomes (Hagiwara et al., 2015) (Filipenko et al., 2004). Sorting of mRNAs into exosomes seems to involve binding to the mRNA 3'UTR and the short motif CTGCC (Villarroya-Beltri et al., 2014). Interestingly, mRNA sorting also appeared to be dependent on certain miRNAs (Zhang et al., 2015).

Viral infection of regulatory T cells

As mentioned, regulatory T cells have been implicated in supporting chronic viral infection by dampening necessary cytotoxic immune responses that would otherwise eliminate infected cells. However, there is little information available on the role of exosomes in viral infection of Tregs. Indeed, there are only 2 viruses demonstrated to infect regulatory T cells in the literature: human herpes virus-6 (HHV-6) and HTLV-1(**Fig. 3)** (Mine et al., 2014; Yamano et al., 2004). Interestingly, HHV-6B infection of Tregs was documented in a case of drug reaction with eosinophilia and systemic

symptoms (DRESS) which resulted in fatal death from inflammatory disease as described by Mine et al. Therefore, there are other isolated cases in which viral infection of Tregs lead to loss of regulatory function and resulted in unchecked inflammation in the brain. This is similar to what occurs with HTLV-1 infection in HAM/TSP patients.

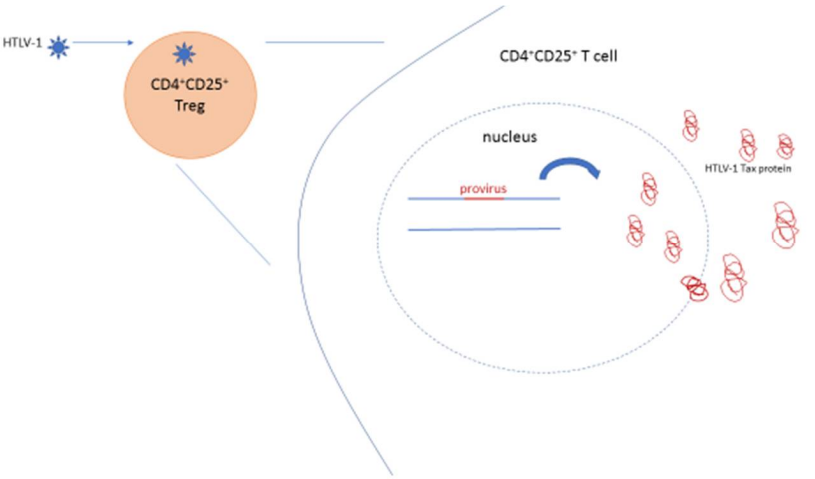

Figure 3: HTLV-1 actively infects regulatory T cells, allowing for HTLV-1 protein expression and potential packaging into exosome

While evidence of viral infection of Tregs is rare in the literature, this may be attributed to the rarity of the Treg subset in peripheral blood and/or to the absence of necessary cellular receptors for viral entry on Tregs for other viruses. GLUT1, HSPGs and Neuropilin-1 have been postulated to be cellular receptors for HTLV-1. Interestingly, neuropilin-1 is a marker of nTregs and may explain the predilection of HTLV-1 for this subset. Indeed, many of the cell lines used to study HTLV-1 are characterized as $CD4^+CD25^+FoxP3^+$ T cells, and two in particular (MT2 and TL-Om1) have been demonstrated to have a completely demethylated TSDR (**Chapter 2)**. Furthermore, TL-Om1 is distinguished from other HTLV-1 infected cell lines by a mutation in the HTLV-1 Tax region, which is thought to be involved in Treg dysfunction.

Prior work showed that HTLV-1 infected cells lines shed exosomes containing HTLV-1 viral antigens. It was demonstrated that exosomes isolated by ultracentrifiguration of supernatant from HTLV-1 infected cell lines contained HTLV-1 Tax protein (Jaworski et al., 2014a). This showed that transformed cells bearing Treg characteristics shed exosomes containing HTLV-1 antigens and therefore suggested that further study of exosomes in HAM/TSP, where Treg infection and dysfunction is a hallmark of the disease, should be undertaken. As such, the work presented in this chapter will demonstrate the presence of HTLV-1 antigens in exosomes isolated from HAM/TSP patient PBMCs and from HAM/TSP patient cerebrospinal fluid (CSF). The mechanisms underlying HTLV-1 protein and RNA sorting into exosomes are not currently well understood. However, it is well known that HTLV-1 Tax undergoes several modifications inside the cell. The following experiments explore the detection of HTLV-1 proteins and mRNA in exosomes present in HAM/TSP patient PBMCs and CSF, and furthermore explore the functional consequences of exosomes carrying HTLV-1 proteins in the pathogenesis of HAM/TSP.

Results

Nanotrapping exosomes from tissue culture supernatants

We initially isolated exosomes from tissue culture supernatant from HTLV-1 infected cell lines HUT102 and HTLV-1 uninfected cell line Jurkat using Nanotrap technology. Nanotrap® particles (NT80+82) pulled down exosomes from both cell lines, regardless of HTLV-1 infection status, as demonstrated by the presence of Alix, CD63, and Actin (**Fig. 4A**, lanes 3 and 4). Control Nanotrap® particles, NT86 (known to isolate viruses but not exosomes (Jaworski et al., 2014b)), was unable to isolate exosomes from tissue culture supernatant, as shown by a lack of Alix, CD63, or Actin (**Fig. 4A**, lanes 5 and 6).

Next, exosomes were nanotrapped from additional cell lines and assessed for CD81, another exosomal marker. As shown in **Fig. 4B**, using an electrochemical based ELISA, CD81 signal for exosomes isolated by Nanotrap® particles from 1mL of tissue culture media from Jurkat, C8166, and HUT102 was equal to or greater than CD81 signal detected from ultracentrifuged Jurkat exosomes from 10mL of starting material (**Fig. 4B**).

To verify further that vesicles isolated by Nanotrap® particles were exosomes, samples were assessed for acetylcholinesterase (AchE) activity, a marker of the exosome fraction (Cantin et al., 2008; Johnstone et al., 1989). Prior to Nanotrap® isolation, exosomes were present in tissue culture supernatant of Jurkat, C81 (C8166), MT2, and HUT102, although at a lower concentration as demonstrated by low levels of AchE activity (**Fig. 4C**, blue bars). However, after nanotrapping with NT80+82, there was a 4-fold increase in AchE activity consistent with an increase in exosome concentration (**Fig. 4C**, red bars).

Samples were also analyzed by nanoFACS, a technique which quantifies vesicles in media by forward and side scatter (FSC, SSC)(Danielson et al., 2016). As seen in **Fig. 4D**, there is a population of vesicles approximately 100nm in size in tissue culture supernatants (**Fig. 4D**, left panel). After the addition of Nanotrap® particles to the supernatant, these Nanotrap® particles could be visualized by a shift in FSC vs. SSC (**Fig. 4D**, middle panel). Moreover, the decrease in the 100nm population was visualized after the addition of the Nanotrap® particles, signifying extraction of the exosomes by the Nanotrap® particles (**Fig. 4D**, middle panel). After trapping, the 100nm vesicles (exosomes) were removed from the tissue culture supernatant, leaving the post-NT sample absent of this population (**Fig. 4D**, right panel).

In addition, exosome visualization was performed by laser capture of the Brownian motion of microvesicles. This technique is a frequently utilized tool for the visualization, characterization, and quantification of exosomes. As seen in **Fig. 4E** (left panel), a population of vesicles with a mean size of 109nm at a concentration of approximately $2x10^9$ vesicles/mL prior to nanotrapping can be visualized from tissue culture supernatant from HTLV-1 infected cells. Nanotraps could be distinguished from exosomes by size, as nanotraps displayed an expected average size of 215nm (**Fig. 4E**, middle panel)(Luchini et al., 2008). When nanotraps were added to tissue culture supernatant, they could be distinguished from exosomes by size and are represented with a size range from 200-500nm were extracted from the media, as shown by an additional peak at ~145nm (**Fig. 4E**, right panel). When comparing pre-NT (inset black bar) and post-NT (inset gray bar) tissue culture supernatant, the concentration of smaller vesicles (<150nm) decreased after nanotrapping in the post-NT sample (gray bar), while medium

(200-300nm) and large vesicles (>300nm) were increased in the remainder of the culture (**Fig. 4E**, right panel inset). The observed decrease in smaller vesicles by NT80+82 is consistent with the AchE results (**Fig. 4C**) and NanoFACS data presented in **Fig. 4D** which further supports the observation that the vesicles isolated by these nanotraps were exosomes. Collectively, these results support nanotrapping as a method for exosome isolation.

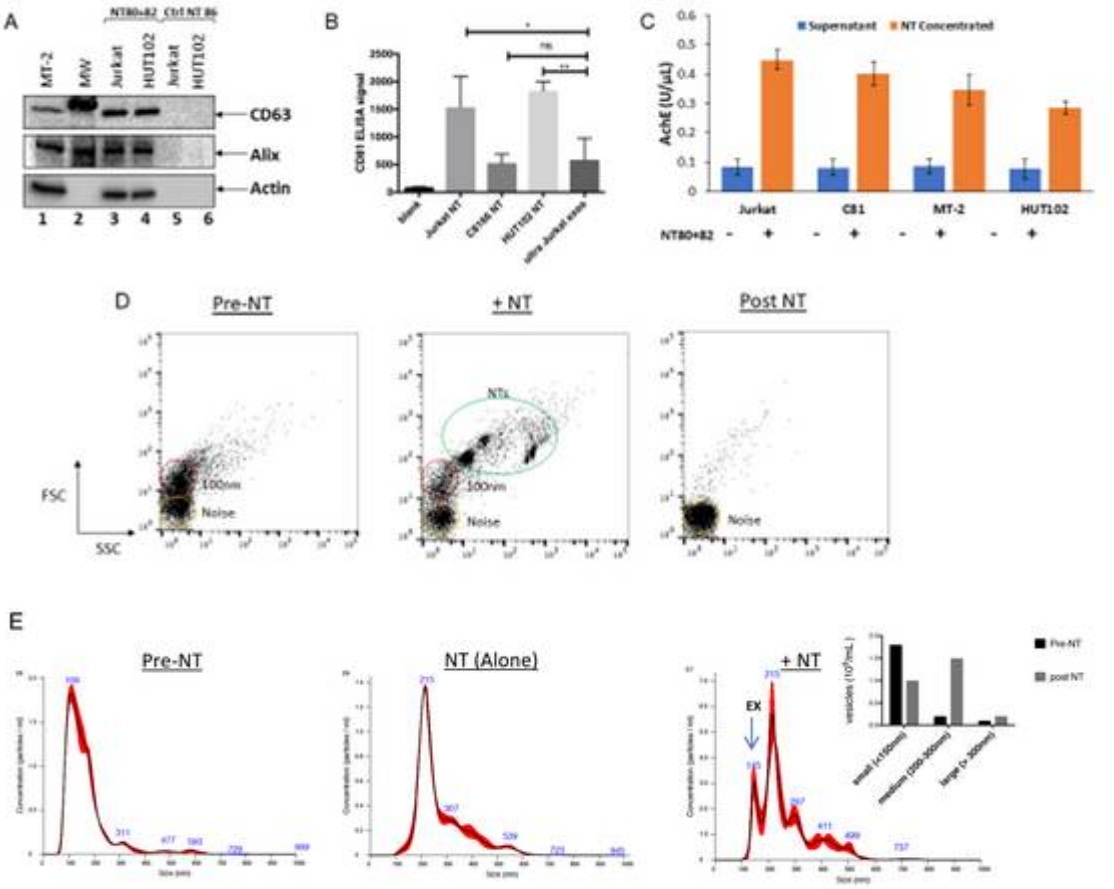

Fig. 4 Nanotrapping exosomes from tissue culture supernatants. (A) CD63, Alix, and Actin signal from (1) MT2 cell lysate (2) MW (3) nanotrapped exosomes from HTLV-1 negative Jurkat tissue culture supernatant using exosome-specific NT 80+82 (4) nanotrapped exosomes from HTLV-1 infected HUT102 tissue culture supernatant using exosome-specific NT 80+82 (5 and 6) Jurkat and HUT102 tissue culture supernatant trapped with control nanotrap (ctrl NT) which is unable to

isolate exosomes from material (B) CD81 ELISA signal was measured from isolated exosomes as a measure of exosome concentration. Nanotrapped exosomes are designated by NT. Nanotrapped exosomes from HTLV-1 negative Jurkat, HTLV-1 infected C8166 and HUT102 from 1 mL of starting tissue culture supernatant all showed an elevated CD81 ELISA signal above background (blank). (C) Measurement of acetylcholinestarse (AchE) activity which is associated with exosome fractions. Initial tissue culture supernatant prior to nanotrapping (blue bars) was measured for AchE activity from HTLV-1 uninfected Jurkat, HTLV-1 infected C8166 (C81), MT2, and HUT102. After addition of NT 80+82 and subsequent exosome isolation, NT concentrated exosomes are shown (orange bars). (D) Tissue culture supernatants from HTLV-1 infected cells were analyzed by specialized flow cytometry, NanoFACS. Left panel represents a representative sample prior to addition of Nanotrap® particle (NT), middle panel represents sample with addition of Nanotrap® particle (NT) and right panel represents sample after Nanotrap® particle and exosomes have been removed. NTs are shown circled in green, while 100 nm vesicles are circled in red, and noise is circled in yellow. (E) Nanotrapped (NT 80+82) exosomes can be visualized. Initial tissue culture supernatant from HTLV-1 infected cells prior to nanotrapping (Pre-NT) was analyzed for size and concentration by Nanosight. NT 80 +82 (NT Alone) were characterized as well in middle panel. Nanotrapped exosomes were assessed after nanotrapping of initial tissue culture supernatant (+NT) in right panel. Exosome (EX) is denoted with arrow.

HTLV-1 Infected Cell Lines have exosomes containing HTLV-I Tax protein

All cell lines produce exosomes in culture, regardless of infection status. However, it has also been shown that viral infection can alter exosome cargo. Indeed, HTLV-1 infected cell lines were shown to produce exosomes that contained HTLV-1 Tax protein which could be isolated by ultracentrifugation (Jaworski et al., 2014a). Here, using 1mL of cell-free, filtered tissue culture supernatant, we demonstrate that of the nanotrapped exosomes isolated from Jurkat, C8166, HUT102, HTLV-1 Tax protein was only detectable by western blot from the exosomes isolated from the HTLV-1 infected cell lines C8166 and HUT102 (**Fig. 5A**, lanes 3 and 4). In addition to these western blot observations, exosomes containing HTLV-I Tax were also confirmed using ELISA.

Exosomes were freeze-thawed after nanotrapping to open the vesicles, after which only exosomes isolated from the HTLV-1 infected cell lines C8166 and Hut 102 showed ELISA reactivity signal for HTLV-1 Tax above background (**Fig. 5B**).

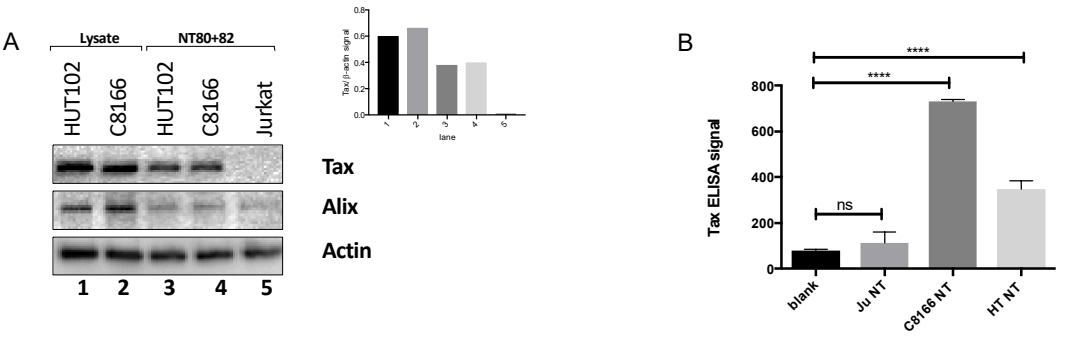

Fig.5 HTLV-1 Infected cell lines have exosomes containing HTLV-1 Tax protein. (A) HTLV-1 Tax, Alix and β-Actin were probed from cell lysates for nanotrapped exosomes from HTLV-1 infected cell lines HUT102 and C8166 (C81) or HTLV-1 uninfected Jurkat. (1) HUT102 lysate (2) C81 lysate both show detection of HTLV-1 Tax, Alix and β-Actin. (3) Exosomes nanotrapped from HUT102 and (4) exosomes nanotrapped from C8166 both show the presence of HTLV-1 Tax, Alix and β-Actin. (5) exosomes nanotrapped from Jurkat show the presence of Alix and β-Actin but do not contain HTLV-1 Tax. (inset)Tax compared to β-actin signal is quantified from graph picture in A with corresponding lanes (B) HTLV-1 Tax was also measured by electrochemical ELISA. Nanotrapped exosomes from Jurkat (Ju), C8166 (C81), and HUT102 (HT) were freeze-thawed and then measured for HTLV-1 reactivity. Ju NT did not show signal above background (blank) while C81 NT and HT NT both showed significantly increased HTLV-1 Tax signal above background from nanotrapped exosomes.

Exosome production from cultured PBMCs

We next investigated peripheral blood mononuclear cells (PBMCs) as a potential source of exosomes in HAM/TSP, since HTLV-1 primarily infects immune cells (Sibon et al., 2006). Exosomes were isolated from normal donor (ND) and HAM/TSP PBMCs after a short term 5-day culture. Through a process of spontaneous lymphoproliferation, it is well known that HAM/TSP PBMCs can proliferate in culture without the addition of

exogenous antigens or cytokines (Miyano-Kurosaki et al., 2007; Sakai et al., 2001). Maximum proliferation is seen after 5d in culture, as demonstrated by peak ^{3}H-TdR uptake by representative HAM/TSP patients compared to a ND (**Fig. 6A**, red and purple lines versus blue line). Moreover, both $CD4^{+}$ and $CD8^{+}$ T cells proliferated as seen by CFSE diminution on flow cytometry (**Fig. 6B**). Maximum CD81 detection, another exosomal marker, also occurred after 5d in culture for both HAM/TSP (HAM) and normal donor (ND) PBMCs (**Fig. 6C**). Unlike HAM/TSP PBMCs, ND PBMCs were primed with recombinant human IL-2 to aid with survival *ex vivo*. Interestingly, exosome production was not significantly different between ND and HAM/TSP PBMCs (**Fig. 6D**). HAM/TSP PBMCs from 2 different patients had maximum exosome detection as measured by CD81 ELISA at 5d (**Fig. 6E**). The vesicles being isolated from HAM/TSP PBMC 5 day cultures were further confirmed to be exosomes by detection of AchE activity from samples (**Fig. 6F**). From these results, 5d was therefore chosen as the optimal time point for analysis of exosomes isolated from PBMC short-term cultures.

HAM/TSP patients are associated with an activated immune response and were shown to produce exosomes (**Fig. 6E, 6F**). Given prior reports that demonstrated that exosome production increases after activation of mouse and human PBMCs (Blanchard et al., 2002), it was of interest to determine in which T cell subset exosome production was most influenced by activation. Therefore, the effect of activation on T cell exosome production was first evaluated in NDs (**Fig. 6G**). PBMC were either activated prior to sorting into T cell subsets or sorted first into T cell subpopulations and then maintained in culture. As shown in **Fig. 6G**, relative to non-stimulated T cell cultures, activation

increased exosome production from predominantly $CD4^+CD25^+$ and $CD8^+CD25^+$ T cell subsets.

Since ND activated $CD4^+CD25^+$ and $CD8^+CD25^+$ produce exosomes and in HAM/TSP patients HTLV-1 is known to predominantly infect and activate $CD4^+$ T cells(Richardson et al., 1990), we analyzed the production of exosomes in HAM/TSP T cell subsets. Similar to exogenously activated ND PBMCs, endogenously stimulated HAM/TSP $CD4^+CD25^+$ produce more exosomes than $CD4^+C25^-$ cells (**Fig. 6H**) and $CD8^+$ T cells.

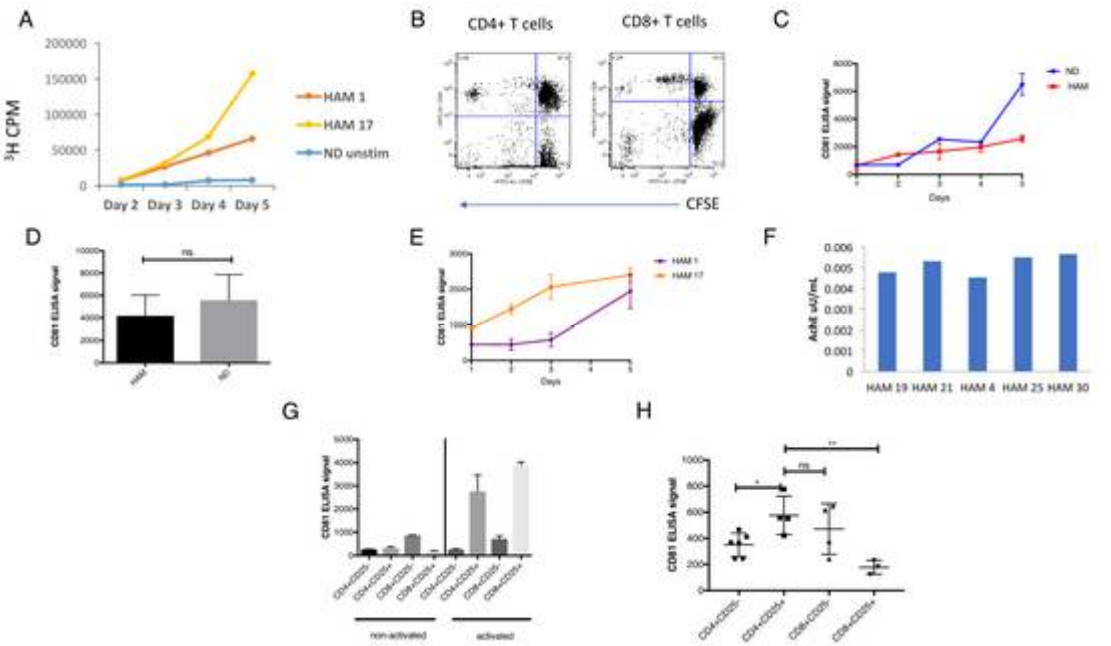

Fig. 6 Exosome production from cultured PBMCs (A) Normal donor (ND) or HAM/TSP (HAM) PBMCs were cultured in exosome free media (Exo free) and measured for ^3H uptake over 5 days. HAM 1 (orange line) and HAM 17 (yellow line) show increasing ^3H uptake at day 3, 4 and 5. ND unstimulated (ND unstim, blue line) does not show an appreciable increase in ^3H uptake. (B) Carboxyfluoroscein succinimidyl ester (CFSE) signal by HAM/TSP PBMCs was measured after 5 days in culture. One representative graph is pictured. Both $CD4^+$ and $CD8^+$T cells undergo proliferation after 5 days (C) CD81 ELISA signal was

assessed from nanotrapped exosomes from ND and HAM. Exosomes trapped from cell supernatant increased as denoted by increased CD81 ELISA signal from trapped exosomes. (D) Exosomes trapped after 5d culture of PBMCs did not show a statistically significant difference in the amount of exosomes isolated from HAM or NDs. (E) Vesicles isolated from HAM PBMC short-term culture were measured for AchE activity for exosome verification. (F) CD81 ELISA signal increased from nanotrapped exosomes isolated from HAM 1 and HAM 17 after 5d in culture (G) ND PBMC were sorted immediately after thawing (non-activated) or after activation for 1d with anti-CD3 100ng/mL and 100IU/mL IL-2 (activated). Of the non-activated T cells, $CD8^+CD25^-$ T cells produced the most in this representative sample. Upon activation, both $CD4^+CD25^+$and $CD8^+CD25^+$ T cells greatly increase exosome production as denoted by CD81 ELISA signal. (H) HAM/TSP PBMCs were cultured for 24h prior to FACS sorting into $CD4^+CD25^-$, $CD4^+CD25^+$, $CD8^+CD25^-$, and $CD8^+CD25^-$ T cells. Increased CD81 ELISA signal was detected from exosomes isolated from $CD4^+CD25^+$ T cells.

Cultured HAM/TSP PBMCs produce exosomes containing HTLV-1 Tax

HTLV-1 infected T-cell lines were shown to produce exosomes that contained HTLV-1 Tax protein (**Fig. 5**). HAM/TSP PBMCs were cultured for 1-5 days to determine if HTLV-1 Tax protein could similarly be demonstrated in nanotrapped exosomes. As shown in **Fig. 7A**, cultured PBMC from 2 HAM/TSP patients produced exosomes containing HTLV-1 Tax that increased over this 5-day period, similar to total exosome production from cultured PBMCS from ND and HAM/TSP patients (**Fig. 6**). As expected, only exosomes isolated from HAM/TSP PBMCs contained HTLV-1 Tax while exosomes isolated from a representative ND PBMC did not (**Fig. 7B**). Quantification of these observations are shown in **Fig. 7B inset** as Tax signal above β-actin, demonstrating tax signal from representative samples of 7 HAM/TSP patients and 1 ND. Cross-sectional analysis of a larger HAM/TSP cohort demonstrated that 71% (25/35) were positive for HTLV-1 Tax in exosomes isolated from cultured PBMC while no Tax positive (Tax^+) exosomes were produced from cultured PBMC of HTLV-1 seronegative

controls (0/10) (Fisher exact test: P-value=0.0001).

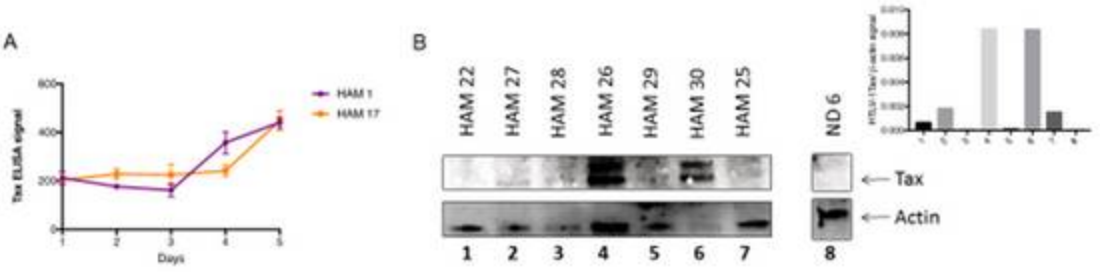

Fig. 7 Cultured HAM/TSP PBMCs produce exosomes containing HTLV-1 Tax. (A) HAM 1 (purple line) and HAM 17 (orange line) were assessed for HTLV-1 Tax content from isolated exosomes by electrochemical ELISA. (B) A representative western blot of HTLV-1 Tax and Actin from nanotrapped exosomes of HAM/TSP PBMC short term 5d culture. HTLV-1 Tax was detected in HAM 27 (lane 2), HAM 26 (lane 4), HAM 30 (lane 6), and HAM 25 (lane 7). Inset: Quantification of western blot (B) as Tax compared to β-actin signal.

Detection of exosomes containing HTLV-1 Tax in CSF of HAM/TSP patients

HAM/TSP is a neuropathologically mediated disorder and therefore the detection of exosomes in the CSF is of significant interest. Cell-free CSF supernatant was obtained from 5 HAM/TSP patients and 5 HTLV-1 seronegative multiple sclerosis (MS) control patients and directly trapped by NT080+082 to be analyzed by western blot for the presence of HTLV-1 Tax. Initially, measurable exosome levels were detected from both HAM/TSP and MS CSF samples as quantified by CD81 ELISA reactivity (**Fig. 8A**) and was variable among this group. Moreover, 3 of the 5 HAM/TSP CSF had exosomes with detectable Tax compared to none of the control MS CSF (**Fig. 8B**). This is quantified as Tax above β-actin signal, where increased signal is only present in lanes 2,4, and 5 corresponding to 3 HAM/TSP CSF samples (HAM 2,4, and 5) (**Fig. 8B,** inset). These observations were expanded to a total of 11 HAM/TSP patient CSF supernatant from which 7 could be shown to contain Tax positive exosomes (Fisher exact test: P-

value=0.0337). The detection of exosomes containing Tax from HAM/TSP CSF did not correlate with total exosomes (data not shown). It is well established that HTLV-1 is a cell-associated virus and restricted to cells in the CSF (Wodarz et al., 1999), while the CSF supernatant is HTLV-1 virus-free (**Fig. 8C**). We therefore have demonstrated the detection of exosomes containing HTLV-1 Tax in the CSF of HAM/TSP patients in the supernatant compartment from which no HTLV-1 virus can be PCR amplified.

Since subsets of HAM/TSP patients PBMC (**Fig. 7B**) and CSF (**Fig. 8B**) contain HTLV-1 Tax^+ exosomes, we asked if there were correlations between these two compartments. All HAM/TSP patients (7/7) with Tax positive exosomes in the CSF were also positive for Tax in exosomes from cultured *ex vivo* PBMCs. For CSF samples from HAM/TSP patients that were Tax negative in the CSF, 2/4 were also negative in the exosomes isolated from *ex vivo* PBMCs.

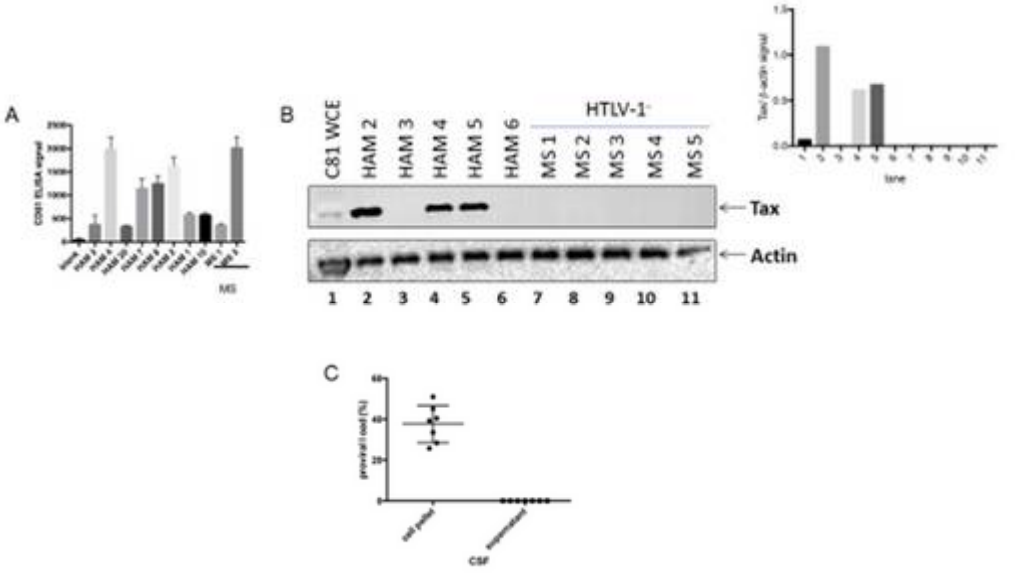

Fig. 8 Detection of exosomes containing HTLV-1 Tax in CSF of HAM/TSP patients (A) CSF supernatant was nanotrapped for exosomes and CD81 ELISA signal was analyzed as a surrogate for isolated exosomes. CD81 was detected for all CSF samples regardless of HTLV-1 infection status and CD81 levels varied from sample to sample. (B) CSF nanotrapped exosomes were probed for HTLV-1 Tax content. C8166 whole cell extract (C8166 WCE, lane 1) was added as a positive control. A representative blot is pictured showing HTLV-1 Tax detection in 3/5 HAM/TSP CSF samples but 0/5 HLTV-1⁻CSF samples. A total of 7/11 HAM/TSP CSF supernatant samples had HTLV-1 Tax detected in isolated CSF exosomes. Actin staining is shown for each exosome sample in this representative blot. Inset: Tax to β-actin signal was quantified. (C) Detection of HTLV-1 proviral load by ddPCR. Provirus was only detected in the cell pellet while virus could not be detected in the CSF supernatant.

HAM/TSP exosomes can sensitize targets to antigen-specific responses

As exosomes containing HTLV-1 Tax in CSF were detectable in the majority of HAM/TSP patients (**Fig. 8B**), it was of interest to determine if these were immunologically functional. Therefore, we investigated the potential of exosomes produced by HAM/TSP PBMCs to sensitize targets for HTLV-1 Tax-specific CTL lysis. HTLV-1 Tax is highly immunogenic and HTLV-1 Tax-specific CTLs have been detected

in brain and spinal cord from HAM/TSP biopsy and autopsy cases (Elovaara et al., 1993; Greten et al., 1998; Kubota et al., 2002; Nagai et al., 2001). To determine if exosomes containing Tax could sensitize target cells for lysis by Tax specific CTL, autologous lymphoblasts from a HAM/TSP patient were pulsed with exosomes generated from HAM/TSP patients or NDs. A representative experiment is shown in **Fig. 9A** where exosomes containing Tax from 2 HAM/TSP patients sensitized target cells for CTL lysis comparable to control Tax-peptide (Hausmann et al., 1999; Kubota et al., 2000) pulsed targets. Exosome from a representative normal donor (4 NDs tested) that was Tax negative did not sensitize targets for CTL lysis (**Fig. 9A**). To demonstrate that these observations were specific for exosomes containing Tax from HAM/TSP patients and not merely cell-free Tax, control nanotraps (ctrl NT86) were used and failed to isolate exosomes that could sensitize targets for CTL lysis (**Fig. 9B**, open symbols) compared to exosomes isolated with NT80+82 (**Fig. 9B**, closed symbols). As shown previously, exosome production increases daily (day1-day5) with *ex vivo* culture with a corresponding increase in Tax detection from isolated exosomes (**Fig. 6E, 7A**) and this increase in Tax^+ exosomes correlated with increased CTL lysis (**Fig. 9B**, NT d1, d3, d5). Further characterization of Tax^+ exosomes sensitizing targets for CTL lysis is shown in **Fig. 9C** that demonstrates a dose-dependent response with increasing concentrations (250μL-1mL) of Tax^+ exosomes.

While most HAM/TSP PBMC derived exosomes were able to sensitize targets for CTL response, the magnitude of this response varied among patients (**Fig. 9D**) and correlated with the detection of HTLV-1 Tax by western blot (**Fig. 7B**) from HAM/TSP exosomes. Of the 10 HAM/TSP patients PBMC with western blot Tax^+ exosomes, 9

were able to sensitize targets for specific lysis (Fisher exact test P-value=0.005). Collectively, these results demonstrate that exosomes containing HTLV-1 Tax can contribute to a functional immune response by sensitizing target cells to specific lysis by antigen-specific CTLs.

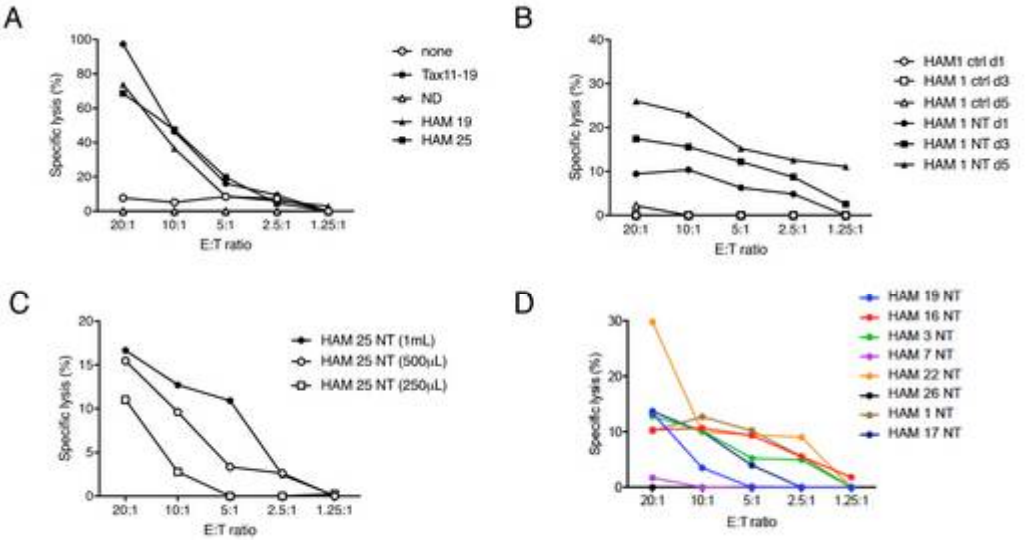

Fig. 9 HAM/TSP exosomes can sensitize targets to Ag-specific responses (A) cytotoxic T lymphocyte (CTL) lysis was analyzed after the addition of PBMC derived exosomes or tax-peptide (11-19). Donor antigen presenting cells (APC) pulsed with Tax11-19 (closed circle) yielded 100% specific lysis at 20:1 E:T ratio and decreased at lower E:T ratios. HAM/TSP PBMC derived exosomes (closed triangle and square) and ND6 (open triangle) derived exosomes are also shown. (B) HAM/TSP PBMC supernatant was either nanotrapped with NT 80+82 (NT) or with a control nanotrap unable to isolate exosomes (ctrl). Supernatants collected after d1, d3, or d5 of short-term culture were used for trapping. Samples trapped with NT are represented with close symbols while samples trapped with ctrl NT are represented with open symbols. Each sample is shown at E:T ratios 20:1 to 1.25:1. (C) Various amounts HAM/TSP 25 PBMC tissue culture supernatant was used as the starting material for nanotrapping (NT). Nanotrapping from the standard 1mL (closed circle), from 500µL (open circle), and from 250µL (open square) of starting tissue culture supernatant are shown at various E:T ratios ranging from of 20:1 to 1.25:1. (D) HAM/TSP PBMC derived exosome samples yielded varying levels of CTL lysis of pulsed targets.

HAM/TSP PBMCs shed exosomes containing HTLV-1 tax mRNA but not HTLV-1 hbz mRNA

In addition to exosomes containing viral proteins, exosomes containing viral mRNAs have been reported in serum from virus-infected individuals (Bukong et al., 2014; Chugh et al., 2013). Therefore, we investigated if HAM/TSP exosomes from PBMC cultures also contained HTLV-I *tax* and *hbz* viral mRNAs, two important regulatory genes involved in HTLV-1 persistence. As shown in **Fig. 10A**, variable levels of HTLV-1 *tax* mRNA were demonstrated in PBMC-derived exosomes isolated from 85% of HAM/TSP patients (17/20). As expected, exosomes from control normal donor PBMC were negative for HTLV-1 mRNAs (data not shown). Of the 17 HAM/TSP patients with exosomes containing HTLV-1 *tax* mRNA, 16 contained HTLV-1 Tax protein. Interestingly, none of the exosome samples tested positive for HTLV-I *hbz* mRNA (data not shown). Since HTLV-1 Tax protein could be detected, exosomes were tested for the presence of HBZ protein as well. 10/17 HAM/TSP PBMC had exosomes that contained HTLV-1 HBZ protein, as seen in a representative blot shown in **Fig. 10B**. Quantitation of this observation was determined as HBZ to β-actin, demonstrating increased densitometry signal from lanes 2 and 3 which represent 2 HAM/TSP samples, but a low to non-existent signal in all other samples (**Fig. 10B,** inset)

As the HTLV-1 mRNA detected in exosomes is produced from cultured PBMC, we measured the levels of cellular HTLV-1 *tax* and *hbz* mRNA in these cultures. As shown in **Fig. 10C**, HTLV-1 *tax* is maximally expressed after 24h in culture (Clarke et al., 1984; Rende et al., 2011) and decreased by 5d (**Fig. 10C**, black). By contrast, HTLV-I *hbz mRNA* could also be detected in cells at 24h although at lower levels than *tax*

mRNA, and remained stable during the 5d culture (**Fig. 10C**, gray). The absence of *hbz* mRNA from isolated PBMC exosomes that nonetheless contained HBZ protein is consistent with the reported localization of *hbz* mRNA to the nucleus of HAM/TSP patients PBMC (Rende et al., 2011; Satou et al., 2006) while HBZ protein was recently reported to be localized to the cytoplasm (Baratella et al., 2017).

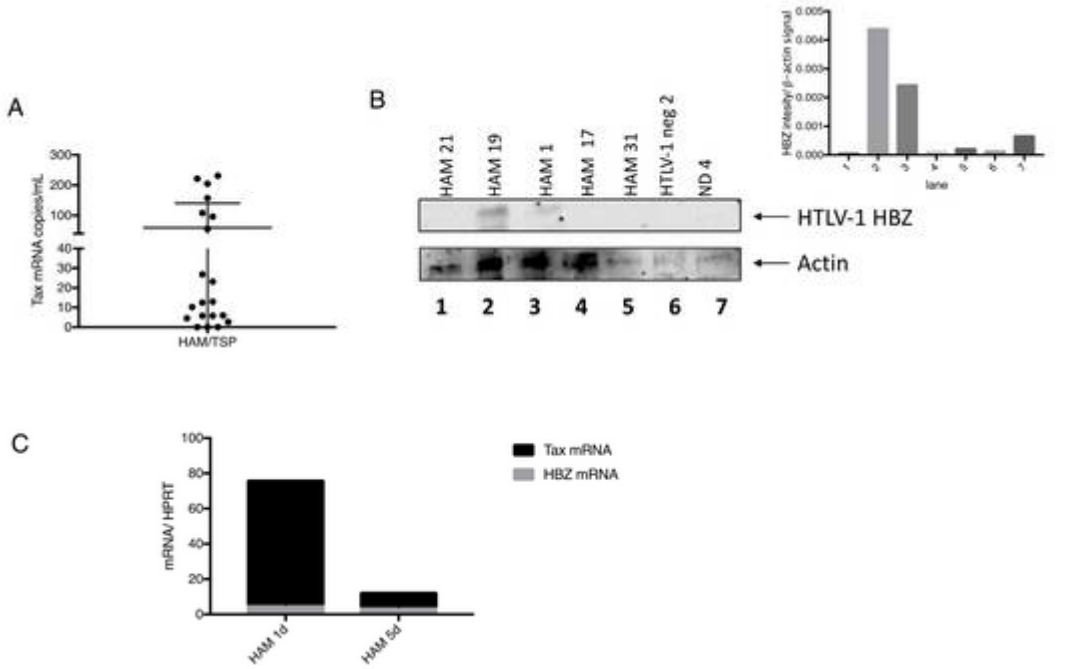

Fig. 10 HAM/TSP PBMCs shed exosomes containing HTLV-1 *tax* mRNA but do not carry HTLV-1 *hbz* mRNA (A) HAM/TSP derived exosomes were probed for HTLV-1 *tax* mRNA content. 17/20 had detectable tax mRNA from nanotrapped exosomes at varying levels. No HTLV-1 *hbz* mRNA could be detected by ddPCR from nanotrapped exosomes. (B) HTLV-1 HBZ protein was assessed by western blot. (inset) HBZ to β-actin signal was analyzed for this blot. (C) HTLV-1 mRNA was analyzed from 8 HAM/TSP PBMC cell lysates. *Tax* mRNA (black bar) and *HBZ* mRNA (gray bar) are quantified against *HPRT* expression after 1d or 5d in culture.

Treatment with Tax-containing HAM/TSP exosomes reduces $CD4^+CD25^+$ T cell population

As mentioned previously, exosomes are thought to contribute to Treg function through the shuttling of various suppressive components, primarily miRNAs, to effector cells (Okoye et al., 2014). This observation was made in mice and has yet to be demonstrated for human Tregs, which have several differences from mouse Tregs that extend beyond phenotypic characterizations (Ziegler, 2006). Therefore, it is possible that human Tregs do not use exosomes for suppressive purposes. Yet, it is clear from **Fig. 6H** that $CD4^+CD25^+$ T cells are predominant producers of exosomes in HAM/TSP T cells. Thus, more must be done to understand how exosomes containing Tax might influence Treg function.

Paradoxically, research has also shown that exosomes help maintain Tregs. In cancer, this is partially through the induction of Tregs by exosomes (Szajnik et al., 2010). Indeed, tumor derived exosomes appeared to not only convert $CD4^+CD25^-$ T cells to Tregs but also upregulated their suppressive capabilities. Separately, it has been demonstrated that exosomes isolated from milk also have the ability to induce Tregs in PBMCs (Admyre et al., 2007). Therefore, we asked whether exosomes from HAM/TSP could also induce Tregs or upregulate Treg function.

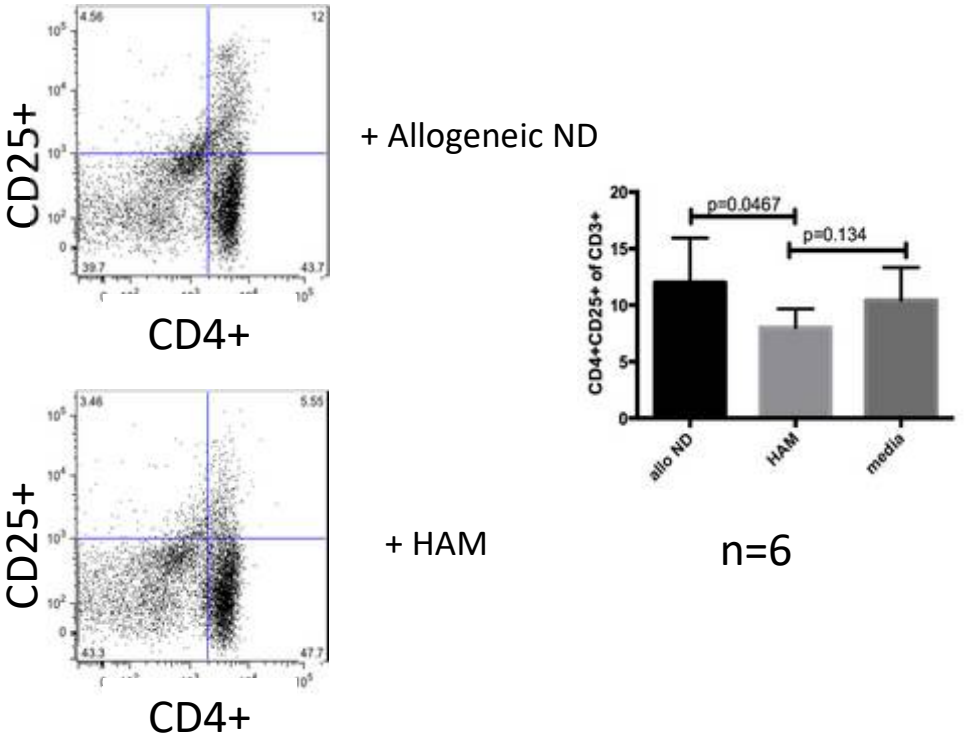

Figure 11: CD4$^+$CD25$^+$ T cells diminish after exposure to HAM/TSP derived exosomes
On the left, plots showing the CD4$^+$CD25$^+$ subset of ND PBMCs after exposure to allogeneic ND PBMC derived exosomes or HAM/TSP (HAM) PBMC derived exosomes. This is quantified for a subset of allogeneic ND PBMC derived exosomes and HAM/TSP PBMC derived exosomes (n=6). Media denotes ND PBMCs that were cultured in media only without addition of exosomes.

To elucidate whether exosomes containing HTLV-1 Tax are deleterious or beneficial in maintaining the Treg population and/or Treg function, exosomes from PBMC cultures of HAM/TSP or ND PBMC cultures were nanotrapped and then added to exosome-free cultures of 2 x10^6 allogeneic ND PBMCs. CTLA-4 and FoxP3 are well known in their role in Treg suppressive function. Additionally, the programmed death (PD) PD-1/PDL-1 axis has recently been implicated in Treg suppression of immune subsets (Gotot et al., 2012; Sage et al., 2013). After 3d, ND PBMCs were assessed by flow cytometry for CD3, CD4, CD25, CTLA4, PD-1, Tax-FITC, and FoxP3 expression

levels and compared to PBMCs with no exosome treatment. Tax-FITC was never detected in ND cells treated with HAM/TSP exosomes (data not shown). This may be due to levels of exosomal Tax protein being below the limits of detection of flow cytometry. Alternatively, it may be attributable to the short longevity of Tax protein upon transfer. Regardless, clear changes in the $CD4^+CD25^+$ T cell population were observed upon exposure to HAM/TSP derived exosomes as compared to ND-derived exosomes (**Fig. 11;** p-value=0.0467). There was also a slight decrease in the $CD4^+CD25^+$ population as compared to ND PBMC that were untreated (media).

In addition, the $CD4^+PD\text{-}1^+$ T cell population also appeared to be reduced, although this did not reach statistical significance (**Fig. 12A,** p=0.2405). Since, there were no observed changes in FoxP3 (**Fig. 12B)** or CTLA-4 (**Fig. 12C**) which are associated with Treg function, after exposure to HAM/TSP exosomes, this may suggest that despite a reduction in $CD4^+CD25^+$ T cell population after HAM/TSP exosome exposure, remaining Tregs may retain their function. Additionally, although PD-1 on $CD4^+CD25^+$ T cells did not change (data not shown), reduced PD-1 on $CD4^+$ T cells may also have implications in immune suppression. Increased PD-1 expression on non-Tregs has been associated with resistance to immune suppression by Tregs (Mercadante and Lorenz, 2016), and therefore $CD4^+$T cells exposed to HAM/TSP exosomes may also respond to Treg suppression.

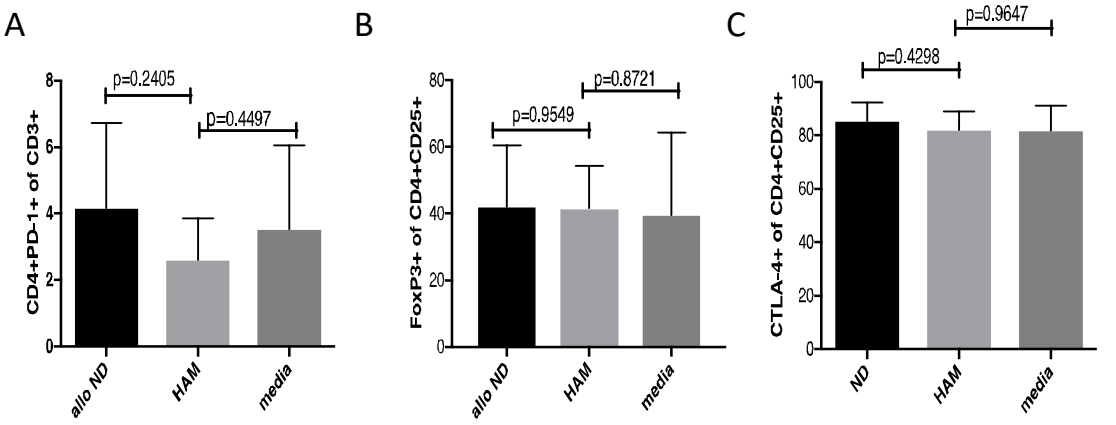

Figure 12: PD-1, FoxP3, and CTLA-4 expression in ND PBMCs after exposure to HAM/TSP derived exosomes (A) % $CD4^+PD\text{-}1^+$ of CD3 population in ND PBMCs exposed to allogeneic ND (allo ND) PBMC derived exosomes or HAM/TSP PBMC (HAM) derived exosomes or no exosomes (media) (B) %$FoxP3^+$ of $CD4^+CD25^+$ T cells in ND PBMC 3d after exposure to allo ND, HAM or media (C) %$CTLA\text{-}4^+$of $CD4^+CD25^+$ in ND PBMC 3d after exposure to exosomes from allo ND, HAM or media

Asymptomatic carriers (ACs) produce exosomes containing Tax but not HBZ

It is unclear how HTLV-1 proteins are targeted to secreted exosomes and how they influence Treg function, if at all. One way to understand how important exosomes containing HTLV-1 proteins might be in HAM/TSP pathogenesis is to compared patients with at asymptomatic carriers (ACs). ACs usually have lower proviral loads and rates of spontaneous proliferation, but still express HTLV-1 proteins (Nagai et al., 1998). We therefore investigated an initial cohort of ACs for exosome content. In a small cohort of 5 ACs, we were able to demonstrate the presence of Tax protein in 2/5 AC PBMC derived exosomes (**Fig. 13,** lanes 5 and 6**)** along with detecting Tax in the exosomes of HTLV-1 infected cell lines C8166 (C81) and HUT102 (HT) indicated by arrows. Interestingly, we were unable to detect the presence of HBZ protein (data not shown),

which was typically present in ~50% of HAM/TSP PBMC exosomes (**Fig. 10B)**

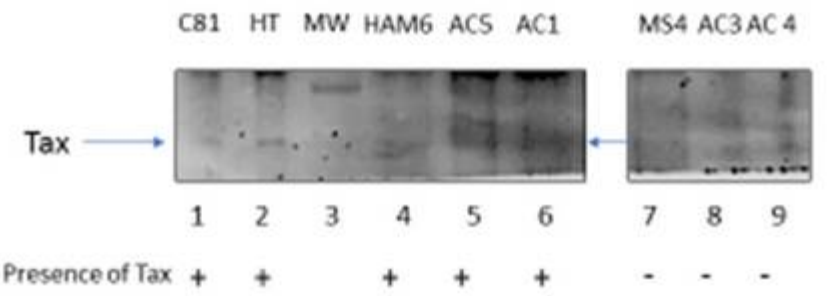

Figure 13: Tax detection in exosomes isolated from AC PBMC culture. Lane 1: C8166 (C81) exosomes. Lane 2: HUT102 (HT) exosomes. Lane 3: Molecular weight (MW). Lane 4: HAM/TSP patient PBCM derived exosomes. Lane 5: Detection of Tax in AC5 derived exosomes. Lane 6: Detection of Tax in AC1 derived exosomes. Lane 7: Multiple sclerosis (MS4) patient PBMC derived exosomes. Lane 8: AC3 derived exosomes. Lane 9: AC4 derived exosomes

.

These observations suggest that the presence of HBZ in exosomes may differentiate between HAM/TSP patents and ACs. It was interesting to note that one of the ACs (AC 1), which showed the presence of Tax in exosomes isolated from PBMC culture (**Fig. 13**, lane 6), subsequently demonstrated a spike in CSF proviral load. This coincided with onset of clinical symptoms consistent with neurologic decline. When his CSF sample was probed for the presence of exosomes containing Tax, there was a signal for Tax in exosomes isolated from his 2014 CSF sample (**Fig 14,** lane 3) which increased in exosomes isolated from a CSF sample from a later date (**Fig. 14,** lane 4), at which point he had developed clinical symptoms. Due to the new onset of neurologic symptoms and increased proviral load in the CSF, this individual has been reclassified as a non-AC/ HAM/TSP. He will be followed closely for further changes in exosomes isolated from PBMC culture and CSF supernatant.

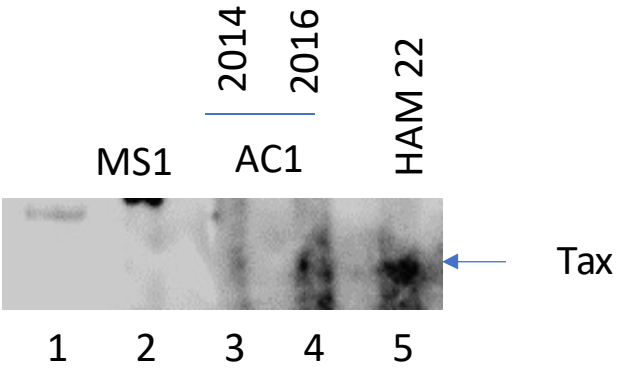

Figure 14: HTLV-1 Tax detected in exosomes from AC and HAM/TSP CSF. Lane 1: ladder. Lane 2: MS1 CSF exosomes. Lane 3: 2014 AC1 CSF exosomes. Lane 4: Tax detection in 2016 AC1 CSF exosomes. Lane 5: Tax detection in HAM 22 CSF derived exosomes

HTLV-1 Tax entry into exosomes shed by AC PBMCs in culture was at a lower frequency (2/5) than what was observed in HAM/TSP (25/35) (40% vs. 70%). Larger numbers of ACs and HAM/TSP patients will be needed to determine if this represents yet another biomarker that differentiates ACs from HAM/TSP patients. Indeed, a lower frequency of exosomes carrying HTLV-1 antigens would support the hypothesis that production of these exosomes perpetuates an inflammatory immune environment, as we suggested in the immunopathogenesis model pictured in **Fig. 15**. HTLV-1 infected PBMCs (mostly $Tax^{+}CD4^{+}CD25^{+}$ T cells) produce exosomes containing HTLV-1 Tax and exosomes with no HTLV-1 antigen. Both Tax^{+} and Tax^{-} exosomes along with HTLV-1 infected and uninfected $CD4^{+}CD25^{+}$ T cells can cross the BBB. Both types of exosomes can be taken up by resident CNS cells such as glia and oligodendrocytes, allowing for the expression of HTLV-1 Tax by uninfected cells. These exosomes-stimulated CNS resident cells could be targets for HTLV-1 Tax-specific CTL, a concept demonstrated by experiments shown in **Fig.9.**

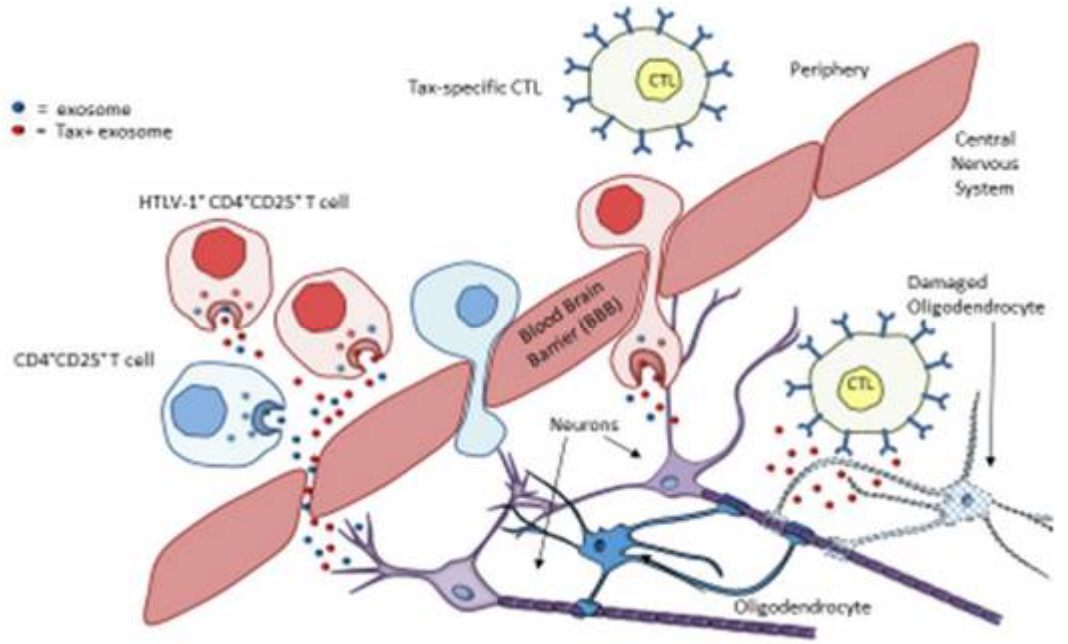

Figure 15: Hypothesized contribution of exosomes to HAM/TSP pathogenesis.

Detection of HTLV-1 Tax in exosomes produced by different HAM/TSP T cell subsets

While HTLV-1 principally infects $CD4^+CD25^+$ T cells, as mentioned in the **Introduction**, HTLV-1 is capable of infecting all T cells. $CD4^+CD25^+$ T cells, which contain the subset of regulatory T cells, produce more exosomes than other T cell subsets, as was observed in **Fig. 6H**. However, HTLV-1 Tax expression is best characterized in T cell subsets when they are still in culture with other PBMCs (Richardson et al., 1990). The phenomenon of spontaneous lymphoproliferation has only been observed in T cells cultured in total PMBCs (**Fig. 6B**) and diminishes upon separation of each immune subset (Itoyama et al., 1988; Macatonia et al., 1992). Therefore, it was still unclear if exosomes produced by individual T cell subsets would contain HTLV-1 antigen if T cell subsets were maintained in isolation. An initial western blot demonstrated the presence

of HTLV-1 Tax in exosomes isolated from $CD4^+CD25^+$ T cells from HAM/TSP patient #16 (HAM16) (**Fig. 16,** lane 4**)** but not from exosomes produced by HAM 16 $CD4^+CD25^-$ T cells (**Fig. 16,** lane 5**)**)

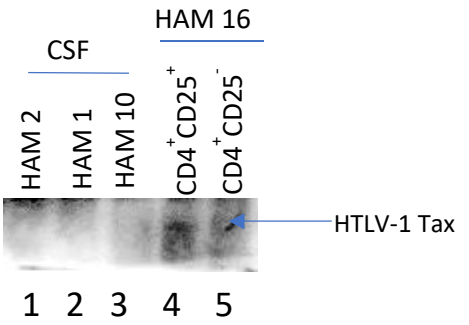

Figure 16: Detection of HTLV-1 Tax in exosomes produced by HAM/TSP T cell subsets. Lane 1: HAM 2 CSF exosomes. Lane 2: HAM 1 CSF exosomes. Lane 3: HAM 10 CSF exosomes. Lane 4: Detection of HTLV-1 Tax in HAM 16 PBMC derived exosomes. Lane 5: No Tax detected in HAM 16 PBMC derived exosomes.

A larger cohort of HAM/TSP patients will need to be sorted and examined for HTLV-1 antigen content in exosomes isolated from T cell subset culture. CD8 T cell exosomes could not be examined because the number of cells yielded after sorting was too low for additional experiments. Future experiments will focus on exosome production and content by HAM/TSP T cell subsets when co-cultured with irradiated allogeneic PBMCs, which should allow for spontaneous proliferation to occur similar to what is observed when PBCMs are cultured without cell separation and permit analysis of additional T cell subsets.

Isoforms of HTLV-1 Tax are present in exosomes isolated from ex vivo PBMC culture

HTLV-1 Tax is phosphorylated, ubiquitinated, sumoylated, and acetylated (Currer et al., 2012). Phosphorylation of Tax occurs at multiple serine residues present in the protein and is thought to be important in nuclear localization of the protein and in the activation of CREB and NF-kB pathways (Currer et al., 2012). Alternatively,

ubiquitination is critical for Tax localization to the cytoplasm (Gatza et al., 2007). This occurs at multiple lysine residues, lysine 263, 280 and 284 being the most important of these via the ubiquitin-conjugating enzyme (Ubc) 13, an E2 enzyme (Chiari et al., 2004; Lavorgna and Harhaj, 2014). Cytoplasmic retention is essential for IKK and NF-kB activation, and may be important for exosome localization as detailed earlier (Currer et al., 2012). HTLV-1 Tax also undergoes sumolyation, which aids in nuclear retention and the formation of nuclear bodies that consist of Tax and binding partners CBP and p300 (Kfoury et al., 2011). The sites for sumoylation on the protein overlap with the sites of ubiquitination. Interestingly, Tax acetylation also occurs at lysine residues, suggesting that each modification competes for lysine residues (Lodewick et al., 2009). Typically, acetylation occurs at position 246 in the C-terminus and modulates its DNA binding affinity, stability and ability to interact with coactivators and corepressors (Shembade and Harhaj, 2010). While there were several forms of modified Tax present in isolated PBMC exosomes (**Fig. 17)**, it was unclear if there was any predominant post-translational modification.

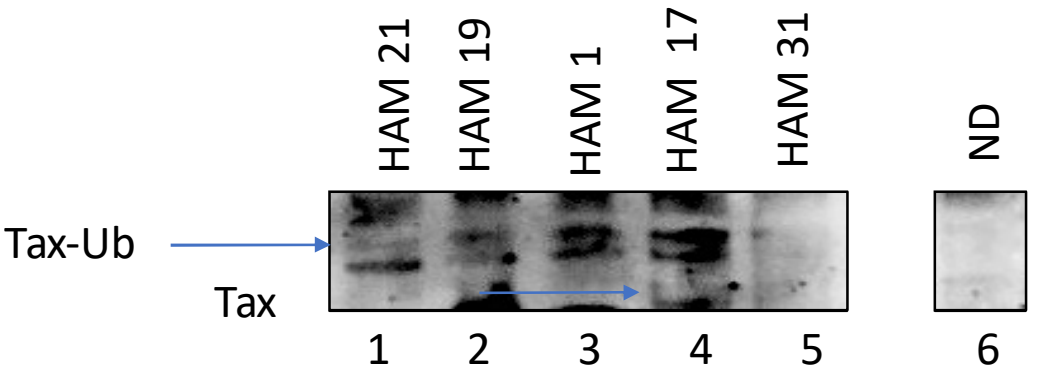

Figure 17: Detection of unmodified HTLV-1 Tax in HAM 17 (lane 4) along with ubiquitinated Tax (Tax Ub) in several HAM/TSP PBMC derived exosomes samples (lanes 1, 2, 3, 4, and 5).

Only unmodified Tax detected from exosomes isolated from transfected cells

Considering that several modified forms of Tax could be detected, but not definitely identified, it was of interest to understand if some of the modified forms were due to ubiquitination. As mentioned earlier, ubiquitination is an important modification to Tax that is involved in both cellular localization and function.

HTLV-1 Tax plasmids with a cytomegalovirus (CMV) promoter were used to transfect HEK 293T cells after which exosomes were collected and assessed for Tax content. The plasmid M22 (T130A/L1315S) has been used for studies in NF-kB activation and this particular mutation is observed to cause alteration in NF- kB activation but retention of CREB binding (Smith and Greene, 1990). M22 is also impaired in its binding to the proteasome due to decreased ubiquitination (Chiari et al., 2004). The plasmid M47 (L319R/ L320S) has increased ubiquitination and increased binding to the proteasome as well as lost CREB binding (**Fig. 18**) (Chiari et al., 2004; Smith and Greene, 1990). The plasmid K88A has lost CBP binding but maintains CREB binding, similar to plasmid M22 in terms of loss of ubiquitination, though this has not been reported (Harrod et al., 1998).To determine if ubiquitination is necessary for localization of HTLV-1 Tax in secreted PBMC exosomes, we transfected Tax and Tax mutant plasmids into HEK 293T cells and examined resulting exosome content. After transfection, cells were washed and subsequently switched to Exo-Free media. 5 days later, supernatants were collected and

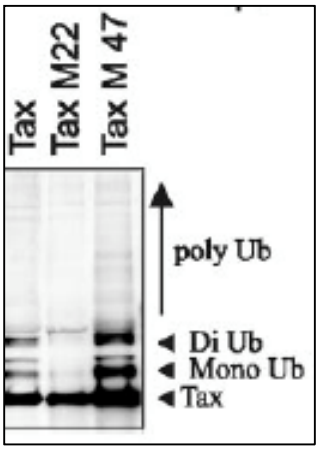

Figure 18: CMV-Tax (Tax) and Tax mutants (Tax M22 and Tax M47) levels of ubiquitination (Chiari et al., 2004)

spun. Initial experiments **(Fig 19)** demonstrated the presence of unmodified Tax and monoubiquinated Tax (Tax mono-Ub) in transfected cell lysates.

Figure 19: HTLV-1 Tax and Tax monoubiquinated (Tax mono-Ub) after transfection with CMV-K88A, M22, M47, Tax, and empty plasmids into HEK 293T cells. Lane 1: Tax detection in CMV-K88A transfected cell lysates. Lane 2: Tax and Tax mono-Ub detection in CMV-M22 transfected cell lysates. Lane 3: Tax and Tax mono-Ub detection in CMV-M47 transfected cell lysates. Lane 4: Tax and Tax mono-Ub detection in CMV-Tax transfected cell lysates. Lane 5: No tax detection after transfection with empty plasmid

However, only unmodified Tax was detected in in the exosomes isolated from transfected cells, regardless of the transgene (**Fig. 20)**. The only difference noted was increased Tax detection in exosomes isolated from M22 and M47 transfected 293T cells. This was likely due to increased HTLV-1 Tax detection from these cell lysates. These initial results suggest that ubiquitinated Tax does not localize to secreted exosomes from 293T cells. Furthermore, ubiquitination of Tax may have no effect on entry of unmodified Tax into secreted exosomes since both M22 (low ubiquitination) and M47 (increased ubiquitination) demonstrated increased Tax in secreted exosomes.

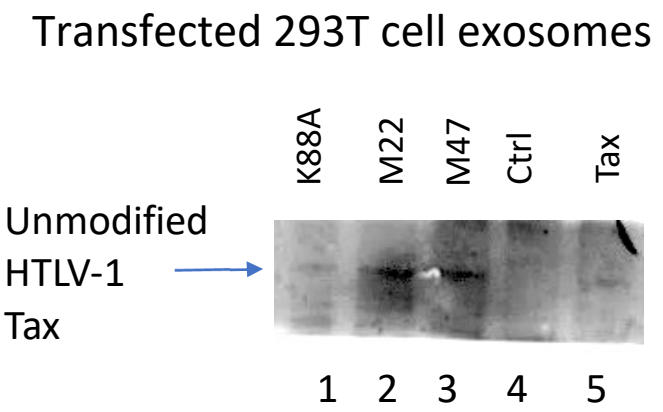

Figure 20: unmodified Tax detected in exosomes secreted by transfected 293T cells. Unmodified HTLV-1 Tax present in lanes 1-3, and 5. No Tax detected in Ctrl transfected cell exosomes which were transfected with a HBZ plasmid (lane 4). No detection of Tax mono-Ub in any lane

Lactacystin treatment has no effect on localization of Tax to exosomes

To further interrogate the potential role of ubiquitination on HTLV-1 Tax entry into secreted exosomes, transfected 293T cells were subjected to lactacystin treatment 24h after transfection. Lactacystin is a proteasome inhibitor which should increase Tax in cell lysates due to lack of proteasomal degradation, but it potentially may have no effect on Tax mutants which have defects in proteasome binding (i.e. M22).

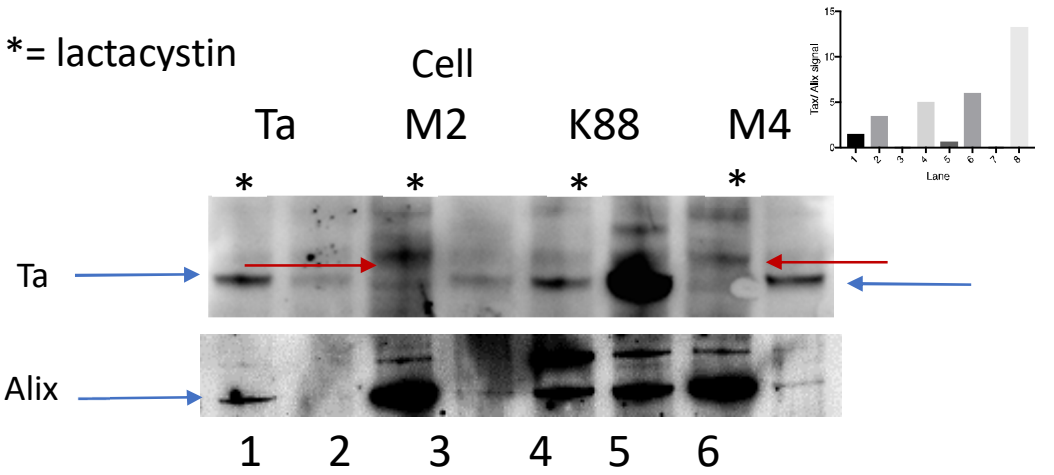

Figure 21: Lactacystin treatment of HTLV-1 Tax mutant transfected 293T cells alters Tax localization in exosomes isolated from M22 transfected cells. Lanes 1, 3, 5, and 7 represent cell lysates after lactacystin treatment. Lanes 2, 4, 6, and 8 represent cell lysates without lactacystin treatment. Top gel shows Tax (blue arrows) and mono- ubiquitinated Tax (red arrows) in treated and untreated cell lysates. Bottom gel shows Alix (blue arrow) in treated and untreated cell lysates. (inset) Unmodified Tax to Alix signal is quantified by densitometry for each lane in pictured blot

As can be seen in **Fig. 21**, lactacystin increased unmodified Tax (blue arrow) in cell lysates from HTLV-1 Tax transfected cells (lane 1), but only increased detection of modified Tax (highlighted with red arrows) in lactacystin treated M22, and M47 (lane 3 and lane 7 respectively). Unexpectedly, K88A transfected cells appear to have a decrease in Tax and modified Tax detection after lactacystin treatment (lane 5). Additionally, Tax expression relative to Alix expression as calculated by western blot densitometry demonstrates that the amount of unmodified Tax was decreased in the samples treated with lactacystin (**Fig. 21** inset, lanes 1,3,5, and 7). This is likely due to the non-specific increase in all proteins as a result of proteasome inhibition.

In comparing the Tax content of isolated exosomes from treated cells, lactacystin treatment increased unmodified Tax in exosomes isolated from Tax, K88A, and M47 transfected cells (**Fig. 22,** lanes 1, 5 and 7). This is despite the observation of increased Tax relative to Alix in untreated cell lysates (**Fig. 21)**. Only M22 appears to have more Tax present in exosomes from untreated transfected 293T cells (**Fig. 22,** lanes 3 and 4, inset). Interestingly, M22 is the only plasmid described that decreases ubiquitination and impairs binding to the proteasome (**Fig. 18**).

Figure 22: Unmodified Tax was detected at higher levels in lactacystin treated exosomes (lanes 1, 5, and 7) for each transfected Tax plasmid except M22 (lane 3). This was confirmed by calculation of band intensity with densitometry (inset)

Therefore, despite proteasome inhibition increasing unmodified Tax localization in isolated exosomes, proteasome inhibition did not increase detection of other Tax isoforms. This suggests that ubiquitination may be important for unmodified Tax entry into exosomes through an indirect mechanism which does not require localization of ubiquitinated forms of Tax into exosomes.

GW48699 treatment decreases exosome isolation from HAM/TSP treated PMBCs

Lactacystin is a non-specific proteasome inhibitor such that all proteins should increase in the cell due to lack of proteasomal degradation. Therefore, we proposed treatment of HAM/TSP PBMCs with GW4869, which blocks exosome production, to see if there was any reduction in HTLV-1 Tax detected in released exosomes. One HAM/TSP patient was selected for treatment of PBMCs with GW4869. Various amounts of GW4869 were added to $8x10^6$ cells, at which point cells were maintained in culture for the typical 5d followed by exosome isolation by nanotrap particles. Alix decreased with increased concentrations of GW4869 by western blot analysis with densitomery calculation by band intensity, indicating decreased exosome isolation in treated cultures, particularly at concentrations above 10 μM (**Fig. 23**). Considering the changes in exosome production detected at 10 μM, this level can be used for potential future experiments that expand on exploring whether Tax content is also altered upon treatment with exosome inhibitors. These observations suggest that exosome production inhibitors such as GW4869 can potentially be used for treatment of HAM/TSP PBMCs in *ex vivo* culture with the goal of assessing the use of this category of drug for future clinical trials in HAM/TSP.

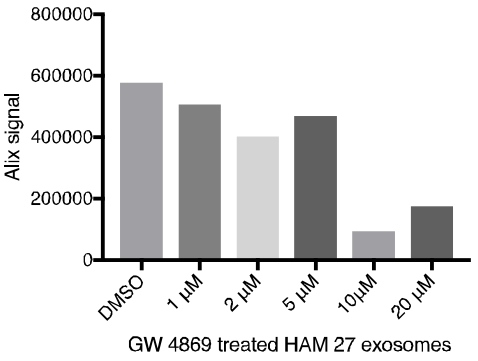

Figure 23: Alix detection in exosomes post GW 4869 treatment decreased at doses above 10 µM.

Methods

Storage of PBMCs and cell lines

PBMCs were isolated by Ficoll-Hypaque (Lonza, Walkersville, MD) centrifugation, and were cryopreserved in liquid nitrogen prior to use. All NDs were noted to be healthy and HTLV-1 negative. HTLV-1 infected cell lines TL-Om1, HUT102, MT2 and C8166 and the uninfected cell lined Jurkat and MOLT3 were also cryopreserved prior to use.

Maintenance of cell lines

For maintenance in cell culture, cell lines were slowly thawed with the addition of C-RPMI (RPMI 1640 supplemented with 10% FBS, 100U/mL penicillin, 100µg/ml streptomycin sulfate, and 2mM L-glutamine) and maintained in this media with weekly splitting.

Cell line culture for exosome cultivation

Cell lines were maintained in Exosome free CRPMI, whereby FBS was spun at >90,000 x g for 2h for removal of exosomes and added to RPMI 1640 supplemented with 100U/mL penicillin, 100µg/ml streptomycin sulfate, and 2mM L-glutamine, for 5 days. Tissue culture media was collected by removal of cells with a 1300rpm for 10 min spin, followed by filtration through a 0.22µm MCE filter (EMD Millipore, Billerica, MA). Media containing exosomes was frozen at 1mL per microcentrifuge tube and stored at -80º C prior to use.

PBMC culture for exosome cultivation

A total of 35 HAM/TSP, 8 ND, and 2 HTLV-II patient PBMC samples were used for *ex vivo* incubation and later exosome isolation. PBMCs were isolated by Ficoll-Hypaque (Lonza, Walkersville, MD) centrifugation, and were cryopreserved in liquid nitrogen prior to use. All NDs were noted to be healthy and HTLV-1 negative. Briefly, PBMCs were placed in Exosome-free CRPMI at $8x10^6$ cells per well in a 12-well plate and incubated at 37^0C for 5d. ND PBMCs were maintained in culture with the addition of 100 IU/mL recombinant human (rh)IL-2. Culture supernatant was collected and then spun at 1300rpm for 10min to remove cells. Spun supernatant was then pushed through a 0.22µm MCE filter (EMD Millipore) to remove large debris, apoptotic bodies and extracellular vesicles >200µm. Cerebrospinal fluid (CSF) was obtained through lumbar puncture of study participants by neurologist and nurse practitioners of the Neuroimmunology Clinical group. CSF was spun at 1300rpm for 10min to remove cells and supernatant was stored in 1mL aliquots at -80^0C prior to use.

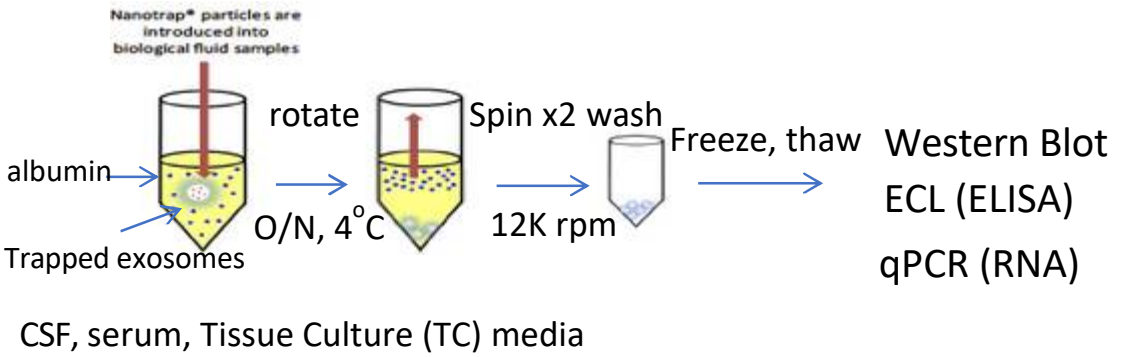

Figure 24: Nanotrap particle technique for exosome isolation

The study was reviewed and approved by the National Institute of Neurological Disorders and Stroke Institutional Review Board. Informed consent was written and obtained from each subject in accordance with the Declaration of Helsinki.

Exosome isolation

Nanotraps 80 and 82 were provided by Ceres Nanosciences (Manassas, VA) and previously shown to isolate exosomes from media (Jaworski et al., 2014b). Each was mixed with PBS (w/o Ca^+ or Mg^+) for final 30% EXNT slurry (*ex* 15µL NT 80+ 15µL NT 82 + 70µL PBS). After thawing of culture supernatants, 30µL of 30% slurry was added to 1 mL of *ex vivo* culture supernatant and rotated O/N at 4ºC or at RT for 1h as shown in **Fig. 24**. After trapping, samples were spun at 13K rpm for 7 min, and then washed with 500µL DEPC H_2O and respun at 13K rpm for 5 min. A second wash with 500µL of DEPC H_2O was performed. Exosome control NT (NT 86) was similarly diluted in PBS for a 30% slurry. When working with CSF, samples were first diluted 1:1 in PBS (w/o Ca^+ or Mg^+) for a total volume of 500µl to which 30µl of EX NT slurry was added.

Western blotting

HTLV-1 Tax, Alix, CD63, HBZ, and actin were detected from NT exosomes by western blot. After spin and wash, samples were resuspended in 8µL of 100µM Tris-HCl, 8µM Urea, 1% Triton lysis buffer with 1X protease inhibitor. After the addition of 4X LDS (Thermo Fisher Scientific) and DTT, samples were heated at 95ºC for 6 min, with vigorous vortexing for 5-10s every 2 min. After heating, samples were pulse-spun and run on a 4-12% Novex Bis-Tris 1.00mm gel (Thermo Fisher Scientific) with MES buffer and then transferred in an X-blot module onto a 0.45µm Nitrocellulose membrane. After blocking for 1h with 3% BSA in 1X TBS, membranes were probed with anti-Tax 1:100

(Lt4, mIgG3. Kindly provided by Dr. Yuetsu Tanaka), anti-Alix 1:100 (1A12, mIgG1, Santa Cruz Biotechnologies, Dallas, TX), anti-HBZ 1:250 (AB9, kindly provided by Dr. Jean-Marie Peloponese), and actin 1:100 (C4, Santa Cruz Biotech). Primary antibodies were incubated O/N at 4ºC with rotation. For imaging, anti-ms HRP secondary antibody (Jackson ImmunoResearch, West Grove, PA) was applied at 1:5000 or goat anti-ms IR (Li-cor Biosciences, Lincoln, NE) (1:10000) secondary was used for CSF samples for 1h shaking at room temperature after washing with 1X TBS 0.1% Tween 3 X 10 min. For detection of actin, blots were stripped for 5-10min with Restore PLUS Western Blot Stripping Buffer (Thermo Fisher Scientific) followed by reblocking in 3% BSA, TBS and reprobed with anti-actin (Santa Cruz Biotech) at 1:100 O/N at 4ºC. For imagaing, HRP substrate (Advansta western bright Sirius). For cell lysates, either 2µg or 10µg of lysate was run with 4X LDS buffer and DTT. Transfer occurred as detailed above onto a 0.45µm Nitroceullulose membrane. Resulting blots were blocked and stained with primary and seconday antibody as detailed above. For imaging, HRP substrate Advansta Western Bright Quantaum was applied and filmed using the Bio Express Lum C Imager.

MESO ELISA

For CD81 and HTLV-1 Tax detection, NT exosomes were resuspended in 1X TBS for assessment by MESO ELISA (MSD Technologies, Rockville, MD). Samples were freeze-thawed for 4 cycles of 5 min each and then applied to a MESO Sector Imager 96-well High-Bind plate (MSD Technologies) at 5µL per well in duplicate O/N. The plate was then blocked with Blocker A for 2h, washed with PBS x2 and then probed with anti-CD81(Santa Cruz Biotech) or anti-HTLV-1 Tax (Lt4) or anti-HTLV-1 Tax (1A3 clone.

Santa Cruz Biotech) for 1h, shaking. After a repeat wash, the plate was probed with secondary Ab (goat anti-ms Sulfa 1:100, MSD Technologies). After a final wash, MSD Read Buffer was added at a 1:2 diluted in in Ultra Pure water and the plate was read using a MSD Sector Imager (courtesy Dr. Avi Nath).

Acetylcholinesterase Ezyme (AchE) Activity Assay

AchE activity of exosomes after nanotrapping was carried out as described in detail previously (Cantin et al., 2008) with brief modification. Amplex® Acetylcholine/Acetylcholine Esterase Activity Assay Kit (Thermo A12217) was used following the manufacturer's instructions. Briefly, a 1x running buffer negative control (20 mL of H_2O and 5 mL of 5x reaction buffer) and two positive controls, one consisting of acetylcholine esterase and one consisting of hydrogen peroxide, were made and plated on a 96-well plate. Exosomes were treated and fluorescence of acetylcholine esterase activity was measured with a GLOMAX multidetection system (Promega, Madison, WI) every fifteen minutes for one hour to find optimal activity. Changes in absorption were monitored at 412 nm during incubation period at 37 °C (Narayanan et al., 2013).

Exosomal RNA isolation and detection

RNA was extracted from NT exosomes using the Trizol-Chloroform method described previously (Jaworski et al., 2014b). Briefly, Trizol reagent (750µL, Invitrogen) was added to pelleted nanotrap-bound exosomes. After a 5min incubation at RN, 200µL of chloroform was added and the samples vortexed vigorously. After an additional 3min incubation at RT, samples were spun at 12K x g for 15min at 4ºC. The aqueous phase

was removed and placed in a separate tube, to which 350µL of 100% Isopropranol was added. Samples were incubated at RT for 10min and then spun at 12K x g for 10min at 4ºC. The resulting pellet was then washed with 750µL of 75% EtOH and spun at 7500 x g for 5min at 4ºC. The RNA pellet was air dried for 10min and then reconstituted in 40µL 1X TE buffer, heated at 65^0C for 10min and stored at -20^0C. RNA was extracted from $<5x10^6$ PBMCs using the RNEasy kit (Qiagen, Hilden, Germany) per provided protocol. 100ng of RNA was used for cDNA synthesis in a total reaction volume of 40µL using the High Capacity cDNA kit (Thermo Fisher Scientific) and cycled as noted in the company protocol on a GeneAmp PCR System 9700. *tax* mRNA (Tax F: 5' ATCCCGTGGAGACTCCTCAA 3', Tax R 5' CCAAACACGTAGACTGGGTATCC 3', probe 5' FAM CCCCGCCGATCCCAAA TAMRA 3'), *hbz* mRNA (HBZ F: AGAACGCGACTCAACCGG. HBZ R: TGACACAGGCAAGCATCGA, probe: ATGGCGGCCTCAGGGCT) and HPRT mRNA (TaqMan Gene Expression assay Hs02800695_m1, Thermo Fisher Scientific) were probed on the digital droplet PCR platform (BioRad). PCR was run as: 95°C × 10 minutes (1 cycle), 94°C × 30 seconds, 59°C × 60 seconds (40 cycles), 98°C × 10 minutes (1 cycle), 12°C hold. The assays were verified for each run with MT2 cellular cDNA

CTL assay

HTLV-1 Tax specific CTLs and target B cells were generated from an HLA A0201 HAM patient and cryopreserved prior to use. Upon thaw, CTLs were primed with Tax peptide 11-19 weekly for expansion and maintenance in CTLA media (IMDM with 5% FBS, 100µg/mL penicillin, 100µg/mL streptomycin sulfate, 12.5mM sulfinpyrazone, 2mL L-

glutamine) for up to one month. Clones were tested for efficiency of target killing after priming with peptide. Targets (HLA A0201 B cells) were pulsed for 1h at 37ºC with Tax peptide 11-19 or nanotrapped exosomes from 1mL of tissue culture supernatants from 10 HAM/TSP or 4 ND PBMC *ex vivo* cultures. One HAM/TSP supernatant was nanotrapped with a control non-exosome NT 86 as a negative control. The CTL Europium cytotoxicity release assay was performed as outlined in the DELFIA protocol (Perkin Elmer Inc., Waltham, MA). Specific lysis was calculated as a percentage (sample x- $Target_{only}$)/ ($Target_{max-}$ $Target_{only}$) x100.

T cell isolation

To understand which T cell subsets were responsible for exosome production found in PBMC culture, sorting was performed on thawed or previously activated ND PBMCs. Activation occurred with addition of 100ng/mL anti-CD3 (HIT3a, eBiosciences) and 300IU/mL rhIL-2 24h prior to sorting. At least $5x10^7$ PBMCs were stained in FACS buffer (1% FBS, 0.1% Sodium azide, PBS) with $10\mu L/1x10^7$ cells of anti-CD4 APC, anti-CD8 FITC and anti-CD25 PE (all from BD Biosciences). Cells were then sorted into $CD4^+CD25^-$, $CD4^+CD25^+$, $CD8^+CD25^-$, $CD8^+CD25^+$ T cell subsets on a BD FACS Aria flow cytometer. After sorting, cells were briefly placed in 20%FBS, 2X antimycobacterial, antibacterial (Thermo Fisher Scientific) RPMI 2mM L-glutamine. Cells were then spun at 1300rpm for 10min and resuspended in Exo-free CRPMI supplemented with 100IU/mL hrIL-2 and plated at $7.5 x10^5$ cells per well in a 12-well plate for 5d at 37^0C. For HAM/TSP PBMCs, no exogenous stimulation was provided.

Endogenous activation of HAM/TSP PBMC was achieved by incubation of PBMCs for 18-24h prior to FACS sorting as described above.

Statistical analysis

Bar graphs and scatter plots were generated in GraphPad Prism 7.0 (GraphPad, San Diego, CA). Two-tailed unpaired t tests were run to establish difference between groups and significance was considered anything with a P-value <0.05. The two-tailed Fisher exact test was used to assess differences between groups on parametric questions (Tax^+ or Tax^- exosomes) using GraphPad QuickCalcs software. Statistical analyses of 2x2 contingency tables were performed using GraphPad QuickCalcs software with two-tailed Fisher exact tests. P-values <0.05 were considered significant.

Staining of T cells post-exosome exposure

$2x10^6$ PBMCs were incubated for 72h in the presence of NT exosomes or PBMC culture supernatant in RPMI, 10% Exosome-free FBS, 100U/mL penicillin, 100µg/ml streptomycin sulfate, and 2mM L-glutamine. After culture, 1×10^6 cells were stained with CD3-Pacific Blue, CD4-Alexa 700, CD25-PE-Cy7. FoxP3-APC, PD-1-APC-Cy7, CTLA-4-PE, Tax-FITC on a BD LSRII flow cytometer. CD4 populations were analyzed by FlowJo.

PBMC treatment with exosomal inhibitors and/or activators

7×10^6 PBMCs from HAM 27 or ND 3 were placed in 1mL of Exo-free CRPMI in a 12-well plate. Cells were treated with: DMSO, 1µM, 2µM, 5µM, 10µM or 20µM of

exosome production inhibitor GW4869 (Santa Cruz Biotech) reconstituted in DMSO or DMSO, 1μg, 5μg, 10μg, 20μg, or 50μg of IFN-α. Cell count and viability were assessed after 5d culture. Cell supernatant was collected and processed for exosome collection as described earlier. Exosomes were nanotrapped and assessed for HTLV-1 Tax content.

Listing and growth of HTLV-1 Tax, HBZ plasmids

Tax-HA, Tax-Ub-HA, Tax-Ub-Flag were prepared in the pcDNA3 plasmid and obtained from Dr. Iha's laboratory and originally described in Peloponese Jr et al JVI 2004. HBZ-GFP plasmid was obtained from Veffa Franchini's laboratory. pCMV-Tax, pCMV-M22, pCMV-M47, and pCMV-Tax were available in house. pCMV-Tax, p-CMV-M22 and pCMV-M47 are previously described (Smith and Greene, 1990). pCMV-K88A was previously described (Harrod et al., 1998). HBZ-AU1 is prepared in a luciferase vector and grown in LB with 50μg/mL kanamycin for amplification. All other plasmids are grown with ampicillin 50μg/mL after transformation into DH5α e. coli. Amplification for all plasmids was conducted in LB at 37ºC. For gene and protein expression, 2.5 x 10^5 HEK 293T cells were plated on 10cm plates 24h prior to transfection. Cells were then transfected with 2μg of plasmid of interest in OPTIMEM using XtremeGene HP at a 3:1 ratio. Cell supernatants were then collected 5d post-transfection where cell count should be 8 x 10^6 per plate. Supernatants were spun at 1300rpm for 10min to remove cells and debris and then filtered by 0.22μm MCE (Millipore) filter. Filtered supernatants were stored in 1mL aliquots and stored at -80ºC. Exosomes were nantorapped and analyzed by western blot as detailed above.

Chapter 4

Consequences of HAM/TSP Treg dysfunction to non-T cells

Introduction

Much of the work pursued in this thesis has focused on the relationship between Tregs and both $CD4^+$ and $CD8^+$ T cells, as these subsets are thought to cause much of the damage that occurs in the CNS of HAM/TSP patients. Indeed, the proposed models of HAM/TSP pathogenesis focus specifically on the potential damage caused by both $CD4^+$ and $CD8^+$ T cells (Fuzii et al., 2014). The results presented in **Chapter 3** suggest that exosomes may play a role in perpetuating this damage by the packaging and delivery of HTLV-1 antigens in the CNS to uninfected target cells. Importantly, preliminary experiments suggest that PMBC exposure to exosomes decreases the $CD4^+CD25^+$T cells and reduces the PD-1 and $CD4^+$ T cells (**Chapter 3 Fig. 12, Fig. 13**). However, it is well known that Tregs inhibit the immune response of several immune subsets, both adapative and innate (Schmidt et al., 2012), including B cells which are often implicated in autoimmunity.

Antibody secreting cells (ASC) are a subset of B cells responsible for antibody production. In humans, this encompasses short-lived plasmablasts as well as plasma cells (Lee et al., 2010). Although it has been well established that ASCs are vital to the regulation and elimination of other infections, their role in the control of HTLV-1 is gaining more recognition. HIV has demonstrated how important a robust B cell response is for control of viral loads (Huang et al., 2010). Indeed, most elite controllers show higher levels of circulating antibodies against HIV. While it is clear that abs against specific HLTV-1 proteins can be detected in HAM/TSP patients and at higher levels than in ACs (Kitze et al., 1996) (Enose-Akahata et al., 2013), the role HTLV-1 specific

antibodies could play in pathogenesis is unclear. Some postulate that HTLV-1 specific abs in the CSF are in fact detrimental (Ribeiro et al., 2013).

As mentioned, Tregs in HAM/TSP are dysfunctional in their ability to suppress immune responses which may also include a lack of suppression to HTLV-1 specific B-cells present in the CSF. Considering the presence of exosomes in the CSF of HAM/TSP patients (**Chapter 3**), and their demonstrated HTLV-1 antigen content, we asked whether BCRs present in the CSF are preferentially enriched for those BCRs that recognize HTLV-1 antigens. Furthermore, the observation of sensitization of targets to HTLV-1 specific $CD8^+$ T cell lysis (**Chapter 3 Fig. 9**), suggested that there may be other potential consequences of exosome exposure to B cells. Stimulation of B cells by exosomes has been reported, demonstrating the specific enhancement of B cell populations that recognized autoantigens packaged in the exosomes (Bashratyan et al., 2013). We sought to understand if HTLV-1 antigens packaged in HAM/TSP exosomes are involved in observed increased ASC responses in HAM/TSP (unpublished data, Jacobson lab). We therefore asked whether BCRs present in the CSF of HAM/TSP patients recognize HTLV-1 antigens and whether these were related to antigens present in HAM/TSP exosomes.

Results

HAM/TSP patient CSF BCRs recognize proteins only expressed by HTLV-1 infected cell line MT2

In collaboration with Brandon DeKosky and Erica Normandin at the Viral Research Center (VRC) at the NIH, single cell sorting of B cells was performed followed by high throughput deep sequencing of BCRs present in HAM/TSP CSF. Sorting of the 20 most prevalent BCR sequences was done followed by transfection of the resulting light and heavy chains into Expi 293F cells (Thermo Fisher Scientific). The resulting cloned antibodies (Abs) were collected and tested for specificity to HTLV-1 antigens. 19 BCRs of interest were selected after analysis by high throughput sequencing; clones #1, 4, 6,8, 9-12 were derived from IgG expressing B cells, clones #2,3,5, and 7 were derived from IgA expressing B cells and clones #13-19 were derived from IgM expressing B cells. Each BCR was cloned into 293F cells in an IgG backbone. The specificity of each antibody was unknown, but HTLV-1 was hypothesized as a potential target. Therefore, homogenized cell lysates of HTLV-1 infected MT2 or uninfected Jurkat (Ju) cells were used for initial testing. 1 μg of cell lysate was applied to each well of an electrochemical ELISA plate (MESO, MSD) plate and stained with 1 μg of each Ab, after which electrochemical signal was quantified. In addition, several control antibodies with known reactivity to non-HTLV-1 antigens were tested (clone #4, VRC01, CR9114, PGT 128, and 2F5). As can be seen in **Fig. 1**, antibodies #4 and #12 both demonstrated increased binding to proteins in MT2 lysate as compared to Jurkat proteins as calculated by a MESO signal ratio for MT2: Ju >2:1. No other HAM/TSP BCR derived antibody demonstrated increased reactivity to MT2 lysate. Importantly, the control antibodies also

did not demonstrate increased reactivity to MT2 lysate as compared to uninfected Ju lysate (PGT128 MT2: Ju <2:1). This relationship was maintained through multiple subsequent trials.

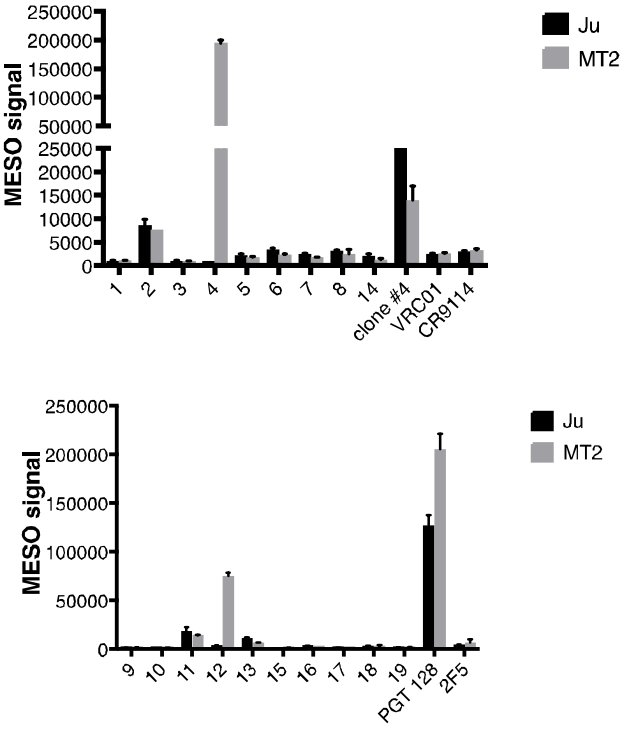

Figure 1: Electrochemical ELISA of Abs generated from HAM/TSP CSF BCRs against Jurkat (Ju) and MT2 lysates. Control HTLV-1 negative antibodies clone #4, VRC01, CR9114, PGT 128, and 2F5 were also tested. Only HAM/TSP CSF BCR generated Abs #4 and #12 show MT2: Ju signal > 2:1.

HAM/TSP CSF BCRs recognize proteins expressed by several HTLV-1 infected cell lines

To verify that increased reactivity to MT2 lysate was HTLV-1 specific, antibodies were further tested against lysates from HTLV-1 infected cell lines C8166 (C81), HUT102 (HT), TL-Om1 (TL) and MT2. Each cell line has differing levels of expression

of HTLV-1 proteins. Again Abs #4 and 12 showed increased reactivity to HTLV-1 infected cell lysates, although reactivity was greatest to MT2 (**Fig. 2**, red bars). Interestingly, neither antibody showed increased reactivity to C8166 (green bar), a cell line which almost exclusively express HTLV-1 Tax (Manuel et al., 2009). As it was initially thought that the HAM/TSP CSF BCRs could recognize HTLV-1 Tax, this observation suggested that Abs #4 and 12 may potentially recognize other non-HTLV-1 antigens. Therefore, an additional uninfected cell line, MOLT3 (Mo= yellow) was tested.

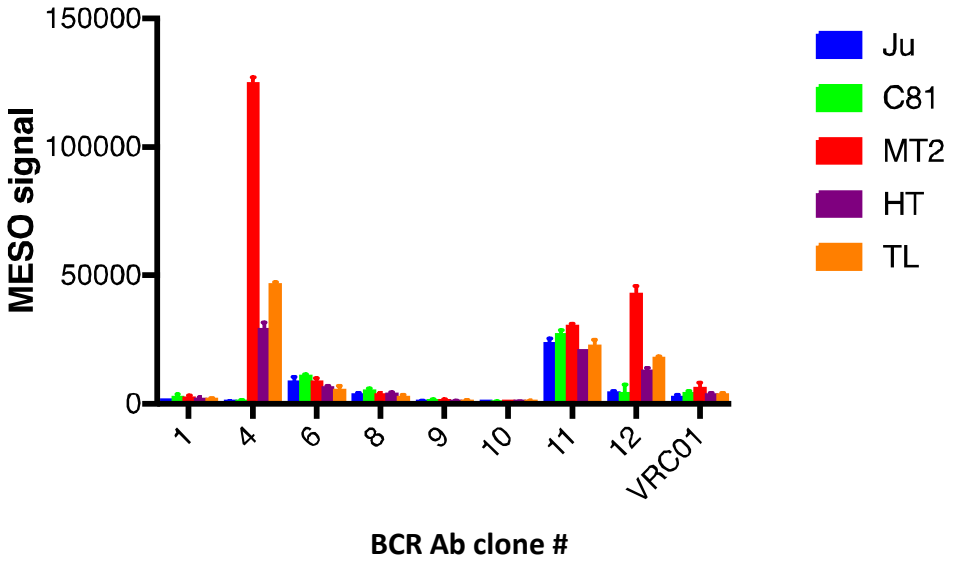

Figure 2: IgG Ab reactivity to HTLV-1 infected cell lines C8166 (C81), MT2, HUT102 (HT), and TL-Om1 and HTLV-1 uninfected cell line Jurkat (Ju)

As can be seen in **Figure 3**, no additional reactivity was measured to lysates of either the uninfected T cell lines Jurkat or MOLT3, suggesting that the HAM/TSP CSF BCRs are not recognizing non-HTLV-1 Ags.

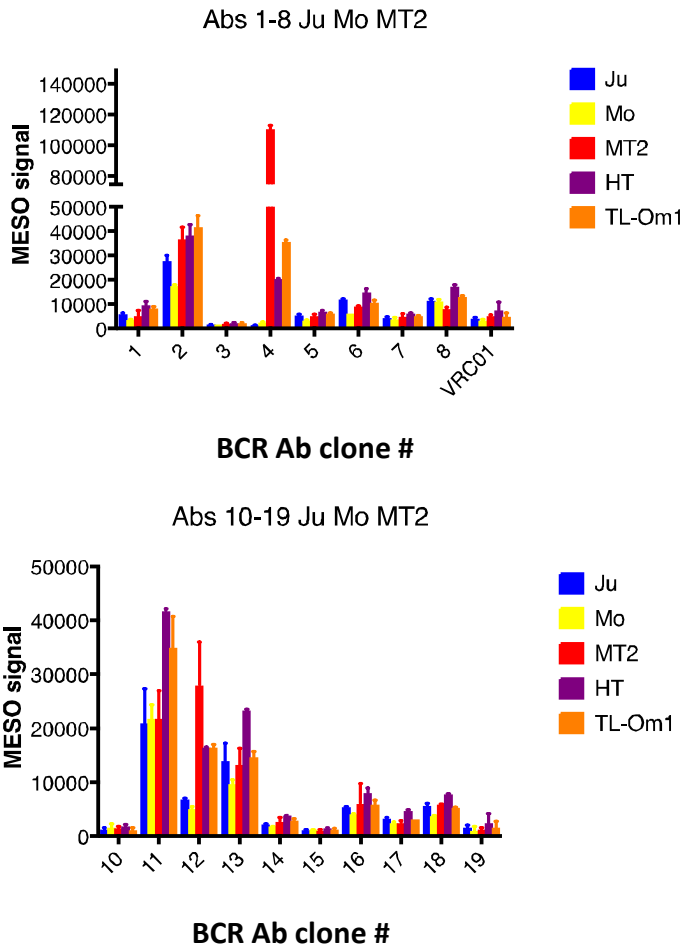

Figure 3: Ab reactivity to HTLV-1 infected cell lines (MT2, HUT102 (HT), TL-Om1) and HTLV-1 uninfected cell lines Jurkat (Ju) and MOLT3 (Mo)

HAM/TSP patient CSF BCRs recognize antigens expressed by HAM/TSP PBMCs but not ND PBMCs

Since long-term, immortalized cell lines may have properties that differ from primary cells, it was suggested that the HAM/TSP CSF BCRs clones #4 and 12 that were shown to be reactive to HTLV-1 infected cell lysates (**Fig. 3,** MT2, HUT102, TL-Om1) but may not be recognizing and HTLV-1 proteins but an HTLV-1 induced cell protein. Freshly thawed HAM/TSP PBMCs were used as primary HTLV-1 infected cells. Lysates from primary cells were compared to lysates from 1-5d cultured PMBC cell

lines. Reactivity was observed to HAM/TSP lysates (HAM 21 and HAM 19) when probed with Ab#4 (**Fig. 4A**) and for #12 (**Fig. 4B**) at 5d, with increased reactivity to HAM/TSP cell lysates over time in culture (**Fig. 4A and 4B**). Reactivity to ND 24910 lysate (green) did not increase over time in culture and was always decreased as compared to reactivity to HAM cell lysates (pink and blank bars). In addition, there was no increased reactivity relative with time or lysate type (ND vs. HAM) when using the control (non-HTLV) 2F5 antibody. In general, patient generated lysates yielded higher backgrounds than tissue culture cell lines and therefore all values were compared to the ND.

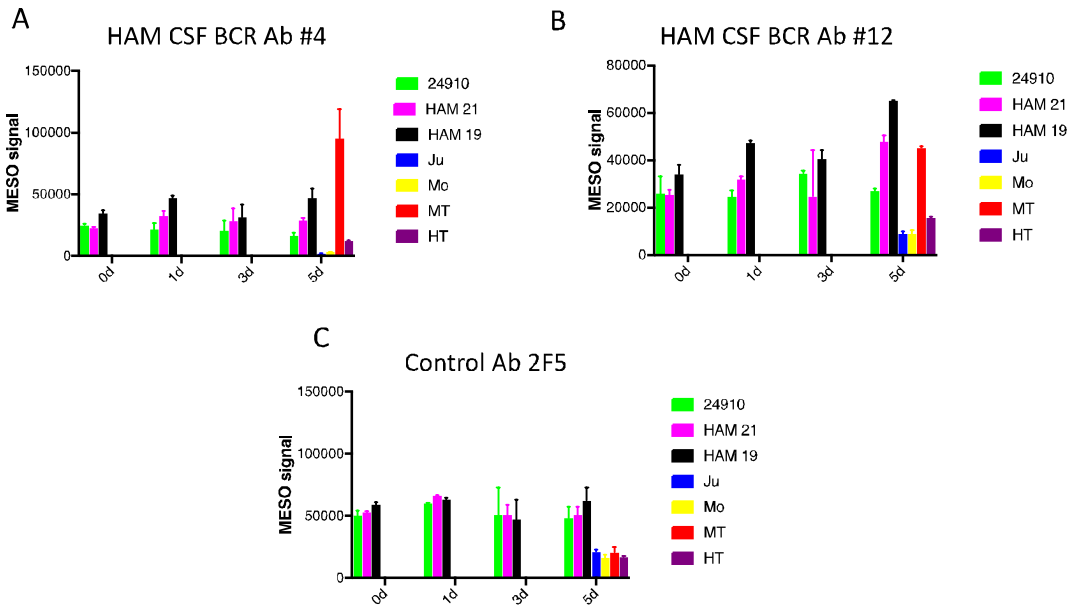

Figure 4: Reactivity to ND and HAM/TSP lysates using Abs generated from HAM/TSP CSF BCRs. (A) Electrochemical ELISA signal results for HAM/TSP CSF BCR (HAM CSF BCR) Ab #4 applied to cell lysates (B) Electrochemical ELISA signal results for HAM/TSP CSF BCR (HAM CSF BCR) Ab #12 applied to cell lysate (C) Electrochemical ELISA signal results for non-HTLV-1 reactive control Ab 2F5 applied to cell lysate

HAM/TSP CSF generated BCRs recognize an HTLV-1 protein similar to p19

In order to specify the HTLV-1 antigen or antigens being recognized by Abs #4 and #12 from HAM/TSP patient CSF, western blots of Jurkat (Ju) and MT2 lysates were performed. Membranes were probed with either HAM TSP patient sera, HTLV-1 p19, HAM Ab #4, HAM Ab #12, and a non-HTLV-1 Ab VRC01.

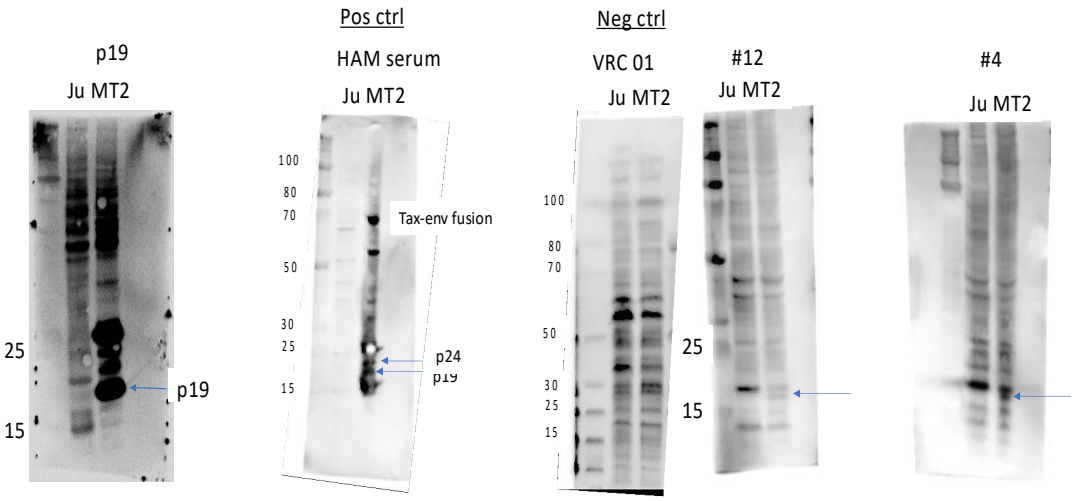

Figure 5: Western blots demonstrating reactivity of Abs generated from HAM/TSP BCRs against proteins expressed by Ju or MT2. P19 blot (far left) represents Jurkat (Ju) and MT2 lysate probed with monocolonal p19 Ab. Positive control (Pos ctrl) represents Ju and MT2 lysate probed with HAM/TSP (HAM) patient serum. Negative control (Neg ctrl) represents Ju and MT2 lsyates probed with non-HTLV-1 related ab (VRC 01). #12 represents Ju and MT2 lysates probed with HAM/TSP CSF BCR Ab #12. #4 represents Ju and MT2 lysates probed with HAM/TSP CSF BCR Ab #4. Blue arrows indicate HTLV-1 p19 band

When analyzing the blots probed with HAM Ab #12 and HAM Ab #4, there is a band between 15 and 25kDa that only appears in MT2 lysates, directly below a band that appears in both Ju and MT2 lysates (**Fig. 5**). Importantly, it appears to be a band similar in size to a protein that is enhanced in MT2 lysates probed with an anti-p19 monoclonal Ab and with HAM/TSP (HAM) patient sera. These results suggest that HAM/TSP CSF

BCR Abs #4 and 12 recognize HTLV-1 p19. Immunoprecipitation assays are currently in progress in which bands of the appropriate molecular weight will be excised and analyzed by mass spectrometry by O. John Semmes, EVMS.

Methods

Growth of Expi 293F cells

Cells are typically grown at 0.5 x10^6 cells/mL in Expi293 Expression Medium (ThermoFisher Scientific) in 250mL flasks.

Transfection of Expi 293F cells

For transfection of plasmids expressing sequenced BCRs into Expi 293F cells, cells should be split at 2 x 10^6/mL in a total volume of 15mL 24h prior to planned transfection. The next day, warm OptiMEM in a 37ºC water bath prior to use. Count cells to ensure viability and growth as they should be at ~3.5 x10^6 cells/mL with >95% viability. Calculate volume of heavy chain (H) and light chain (L) plasmids to get 8μg each. Dilute the H and L plasmid in 400μL of warmed OptiMEM and spin at highest speed for 4 min through .22μm filter (Ultrafree Millipore). Separately combine 1mL of warmed OptiMEM with 40 μL of ExpiFectamine 293 Reagent multiplied by the number of transfections being performed and incubate at room temperature for 5 min. Remove filter from spun plasmids and add 1mL of OptiMEM/ExpiFectamine solution. Incubate for 20min at room temperature. During incubation, seed 15mL of Expi293F cells into 50Ml Bio-Reaction tubes with vented cap (Cell Treat, Pepperell, MA). After incubation, add DNA-reagent mix to cells and incubate in tissue culture incubator with shaking at 37ºC for 16-18h. After 16-18h, add 750μL each of ExpiFectamine 293 Transfection Enhancer 1 and ExpiFectamine 293 Transfection Enhancer 2. Incubate cells with shaking at 37ºC for an additional 4+ (typically 4) days. Supernatant can then be collected for antibody purification. The workflow for this procedure is illustrated in **Fig. 6.**

Purification of antibodies

Regardless of initial isotype sequenced, all antibodies produced were IgG. As such, antibodies were purified from tissue culture supernatants via affinity chromatography.

BCR Antibody testing

BCRs were cloned from 3 HAM/TSP CSF samples and subsequently transfected in 293 F cells for antibody purification (Brandon DeKosky, Vaccine Research Center, NIH). Purified antibodies were tested for anti-HTLV-1 reactivity using HTLV-1 infected lysates C8166, HUT102, TL-Om1, and MT2 with the use of Jurkat and MOLT-3 lysates as negative controls. Lysates were generated from cell pellets homogenized on a Misonix sonicator 3000 in 1X PBS. This was also done for freshly thawed and 1,2,3,4 and 5d culture PBMCs from 2 HAM/TSP patients and 1 ND. Lysates were applied to MESO Sector Imager 96-well High-Bind plate (MSD Technologies) at 1μg per well in duplicate O/N. The plate was then blocked with Blocker A for 2h, washed with PBS x2 and then probed with antibodies generated from HAM CSF BCRs (1μg/ well) for 1h with shaking in diluent 100. After a repeat wash, the plate was probed with secondary Ab (goat Anti-hu IgG Sulfa, 1:100, MSD Technologies). After a final wash, MSD Read buffer was added at 1:2 dilution (2X) in Ultra Pure Water and the plate was read using a MSD Sector Imager (courtesy of Dr. Avi Nath).

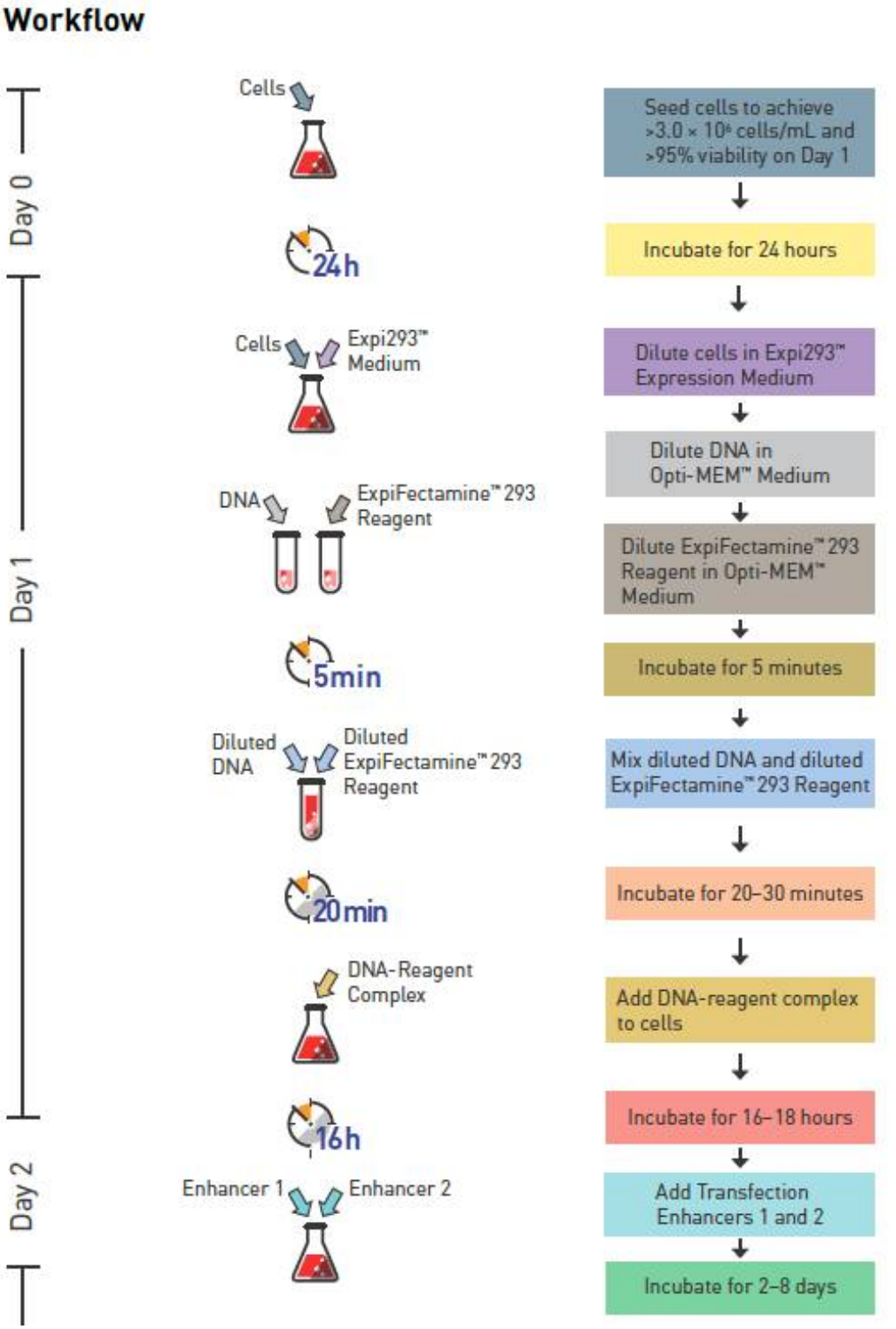

Figure 6: Schematic of transfection of Expi293F cells for antibody production https://assets.thermofisher.com/TFS-Assets/LSG/manuals/MAN0006694_ExpiFectamine293_Transfec_QR.pdf

Anti-HTLV-1 protein verification

Jurkat and MT2 lysates (sonicated) were loaded (10µg) into a 4-12% Bis-Tris gel and run at 200V for 45min. Transfer occurred in an X-blot module onto 0.45µm Nitrocellulose membrane. After blocking, primary Ab (Ab #4, #12, p19 and ctrl VRC01) were applied overnight. After processing, bands were imaged on an ECL Imager (Bio Express Lum C) with HRP (Advansta Western Bright Quantum, Menlo Park, CA). For band verification, lysates were run on a 4-12% Bis-Tris gel for 45min at 200V, after which the gel was wash 3x with 100mL of deionoized water. The gel was then stained with Coomassie dye (Thermo Fisher Scientific Simply Blue SafeStain) for 1h at RT followed by a wash O/N with deionized water at RT. This was followed by another wash for 1h the following day. Gel fragments were sent to Dr. John Semmes for band analysis by mass spectrometry.

Immunoprecipitation

10µg of Jurkat and MT2 homogenized lysates diluted in 200µL of 1X PBS were used for immunoprecipitation (IP). Prior to IP, 50µL of Immunoprecipitation Kit Dynabeads® Protein G (Thermo Fisher Scientific) were placed on a magnet, followed by removal of supernatant. The beads were resuspended with 10µg of ab of choice diluted into 200µL of Binding & Wash Buffer. Incubate with rotation 20min at room temperature (RT). Magnetize suspension to remove supernatant and wash 1X with 200µL of Binding and Washing Buffer. Add Resuspended lysate (200µL) and incubate at RT with rotation for 1h30min (up to 2h). Magnetize suspension to remove supernatant and wash beads 3 x

200µL with Washing Buffer. Resuspend beads in 100µL of Washing Buffer and transfer to a clean microcentrifuge tube. Magnetize and remove supernatant. Resuspend in 20µL of Elution buffer and 10.5µL of LDS Sample (7.5µL 4X LDS and 3.0µL 10X DTT). Gently pipet to resuspend and then heat at 95^0C for 3-5min. Magnetize and load the supernatant onto 4-12% Bis-Tris gel (Thermo Fisher Scientific). Run at 200V for 55min in 1X MES Running Buffer.

Immunoprecipitation with crosslinking

Prior to IP, make 20mM Na_2HPO_4, 0.15M NaCl, 100mM BS^3 (Stock Solution), 5mM BS^3, and 1M Tris-HCl pH 7.5 (Quenching Buffer). 10µg of Jurkat and MT2 homogenized lysates diluted in 200µL of 1X PBS were used for immunoprecipitation (IP). Prior to IP, 50µL of Immunoprecipitation Kit Dynabeads® Protein G (Thermo Fisher Scientific) were placed on a magnet, followed by removal of supernatant. The beads were resuspended with 10µg of ab of choice diluted into 200µL of Binding & Wash Buffer. Incubate with rotation 30min at room temperature (RT). Magnetize suspension to remove supernatant and wash 2X with 200µL of Conjugation Buffer (20mM Na_2HPO_4, 0.15M NaCl). Resuspend in 250µL of 5mM BS^3 and incubate with rotation at RT for 30min. Quench crosslinking reaction with 12.5µL Quenching Buffer. Incubate with rotation for 15min at RT. Wash crosslinked beads 3X 200µL Binding and Washing Buffer. Add Resuspended lysate (200µL) and incubate at RT with rotation for 1h30min (up to 2h). Magnetize suspension to remove supernatant and wash beads 3 x 200µL with Washing Buffer. Resuspend beads in 100µL of Washing Buffer and transfer

to a clean microcentrifuge tube. Magnetize and remove supernatant. Resuspend in 20µL of Elution buffer and 10.5µL of LDS Sample (7.5µL 4X LDS and 3.0µL 10X DTT). Gently pipet to resuspend and then heat at 95^0C for 3-5min. Magnetize and load the supernatant onto 4-12% Bis-Tris gel (Thermo Fisher Scientific). Run at 200V for 55min in 1X MES Running Buffer.

Staining gels for band visualization

After gels were run, they were carefully removed from packaging and placed in 100cm plate for washing. Wash gel 3X 5 min with 100mL Ultra Pure or Molecular Biology Grade Water. Add Simply Blue (Thermo Fisher Scientific) Coomassie Stain and incubate for 1-2h with shaking at RT. Remove stain and add 100mL Ultra Pure or Molecular Biology Grade water and rotate with shaking O/N. Remove water and re-wash with 100mL UltraPure or Molecular Biology Grade water for 1h and then proceed with gel imaging or excision of bands of interest.

Chapter 5

Discussion and Future Directions

Discussion

HTLV-1 is a human retrovirus that is prevalent in endemic regions scattered around the globe. Although HTLV-1 can be transmitted with high efficiency by acquisition of large boluses of virus through blood transfusions or organ donations, the virus is considered to have a low efficiency of infection due to low levels of cell-free virus; indeed, *in vitro* infections are performed with the addition of infected cells (Donegan et al., 1994; Lairmore et al., 2012; Yamamoto et al., 1982). Most infection occurs through breast-feeding, with up to 20% of children breastfed >6mo acquiring the virus (Goncalves et al., 2010). Since, HTLV-1 infection has been in the population for millions of years, most individuals remain asymptomatic, however up to 10% can go on to develop Adult T cell leukemia (ATLL) or HTLV-1 associated myelopathy/tropical spastic paraparesis (HAM/TSP (Li et al., 1999).

HTLV-1 primarily infects $CD4^+$ T cells, in particular the subset of $CD4^+CD25^+$ T cells or regulatory T cells. The vast majority of virus in HAM/TSP patients can be isolated from this subset and thus it serves as a viral reservoir (Yamano et al., 2009; Yamano et al., 2004). In ATLL, circulating leukemic cells are usually characterized as $CD4^+CD25^+$ T cells expressing FoxP3 (Karube et al., 2004). This has led to a prevailing theory suggesting that ATLL results from the clonal expansion of infected regulatory T cells, resulting in a largely suppressive immune environment that allows for leukemic cells to escape immune detection (Chen et al., 2006; Yano et al., 2007). Indeed, isolated ATLL patient Tregs suppress as well as Tregs from a ND (Chen et al., 2006; Yano et al., 2007) and have hypomethylation of the FoxP3 TSDR (Shimazu et al., 2016). Paradoxically, despite the presence of infected Tregs in HAM/TSP as well, isolated

HAM/SP patient Tregs do not suppress the activation of Teffs and instead have been shown to be pro-inflammatory (Araya et al., 2014; Yamano et al., 2005). Since ATLL and HAM/TSP are both consequences of HTLV-1 infection, how does the virus lead to different immune consequences while infecting the same cell type? This question is likely answered in the analysis of virus, host, and environmental factors, all of which contribute to diseases caused by ubiquitous viruses. When several variables are analyzed, one particular factor stands out: HTLV-1 gene expression. Specifically, HTLV-1 Tax and HBZ are expressed differentially in patients with ATLL vs. HAM/TSP **(Fig. 1)** (Araya et al., 2011). These initial observations, along with the reduced functional suppression of HAM/TSP Tregs, prompted the question of how HTLV-1 gene expression ultimately leads to Treg dysfunction and overall immune dysregulation in HAM/TSP. Though controversial, this has been explored from several angles through experiments described in this thesis.

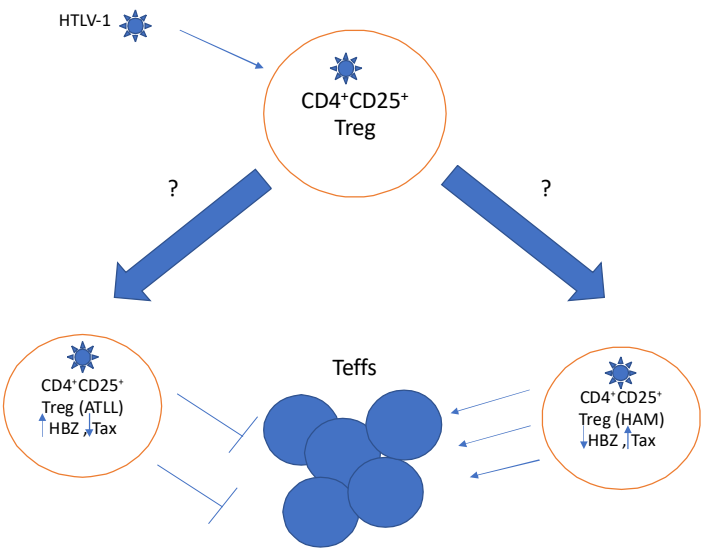

Figure 1: Certain factors allow HTLV-1 infected Tregs to favor the development of ATLL or HAM/TSP

In **Chapter 2**, the alterations in HAM/TSP Tregs were explored from a genetic approach. In addition to a reduced ability to suppress proliferation, HAM/TSP Tregs were found to have decreased demethylation (or increased methylation) in the FoxP3 Treg-specific demethylated region (TSDR). As discussed in the **Introduction,** this area of the FoxP3 locus confers stable expression of FoxP3 in Tregs. It allows Tregs to maintain an inhibitory phenotype even in activated environments, as would be encountered in the CNS of HAM/TSP patients. Prior experiments in the Jacobson laboratory suggested that HTLV-1 Tax reduced FoxP3 expression (Yamano et al., 2005). In **Chapter 2 Fig. 9**, incubation of HAM/TSP PBMCs and $CD4^+$ T cells resulted in a decline in TSDR demethylation concomitant with an increase in HTLV-1 Tax expression. This suggests that the previous observations of decreased FoxP3 mRNA expression that occurred with Tax transfection was due to reduced demethylation of the FoxP3 TSDR. Furthermore, reduced demethylation of the TSDR correlated with reduced Treg suppressive capacity (Anderson et al., 2014).

There has been some debate in the field over the observed changes in Treg suppression in proliferation assays. Some have postulated that effects seen are due to induction of CD25 on non-Tregs with HTLV-1 infection, thereby creating cells that phenotypically resemble Tregs but which are incapable of immune suppression (Satou et al., 2011). Other researchers suggest that that HTLV-1 preferentially induces the formation of pTregs, which as noted in the **Introduction,** can be slightly less stable in inflammatory environments depending on method of induction (Satou et al., 2011). HBZ has been reported to induce pTregs (Satou et al., 2011; Yamamoto-Taguchi et al., 2013). Induction of pTregs might explain why HTLV-1 infected Tregs are more prone to

convert to IFN-λ producing cells and also might explain the reduced levels of TSDR demethylation detected (Anderson et al., 2016; Yamano et al., 2009). These explanations would argue that HAM/TSP is a result of an increase in pTregs which are more prone to convert to non-Tregs in inflammatory environments, thus lowering the ratio of suppressive nTregs entering into inflammatory sites which may result in a loss of the immunosuppressive response. Yet, recent experiments conducted in the Yamano laboratory revealed reduced Treg suppression upon Tax-GFP transduction of ND $CD4^+CD25^+$ T cells. ND $CD4^+CD25^+$ T cells transduced with GFP without a transgene did not show altered suppression of Teffs (Araya et al., 2014). Initial experiments shown in **Chapter 2** suggests that this reduced proliferation is due to a reduction in TSDR demethylation, although it is too early to conclude that this was a result of HTLV-1 specific genes.

Other viral genes could potentially have a similar effect on the TSDR and Treg suppression, but since HTLV-1 uniquely infects Tregs, a reduction in Treg suppression may only be observable with viruses that infect $CD4^+CD25^+$ T cells. However, transfected HTLV-1 *env* did not result in a similar decline in FoxP3 expression (Yamano et al., 2005). Furthermore, preliminary experiments presented in **Chapter 2** showed that the decline in FoxP3 TSDR demethylation is likely HTLV-1 Tax specific. To confirm that Tax is increasing methylation in the TSDR, there are ongoing experiments which are utilizing a FoxP3 TSDR plasmid that has been shown to decrease luciferase activity when exposed to methylating agents (Polansky et al., 2010). We hope to observe similar changes to the luciferase activity of this plasmid after transduction of HTLV-1 Tax as compared to the control and HBZ pseudoviruses. Those results will build into an overall

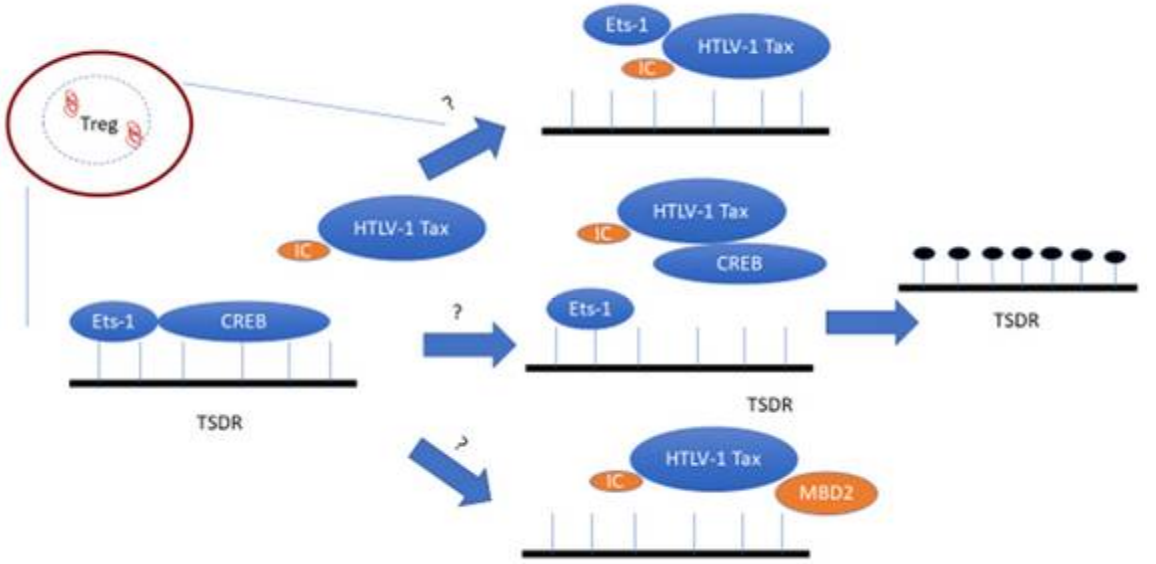

Figure 2: HTLV-1 Tax interferes with transcriptional regulators or binds to methyltransferases to increase TSDR methylation

pathogenesis model where HTLV-1 integrates into the genome of Tregs, infecting them through binding of a combination of three separate cell receptors postulated to be necessary for HTLV-1 infection: neuropilin-1 which is highly expressed on Tregs, GLUT1, and HSPGs. After integration, the virus begins to express several genes, most important of which is HTLV-1 Tax, a multifunctional regulatory protein that has several binding partners discussed in the **Introduction**. HTLV-1 Tax directly leads to reduced Treg suppression possible through reduced demethylation of state of FoxP3 TSDR (Anderson et al., 2014).

As outlined in **Fig. 2**, HTLV-1 Tax can lead to increased methylation in the TSDR through several potential mechanisms. Increased methylation may occur through Tax binding of either Ets1 or CREB, both of which bind to the TSDR while it is in a demethylated state. There are suggestions that de novo methylation occurs in areas of the

genome if there are inappropriate levels of transcription factors for binding of the demethylated region (Domcke et al., 2015; Palacios et al., 2010). Tax could also bind and recruit MBD2, a methyltransferase, and induce increased methylation in the TSDR. Future experiments will need to delineate the mechanisms involved in increased methylation at the TSDR that occurs in Tregs in HAM/TSP.

As discussed in the **Introduction**, Tregs have been observed to suppress by several mechanisms. Thus far, this involves: 1) direct cell-cell contact with interactions between CTLA-4, lymphocyte function -ssociated antigen 1 (LFA-1), latency associated protein (LAP), PD-1/PDL-1, neuropilin-1, CD95, LAG3, CD73 and their cognate receptors on effector cells (Delgoffe et al., 2013; Gotot et al., 2012) (Schmidt et al., 2012) ;2) production of inhibitory cytokines and other factors including IL-10, TGF-β, IL-35, Granzyme A, and perforin ;3) Absorption of stimulatory molecules such as Il-2 and ATP ;4) modulation of DC activity and ;5) a newly discovered method of delivery of inhibitory miRNAs to effector cells via exosomes (Okoye et al., 2014; Vignali et al., 2008).

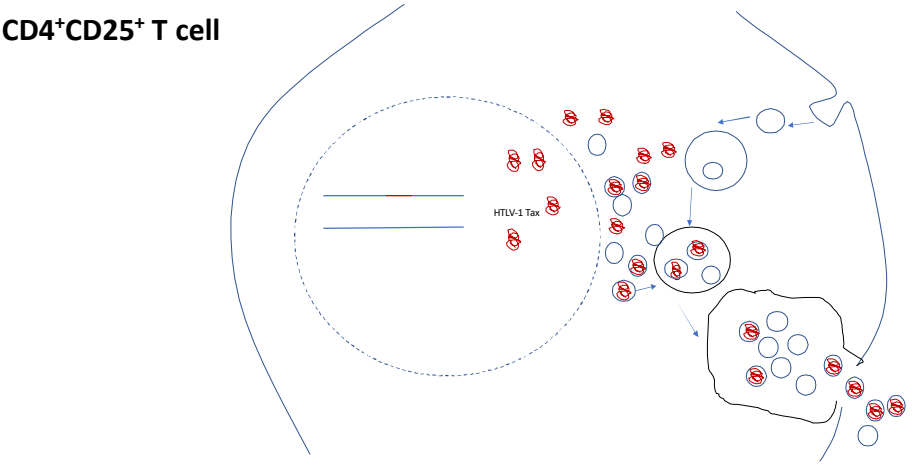

Figure 3: Infected $CD4^{+}CD25^{+}$ T cells produce exosomes containing Tax

While the observation of exosome production was made in mice (Okoye et al., 2014), **Chapter 3** demonstrated that human Tregs, along with several other T cell subsets in the immune system, produce exosomes (**Chapter 3 Fig 6H)**. Since Treg exosomes typically carry inhibitory molecules such as miRNAs in the lumen and CD39/CD73 at the membrane (Schuler et al., 2014), introduction of HTLV-1 products into shed exosomes (**Fig. 3**) would necessarily alter the function of Treg exosomes. Indeed, we found evidence for the presence of HTLV-1 Tax protein, HTLV-1 *tax* mRNA, and HTLV-1 HBZ protein in exosomes isolated from HAM/TSP PBMCs (**Chapter 3**). Based on the observation of $CD4^+CD25^+$ T cells expressing HTLV-1 Tax at much higher levels than any other immune subset in HAM/TSP, it was postulated that these cells are likely the major source of Tax^+ exosomes. Initial experiments testing the levels of Tax present in exosomes produced by $CD4^+$ and $CD8^+$ T cells were inconclusive and must be repeated (data not shown). HAM/TSP T cells spontaneously proliferate when in the presence of other immune subsets, thus cell sorting may actually diminish HTLV-1 gene expression as well as exosome production. Future experiments will pair sorted T cells with irradiated autologous PBMCs which should support T cell proliferation. This should allow for the capture of exosomes from sorted T cell culture such that the question of which subset produces the most Tax^+ exosomes is better answered. Regardless, it can currently be stated that without feeder cells, $CD4^+CD25^+$ T cells from HAM/TSP patients produce more exosomes than other HAM/TSP subsets (**Chapter 3 Fig. 6H**).

In addition to differences in the cargo in exosomes produced by HAM/TSP PBMCs compared to ND PBMCs, there were clear differences in the function of these exosomes. Specifically, Tax^+ exosomes could sensitize targets for CTL lysis in an Ag-

specific immune response. This is in contrast to ND exosomes which were never able to sensitize targets for Tax-specific lysis (**Chapter 3 Fig. 9**). Exosomes from conventional Tregs should not prime an activated immune response and instead usually suppress activated responses in effectors (**Fig. 4**). The presence of HTLV-1 products, in particular Tax, has thus changed the function of secreted exosomes from suppressive to inflammatory. Indeed, to our knowledge, this the first time that uptake of exosomes by target cells has been shown to lead to their lysis, suggesting similar mechanisms occurring *in vivo*. Exosome uptake by uninfected recipient cells may be a method by which uninfected cells can "carry" HTLV-1 proteins and RNA, however briefly, making them targets for HTLV-1 specific immune recognition. Furthermore, Tax^+ exosomes reduced the stability of Tregs (**Chapter 3 Fig. 11**) and also decreased the number of $CD4^+PD\text{-}1^+$ T cells. This suggests that in addition to a reduced Treg subset, exosome exposure may also reduce T cell susceptibility to suppression. These observations will need to be expanded upon in future studies.

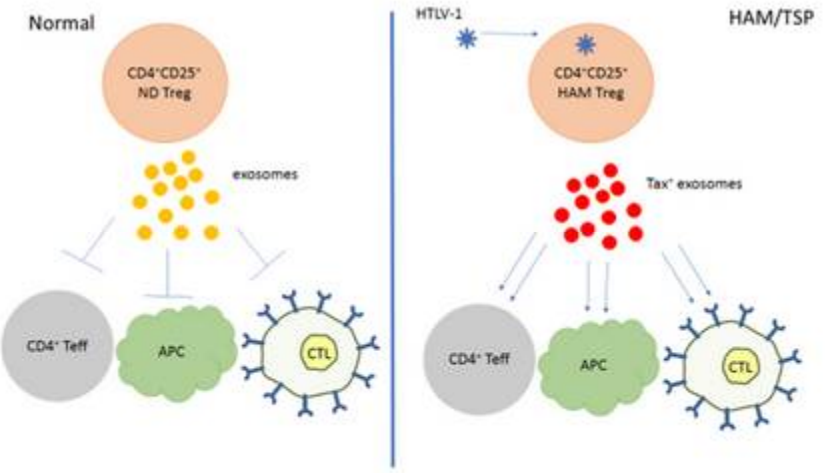

Figure 4: Tax containing exosomes are activating in HAM/TSP, whereas exosomes produced by ND $CD4^+CD25^+$ Tregs are instead of inhibitory

In addition to changes in $CD4^+$ T cell populations, the potential consequences of Treg dysfunction were expanded upon by analyzing HAM/TSP CSF BCRs in **Chapter 4**. Tregs are able to reduce proliferation in several immune subsets including B cells. It was demonstrated that BCRs do recognize HTLV-1 associated proteins, as they were able to detect antigens expressed by both HTLV-1 infected cell lines (**Chapter 4 Fig. 3**) and HAM/TSP PBMC lysates (**Chapter 4 Fig. 4**). Although initial western blots did not show detection of HTLV-1 Tax by Abs generated from HAM/TSP CSF BCRs, we did demonstrate detection of the HTLV-1 specific protein, p19 (**Chapter 4 Fig. 5)**. P19 is a portion of the envelope of HTLV-1 and was not in the initial group of proteins that were probed in HAM/TSP derived exosomes. However, given data that other viral envelope proteins have been detected in exosomes in other diseases (Masciopinto et al., 2004), p19 will be added to future studies of HAM/TSP exosome content from PBMCs and in the CSF. This will be important given additional observations of B cell reactivity to exosome content (Bashratyan et al., 2013).

One question that arises with the finding of HTLV-1product sorting into exosomes is whether transference of Tax by exosomes perpetuates Treg dysfunction by altering the methylation state of recipient Tregs. Preliminary experiments could not detect Tax protein by flow cytometry 24h or 72h in cells exposed to Tax^+ exosomes, suggesting that either the Tax is expressed only transiently in recipient cells or that the amounts of protein transferred are too low to be detected by this method (data not shown). ELISA and western blotting also suggested that the amount of Tax protein carried by exosomes would be in the range of ng, an amount that may not be sufficient to cause changes in the epigenome.

The observation of immune directed responses from exposure to HAM/TSP exosomes is even more pertinent considering the detection of exosomes containing Tax in the cell-free CSF of HAM/TSP patients (**Chapter 3 Fig. 8B**). HAM/TSP is characterized by demyelination of the pyramidal tracts resulting in spinal cord atrophy (Jacobson, 2002). HAM/TSP patients are distinguished from ACs by the increased presence of HTLV-1 specific T cells in both the CSF and peripheral blood (Elovaara et al., 1993; Kubota et al., 2002). The loss of oligodendrocytes and neurons has been attributed to the actions of HTLV-1 specific T cell through: a bystander effect of neurotoxic cytokines, CNS damage through direct CTL lysis of oligodendrocytes and neurons by viral mimicry, and/or an off-shoot of autoimmune responses initiated in an inflammatory milieu. Each of these hypothesized immunopathogenic mechanisms suggests that CNS damage is not necessarily due to HTLV-1 expression in CNS resident cells. Indeed, there is no evidence for infection of oligodendrocytes or neurons by HTLV-1 (Lepoutre et al., 2009). Could uptake of Tax^{+} exosomes by resident glial cells then explain HTLV-1 specific responses occurring in the CNS? Uptake of exosome by oligodendrocytes, neurons, astrocytes and/or microglia endocytose exosomes has been reported (Fitzner et al., 2011; Frohlich et al., 2014; Fruhbeis et al., 2013). Furthermore, dissemination and processing of exosomes by these cell types has already been implicated in the immunopathogenesis of several other neurodegenerative diseases, including Alzheimer's disease and Creutzfeld-Jacob Disease (CJD) (Bellingham et al., 2012; Xiao et al., 2017). While *in vitro* experiments suggest uptake of exosomes carry HTLV-1 Ag by target cells may be a mechanism of Ag-specific immune directed responses to the CNS resident cells in

HAM/TSP patients, observations of responses to exosome exposure in CNS resident cells must still be made.

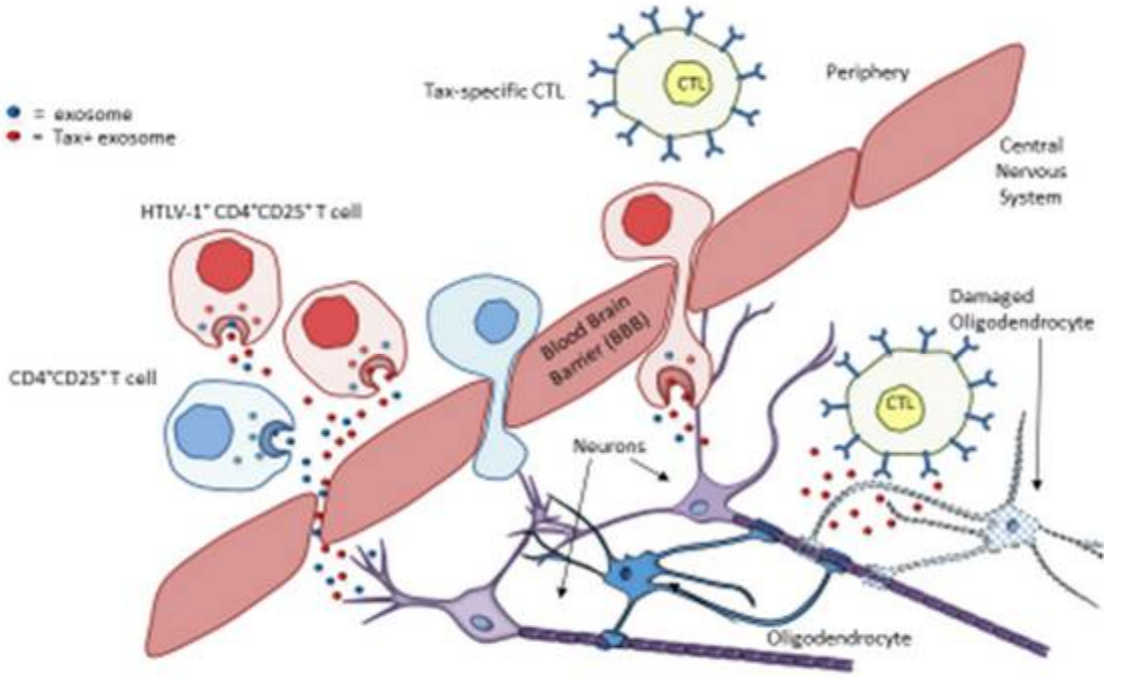

Figure 5: How HTLV-1 Tax$^+$ exosomes may contribute to the immunopathogenesis of HAM/TSP in CNS

Currently, while there are animal models of HTLV-1 infection, none have resulted in neurologic disease. Newer humanized mice models were created in the hopes of more precisely recapitulating what occurs in the human host. Thus, future experiments should involve *in vitro* application of HTLV-1 Tax$^+$ exosomes to oligodendrocyte, astrocytes, and neurons to assess for increased cell death or similar Ag recognition by HTLV-1 Tax-specific CTLs. Additionally, if possible, purified exosomes should be administered intrathecally to mice previously infected with HTLV-1 with intact immune responses. This could represent the next stage in animal models for HAM/TSP and

would help to clarify the extent to which exosomes containing HTLV-1 gene products perpetuate inflammatory immune responses in the CNS in HAM/TSP.

The picture being built demonstrates that HTLV-1 infects Tregs, altering their ability to suppress through reduced demethylation in the TSDR and altered exosomes that can sensitize an immune response rather than suppress. Furthermore, exosomes found in the CNS, likely produced by infiltrating T cells or independently crossing over the blood brain barrier (BBB) after being produced in the periphery, can potentially be captured by uninfected CNS resident cells. These viral-exosome stimulated CNS resident cells can then be recognized by HTLV-1 Tax specific CTLs and subsequently lysed (**Fig. 5**). With so many facets of the inflammatory milieu developing from the alteration in Treg function that occurs upon infection with the HTLV-1, treatment strategies that target the virus or Treg subset should be considered. Currently, there is a trial of raltegravir which is an HIV integrase inhibitor and has been shown to have activity against HTLV-1, being conducted in our lab. A preliminary western blot on exosomes isolated from the PBMCs of one trial patient showed that Tax content in isolated exosomes diminished after 6mos on trial (data not shown). Future work will analyze changes in Tax and HBZ protein in isolated exosomes from trial patients, as this could be an "off-target" benefit of antiretroviral therapy.

There are other potential methods to reduce Tax^+ exosomes present in HAM/TSP patients. One alternative is to treat with exosome-inhibitors. In addition to GW4869, there are other exosome release inhibitors such as chloramidine and bisindolymaleimide-I which have been shown to be effective while maintaining cell viability *in vitro* (Kosgodage et al., 2017). However, none of these agents has been used clinically to treat

patients to date and it is unclear if they have associated toxicities. Another agent proposed to potentially reduce HTLV-1 Tax content in exosomes, if not exosome production, was IFN-α. Western blots comparing exosomes isolated from untreated and INF-α-treated HAM/TSP PBMCs are still in process.

Rather than targeting exosome content or production, restoration of TSDR demethylation could potentially restore Treg suppressive capacity. It has been shown that Teffs can be transformed into suppressive Tregs after treatment with demethylating agents (Chan et al., 2014). These "transformed" Tregs were capable of inhibiting immune responses to self (Wong et al., 2011; Zheng et al., 2009). It remains to be seen if demethylating agents such as 5-Azacytidine or Epigallocatechin-3-gallate (ECCG, a key component of green tea) would have similar results in HAM/TSP. As of yet, "transformed" Tregs have not been assessed for changes in exosome production or content.

How Tregs and exosomes contribute to the overall immunopathogenesis in HAM/TSP has brought about many ideas for future therapies for patients in a disease which currently does not have a standard treatment or cure. Importantly, screening of exosomes in asymptomatic carriers (ACs) could identify individuals who may develop into HAM/TSP. As demonstrated in **Chapter 3 Fig. 14, Fig. 15,** Tax^{+} exosomes could be detected from an individual who was initially classified as an AC, at a point when he was beginning to present with neurologic symptoms. He is now being followed closely by our clinical staff. Of note, he has yet to show the typical spinal cord atrophy seen in HAM/TSP patients, although this may take years to decades to observe. Therefore, this individual could be targeted for early interventions such as steroids or immune

modulators, prior to the onset of more damage to his CNS. The goal would be to find patients at the early onset of disease and hopefully halt the deleterious inflammatory response in the CNS that leads to neurologic functional decline.

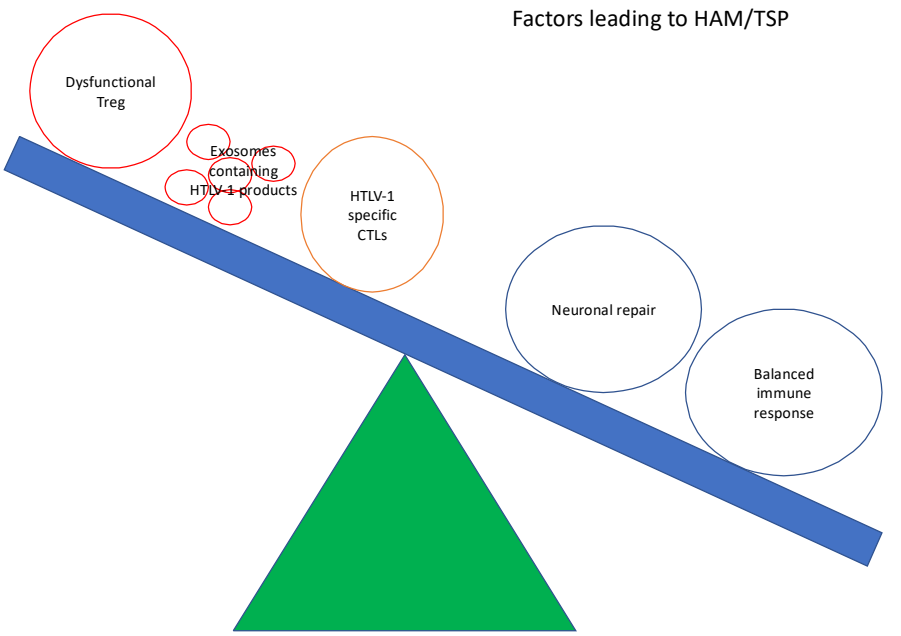

Figure 6: Dysfunctional Tregs, exosomes with HTLV-1 products, and HTLV-1 specific CTLs create imbalanced immune responses that lead to HAM/TSP

One of the challenges in HAM/TSP is that most patients are not diagnosed and do not receive any form of treatment until they have had long-standing disease. For example, the HAM/TSP cohort at the NIH consists mostly of patients who have had neurologic symptoms for more than 10 years. A concern in the field is that for the vast majority of HAM/TSP patients, therapeutic interventions may not be beneficial because they are now far removed chronologically from the initial insults leading to their current level of disability. Of course, halting further inflammation and plateauing of disease progression is also a reasonable outcome of therapy. There is evidence for some clinical recovery in models of MS after immune subsets involved in the pro-inflammatory

response have been removed or controlled (Atkins et al., 2016). Perhaps remodeling or removing secreted exosomes containing HTLV-1 products would remove one part of the fulcrum pushing the HAM/TSP immune response into imbalance (**Fig. 6**). Improving Treg function would further right the balance to a hopefully more normal immune response in which neuronal repair could occur.

Understanding the role of exosomes and Tregs in HAM/TSP is not solely beneficial to HAM/TSP but also to other neuroinflammaotry diseases in which Treg dysfunction and/or exosomes are implicated. As mentioned, MS, progressive multifocal leukoencephalopathy (PML), and many undiagnosed encephalitides may be associated with Treg and/ or exosome involvement in disease pathology. Indeed, we were able to isolate exosomes from the CSF of MS patients (**Chapter 3 Fig. 8**) although these were not probed for content. When exosomes from MS sera were assayed for protein content by another group, Mog proteins were detected (Galazka et al., 2017). Furthermore, Treg dysfunction has long been implicated in MS progression, suggesting that alterations in the TSDR and exosome production or content could serve as potential therapeutic targets in the disease (Buc, 2013; Dalla Libera et al., 2011). Moreover, there are many indications in the literature that MS has a viral trigger (Kakalacheva et al., 2011; Virtanen and Jacobson, 2012). Probing of exosomes could potentially reveal footprints of the triggering virus that initiated a proinflammatory response. Similarly, free virus cannot be detected in the CSF of the majority of encephalitides in which a viral agent is implicated, but may have been cleared or established latency in an undefined reservoir. Analysis of exosomes containing likely viral candidate proteins and/or mRNAs could help to direct future treatments and identify the inciting agent in encephalitides of unknown origin.

Collectively, the work pursued through the body of this thesis represents a step forward in the understanding of the factors involved in the immunopathogenesis of a virus-associated neurologic disease. HTLV-1 Tax is widely accepted to alter the function of Tregs in HAM/TSP. This dysfunction can now be better defined as originating from decreased demethylation of the FoxP3 TSDR, which typically allows for stable FoxP3 expression and suppressive function, and altered cargo in secreted exosomes. Packaging of HTLV-1 Tax and other HTLV-1 products alters non-inflammatory exosomes to exosomes that can sensitize targets for immune recognition by HTLV-1 specific CTLs, perhaps perpetuating damage to uninfected CNS resident cells in HAM/TSP. Proposed treatment strategies that target exosome production and Treg function could potentially restore immune stability, thereby allowing a milieu favorable to CNS repair. This work has applications in other neuroinflammatory disorders such as MS and could help in the diagnosis of previously "asceptic" encephalitides. Our patients are what motivate the continued search for a full understanding of HAM/TSP, so we hope that the research presented here can increase the treatment options available for HAM/TSP patients and those suffering from other neuroinflammatory and neuroviral diseases.

Future directions

As suggested by the research presented in this thesis, more experiments are needed to explore the role that changes in exosome content might play in Treg suppressive capacity and how these factors contribute to HAM/TSP immunopathogenesis. Currently, the data presented suggests that altered exosome

content in HAM/TSP is associated with increased inflammation, but a causative relationship between loss of Treg suppression/ increased inflammation and altered exosome content has not be defined. An experiment introducing HTLV-1 proteins into produced exosomes and measuring changes in effector cell proliferation in the presence of altered exosomes could better illustrate the relationship between Treg suppression and exosome content. Other ways to further explore potential increases in inflammation due to the presence of HTLV-1 antigens in exosomes could include exploring the differences in the contents of exosomes produced by ND and HAM/TSP Tregs. While we demonstrated the presence of HTLV-1 Tax protein, *tax* mRNA, and HBZ protein (**Chapter 3**), there are other HTLV-1 proteins such as Env, p19, p24, and Rex that may potentially also incorporate into produced exosomes. Initial work suggested that ubiquitination might increase localization of unmodified forms of proteins into the exosome (**Chapter 3, Fig. 22**), but the mechanisms involved in shuttling specific proteins into HAM/TSP exosomes are poorly understood and thus far do not appear to preclude the inclusion of several HTLV-1 proteins.

Other ways to explore the role of altered exosome content in HAM/TSP immunopathogenesis might include studying exosomes in larger subsets of ACs. Initial work demonstrated that the detection of HTLV-1 Tax in exosomes in AC CSF were related to early neurologic decline (**Chapter 3, Fig. 14**). While most AC do not typically undergo lumbar puncture, the initial cohort of AC PBMC samples showed that AC PBMC exosomes are less likely to contain HTLV-1 Tax (**Chapter 3, Fig. 13**). Therefore, it would be important to expand on this observation in a larger cohort and include other HTLV-1 proteins to gain a better understanding of whether the presence of

HTLV-1 antigens in produced exosomes might contribute to neurologic decline. Culture of isolated PBMCs from AC and analysis of their produced exosomes could serve as an experimental tool in determining which AC should be followed closely for development of HAM/TSP. These individuals would also be ideal targets for early clinical interventions in the hopes of preventing progression to neurologic dysfunction.

In addition to proteins, *tax* mRNA was found to be present in exosomes while *hbz* mRNA could not be detected (**Chapter 3, Fig. 10**). It had been suggested that this was due to differential cellular localization (Rende et al., 2011). However, due to the role of *hbz* as an antisense RNA, *hbz* could be hybridized with other mRNAs, preventing its detection (Barbeau and Mesnard, 2011). Future experiments could focus on methods for denaturation of cellular RNAs to understand if lack of *hbz* mRNA in HAM/TSP exosomes is due to cellular localization or due to oligomerization.

In addition, one of the premises introduced in the **Discussion** was that secreted HAM/TSP Treg exosomes are inflammatory rather than inhibitory, due to the inclusion of HTLV-1 products. The ability of the exosomes to sensitize targets for CTL lysis supported this hypothesis, however an altered Treg suppression due to these HTLV-1 antigen containing exosomes still remains to be seen. Treg exosomes have been suggested to be inhibitory both through their miRNA profile and through suppression experiments (Okoye et al., 2014). Future experiments could incorporate a miRNA profile of HAM/TSP Treg exosomes vs ND Treg exosomes to determine if changes in proliferation or suppression in effector cells could be observed. Effects on effector cells were preliminarily investigated by probing BCR profiles in HAM/TSP patients. While early results suggest the presence of BCRs that recognize HTLV-1 p19 in HAM/TSP

patient CSF (**Chapter 5, Fig. 5**), this particular protein was not assessed in exosomes. Therefore, as suggested earlier, p19 should be profiled in HAM/TSP vs ND exosomes, especially those isolated form the CSF. Additionally, B cells and other effector T cells could be assessed for their proliferative or suppressed responses after exposure to ND or HAM/TSP exosomes.

Considering the initial observations of TSDR demethylation accurately recapitulating Treg dysfunction in HAM/TSP (**Chapter 2**), it would be of interest to assess changes in exosome protein and RNA profiles with decreasing TSDR demethylation. This could be accomplished with the application of HDAC inhibitors and other epigenetic modifiers to ND Tregs and assessing both changes to the TSDR and exosome content, or by treatment of HAM/TSP Tregs with similar agents and assessing changes to the TSDR and contents of exosomes. Such experiments may support the use of these drugs in clinical trials for HAM/TSP treatment. Alternatively, treatments that directly target exosome content, such as exosome inhibitors like GW4869 or treatments that decrease HTLV-1 gene expression such as integrase inhibitors like raltegravir could decrease HTLV-1 product localization to exosomes. While other anti-retroviral therapies (ARTs) have not been shown to be effective (Bangham et al., 2015), there is new interest in trials for HAM/TSP patients with newer generations of ARTs. If these could decrease the HTLV-1 proviral load and consequently improve Treg function and exosome content, these could have life-altering benefits.

Additionally, it was suggested that other viruses, such as HHV-6, can infect Tregs (Mine et al., 2014). Therefore, it would be of interest to assess the TSDR methylation status and exosome profiles of HHV-6 infected patients, some of whom develop

neuroinflammatory disease and encephalomyelitis (Reynaud and Horvat, 2013). MS, another neuroinflammatory disorder proposed to have viral triggers has also been suggested to have Treg dysfunction (Fierz, 2017; Virtanen and Jacobson, 2012; Zozulya and Wiendl, 2008). As such, exosome profiling with an emphasis on testing for proteins from commonly implicated viruses such as EBV, CMV and HHV-6 could be undertaken in conjunction with TCR and BCR profiling that is ongoing in the Jacobson lab. This would enable an understanding of whether the content of exosomes in MS might be reflected in the specificities of T cells and B cells that infiltrate the CNS.

Mollaret's meningitis, a recurrent inflammatory meningitis, is potentially associated with HSV-2 infection (Berger and Houff, 2008). Given the ability to detect viral antigens in virus-free cell-free HAM/TSP patient CSF, it would be of interest to perform exosome profiling on the CSF of Mollaret's meningitis patients to assess the presence of viral products, focusing on neurotropic viruses. Similarly, while PML is often thought to be due to a poor immune response to John Cunningham Virus (JCV) in immunocompromised individuals (Saribas et al., 2010), the cell-free virus can be difficult to detect in some PML patients. Exosomes may therefore serve as another potential tool in assessing clinical progression in PML patients undergoing treatment. For example, diminution in the presence of JCV proteins or RNAs could suggest improvement in disease status.

Collectively, the suggested experiments would broaden our understanding of the role of exosomes in Treg suppression and in overall immune activation and neuroinflammation in HAM/TSP and in other virally mediated neuroinflammatory disorders. These observations could guide strategies on which immune subsets to target

or drug treatments to initiate in patients suffering from similar disorders. It is our hope that the work provided in this thesis in conjunction with continuing and future experiments described in this section will explain how altered Treg function and exosome content are related to deleterious effects in neuroinflammatory disease.

References:

Admyre, C., S.M. Johansson, K.R. Qazi, J.J. Filen, R. Lahesmaa, M. Norman, E.P. Neve, A. Scheynius, and S. Gabrielsson. 2007. Exosomes with immune modulatory features are present in human breast milk. *Journal of immunology* 179:1969-1978.

Aida, Y., H. Murakami, M. Takahashi, and S.N. Takeshima. 2013. Mechanisms of pathogenesis induced by bovine leukemia virus as a model for human T-cell leukemia virus. *Frontiers in microbiology* 4:328.

Alenquer, M., and M.J. Amorim. 2015. Exosome Biogenesis, Regulation, and Function in Viral Infection. *Viruses* 7:5066-5083.

Anderson, M.R., Y. Enose-Akahata, R. Massoud, N. Ngouth, Y. Tanaka, U. Oh, and S. Jacobson. 2014. Epigenetic modification of the FoxP3 TSDR in HAM/TSP decreases the functional suppression of Tregs. *J Neuroimmune Pharmacol* 9:522-532.

Anderson, M.R., F. Kashanchi, and S. Jacobson. 2016. Exosomes in Viral Disease. *Neurotherapeutics* 13:535-546.

Andreu, Z., and M. Yanez-Mo. 2014. Tetraspanins in extracellular vesicle formation and function. *Front Immunol* 5:442.

Araya, N., T. Sato, H. Ando, U. Tomaru, M. Yoshida, A. Coler-Reilly, N. Yagishita, J. Yamauchi, A. Hasegawa, M. Kannagi, Y. Hasegawa, K. Takahashi, Y. Kunitomo, Y. Tanaka, T. Nakajima, K. Nishioka, A. Utsunomiya, S. Jacobson, and Y. Yamano. 2014. HTLV-1 induces a Th1-like state in CD4+CCR4+ T cells. *The Journal of clinical investigation* 124:3431-3442.

Araya, N., T. Sato, N. Yagishita, H. Ando, A. Utsunomiya, S. Jacobson, and Y. Yamano. 2011. Human T-lymphotropic virus type 1 (HTLV-1) and regulatory T cells in HTLV-1-associated neuroinflammatory disease. *Viruses* 3:1532-1548.

Arenaccio, C., C. Chiozzini, S. Columba-Cabezas, F. Manfredi, E. Affabris, A. Baur, and M. Federico. 2014. Exosomes from human immunodeficiency virus type 1 (HIV-1)-infected cells license quiescent CD4+ T lymphocytes to replicate HIV-1 through a Nef- and ADAM17-dependent mechanism. *Journal of virology* 88:11529-11539.

Asquith, B., Y. Zhang, A.J. Mosley, C.M. de Lara, D.L. Wallace, A. Worth, L. Kaftantzi, K. Meekings, G.E. Griffin, Y. Tanaka, D.F. Tough, P.C. Beverley, G.P. Taylor, D.C. Macallan, and C.R. Bangham. 2007. In vivo T lymphocyte dynamics in humans and the impact of human T-lymphotropic virus 1 infection. *Proceedings of the National Academy of Sciences of the United States of America* 104:8035-8040.

Atkins, H.L., M. Bowman, D. Allan, G. Anstee, D.L. Arnold, A. Bar-Or, I. Bence-Bruckler, P. Birch, C. Bredeson, J. Chen, D. Fergusson, M. Halpenny, L. Hamelin, L. Huebsch, B. Hutton, P. Laneuville, Y. Lapierre, H. Lee, L. Martin, S. McDiarmid, P. O'Connor, T. Ramsay, M. Sabloff, L. Walker, and M.S. Freedman. 2016. Immunoablation and autologous haemopoietic stem-cell transplantation for aggressive multiple sclerosis: a multicentre single-group phase 2 trial. *Lancet* 388:576-585.

Baecher-Allan, C., J.A. Brown, G.J. Freeman, and D.A. Hafler. 2001. CD4+CD25high regulatory cells in human peripheral blood. *Journal of immunology* 167:1245-1253.

Baecher-Allan, C., V. Viglietta, and D.A. Hafler. 2004. Human CD4+CD25+ regulatory T cells. *Seminars in immunology* 16:89-98.

Baglio, S.R., M.A. van Eijndhoven, D. Koppers-Lalic, J. Berenguer, S.M. Lougheed, S. Gibbs, N. Leveille, R.N. Rinkel, E.S. Hopmans, S. Swaminathan, S.A. Verkuijlen, G.L. Scheffer, F.J. van Kuppeveld, T.D. de Gruijl, I.E. Bultink, E.S. Jordanova, M. Hackenberg, S.R. Piersma, J.C. Knol, A.E. Voskuyl, T. Wurdinger, C.R. Jimenez, J.M. Middeldorp, and D.M. Pegtel. 2016. Sensing of latent EBV infection through exosomal transfer of 5'pppRNA. *Proceedings of the National Academy of Sciences of the United States of America* 113:E587-596.

Bai, X.T., U. Sinha-Datta, N.L. Ko, M. Bellon, and C. Nicot. 2012. Nuclear export and expression of human T-cell leukemia virus type 1 tax/rex mRNA are RxRE/Rex dependent. *Journal of virology* 86:4559-4565.

Baietti, M.F., Z. Zhang, E. Mortier, A. Melchior, G. Degeest, A. Geeraerts, Y. Ivarsson, F. Depoortere, C. Coomans, E. Vermeiren, P. Zimmermann, and G. David. 2012. Syndecan-syntenin-ALIX regulates the biogenesis of exosomes. *Nature cell biology* 14:677-685.

Bangham, C.R., A. Araujo, Y. Yamano, and G.P. Taylor. 2015. HTLV-1-associated myelopathy/tropical spastic paraparesis. *Nat Rev Dis Primers* 1:15012.

Baratella, M., G. Forlani, G.U. Raval, A. Tedeschi, O. Gout, A. Gessain, G. Tosi, and R.S. Accolla. 2017. Cytoplasmic Localization of HTLV-1 HBZ Protein: A Biomarker of HTLV-1-Associated Myelopathy/Tropical Spastic Paraparesis (HAM/TSP). *PLoS Negl Trop Dis* 11:e0005285.

Barbeau, B., and J.M. Mesnard. 2011. Making sense out of antisense transcription in human T-cell lymphotropic viruses (HTLVs). *Viruses* 3:456-468.

Barbi, J., D. Pardoll, and F. Pan. 2014. Treg functional stability and its responsiveness to the microenvironment. *Immunol Rev* 259:115-139.

Bashratyan, R., H. Sheng, D. Regn, M.J. Rahman, and Y.D. Dai. 2013. Insulinoma-released exosomes activate autoreactive marginal zone-like B cells that expand endogenously in prediabetic NOD mice. *European journal of immunology* 43:2588-2597.

Bayer, A.L., A. Yu, D. Adeegbe, and T.R. Malek. 2005. Essential role for interleukin-2 for CD4(+)CD25(+) T regulatory cell development during the neonatal period. *The Journal of experimental medicine* 201:769-777.

Begin, P., and K.C. Nadeau. 2014. Epigenetic regulation of asthma and allergic disease. *Allergy, asthma, and clinical immunology : official journal of the Canadian Society of Allergy and Clinical Immunology* 10:27.

Belkaid, Y. 2007. Regulatory T cells and infection: a dangerous necessity. *Nature reviews. Immunology* 7:875-888.

Belkaid, Y., and B.T. Rouse. 2005. Natural regulatory T cells in infectious disease. *Nature immunology* 6:353-360.

Belkaid, Y., and K.V. Tarbell. 2009. Arming Treg cells at the inflammatory site. *Immunity* 30:322-323.

Bellingham, S.A., B.B. Guo, B.M. Coleman, and A.F. Hill. 2012. Exosomes: vehicles for the transfer of toxic proteins associated with neurodegenerative diseases? *Front Physiol* 3:124.

Bennett, C.L., J. Christie, F. Ramsdell, M.E. Brunkow, P.J. Ferguson, L. Whitesell, T.E. Kelly, F.T. Saulsbury, P.F. Chance, and H.D. Ochs. 2001. The immune dysregulation, polyendocrinopathy, enteropathy, X-linked syndrome (IPEX) is caused by mutations of FOXP3. *Nature genetics* 27:20-21.

Berger, J.R., and S. Houff. 2008. Neurological complications of herpes simplex virus type 2 infection. *Arch Neurol* 65:596-600.

Bilal, M.Y., A. Vacaflores, and J.C. Houtman. 2015. Optimization of methods for the genetic modification of human T cells. *Immunol Cell Biol* 93:896-908.

Bissig, C., and J. Gruenberg. 2014. ALIX and the multivesicular endosome: ALIX in Wonderland. *Trends in cell biology* 24:19-25.

Blais, V., and S. Rivest. 2004. Effects of TNF-alpha and IFN-gamma on nitric oxide-induced neurotoxicity in the mouse brain. *Journal of immunology* 172:7043-7052.

Blanchard, N., D. Lankar, F. Faure, A. Regnault, C. Dumont, G. Raposo, and C. Hivroz. 2002. TCR activation of human T cells induces the production of exosomes bearing the TCR/CD3/zeta complex. *Journal of immunology* 168:3235-3241.

Bogenberger, J.M., and P.J. Laybourn. 2008. Human T Lymphotropic Virus Type 1 protein Tax reduces histone levels. *Retrovirology* 5:9.

Boxus, M., J.C. Twizere, S. Legros, J.F. Dewulf, R. Kettmann, and L. Willems. 2008. The HTLV-1 Tax interactome. *Retrovirology* 5:76.

Brunkow, M.E., E.W. Jeffery, K.A. Hjerrild, B. Paeper, L.B. Clark, S.A. Yasayko, J.E. Wilkinson, D. Galas, S.F. Ziegler, and F. Ramsdell. 2001. Disruption of a new forkhead/winged-helix protein, scurfin, results in the fatal lymphoproliferative disorder of the scurfy mouse. *Nature genetics* 27:68-73.

Buc, M. 2013. Role of regulatory T cells in pathogenesis and biological therapy of multiple sclerosis. *Mediators Inflamm* 2013:963748.

Bukong, T.N., F. Momen-Heravi, K. Kodys, S. Bala, and G. Szabo. 2014. Exosomes from hepatitis C infected patients transmit HCV infection and contain replication competent viral RNA in complex with Ago2-miR122-HSP90. *PLoS pathogens* 10:e1004424.

Campbell, T.D., M. Khan, M.B. Huang, V.C. Bond, and M.D. Powell. 2008. HIV-1 Nef protein is secreted into vesicles that can fuse with target cells and virions. *Ethnicity & disease* 18:S2-14-19.

Cantin, R., J. Diou, D. Belanger, A.M. Tremblay, and C. Gilbert. 2008. Discrimination between exosomes and HIV-1: purification of both vesicles from cell-free supernatants. *J Immunol Methods* 338:21-30.

Carpentier, A., P.Y. Barez, M. Hamaidia, H. Gazon, A. de Brogniez, S. Perike, N. Gillet, and L. Willems. 2015. Modes of Human T Cell Leukemia Virus Type 1 Transmission, Replication and Persistence. *Viruses* 7:3603-3624.

Cavallari, I., F. Rende, C. Bender, M.G. Romanelli, D.M. D'Agostino, and V. Ciminale. 2013. Fine tuning of the temporal expression of HTLV-1 and HTLV-2. *Frontiers in microbiology* 4:235.

Chan, M.W., C.B. Chang, C.H. Tung, J. Sun, J.L. Suen, and S.F. Wu. 2014. Low-dose 5-aza-2'-deoxycytidine pretreatment inhibits experimental autoimmune encephalomyelitis by induction of regulatory T cells. *Mol Med* 20:248-256.

Chen, S., N. Ishii, S. Ine, S. Ikeda, T. Fujimura, L.C. Ndhlovu, P. Soroosh, K. Tada, H. Harigae, J. Kameoka, N. Kasai, T. Sasaki, and K. Sugamura. 2006. Regulatory T cell-like activity of Foxp3+ adult T cell leukemia cells. *International immunology* 18:269-277.

Chen, W.W., X. Zhang, and W.J. Huang. 2016. Role of neuroinflammation in neurodegenerative diseases (Review). *Mol Med Rep* 13:3391-3396.

Cheng, J., A.R. Kydd, K. Nakase, K.M. Noonan, A. Murakami, H. Tao, M. Dwyer, C. Xu, Q. Zhu, and W.A. Marasco. 2007. Negative regulation of the SH2-homology containing protein-tyrosine phosphatase-1 (SHP-1) P2 promoter by the HTLV-1 Tax oncoprotein. *Blood* 110:2110-2120.

Chiari, E., I. Lamsoul, J. Lodewick, C. Chopin, F. Bex, and C. Pique. 2004. Stable ubiquitination of human T-cell leukemia virus type 1 tax is required for proteasome binding. *Journal of virology* 78:11823-11832.

Chugh, P.E., S.H. Sin, S. Ozgur, D.H. Henry, P. Menezes, J. Griffith, J.J. Eron, B. Damania, and D.P. Dittmer. 2013. Systemically circulating viral and tumor-derived microRNAs in KSHV-associated malignancies. *PLoS pathogens* 9:e1003484.

Churlaud, G., F. Pitoiset, F. Jebbawi, R. Lorenzon, B. Bellier, M. Rosenzwajg, and D. Klatzmann. 2015. Human and Mouse CD8(+)CD25(+)FOXP3(+) Regulatory T Cells at Steady State and during Interleukin-2 Therapy. *Front Immunol* 6:171.

Clarke, M.F., C.D. Trainor, D.L. Mann, R.C. Gallo, and M.S. Reitz. 1984. Methylation of human T-cell leukemia virus proviral DNA and viral RNA expression in short- and long-term cultures of infected cells. *Virology* 135:97-104.

Coffin, J.M. 2015. The discovery of HTLV-1, the first pathogenic human retrovirus. *Proceedings of the National Academy of Sciences of the United States of America* 112:15525-15529.

Collison, L.W., and D.A. Vignali. 2011. In vitro Treg suppression assays. *Methods in molecular biology* 707:21-37.

Colombo, M., G. Raposo, and C. Thery. 2014. Biogenesis, secretion, and intercellular interactions of exosomes and other extracellular vesicles. *Annual review of cell and developmental biology* 30:255-289.

Cook, L.B., M. Elemans, A.G. Rowan, and B. Asquith. 2013. HTLV-1: persistence and pathogenesis. *Virology* 435:131-140.

Curis, C., F. Percher, P. Jeannin, T. Montange, S.A. Chevalier, D. Seilhean, L. Cartier, P.O. Couraud, O. Gout, A. Gessain, P.E. Ceccaldi, and P.V. Afonso. 2016. Human T-

Lymphotropic Virus Type 1-Induced Overexpression of Activated Leukocyte Cell Adhesion Molecule (ALCAM) Facilitates Trafficking of Infected Lymphocytes through the Blood-Brain Barrier. *Journal of virology* 90:7303-7312.

Currer, R., R. Van Duyne, E. Jaworski, I. Guendel, G. Sampey, R. Das, A. Narayanan, and F. Kashanchi. 2012. HTLV tax: a fascinating multifunctional co-regulator of viral and cellular pathways. *Frontiers in microbiology* 3:406.

Dalla Libera, D., D. Di Mitri, A. Bergami, D. Centonze, C. Gasperini, M.G. Grasso, S. Galgani, V. Martinelli, G. Comi, C. Avolio, G. Martino, G. Borsellino, F. Sallusto, L. Battistini, and R. Furlan. 2011. T regulatory cells are markers of disease activity in multiple sclerosis patients. *PloS one* 6:e21386.

Danielson, K.M., J. Estanislau, J. Tigges, V. Toxavidis, V. Camacho, E.J. Felton, J. Khoory, S. Kreimer, A.R. Ivanov, P.Y. Mantel, J. Jones, P. Akuthota, S. Das, and I. Ghiran. 2016. Diurnal Variations of Circulating Extracellular Vesicles Measured by Nano Flow Cytometry. *PloS one* 11:e0144678.

Delgoffe, G.M., S.R. Woo, M.E. Turnis, D.M. Gravano, C. Guy, A.E. Overacre, M.L. Bettini, P. Vogel, D. Finkelstein, J. Bonnevier, C.J. Workman, and D.A. Vignali. 2013. Stability and function of regulatory T cells is maintained by a neuropilin-1-semaphorin-4a axis. *Nature* 501:252-256.

Domcke, S., A.F. Bardet, P. Adrian Ginno, D. Hartl, L. Burger, and D. Schubeler. 2015. Competition between DNA methylation and transcription factors determines binding of NRF1. *Nature* 528:575-579.

Donegan, E., H. Lee, E.A. Operskalski, G.M. Shaw, S.H. Kleinman, M.P. Busch, C.E. Stevens, E.R. Schiff, M.J. Nowicki, C.G. Hollingsworth, and et al. 1994. Transfusion transmission of retroviruses: human T-lymphotropic virus types I and II compared with human immunodeficiency virus type 1. *Transfusion* 34:478-483.

Ego, T., Y. Tanaka, and K. Shimotohno. 2005. Interaction of HTLV-1 Tax and methyl-CpG-binding domain 2 positively regulates the gene expression from the hypermethylated LTR. *Oncogene* 24:1914-1923.

Elkord, E. 2016. Helios Should Not Be Cited as a Marker of Human Thymus-Derived Tregs. Commentary: Helios(+) and Helios(-) Cells Coexist within the Natural FOXP3(+) T Regulatory Cell Subset in Humans. *Front Immunol* 7:276.

Elovaara, I., S. Koenig, A.Y. Brewah, R.M. Woods, T. Lehky, and S. Jacobson. 1993. High human T cell lymphotropic virus type 1 (HTLV-1)-specific precursor cytotoxic T lymphocyte frequencies in patients with HTLV-1-associated neurological disease. *The Journal of experimental medicine* 177:1567-1573.

Enose-Akahata, Y., A. Abrams, R. Massoud, I. Bialuk, K.R. Johnson, P.L. Green, E.M. Maloney, and S. Jacobson. 2013. Humoral immune response to HTLV-1 basic leucine zipper factor (HBZ) in HTLV-1-infected individuals. *Retrovirology* 10:19.

Evangelou, I.E., R. Massoud, and S. Jacobson. 2014. HTLV-I-associated myelopathy/tropical spastic paraparesis: semiautomatic quantification of spinal cord atrophy from 3-dimensional MR images. *J Neuroimaging* 24:74-78.

Fader, C.M., D.G. Sanchez, M.B. Mestre, and M.I. Colombo. 2009. TI-VAMP/VAMP7 and VAMP3/cellubrevin: two v-SNARE proteins involved in specific steps of the

autophagy/multivesicular body pathways. *Biochimica et biophysica acta* 1793:1901-1916.

Fang, J.Y., J.A. Mikovits, R. Bagni, C.L. Petrow-Sadowski, and F.W. Ruscetti. 2001. Infection of lymphoid cells by integration-defective human immunodeficiency virus type 1 increases de novo methylation. *Journal of virology* 75:9753-9761.

Fang, Y., N. Wu, X. Gan, W. Yan, J.C. Morrell, and S.J. Gould. 2007. Higher-order oligomerization targets plasma membrane proteins and HIV gag to exosomes. *PLoS biology* 5:e158.

Fierz, W. 2017. Multiple sclerosis: an example of pathogenic viral interaction? *Virology journal* 14:42.

Filipenko, N.R., T.J. MacLeod, C.S. Yoon, and D.M. Waisman. 2004. Annexin A2 is a novel RNA-binding protein. *The Journal of biological chemistry* 279:8723-8731.

Fitzner, D., M. Schnaars, D. van Rossum, G. Krishnamoorthy, P. Dibaj, M. Bakhti, T. Regen, U.K. Hanisch, and M. Simons. 2011. Selective transfer of exosomes from oligodendrocytes to microglia by macropinocytosis. *Journal of cell science* 124:447-458.

Flanagan, J., J. Middeldorp, and T. Sculley. 2003. Localization of the Epstein-Barr virus protein LMP 1 to exosomes. *The Journal of general virology* 84:1871-1879.

Fleissner, D., W. Hansen, R. Geffers, J. Buer, and A.M. Westendorf. 2010. Local induction of immunosuppressive CD8+ T cells in the gut-associated lymphoid tissues. *PloS one* 5:e15373.

Floess, S., J. Freyer, C. Siewert, U. Baron, S. Olek, J. Polansky, K. Schlawe, H.D. Chang, T. Bopp, E. Schmitt, S. Klein-Hessling, E. Serfling, A. Hamann, and J. Huehn. 2007. Epigenetic control of the foxp3 locus in regulatory T cells. *PLoS biology* 5:e38.

Fontenot, J.D., M.A. Gavin, and A.Y. Rudensky. 2003. Foxp3 programs the development and function of CD4+CD25+ regulatory T cells. *Nature immunology* 4:330-336.

Frohlich, D., W.P. Kuo, C. Fruhbeis, J.J. Sun, C.M. Zehendner, H.J. Luhmann, S. Pinto, J. Toedling, J. Trotter, and E.M. Kramer-Albers. 2014. Multifaceted effects of oligodendroglial exosomes on neurons: impact on neuronal firing rate, signal transduction and gene regulation. *Philos Trans R Soc Lond B Biol Sci* 369:

Fruhbeis, C., D. Frohlich, W.P. Kuo, and E.M. Kramer-Albers. 2013. Extracellular vesicles as mediators of neuron-glia communication. *Front Cell Neurosci* 7:182.

Fu, S., N. Zhang, A.C. Yopp, D. Chen, M. Mao, D. Chen, H. Zhang, Y. Ding, and J.S. Bromberg. 2004. TGF-beta induces Foxp3 + T-regulatory cells from CD4 + CD25 - precursors. *Am J Transplant* 4:1614-1627.

Fuzii, H.T., G.A. da Silva Dias, R.J. de Barros, L.F. Falcao, and J.A. Quaresma. 2014. Immunopathogenesis of HTLV-1-assoaciated myelopathy/tropical spastic paraparesis (HAM/TSP). *Life Sci* 104:9-14.

Galazka, G., M.P. Mycko, I. Selmaj, C.S. Raine, and K.W. Selmaj. 2017. Multiple sclerosis: Serum-derived exosomes express myelin proteins. *Mult Scler* 1352458517696597.

Gallo, R.C. 2005. The discovery of the first human retrovirus: HTLV-1 and HTLV-2. *Retrovirology* 2:17.

Gasteiger, G., S. Hemmers, M.A. Firth, A. Le Floc'h, M. Huse, J.C. Sun, and A.Y. Rudensky. 2013. IL-2-dependent tuning of NK cell sensitivity for target cells is controlled by regulatory T cells. *The Journal of experimental medicine* 210:1167-1178.

Gatza, M.L., T. Dayaram, and S.J. Marriott. 2007. Ubiquitination of HTLV-I Tax in response to DNA damage regulates nuclear complex formation and nuclear export. *Retrovirology* 4:95.

Gaudray, G., F. Gachon, J. Basbous, M. Biard-Piechaczyk, C. Devaux, and J.M. Mesnard. 2002. The complementary strand of the human T-cell leukemia virus type 1 RNA genome encodes a bZIP transcription factor that down-regulates viral transcription. *Journal of virology* 76:12813-12822.

Gershon, R.K., and K. Kondo. 1970. Cell interactions in the induction of tolerance: the role of thymic lymphocytes. *Immunology* 18:723-737.

Gershon, R.K., and K. Kondo. 1971. Infectious immunological tolerance. *Immunology* 21:903-914.

Gessain, A., and O. Cassar. 2012. Epidemiological Aspects and World Distribution of HTLV-1 Infection. *Frontiers in microbiology* 3:388.

Gessain, A., A. Louie, O. Gout, R.C. Gallo, and G. Franchini. 1991. Human T-cell leukemia-lymphoma virus type I (HTLV-I) expression in fresh peripheral blood mononuclear cells from patients with tropical spastic paraparesis/HTLV-I-associated myelopathy. *Journal of virology* 65:1628-1633.

Ghez, D., Y. Lepelletier, S. Lambert, J.M. Fourneau, V. Blot, S. Janvier, B. Arnulf, P.M. van Endert, N. Heveker, C. Pique, and O. Hermine. 2006. Neuropilin-1 is involved in human T-cell lymphotropic virus type 1 entry. *Journal of virology* 80:6844-6854.

Godoy, A.J., J. Kira, K. Hasuo, and I. Goto. 1995. Characterization of cerebral white matter lesions of HTLV-I-associated myelopathy/tropical spastic paraparesis in comparison with multiple sclerosis and collagen-vasculitis: a semiquantitative MRI study. *J Neurol Sci* 133:102-111.

Gol-Ara, M., F. Jadidi-Niaragh, R. Sadria, G. Azizi, and A. Mirshafiey. 2012. The role of different subsets of regulatory T cells in immunopathogenesis of rheumatoid arthritis. *Arthritis* 2012:805875.

Goncalves, D.U., F.A. Proietti, J.G. Ribas, M.G. Araujo, S.R. Pinheiro, A.C. Guedes, and A.B. Carneiro-Proietti. 2010. Epidemiology, treatment, and prevention of human T-cell leukemia virus type 1-associated diseases. *Clin Microbiol Rev* 23:577-589.

Gotot, J., C. Gottschalk, S. Leopold, P.A. Knolle, H. Yagita, C. Kurts, and I. Ludwig-Portugall. 2012. Regulatory T cells use programmed death 1 ligands to directly suppress autoreactive B cells in vivo. *Proceedings of the National Academy of Sciences of the United States of America* 109:10468-10473.

Grant, C., K. Barmak, T. Alefantis, J. Yao, S. Jacobson, and B. Wigdahl. 2002. Human T cell leukemia virus type I and neurologic disease: events in bone marrow, peripheral blood, and central nervous system during normal immune surveillance and neuroinflammation. *Journal of cellular physiology* 190:133-159.

Grant, C., U. Oh, K. Yao, Y. Yamano, and S. Jacobson. 2008. Dysregulation of TGF-beta signaling and regulatory and effector T-cell function in virus-induced neuroinflammatory disease. *Blood* 111:5601-5609.

Greening, D.W., S.K. Gopal, R. Xu, R.J. Simpson, and W. Chen. 2015. Exosomes and their roles in immune regulation and cancer. *Seminars in cell & developmental biology* 40:72-81.

Greten, T.F., J.E. Slansky, R. Kubota, S.S. Soldan, E.M. Jaffee, T.P. Leist, D.M. Pardoll, S. Jacobson, and J.P. Schneck. 1998. Direct visualization of antigen-specific T cells: HTLV-1 Tax11-19- specific CD8(+) T cells are activated in peripheral blood and accumulate in cerebrospinal fluid from HAM/TSP patients. *Proceedings of the National Academy of Sciences of the United States of America* 95:7568-7573.

Gross, C., and A.K. Thoma-Kress. 2016. Molecular Mechanisms of HTLV-1 Cell-to-Cell Transmission. *Viruses* 8:74.

Groux, H., A. O'Garra, M. Bigler, M. Rouleau, S. Antonenko, J.E. de Vries, and M.G. Roncarolo. 1997. A CD4+ T-cell subset inhibits antigen-specific T-cell responses and prevents colitis. *Nature* 389:737-742.

Hagiwara, K., T. Katsuda, L. Gailhouste, N. Kosaka, and T. Ochiya. 2015. Commitment of Annexin A2 in recruitment of microRNAs into extracellular vesicles. *FEBS Lett* 589:4071-4078.

Han, S.P., L.R. Friend, J.H. Carson, G. Korza, E. Barbarese, M. Maggipinto, J.T. Hatfield, J.A. Rothnagel, and R. Smith. 2010. Differential subcellular distributions and trafficking functions of hnRNP A2/B1 spliceoforms. *Traffic* 11:886-898.

Harrod, R., Y. Tang, C. Nicot, H.S. Lu, A. Vassilev, Y. Nakatani, and C.Z. Giam. 1998. An exposed KID-like domain in human T-cell lymphotropic virus type 1 Tax is responsible for the recruitment of coactivators CBP/p300. *Mol Cell Biol* 18:5052-5061.

Hassfeld, W., G. Steiner, A. Studnicka-Benke, K. Skriner, W. Graninger, I. Fischer, and J.S. Smolen. 1995. Autoimmune response to the spliceosome. An immunologic link between rheumatoid arthritis, mixed connective tissue disease, and systemic lupus erythematosus. *Arthritis Rheum* 38:777-785.

Hausmann, S., W.E. Biddison, K.J. Smith, Y.H. Ding, D.N. Garboczi, U. Utz, D.C. Wiley, and K.W. Wucherpfennig. 1999. Peptide recognition by two HLA-A2/Tax11-19-specific T cell clones in relationship to their MHC/peptide/TCR crystal structures. *Journal of immunology* 162:5389-5397.

Helwa, I., J. Cai, M.D. Drewry, A. Zimmerman, M.B. Dinkins, M.L. Khaled, M. Seremwe, W.M. Dismuke, E. Bieberich, W.D. Stamer, M.W. Hamrick, and Y. Liu. 2017. A Comparative Study of Serum Exosome Isolation Using Differential Ultracentrifugation and Three Commercial Reagents. *PloS one* 12:e0170628.

Henne, W.M., N.J. Buchkovich, and S.D. Emr. 2011. The ESCRT pathway. *Developmental cell* 21:77-91.

Hilburn, S., A. Rowan, M.A. Demontis, A. MacNamara, B. Asquith, C.R. Bangham, and G.P. Taylor. 2011. In vivo expression of human T-lymphotropic virus type 1 basic leucine-zipper protein generates specific CD8+ and CD4+ T-lymphocyte

responses that correlate with clinical outcome. *The Journal of infectious diseases* 203:529-536.

Hori, S., T. Nomura, and S. Sakaguchi. 2003. Control of regulatory T cell development by the transcription factor Foxp3. *Science* 299:1057-1061.

Hoshino, H. 2012. Cellular Factors Involved in HTLV-1 Entry and Pathogenicit. *Frontiers in microbiology* 3:222.

Huang, K.H., D. Bonsall, A. Katzourakis, E.C. Thomson, S.J. Fidler, J. Main, D. Muir, J.N. Weber, A.J. Frater, R.E. Phillips, O.G. Pybus, P.J. Goulder, M.O. McClure, G.S. Cooke, and P. Klenerman. 2010. B-cell depletion reveals a role for antibodies in the control of chronic HIV-1 infection. *Nat Commun* 1:102.

Huehn, J., and M. Beyer. 2015. Epigenetic and transcriptional control of Foxp3+ regulatory T cells. *Semin Immunol* 27:10-18.

Huehn, J., J.K. Polansky, and A. Hamann. 2009. Epigenetic control of FOXP3 expression: the key to a stable regulatory T-cell lineage? *Nature reviews. Immunology* 9:83-89.

Itoyama, Y., S. Minato, J. Kira, I. Goto, H. Sato, K. Okochi, and N. Yamamoto. 1988. Spontaneous proliferation of peripheral blood lymphocytes increased in patients with HTLV-I-associated myelopathy. *Neurology* 38:1302-1307.

Iwasaki, Y. 1990. Pathology of chronic myelopathy associated with HTLV-I infection (HAM/TSP). *J Neurol Sci* 96:103-123.

Izumo, S. 2010. Neuropathology of HTLV-1-associated myelopathy (HAM/TSP). *Neuropathology : official journal of the Japanese Society of Neuropathology*

Jacobson, S. 1996. Cellular immune responses to HTLV-I: immunopathogenic role in HTLV-I-associated neurologic disease. *J Acquir Immune Defic Syndr Hum Retrovirol* 13 Suppl 1:S100-106.

Jacobson, S. 2002. Immunopathogenesis of human T cell lymphotropic virus type I-associated neurologic disease. *The Journal of infectious diseases* 186 Suppl 2:S187-192.

Janson, P.C., M.E. Winerdal, P. Marits, M. Thorn, R. Ohlsson, and O. Winqvist. 2008. FOXP3 promoter demethylation reveals the committed Treg population in humans. *PloS one* 3:e1612.

Jaworski, E., A. Narayanan, R. Van Duyne, S. Shabbeer-Meyering, S. Iordanskiy, M. Saifuddin, R. Das, P.V. Afonso, G.C. Sampey, M. Chung, A. Popratiloff, B. Shrestha, M. Sehgal, P. Jain, A. Vertes, R. Mahieux, and F. Kashanchi. 2014a. Human T-lymphotropic virus type 1-infected cells secrete exosomes that contain Tax protein. *The Journal of biological chemistry* 289:22284-22305.

Jaworski, E., M. Saifuddin, G. Sampey, N. Shafagati, R. Van Duyne, S. Iordanskiy, K. Kehn-Hall, L. Liotta, E. Petricoin, 3rd, M. Young, B. Lepene, and F. Kashanchi. 2014b. The use of Nanotrap particles technology in capturing HIV-1 virions and viral proteins from infected cells. *PloS one* 9:e96778.

Jensen, L., E.L. Kuff, S.H. Wilson, A.D. Steinberg, and D.M. Klinman. 1988. Antibodies from patients and mice with autoimmune diseases react with recombinant hnRNP core protein A1. *J Autoimmun* 1:73-83.

Johnstone, R.M., A. Bianchini, and K. Teng. 1989. Reticulocyte maturation and exosome release: transferrin receptor containing exosomes shows multiple plasma membrane functions. *Blood* 74:1844-1851.

Jones, A., and D. Hawiger. 2017. Peripherally Induced Regulatory T Cells: Recruited Protectors of the Central Nervous System against Autoimmune Neuroinflammation. *Front Immunol* 8:532.

Josefowicz, S.Z., L.F. Lu, and A.Y. Rudensky. 2012. Regulatory T cells: mechanisms of differentiation and function. *Annu Rev Immunol* 30:531-564.

Kakalacheva, K., C. Munz, and J.D. Lunemann. 2011. Viral triggers of multiple sclerosis. *Biochimica et biophysica acta* 1812:132-140.

Kalamvoki, M., and B. Roizman. 2014. HSV-1 degrades, stabilizes, requires, or is stung by STING depending on ICP0, the US3 protein kinase, and cell derivation. *Proceedings of the National Academy of Sciences of the United States of America* 111:E611-617.

Kamma, H., D.S. Portman, and G. Dreyfuss. 1995. Cell type-specific expression of hnRNP proteins. *Exp Cell Res* 221:187-196.

Kannian, P., and P.L. Green. 2010. Human T Lymphotropic Virus Type 1 (HTLV-1): Molecular Biology and Oncogenesis. *Viruses* 2:2037-2077.

Karube, K., K. Ohshima, T. Tsuchiya, T. Yamaguchi, R. Kawano, J. Suzumiya, A. Utsunomiya, M. Harada, and M. Kikuchi. 2004. Expression of FoxP3, a key molecule in CD4CD25 regulatory T cells, in adult T-cell leukaemia/lymphoma cells. *Br J Haematol* 126:81-84.

Kehn, K., R. Berro, C. de la Fuente, K. Strouss, E. Ghedin, S. Dadgar, M.E. Bottazzi, A. Pumfery, and F. Kashanchi. 2004. Mechanisms of HTLV-1 transformation. *Front Biosci* 9:2347-2372.

Kfoury, Y., N. Setterblad, M. El-Sabban, A. Zamborlini, Z. Dassouki, H. El Hajj, O. Hermine, C. Pique, H. de The, A. Saib, and A. Bazarbachi. 2011. Tax ubiquitylation and SUMOylation control the dynamic shuttling of Tax and NEMO between Ubc9 nuclear bodies and the centrosome. *Blood* 117:190-199.

Kitze, B., K. Usuku, S. Izumo, M. Nakamura, H. Shiraki, S. Ijichi, S. Yashiki, T. Fujiyoshi, S. Sonoda, and M. Osame. 1996. Diversity of intrathecal antibody synthesis against HTLV-I and its relation to HTLV-I associated myelopathy. *J Neurol* 243:393-400.

Klibi, J., T. Niki, A. Riedel, C. Pioche-Durieu, S. Souquere, E. Rubinstein, S. Le Moulec, J. Guigay, M. Hirashima, F. Guemira, D. Adhikary, J. Mautner, and P. Busson. 2009. Blood diffusion and Th1-suppressive effects of galectin-9-containing exosomes released by Epstein-Barr virus-infected nasopharyngeal carcinoma cells. *Blood* 113:1957-1966.

Knipe, D.M., P.M. Lieberman, J.U. Jung, A.A. McBride, K.V. Morris, M. Ott, D. Margolis, A. Nieto, M. Nevels, R.J. Parks, and T.M. Kristie. 2013. Snapshots: chromatin control of viral infection. *Virology* 435:141-156.

Kosgodage, U.S., R.P. Trindade, P.R. Thompson, J.M. Inal, and S. Lange. 2017. Chloramidine/Bisindolylmaleimide-I-Mediated Inhibition of Exosome and

Microvesicle Release and Enhanced Efficacy of Cancer Chemotherapy. *Int J Mol Sci* 18:

Koutrolos, M., K. Berer, N. Kawakami, H. Wekerle, and G. Krishnamoorthy. 2014. Treg cells mediate recovery from EAE by controlling effector T cell proliferation and motility in the CNS. *Acta Neuropathol Commun* 2:163.

Kubota, R., M. Nagai, T. Kawanishi, M. Osame, and S. Jacobson. 2000. Increased HTLV type 1 tax specific CD8+ cells in HTLV type 1-asociated myelopathy/tropical spastic paraparesis: correlation with HTLV type 1 proviral load. *AIDS research and human retroviruses* 16:1705-1709.

Kubota, R., S.S. Soldan, R. Martin, and S. Jacobson. 2002. Selected cytotoxic T lymphocytes with high specificity for HTLV-I in cerebrospinal fluid from a HAM/TSP patient. *Journal of neurovirology* 8:53-57.

Lairmore, M.D., R. Haines, and R. Anupam. 2012. Mechanisms of human T-lymphotropic virus type 1 transmission and disease. *Curr Opin Virol* 2:474-481.

Lal, G., and J.S. Bromberg. 2009. Epigenetic mechanisms of regulation of Foxp3 expression. *Blood* 114:3727-3735.

Lamparski, H.G., A. Metha-Damani, J.Y. Yao, S. Patel, D.H. Hsu, C. Ruegg, and J.B. Le Pecq. 2002. Production and characterization of clinical grade exosomes derived from dendritic cells. *J Immunol Methods* 270:211-226.

Lavorgna, A., and E.W. Harhaj. 2014. Regulation of HTLV-1 tax stability, cellular trafficking and NF-kappaB activation by the ubiquitin-proteasome pathway. *Viruses* 6:3925-3943.

Lee, F.E., A.R. Falsey, J.L. Halliley, I. Sanz, and E.E. Walsh. 2010. Circulating antibody-secreting cells during acute respiratory syncytial virus infection in adults. *The Journal of infectious diseases* 202:1659-1666.

Lee, S.M., Y. Morcos, H. Jang, J.M. Stuart, and M.C. Levin. 2005. HTLV-1 induced molecular mimicry in neurological disease. *Curr Top Microbiol Immunol* 296:125-136.

Leibovitch, E., J.E. Wohler, S.M. Cummings Macri, K. Motanic, E. Harberts, M.I. Gaitan, P. Maggi, M. Ellis, S. Westmoreland, A. Silva, D.S. Reich, and S. Jacobson. 2013. Novel marmoset (Callithrix jacchus) model of human Herpesvirus 6A and 6B infections: immunologic, virologic and radiologic characterization. *PLoS pathogens* 9:e1003138.

Leibovitch, E.C., and S. Jacobson. 2014. Evidence linking HHV-6 with multiple sclerosis: an update. *Curr Opin Virol* 9:127-133.

Lemasson, I., M.R. Lewis, N. Polakowski, P. Hivin, M.H. Cavanagh, S. Thebault, B. Barbeau, J.K. Nyborg, and J.M. Mesnard. 2007. Human T-cell leukemia virus type 1 (HTLV-1) bZIP protein interacts with the cellular transcription factor CREB to inhibit HTLV-1 transcription. *Journal of virology* 81:1543-1553.

Lepoutre, V., P. Jain, K. Quann, B. Wigdahl, and Z.K. Khan. 2009. Role of resident CNS cell populations in HTLV-1-associated neuroinflammatory disease. *Frontiers in bioscience* 14:1152-1168.

Levin, M.C., S.M. Lee, F. Kalume, Y. Morcos, F.C. Dohan, Jr., K.A. Hasty, J.C. Callaway, J. Zunt, D. Desiderio, and J.M. Stuart. 2002. Autoimmunity due to molecular mimicry as a cause of neurological disease. *Nature medicine* 8:509-513.

Li, H.C., T. Fujiyoshi, H. Lou, S. Yashiki, S. Sonoda, L. Cartier, L. Nunez, I. Munoz, S. Horai, and K. Tajima. 1999. The presence of ancient human T-cell lymphotropic virus type I provirus DNA in an Andean mummy. *Nature medicine* 5:1428-1432.

Li, M., M. Kesic, H. Yin, L. Yu, and P.L. Green. 2009. Kinetic analysis of human T-cell leukemia virus type 1 gene expression in cell culture and infected animals. *Journal of virology* 83:3788-3797.

Li, S., E.J. Gowans, C. Chougnet, M. Plebanski, and U. Dittmer. 2008. Natural regulatory T cells and persistent viral infection. *Journal of virology* 82:21-30.

Lin, X., M. Chen, Y. Liu, Z. Guo, X. He, D. Brand, and S.G. Zheng. 2013. Advances in distinguishing natural from induced Foxp3(+) regulatory T cells. *Int J Clin Exp Pathol* 6:116-123.

Liu, J., A. Lluis, S. Illi, L. Layland, S. Olek, E. von Mutius, and B. Schaub. 2010. T regulatory cells in cord blood--FOXP3 demethylation as reliable quantitative marker. *PloS one* 5:e13267.

Liu, W., G. Nair, L. Vuolo, A. Bakshi, R. Massoud, D.S. Reich, and S. Jacobson. 2014. In vivo imaging of spinal cord atrophy in neuroinflammatory diseases. *Annals of neurology* 76:370-378.

Lodewick, J., I. Lamsoul, A. Polania, S. Lebrun, A. Burny, L. Ratner, and F. Bex. 2009. Acetylation of the human T-cell leukemia virus type 1 Tax oncoprotein by p300 promotes activation of the NF-kappaB pathway. *Virology* 386:68-78.

Long, S.A., and J.H. Buckner. 2011. CD4+FOXP3+ T regulatory cells in human autoimmunity: more than a numbers game. *Journal of immunology* 187:2061-2066.

Long, X., Q. Cheng, H. Liang, J. Zhao, J. Wang, W. Wang, S. Tomlinson, L. Chen, C. Atkinson, B. Zhang, X. Chen, and P. Zhu. 2017. Memory CD4+ T cells are suppressed by CD8+ regulatory T cells in vitro and in vivo. *Am J Transl Res* 9:63-78.

Longatti, A., B. Boyd, and F.V. Chisari. 2015. Virion-independent transfer of replication-competent hepatitis C virus RNA between permissive cells. *Journal of virology* 89:2956-2961.

Luchini, A., D.H. Geho, B. Bishop, D. Tran, C. Xia, R.L. Dufour, C.D. Jones, V. Espina, A. Patanarut, W. Zhou, M.M. Ross, A. Tessitore, E.F. Petricoin, 3rd, and L.A. Liotta. 2008. Smart hydrogel particles: biomarker harvesting: one-step affinity purification, size exclusion, and protection against degradation. *Nano Lett* 8:350-361.

Lundquist, C.A., M. Tobiume, J. Zhou, D. Unutmaz, and C. Aiken. 2002. Nef-mediated downregulation of CD4 enhances human immunodeficiency virus type 1 replication in primary T lymphocytes. *Journal of virology* 76:4625-4633.

Macatonia, S.E., J.K. Cruickshank, P. Rudge, and S.C. Knight. 1992. Dendritic cells from patients with tropical spastic paraparesis are infected with HTLV-1 and stimulate

autologous lymphocyte proliferation. *AIDS research and human retroviruses* 8:1699-1706.

Madison, M.N., and C.M. Okeoma. 2015. Exosomes: Implications in HIV-1 Pathogenesis. *Viruses* 7:4093-4118.

Maloney, E.M., F.R. Cleghorn, O.S. Morgan, P. Rodgers-Johnson, B. Cranston, N. Jack, W.A. Blattner, C. Bartholomew, and A. Manns. 1998. Incidence of HTLV-I-associated myelopathy/tropical spastic paraparesis (HAM/TSP) in Jamaica and Trinidad. *J Acquir Immune Defic Syndr Hum Retrovirol* 17:167-170.

Mantel, P.Y., N. Ouaked, B. Ruckert, C. Karagiannidis, R. Welz, K. Blaser, and C.B. Schmidt-Weber. 2006. Molecular mechanisms underlying FOXP3 induction in human T cells. *Journal of immunology* 176:3593-3602.

Manuel, S.L., T.D. Schell, E. Acheampong, S. Rahman, Z.K. Khan, and P. Jain. 2009. Presentation of human T cell leukemia virus type 1 (HTLV-1) Tax protein by dendritic cells: the underlying mechanism of HTLV-1-associated neuroinflammatory disease. *Journal of leukocyte biology* 86:1205-1216.

Martin, F., G.P. Taylor, and S. Jacobson. 2014. Inflammatory manifestations of HTLV-1 and their therapeutic options. *Expert Rev Clin Immunol* 10:1531-1546.

Masciopinto, F., C. Giovani, S. Campagnoli, L. Galli-Stampino, P. Colombatto, M. Brunetto, T.S. Yen, M. Houghton, P. Pileri, and S. Abrignani. 2004. Association of hepatitis C virus envelope proteins with exosomes. *European journal of immunology* 34:2834-2842.

Matsuo, H., J. Chevallier, N. Mayran, I. Le Blanc, C. Ferguson, J. Faure, N.S. Blanc, S. Matile, J. Dubochet, R. Sadoul, R.G. Parton, F. Vilbois, and J. Gruenberg. 2004. Role of LBPA and Alix in multivesicular liposome formation and endosome organization. *Science* 303:531-534.

Matsuoka, M., and P.L. Green. 2009. The HBZ gene, a key player in HTLV-1 pathogenesis. *Retrovirology* 6:71.

Matsuura, E., R. Kubota, Y. Tanaka, H. Takashima, and S. Izumo. 2015. Visualization of HTLV-1-specific cytotoxic T lymphocytes in the spinal cords of patients with HTLV-1-associated myelopathy/tropical spastic paraparesis. *J Neuropathol Exp Neurol* 74:2-14.

Matsuura, E., S. Nozuma, Y. Tashiro, R. Kubota, S. Izumo, and H. Takashima. 2016. HTLV-1 associated myelopathy/tropical spastic paraparesis (HAM/TSP): A comparative study to identify factors that influence disease progression. *J Neurol Sci* 371:112-116.

McHugh, R.S., and E.M. Shevach. 2002. The role of suppressor T cells in regulation of immune responses. *The Journal of allergy and clinical immunology* 110:693-702.

Meckes, D.G., Jr., and N. Raab-Traub. 2011. Microvesicles and viral infection. *Journal of virology* 85:12844-12854.

Meekings, K.N., J. Leipzig, F.D. Bushman, G.P. Taylor, and C.R. Bangham. 2008. HTLV-1 integration into transcriptionally active genomic regions is associated with proviral expression and with HAM/TSP. *PLoS pathogens* 4:e1000027.

Melamed, A., D.J. Laydon, H. Al Khatib, A.G. Rowan, G.P. Taylor, and C.R. Bangham. 2015. HTLV-1 drives vigorous clonal expansion of infected CD8(+) T cells in natural infection. *Retrovirology* 12:91.

Melnik, B.C., S.M. John, and G. Schmitz. 2014. Milk: an exosomal microRNA transmitter promoting thymic regulatory T cell maturation preventing the development of atopy? *J Transl Med* 12:43.

Mercadante, E.R., and U.M. Lorenz. 2016. Breaking Free of Control: How Conventional T Cells Overcome Regulatory T Cell Suppression. *Front Immunol* 7:193.

Merrill, J.E., and E.N. Benveniste. 1996. Cytokines in inflammatory brain lesions: helpful and harmful. *Trends Neurosci* 19:331-338.

Mikovits, J.A., H.A. Young, P. Vertino, J.P. Issa, P.M. Pitha, S. Turcoski-Corrales, D.D. Taub, C.L. Petrow, S.B. Baylin, and F.W. Ruscetti. 1998. Infection with human immunodeficiency virus type 1 upregulates DNA methyltransferase, resulting in de novo methylation of the gamma interferon (IFN-gamma) promoter and subsequent downregulation of IFN-gamma production. *Molecular and cellular biology* 18:5166-5177.

Mine, S., K. Suzuki, Y. Sato, H. Fukumoto, M. Kataoka, N. Inoue, C. Ohbayashi, H. Hasegawa, T. Sata, M. Fukayama, and H. Katano. 2014. Evidence for human herpesvirus-6B infection of regulatory T-cells in acute systemic lymphadenitis in an immunocompetent adult with the drug reaction with eosinophilia and systemic symptoms syndrome: a case report. *Journal of clinical virology : the official publication of the Pan American Society for Clinical Virology* 61:448-452.

Mittelbrunn, M., C. Gutierrez-Vazquez, C. Villarroya-Beltri, S. Gonzalez, F. Sanchez-Cabo, M.A. Gonzalez, A. Bernad, and F. Sanchez-Madrid. 2011. Unidirectional transfer of microRNA-loaded exosomes from T cells to antigen-presenting cells. *Nat Commun* 2:282.

Miyano-Kurosaki, N., J. Kira, J.S. Barnor, N. Maeda, N. Misawa, Y. Kawano, Y. Tanaka, N. Yamamoto, and Y. Koyanagi. 2007. Autonomous proliferation of HTLV-CD4+ T cell clones derived from human T cell leukemia virus type I (HTLV-I)-associated myelopathy patients. *Microbiology and immunology* 51:235-242.

Miyao, T., S. Floess, R. Setoguchi, H. Luche, H.J. Fehling, H. Waldmann, J. Huehn, and S. Hori. 2012. Plasticity of Foxp3(+) T cells reflects promiscuous Foxp3 expression in conventional T cells but not reprogramming of regulatory T cells. *Immunity* 36:262-275.

Miyara, M., Y. Yoshioka, A. Kitoh, T. Shima, K. Wing, A. Niwa, C. Parizot, C. Taflin, T. Heike, D. Valeyre, A. Mathian, T. Nakahata, T. Yamaguchi, T. Nomura, M. Ono, Z. Amoura, G. Gorochov, and S. Sakaguchi. 2009. Functional delineation and differentiation dynamics of human CD4+ T cells expressing the FoxP3 transcription factor. *Immunity* 30:899-911.

Miyazato, P., M. Matsuo, H. Katsuya, and Y. Satou. 2016. Transcriptional and Epigenetic Regulatory Mechanisms Affecting HTLV-1 Provirus. *Viruses* 8:

Mori, Y., M. Koike, E. Moriishi, A. Kawabata, H. Tang, H. Oyaizu, Y. Uchiyama, and K. Yamanishi. 2008. Human herpesvirus-6 induces MVB formation, and virus egress occurs by an exosomal release pathway. *Traffic* 9:1728-1742.

Mrizak, D., N. Martin, C. Barjon, A.S. Jimenez-Pailhes, R. Mustapha, T. Niki, J. Guigay, V. Pancre, Y. de Launoit, P. Busson, O. Morales, and N. Delhem. 2015. Effect of nasopharyngeal carcinoma-derived exosomes on human regulatory T cells. *J Natl Cancer Inst* 107:363.

Mukae, H., S. Kohno, N. Morikawa, J. Kadota, S. Matsukura, and K. Hara. 1994. Increase in T-cells bearing CD25 in bronchoalveolar lavage fluid from HAM/TSP patients and HTLV-I carriers. *Microbiology and immunology* 38:55-62.

Murr, C., B. Widner, B. Wirleitner, and D. Fuchs. 2002. Neopterin as a marker for immune system activation. *Curr Drug Metab* 3:175-187.

Nagai, M., R. Kubota, T.F. Greten, J.P. Schneck, T.P. Leist, and S. Jacobson. 2001. Increased activated human T cell lymphotropic virus type I (HTLV-I) Tax11-19-specific memory and effector CD8+ cells in patients with HTLV-I-associated myelopathy/tropical spastic paraparesis: correlation with HTLV-I provirus load. *The Journal of infectious diseases* 183:197-205.

Nagai, M., K. Usuku, W. Matsumoto, D. Kodama, N. Takenouchi, T. Moritoyo, S. Hashiguchi, M. Ichinose, C.R. Bangham, S. Izumo, and M. Osame. 1998. Analysis of HTLV-I proviral load in 202 HAM/TSP patients and 243 asymptomatic HTLV-I carriers: high proviral load strongly predisposes to HAM/TSP. *Journal of neurovirology* 4:586-593.

Nakamaru, Y., A. Ishizu, H. Ikeda, T. Sugaya, K. Fugo, M. Higuchi, H. Yamazaki, and T. Yoshiki. 2001. Immunological hyperresponsiveness in HTLV-I LTR-env-pX transgenic rats: a prototype animal model for collagen vascular and HTLV-I-related inflammatory diseases. *Pathobiology* 69:11-18.

Nakano, K., and T. Watanabe. 2012. HTLV-1 Rex: the courier of viral messages making use of the host vehicle. *Frontiers in microbiology* 3:330.

Nakano, K., and T. Watanabe. 2016. HTLV-1 Rex Tunes the Cellular Environment Favorable for Viral Replication. *Viruses* 8:58.

Nakase, K., J. Cheng, Q. Zhu, and W.A. Marasco. 2009. Mechanisms of SHP-1 P2 promoter regulation in hematopoietic cells and its silencing in HTLV-1-transformed T cells. *Journal of leukocyte biology* 85:165-174.

Narayanan, A., S. Iordanskiy, R. Das, R. Van Duyne, S. Santos, E. Jaworski, I. Guendel, G. Sampey, E. Dalby, M. Iglesias-Ussel, A. Popratiloff, R. Hakami, K. Kehn-Hall, M. Young, C. Subra, C. Gilbert, C. Bailey, F. Romerio, and F. Kashanchi. 2013. Exosomes derived from HIV-1-infected cells contain trans-activation response element RNA. *The Journal of biological chemistry* 288:20014-20033.

Ng, W.F., P.J. Duggan, F. Ponchel, G. Matarese, G. Lombardi, A.D. Edwards, J.D. Isaacs, and R.I. Lechler. 2001. Human CD4(+)CD25(+) cells: a naturally occurring population of regulatory T cells. *Blood* 98:2736-2744.

Niederer, H.A., D.J. Laydon, A. Melamed, M. Elemans, B. Asquith, M. Matsuoka, and C.R. Bangham. 2014. HTLV-1 proviral integration sites differ between asymptomatic carriers and patients with HAM/TSP. *Virology journal* 11:172.

Nishimoto, N., K. Yoshizaki, N. Eiraku, K. Machigashira, H. Tagoh, A. Ogata, T. Kuritani, M. Osame, and T. Kishimoto. 1990. Elevated levels of interleukin-6 in serum and cerebrospinal fluid of HTLV-I-associated myelopathy/tropical spastic paraparesis. *J Neurol Sci* 97:183-193.

Nishimura, M., D.E. McFarlin, and S. Jacobson. 1993. Sequence comparisons of HTLV-I from HAM/TSP patients and their asymptomatic spouses. *Neurology* 43:2621-2624.

Nour, A.M., and Y. Modis. 2014. Endosomal vesicles as vehicles for viral genomes. *Trends in cell biology* 24:449-454.

Oh, U., C. Grant, C. Griffith, K. Fugo, N. Takenouchi, and S. Jacobson. 2006. Reduced Foxp3 protein expression is associated with inflammatory disease during human t lymphotropic virus type 1 Infection. *The Journal of infectious diseases* 193:1557-1566.

Oh, U., and S. Jacobson. 2008. Treatment of HTLV-I-associated myelopathy/tropical spastic paraparesis: toward rational targeted therapy. *Neurol Clin* 26:781-797, ix-x.

Oh, U., Y. Yamano, C.A. Mora, J. Ohayon, F. Bagnato, J.A. Butman, J. Dambrosia, T.P. Leist, H. McFarland, and S. Jacobson. 2005. Interferon-beta1a therapy in human T-lymphotropic virus type I-associated neurologic disease. *Annals of neurology* 57:526-534.

Ohsugi, T., and T. Kumasaka. 2011. Low CD4/CD8 T-cell ratio associated with inflammatory arthropathy in human T-cell leukemia virus type I Tax transgenic mice. *PloS one* 6:e18518.

Okoye, I.S., S.M. Coomes, V.S. Pelly, S. Czieso, V. Papayannopoulos, T. Tolmachova, M.C. Seabra, and M.S. Wilson. 2014. MicroRNA-containing T-regulatory-cell-derived exosomes suppress pathogenic T helper 1 cells. *Immunity* 41:89-103.

Osame, M. 2002. Pathological mechanisms of human T-cell lymphotropic virus type I-associated myelopathy (HAM/TSP). *Journal of neurovirology* 8:359-364.

Ostrowski, M., N.B. Carmo, S. Krumeich, I. Fanget, G. Raposo, A. Savina, C.F. Moita, K. Schauer, A.N. Hume, R.P. Freitas, B. Goud, P. Benaroch, N. Hacohen, M. Fukuda, C. Desnos, M.C. Seabra, F. Darchen, S. Amigorena, L.F. Moita, and C. Thery. 2010. Rab27a and Rab27b control different steps of the exosome secretion pathway. *Nature cell biology* 12:19-30; sup pp 11-13.

Pacholczyk, R., J. Kern, N. Singh, M. Iwashima, P. Kraj, and L. Ignatowicz. 2007. Nonself-antigens are the cognate specificities of Foxp3+ regulatory T cells. *Immunity* 27:493-504.

Palacios, D., D. Summerbell, P.W. Rigby, and J. Boyes. 2010. Interplay between DNA methylation and transcription factor availability: implications for developmental activation of the mouse Myogenin gene. *Mol Cell Biol* 30:3805-3815.

Paschos, K., and M.J. Allday. 2010. Epigenetic reprogramming of host genes in viral and microbial pathogenesis. *Trends in microbiology* 18:439-447.

Pashoutan Sarvar, D., K. Shamsasenjan, and P. Akbarzadehlaleh. 2016. Mesenchymal Stem Cell-Derived Exosomes: New Opportunity in Cell-Free Therapy. *Adv Pharm Bull* 6:293-299.

Perez-Hernandez, D., C. Gutierrez-Vazquez, I. Jorge, S. Lopez-Martin, A. Ursa, F. Sanchez-Madrid, J. Vazquez, and M. Yanez-Mo. 2013. The intracellular interactome of tetraspanin-enriched microdomains reveals their function as sorting machineries toward exosomes. *The Journal of biological chemistry* 288:11649-11661.

Polansky, J.K., L. Schreiber, C. Thelemann, L. Ludwig, M. Kruger, R. Baumgrass, S. Cording, S. Floess, A. Hamann, and J. Huehn. 2010. Methylation matters: binding of Ets-1 to the demethylated Foxp3 gene contributes to the stabilization of Foxp3 expression in regulatory T cells. *J Mol Med (Berl)* 88:1029-1040.

Proietti, F.A., A.B. Carneiro-Proietti, B.C. Catalan-Soares, and E.L. Murphy. 2005. Global epidemiology of HTLV-I infection and associated diseases. *Oncogene* 24:6058-6068.

Puccioni-Sohler, M., E. Gasparetto, M.J. Cabral-Castro, C. Slatter, C.M. Vidal, R.D. Cortes, B.R. Rosen, and C. Mainero. 2012. HAM/TSP: association between white matter lesions on magnetic resonance imaging, clinical and cerebrospinal fluid findings. *Arq Neuropsiquiatr* 70:246-251.

Puccioni-Sohler, M., Y. Yamano, M. Rios, S.M. Carvalho, C.C. Vasconcelos, R. Papais-Alvarenga, and S. Jacobson. 2007. Differentiation of HAM/TSP from patients with multiple sclerosis infected with HTLV-I. *Neurology* 68:206-213.

Ramakrishnaiah, V., C. Thumann, I. Fofana, F. Habersetzer, Q. Pan, P.E. de Ruiter, R. Willemsen, J.A. Demmers, V. Stalin Raj, G. Jenster, J. Kwekkeboom, H.W. Tilanus, B.L. Haagmans, T.F. Baumert, and L.J. van der Laan. 2013. Exosome-mediated transmission of hepatitis C virus between human hepatoma Huh7.5 cells. *Proceedings of the National Academy of Sciences of the United States of America* 110:13109-13113.

Rao, A., N. Kamani, A. Filipovich, S.M. Lee, S.M. Davies, J. Dalal, and S. Shenoy. 2007. Successful bone marrow transplantation for IPEX syndrome after reduced-intensity conditioning. *Blood* 109:383-385.

Ren, T., Y. Takahashi, X. Liu, T.P. Loughran, S.C. Sun, H.G. Wang, and H. Cheng. 2015. HTLV-1 Tax deregulates autophagy by recruiting autophagic molecules into lipid raft microdomains. *Oncogene* 34:334-345.

Rende, F., I. Cavallari, A. Corradin, M. Silic-Benussi, F. Toulza, G.M. Toffolo, Y. Tanaka, S. Jacobson, G.P. Taylor, D.M. D'Agostino, C.R. Bangham, and V. Ciminale. 2011. Kinetics and intracellular compartmentalization of HTLV-1 gene expression: nuclear retention of HBZ mRNAs. *Blood* 117:4855-4859.

Reynaud, J.M., and B. Horvat. 2013. Animal models for human herpesvirus 6 infection. *Frontiers in microbiology* 4:174.

Ribeiro, L.C., C.C. Goncalves, C.M. Slater, S.M. Carvalho, and M. Puccioni-Sohler. 2013. Standardisation of Western blotting to detect HTLV-1 antibodies synthesised in

the central nervous system of HAM/TSP patients. *Mem Inst Oswaldo Cruz* 108:730-734.

Richardson, J.H., A.J. Edwards, J.K. Cruickshank, P. Rudge, and A.G. Dalgleish. 1990. In vivo cellular tropism of human T-cell leukemia virus type 1. *Journal of virology* 64:5682-5687.

Robbins, P.D., and A.E. Morelli. 2014. Regulation of immune responses by extracellular vesicles. *Nature reviews. Immunology* 14:195-208.

Rocha, A.J., I.A. Littig, R.H. Nunes, and C.P. Tilbery. 2013. Central nervous system infectious diseases mimicking multiple sclerosis: recognizing distinguishable features using MRI. *Arq Neuropsiquiatr* 71:738-746.

Romanelli, L.C., P. Caramelli, M.L. Martins, D.U. Goncalves, F.A. Proietti, J.G. Ribas, M.G. Araujo, and A.B. Carneiro-Proietti. 2013. Incidence of human T cell lymphotropic virus type 1-associated myelopathy/tropical spastic paraparesis in a long-term prospective cohort study of initially asymptomatic individuals in Brazil. *AIDS research and human retroviruses* 29:1199-1202.

Rosser, E.C., and C. Mauri. 2015. Regulatory B cells: origin, phenotype, and function. *Immunity* 42:607-612.

Roucourt, B., S. Meeussen, J. Bao, P. Zimmermann, and G. David. 2015. Heparanase activates the syndecan-syntenin-ALIX exosome pathway. *Cell Res* 25:412-428.

Sage, P.T., L.M. Francisco, C.V. Carman, and A.H. Sharpe. 2013. The receptor PD-1 controls follicular regulatory T cells in the lymph nodes and blood. *Nature immunology* 14:152-161.

Sahin, M., E. Sahin, and S. Koksoy. 2013. Regulatory T cells in cancer: an overview and perspectives on cyclooxygenase-2 and Foxp3 DNA methylation. *Human immunology* 74:1061-1068.

Sakaguchi, S. 2005. Naturally arising Foxp3-expressing CD25+CD4+ regulatory T cells in immunological tolerance to self and non-self. *Nature immunology* 6:345-352.

Sakaguchi, S., K. Fukuma, K. Kuribayashi, and T. Masuda. 1985. Organ-specific autoimmune diseases induced in mice by elimination of T cell subset. I. Evidence for the active participation of T cells in natural self-tolerance; deficit of a T cell subset as a possible cause of autoimmune disease. *The Journal of experimental medicine* 161:72-87.

Sakai, J.A., M. Nagai, M.B. Brennan, C.A. Mora, and S. Jacobson. 2001. In vitro spontaneous lymphoproliferation in patients with human T-cell lymphotropic virus type I-associated neurologic disease: predominant expansion of CD8+ T cells. *Blood* 98:1506-1511.

Sampey, G.C., S.S. Meyering, M. Asad Zadeh, M. Saifuddin, R.M. Hakami, and F. Kashanchi. 2014. Exosomes and their role in CNS viral infections. *Journal of neurovirology* 20:199-208.

Saribas, A.S., A. Ozdemir, C. Lam, and M. Safak. 2010. JC virus-induced Progressive Multifocal Leukoencephalopathy. *Future Virol* 5:313-323.

Sato, T., A. Coler-Reilly, A. Utsunomiya, N. Araya, N. Yagishita, H. Ando, J. Yamauchi, E. Inoue, T. Ueno, Y. Hasegawa, K. Nishioka, T. Nakajima, S. Jacobson, S. Izumo, and

Y. Yamano. 2013. CSF CXCL10, CXCL9, and neopterin as candidate prognostic biomarkers for HTLV-1-associated myelopathy/tropical spastic paraparesis. *PLoS Negl Trop Dis* 7:e2479.

Satou, Y., J. Yasunaga, M. Yoshida, and M. Matsuoka. 2006. HTLV-I basic leucine zipper factor gene mRNA supports proliferation of adult T cell leukemia cells. *Proceedings of the National Academy of Sciences of the United States of America* 103:720-725.

Satou, Y., J. Yasunaga, T. Zhao, M. Yoshida, P. Miyazato, K. Takai, K. Shimizu, K. Ohshima, P.L. Green, N. Ohkura, T. Yamaguchi, M. Ono, S. Sakaguchi, and M. Matsuoka. 2011. HTLV-1 bZIP factor induces T-cell lymphoma and systemic inflammation in vivo. *PLoS pathogens* 7:e1001274.

Savina, A., C.M. Fader, M.T. Damiani, and M.I. Colombo. 2005. Rab11 promotes docking and fusion of multivesicular bodies in a calcium-dependent manner. *Traffic* 6:131-143.

Sawant, D.V., and D.A. Vignali. 2014. Once a Treg, always a Treg? *Immunol Rev* 259:173-191.

Schmidt, A., N. Oberle, and P.H. Krammer. 2012. Molecular mechanisms of treg-mediated T cell suppression. *Front Immunol* 3:51.

Schmidt, O., and D. Teis. 2012. The ESCRT machinery. *Curr Biol* 22:R116-120.

Schorey, J.S., Y. Cheng, P.P. Singh, and V.L. Smith. 2015. Exosomes and other extracellular vesicles in host-pathogen interactions. *EMBO reports* 16:24-43.

Schuler, P.J., Z. Saze, C.S. Hong, L. Muller, D.G. Gillespie, D. Cheng, M. Harasymczuk, M. Mandapathil, S. Lang, E.K. Jackson, and T.L. Whiteside. 2014. Human CD4+ CD39+ regulatory T cells produce adenosine upon co-expression of surface CD73 or contact with CD73+ exosomes or CD73+ cells. *Clinical and experimental immunology* 177:531-543.

Shembade, N., and E.W. Harhaj. 2010. Role of post-translational modifications of HTLV-1 Tax in NF-kappaB activation. *World journal of biological chemistry* 1:13-20.

Shen, B., N. Wu, J.M. Yang, and S.J. Gould. 2011. Protein targeting to exosomes/microvesicles by plasma membrane anchors. *The Journal of biological chemistry* 286:14383-14395.

Shimazu, Y., Y. Shimazu, M. Hishizawa, M. Hamaguchi, Y. Nagai, N. Sugino, S. Fujii, M. Kawahara, N. Kadowaki, H. Nishikawa, S. Sakaguchi, and A. Takaori-Kondo. 2016. Hypomethylation of the Treg-Specific Demethylated Region in FOXP3 Is a Hallmark of the Regulatory T-cell Subtype in Adult T-cell Leukemia. *Cancer Immunol Res* 4:136-145.

Shoeibi, A., M. Etemadi, A. Moghaddam Ahmadi, M. Amini, and R. Boostani. 2013. "HTLV-I Infection" Twenty-Year Research in Neurology Department of Mashhad University of Medical Sciences. *Iran J Basic Med Sci* 16:202-207.

Sibon, D., A.S. Gabet, M. Zandecki, C. Pinatel, J. Thete, M.H. Delfau-Larue, S. Rabaaoui, A. Gessain, O. Gout, S. Jacobson, F. Mortreux, and E. Wattel. 2006. HTLV-1 propels untransformed CD4 lymphocytes into the cell cycle while protecting CD8 cells from death. *The Journal of clinical investigation* 116:974-983.

Smith, M.R., and W.C. Greene. 1990. Identification of HTLV-I tax trans-activator mutants exhibiting novel transcriptional phenotypes. *Genes Dev* 4:1875-1885.

Sojka, D.K., Y.H. Huang, and D.J. Fowell. 2008. Mechanisms of regulatory T-cell suppression - a diverse arsenal for a moving target. *Immunology* 124:13-22.

Stockis, J., W. Fink, V. Francois, T. Connerotte, C. de Smet, L. Knoops, P. van der Bruggen, T. Boon, P.G. Coulie, and S. Lucas. 2009. Comparison of stable human Treg and Th clones by transcriptional profiling. *European journal of immunology* 39:869-882.

Stoorvogel, W. 2015. Resolving sorting mechanisms into exosomes. *Cell Res* 25:531-532.

Stuffers, S., C. Sem Wegner, H. Stenmark, and A. Brech. 2009. Multivesicular endosome biogenesis in the absence of ESCRTs. *Traffic* 10:925-937.

Sugata, K., J. Yasunaga, H. Kinosada, Y. Mitobe, R. Furuta, M. Mahgoub, C. Onishi, K. Nakashima, K. Ohshima, and M. Matsuoka. 2016. HTLV-1 Viral Factor HBZ Induces CCR4 to Promote T-cell Migration and Proliferation. *Cancer research* 76:5068-5079.

Suvas, S., A.K. Azkur, B.S. Kim, U. Kumaraguru, and B.T. Rouse. 2004. CD4+CD25+ regulatory T cells control the severity of viral immunoinflammatory lesions. *Journal of immunology* 172:4123-4132.

Szajnik, M., M. Czystowska, M.J. Szczepanski, M. Mandapathil, and T.L. Whiteside. 2010. Tumor-derived microvesicles induce, expand and up-regulate biological activities of human regulatory T cells (Treg). *PloS one* 5:e11469.

Szurek, E., A. Cebula, L. Wojciech, M. Pietrzak, G. Rempala, P. Kisielow, and L. Ignatowicz. 2015. Differences in Expression Level of Helios and Neuropilin-1 Do Not Distinguish Thymus-Derived from Extrathymically-Induced CD4+Foxp3+ Regulatory T Cells. *PloS one* 10:e0141161.

Tamai, K., N. Tanaka, T. Nakano, E. Kakazu, Y. Kondo, J. Inoue, M. Shiina, K. Fukushima, T. Hoshino, K. Sano, Y. Ueno, T. Shimosegawa, and K. Sugamura. 2010. Exosome secretion of dendritic cells is regulated by Hrs, an ESCRT-0 protein. *Biochemical and biophysical research communications* 399:384-390.

Tamburro, D., C. Fredolini, V. Espina, T.A. Douglas, A. Ranganathan, L. Ilag, W. Zhou, P. Russo, B.H. Espina, G. Muto, E.F. Petricoin, 3rd, L.A. Liotta, and A. Luchini. 2011. Multifunctional core-shell nanoparticles: discovery of previously invisible biomarkers. *Journal of the American Chemical Society* 133:19178-19188.

Tanaka, A., A. Jinno-Oue, N. Shimizu, A. Hoque, T. Mori, S. Islam, Y. Nakatani, M. Shinagawa, and H. Hoshino. 2012. Entry of human T-cell leukemia virus type 1 is augmented by heparin sulfate proteoglycans bearing short heparin-like structures. *Journal of virology* 86:2959-2969.

Tanoue, T., K. Atarashi, and K. Honda. 2016. Development and maintenance of intestinal regulatory T cells. *Nature reviews. Immunology* 16:295-309.

Thornton, A.M., P.E. Korty, D.Q. Tran, E.A. Wohlfert, P.E. Murray, Y. Belkaid, and E.M. Shevach. 2010. Expression of Helios, an Ikaros transcription factor family member, differentiates thymic-derived from peripherally induced Foxp3+ T regulatory cells. *Journal of immunology* 184:3433-3441.

Thornton, A.M., and E.M. Shevach. 1998. CD4+CD25+ immunoregulatory T cells suppress polyclonal T cell activation in vitro by inhibiting interleukin 2 production. *The Journal of experimental medicine* 188:287-296.

Toker, A., and J. Huehn. 2011. To be or not to be a Treg cell: lineage decisions controlled by epigenetic mechanisms. *Science signaling* 4:pe4.

Trajkovic, K., C. Hsu, S. Chiantia, L. Rajendran, D. Wenzel, F. Wieland, P. Schwille, B. Brugger, and M. Simons. 2008. Ceramide triggers budding of exosome vesicles into multivesicular endosomes. *Science* 319:1244-1247.

Umehara, F., S. Izumo, M. Takeya, K. Takahashi, E. Sato, and M. Osame. 1996. Expression of adhesion molecules and monocyte chemoattractant protein -1 (MCP-1) in the spinal cord lesions in HTLV-I-associated myelopathy. *Acta Neuropathol* 91:343-350.

Urbanelli, L., A. Magini, S. Buratta, A. Brozzi, K. Sagini, A. Polchi, B. Tancini, and C. Emiliani. 2013. Signaling pathways in exosomes biogenesis, secretion and fate. *Genes (Basel)* 4:152-170.

van Niel, G., S. Charrin, S. Simoes, M. Romao, L. Rochin, P. Saftig, M.S. Marks, E. Rubinstein, and G. Raposo. 2011. The tetraspanin CD63 regulates ESCRT-independent and -dependent endosomal sorting during melanogenesis. *Developmental cell* 21:708-721.

Verweij, F.J., M.A. van Eijndhoven, E.S. Hopmans, T. Vendrig, T. Wurdinger, E. Cahir-McFarland, E. Kieff, D. Geerts, R. van der Kant, J. Neefjes, J.M. Middeldorp, and D.M. Pegtel. 2011. LMP1 association with CD63 in endosomes and secretion via exosomes limits constitutive NF-kappaB activation. *EMBO J* 30:2115-2129.

Vieira, P.L., J.R. Christensen, S. Minaee, E.J. O'Neill, F.J. Barrat, A. Boonstra, T. Barthlott, B. Stockinger, D.C. Wraith, and A. O'Garra. 2004. IL-10-secreting regulatory T cells do not express Foxp3 but have comparable regulatory function to naturally occurring CD4+CD25+ regulatory T cells. *Journal of immunology* 172:5986-5993.

Vignali, D.A., L.W. Collison, and C.J. Workman. 2008. How regulatory T cells work. *Nature reviews. Immunology* 8:523-532.

Villarroya-Beltri, C., F. Baixauli, C. Gutierrez-Vazquez, F. Sanchez-Madrid, and M. Mittelbrunn. 2014. Sorting it out: regulation of exosome loading. *Semin Cancer Biol* 28:3-13.

Villarroya-Beltri, C., C. Gutierrez-Vazquez, F. Sanchez-Cabo, D. Perez-Hernandez, J. Vazquez, N. Martin-Cofreces, D.J. Martinez-Herrera, A. Pascual-Montano, M. Mittelbrunn, and F. Sanchez-Madrid. 2013. Sumoylated hnRNPA2B1 controls the sorting of miRNAs into exosomes through binding to specific motifs. *Nat Commun* 4:2980.

Virtanen, J.O., and S. Jacobson. 2012. Viruses and multiple sclerosis. *CNS Neurol Disord Drug Targets* 11:528-544.

Wager-Smith, K., and A. Markou. 2011. Depression: a repair response to stress-induced neuronal microdamage that can grade into a chronic neuroinflammatory condition? *Neurosci Biobehav Rev* 35:742-764.

Wang, G.J., Y. Liu, A. Qin, S.V. Shah, Z.B. Deng, X. Xiang, Z. Cheng, C. Liu, J. Wang, L. Zhang, W.E. Grizzle, and H.G. Zhang. 2008. Thymus exosomes-like particles induce regulatory T cells. *Journal of immunology* 181:5242-5248.

Wang, J., A. Ioan-Facsinay, E.I. van der Voort, T.W. Huizinga, and R.E. Toes. 2007. Transient expression of FOXP3 in human activated nonregulatory CD4+ T cells. *European journal of immunology* 37:129-138.

Wang, L., Y. Liu, R. Han, U.H. Beier, R.M. Thomas, A.D. Wells, and W.W. Hancock. 2013. Mbd2 promotes foxp3 demethylation and T-regulatory-cell function. *Molecular and cellular biology* 33:4106-4115.

Wang, Y.M., and S.I. Alexander. 2009. CD8 regulatory T cells: what's old is now new. *Immunol Cell Biol* 87:192-193.

Weiss, R.A., and P.K. Vogt. 2011. 100 years of Rous sarcoma virus. *The Journal of experimental medicine* 208:2351-2355.

Whiteside, T.L. 2016. Exosomes and tumor-mediated immune suppression. *The Journal of clinical investigation* 126:1216-1223.

Wildin, R.S., F. Ramsdell, J. Peake, F. Faravelli, J.L. Casanova, N. Buist, E. Levy-Lahad, M. Mazzella, O. Goulet, L. Perroni, F.D. Bricarelli, G. Byrne, M. McEuen, S. Proll, M. Appleby, and M.E. Brunkow. 2001. X-linked neonatal diabetes mellitus, enteropathy and endocrinopathy syndrome is the human equivalent of mouse scurfy. *Nature genetics* 27:18-20.

Wodarz, D., M.A. Nowak, and C.R. Bangham. 1999. The dynamics of HTLV-I and the CTL response. *Immunol Today* 20:220-227.

Wong, C.P., L.P. Nguyen, S.K. Noh, T.M. Bray, R.S. Bruno, and E. Ho. 2011. Induction of regulatory T cells by green tea polyphenol EGCG. *Immunol Lett* 139:7-13.

Xiao, T., W. Zhang, B. Jiao, C.Z. Pan, X. Liu, and L. Shen. 2017. The role of exosomes in the pathogenesis of Alzheimer' disease. *Transl Neurodegener* 6:3.

Yadav, M., C. Louvet, D. Davini, J.M. Gardner, M. Martinez-Llordella, S. Bailey-Bucktrout, B.A. Anthony, F.M. Sverdrup, R. Head, D.J. Kuster, P. Ruminski, D. Weiss, D. Von Schack, and J.A. Bluestone. 2012. Neuropilin-1 distinguishes natural and inducible regulatory T cells among regulatory T cell subsets in vivo. *The Journal of experimental medicine* 209:1713-1722, S1711-1719.

Yadav, M., S. Stephan, and J.A. Bluestone. 2013. Peripherally induced tregs - role in immune homeostasis and autoimmunity. *Front Immunol* 4:232.

Yagi, H., T. Nomura, K. Nakamura, S. Yamazaki, T. Kitawaki, S. Hori, M. Maeda, M. Onodera, T. Uchiyama, S. Fujii, and S. Sakaguchi. 2004. Crucial role of FOXP3 in the development and function of human CD25+CD4+ regulatory T cells. *International immunology* 16:1643-1656.

Yamamoto, N., M. Okada, Y. Koyanagi, M. Kannagi, and Y. Hinuma. 1982. Transformation of human leukocytes by cocultivation with an adult T cell leukemia virus producer cell line. *Science* 217:737-739.

Yamamoto-Taguchi, N., Y. Satou, P. Miyazato, K. Ohshima, M. Nakagawa, K. Katagiri, T. Kinashi, and M. Matsuoka. 2013. HTLV-1 bZIP factor induces inflammation through labile Foxp3 expression. *PLoS pathogens* 9:e1003630.

Yamano, Y., N. Araya, T. Sato, A. Utsunomiya, K. Azakami, D. Hasegawa, T. Izumi, H. Fujita, S. Aratani, N. Yagishita, R. Fujii, K. Nishioka, S. Jacobson, and T. Nakajima. 2009. Abnormally high levels of virus-infected IFN-gamma+ CCR4+ CD4+ CD25+ T cells in a retrovirus-associated neuroinflammatory disorder. *PloS one* 4:e6517.

Yamano, Y., C.J. Cohen, N. Takenouchi, K. Yao, U. Tomaru, H.C. Li, Y. Reiter, and S. Jacobson. 2004. Increased expression of human T lymphocyte virus type I (HTLV-I) Tax11-19 peptide-human histocompatibility leukocyte antigen A*201 complexes on CD4+ CD25+ T Cells detected by peptide-specific, major histocompatibility complex-restricted antibodies in patients with HTLV-I-associated neurologic disease. *The Journal of experimental medicine* 199:1367-1377.

Yamano, Y., and T. Sato. 2012. Clinical pathophysiology of human T-lymphotropic virus-type 1-associated myelopathy/tropical spastic paraparesis. *Frontiers in microbiology* 3:389.

Yamano, Y., N. Takenouchi, H.C. Li, U. Tomaru, K. Yao, C.W. Grant, D.A. Maric, and S. Jacobson. 2005. Virus-induced dysfunction of CD4+CD25+ T cells in patients with HTLV-I-associated neuroimmunological disease. *The Journal of clinical investigation* 115:1361-1368.

Yang, M., K. Rui, S. Wang, and L. Lu. 2013. Regulatory B cells in autoimmune diseases. *Cell Mol Immunol* 10:122-132.

Yano, H., T. Ishida, A. Inagaki, T. Ishii, S. Kusumoto, H. Komatsu, S. Iida, A. Utsunomiya, and R. Ueda. 2007. Regulatory T-cell function of adult T-cell leukemia/lymphoma cells. *Int J Cancer* 120:2052-2057.

Yin, J.C., and T. Tully. 1996. CREB and the formation of long-term memory. *Curr Opin Neurobiol* 6:264-268.

Yoshioka, A., G. Hirose, Y. Ueda, Y. Nishimura, and K. Sakai. 1993. Neuropathological studies of the spinal cord in early stage HTLV-I-associated myelopathy (HAM). *J Neurol Neurosurg Psychiatry* 56:1004-1007.

Zalckvar, E., C. Paulus, D. Tillo, A. Asbach-Nitzsche, Y. Lubling, C. Winterling, N. Strieder, K. Mucke, F. Goodrum, E. Segal, and M. Nevels. 2013. Nucleosome maps of the human cytomegalovirus genome reveal a temporal switch in chromatin organization linked to a major IE protein. *Proceedings of the National Academy of Sciences of the United States of America* 110:13126-13131.

Zeringer, E., T. Barta, M. Li, and A.V. Vlassov. 2015. Strategies for isolation of exosomes. *Cold Spring Harb Protoc* 2015:319-323.

Zhang, J., S. Li, L. Li, M. Li, C. Guo, J. Yao, and S. Mi. 2015. Exosome and exosomal microRNA: trafficking, sorting, and function. *Genomics Proteomics Bioinformatics* 13:17-24.

Zhao, T., Y. Satou, K. Sugata, P. Miyazato, P.L. Green, T. Imamura, and M. Matsuoka. 2011. HTLV-1 bZIP factor enhances TGF-beta signaling through p300 coactivator. *Blood* 118:1865-1876.

Zheng, Q., Y. Xu, Y. Liu, B. Zhang, X. Li, F. Guo, and Y. Zhao. 2009. Induction of Foxp3 demethylation increases regulatory CD4+CD25+ T cells and prevents the occurrence of diabetes in mice. *J Mol Med (Berl)* 87:1191-1205.

Zheng, Y., S. Josefowicz, A. Chaudhry, X.P. Peng, K. Forbush, and A.Y. Rudensky. 2010. Role of conserved non-coding DNA elements in the Foxp3 gene in regulatory T-cell fate. *Nature* 463:808-812.

Zhi, H., L. Yang, Y.L. Kuo, Y.K. Ho, H.M. Shih, and C.Z. Giam. 2011. NF-kappaB hyper-activation by HTLV-1 tax induces cellular senescence, but can be alleviated by the viral anti-sense protein HBZ. *PLoS pathogens* 7:e1002025.

Ziegler, S.F. 2006. FOXP3: of mice and men. *Annu Rev Immunol* 24:209-226.

Zozulya, A.L., and H. Wiendl. 2008. The role of regulatory T cells in multiple sclerosis. *Nat Clin Pract Neurol* 4:384-398.

Appendix I

Publications

J Neuroimmune Pharmacol (2014) 9:522–532
DOI 10.1007/s11481-014-9547-z

ORIGINAL ARTICLE

Epigenetic Modification of the FoxP3 TSDR in HAM/TSP Decreases the Functional Suppression of Tregs

Monique R. Anderson · Yoshimi Enose-Akahata · Raya Massoud · Nyater Ngouth · Yuetsu Tanaka · Unsong Oh · Steven Jacobson

Received: 27 January 2014 / Accepted: 4 May 2014 / Published online: 21 May 2014

Abstract HTLV-1 is a human retrovirus that is associated with the neuroinflammatory disorder HTLV-1 associated myelopathy/tropical spastic paraparesis (HAM/TSP). In these patients, HTLV-1 is primarily found in the $CD4^+CD25^+$ T cell subset (Regulatory T cells:Tregs), which is responsible for peripheral immune tolerance and is known to be dysfunctional in HAM/TSP. Recent evidence suggests that FoxP3 expression and function is determined epigenetically through DNA demethylation in the Treg-specific demethylated region (TSDR). We analyzed the methylation of the TSDR in PBMCs, $CD4^+$ T cells, and $CD4^+CD25^+$ T cells from normal healthy donors (NDs) and HAM/TSP patients. We demonstrated that there is decreased demethylation in analyzed PBMCs and $CD4^+CD25^+$ T cells from HAM/TSP patients as compared to NDs. Furthermore, decreased TSDR demethylation was associated with decreased functional suppression by Tregs. Additionally, increased HTLV-1 Tax expression in HAM/TSP PBMC culture correlated with a concomitant decline in FoxP3 TSDR demethylation. Overall, we suggest that HTLV-1 infection decreases Treg functional suppressive capacity in HAM/TSP through modification of FoxP3 TSDR demethylation and that dysregulated Treg function may contribute to HAM/TSP disease pathogenesis.

Keywords Regulatory T cells · HTLV-1 · Treg specific demethylation region (TSDR) · Epigenetic regulation · Suppressive capacity · Demethylation

Introduction

Human T cell Lymphotropic Virus-1 (HTLV-1) is a human retrovirus initially isolated in 1980 from a patient with a cutaneous T cell lymphoma (Poiesz et al. 1980). It is estimated that 15–20 million people worldwide are infected, though the vast majority will remain asymptomatic carriers (Proietti et al. 2005; Osame et al. 1986). Approximately 0.25–4 % will develop HTLV-1 associated myelopathy/tropical spastic paraparesis (HAM/TSP) with another 1–5 % developing Adult T cell leukemia/lymphoma (ATLL) (Proietti et al. 2005). HAM/TSP is a neuroinflammatory disorder characterized by perivascular inflammatory infiltration in the brain and spinal cord (Izumo 2010). Activated cytotoxic T cells ($CD8^+$ T cells) and the production of inflammatory cytokines, including IFN-γ and TNF-α, have been associated with damage to the central nervous system (CNS) (Barmak et al. 2003), eventually leading to urinary and bowel incontinence, spastic limb paraparesis, parasthesias and ataxia manifesting after a long asymptomatic phase of infection (Evangelou et al. 2012). In all HTLV-1 infected

M. R. Anderson · Y. Enose-Akahata · R. Massoud · N. Ngouth · S. Jacobson (✉)
Neuroimmunology Branch, Viral Immunological Section, National Institute of Neurological Disorders and Stroke, National Institutes of Health, 10 Center Drive Rm 5C103, Bethesda, MD 20892, USA
e-mail: jacobsons@ninds.nih.gov

M. R. Anderson
Howard Hughes Medical Institute-National Institutes of Health Research Scholars Program, Howard Hughes Medical Institute, Chevy Chase, MD 20815, USA

M. R. Anderson
Department of Pathology, University of Virginia School of Medicine, Molecular and Cellular Basis of Disease Graduate Program, Charlottesville, VA 22908, USA

Y. Tanaka
Department of Immunology, Graduate School of Medicine, University of the Ryukyus, Nishihara-cho, Okinawa 903-0125, Japan

U. Oh
Department of Neurology, Virginia Commonwealth University, Richmond, VA 23298, USA

individuals the primary viral reservoir is $CD4^+CD25^+$ T cells (Yamano et al. 2004), a subset of which is comprised of regulatory T cells (Tregs). Given that Treg dysfunction has been reported in HAM/TSP patients (Yamano et al. 2005), proper characterization of Tregs and their functional abnormalities may provide an assessment of the immune dysregulation observed in HAM/TSP patients and serve as a valuable biomarker in clinical trials.

Tregs are essential in maintaining peripheral immune tolerance through their ability to actively suppress auto-reactive T cells and other inflammatory immune responses (Sakaguchi 2005). They have been implicated in cancer, infectious disease, autoimmunity, transplant medicine and allergy, but their characterization and isolation has proven to be complex (Balandina et al. 2005; Chen et al. 2007; Weiss et al. 2012). Although the cell surface markers CD4 and CD25 are routinely used for their isolation, in humans the $CD4^+CD25^+$subset also includes activated T cells. Notably, only the top 1–2 % of these cells ($CD4^+CD25^{hi}$) is considered to be functionally suppressive (Baecher-Allan et al. 2001), and this frequency varies physiologically, especially with increased age (Gregg et al. 2005). Several additional markers used to characterize Tregs in healthy donors, including GITR, CD127, and CTLA4, are unreliable here due to their alteration by HTLV-1 related activation (Ramirez et al. 2010; Michaelsson et al. 2008).

FoxP3 was first identified as a specific Treg marker in the context of the genetic disorder Immunodysregulation polyendocrinopathy enteropathy X-linked syndrome (IPEX) in which the gene is mutated (Wildin et al. 2001). IPEX patients develop life-threatening autoimmune complications due to a defect in Tregs (van der Vliet and Nieuwenhuis 2007). Furthermore, when $CD4^+CD25^-$ T cells (Teffs) were induced to express FoxP3, they acquired a Treg phenotype indicating that FoxP3 is a Treg lineage specific factor (Loser et al. 2005). However, in the human immune system, the FoxP3 expressing subset includes many cell types (i.e. natural, induced, naive, memory, etc.) with different functions and FoxP3 expression levels (Miyara et al. 2009). Additionally, there is up-regulation of FoxP3 transiently upon activation of T cells (Wang et al. 2007). Therefore, in inflammatory disorders such as HAM/TSP, Foxp3 expression may not be a reliable marker of Tregs.

Recent research has highlighted the importance of DNA methylation in the epigenetic control of Foxp3 gene expression (Bettini et al. 2012; Lal and Bromberg 2009). Studies have shown that selective demethylation of a conserved CpG island within the Foxp3 locus termed the Treg-specific demethylated region (TSDR) leads to stable Foxp3 expression and defines thymic-derived natural Tregs (Toker and Huehn 2011). On the other hand, activated T cells and peripherally-induced Tregs (iTregs) exhibit a variably methylated FoxP3 TSDR (Baron et al. 2007). Importantly, stable expression of FoxP3 through demethylation of the TSDR is necessary for Treg suppression (Polansky et al. 2010).

We examined levels of TSDR demethylation in PBMCs, $CD4^+$ T cells and $CD4^+CD25^+$ T cells obtained from normal healthy donors (NDs) and HAM/TSP patients. The results demonstrated decreased demethylation in the FoxP3 TSDR of HAM/TSP patients as compared to NDs that correlates with the decreased suppressive capacity of $CD4^+CD25^+$ T cells in these patients. The lower levels of demethylation seen in the $CD4^+CD25^+$ subset of our HAM/TSP patients may also serve as an indicator of disease progression and suggests that a virus or viral gene may contribute to dysregulation of Tregs.

Materials and Methods

Patient Samples

A total of 10 ND PBMCs and 9 HAM/TSP PBMCs samples were used for this study. An additional 3 ND PBMC samples and 6 HAM/TSP samples were used for 24 h PBMC culture. ND ranged from 28 to 64 years old while HAM/TSP patients ranged from 31 to 70 years old. PBMCs were isolated by Ficoll-Hypaque (Lonza, Walkersville, MD) centrifugation, and were cryopreserved in liquid nitrogen until use. All NDs were noted to be healthy and HTLV-1 negative. The study was reviewed and approved by the National Institute of Neurological Disorders and Stroke Institutional Review Board. Informed consent was written and obtained from each subject in accordance with the Declaration of Helsinki.

Cell Lines

HTLV-1-infected human cell lines HUT102 and MT2 and the uninfected cell lines Jurkat and MOLT3 were used. All the cells were cultured in RPMI 1640 supplemented with 10 % FBS, 100 U/mL penicillin, 100 μg/mL streptomycin sulfate, and 2 mM L-glutamine in 5 % CO_2 incubator at 37 °C.

DNA Isolation

Total DNA was isolated from cell lines or cells obtained from NDs and HAM/TSP patients using the DNeasy Blood and Tissue Kit (Qiagen, Germantown, MD). All samples were incubated with RNAse A at 37 °C for 30 min to ensure removal of all RNA.

Bisulfite Conversion

Due to the harshness of the reaction, at least 1 μg of DNA was utilized when possible. All samples were initially cut with Fast Digest EcoRI (Fermentas, Glen Burnie, MD).

Bisulfite conversions were completed using the Cells-to-CpG kit (Applied Biosystems, Foster City, CA) according to the manufacturer's instructions.

Quantitative PCR

Bisulfite converted DNA was amplified in two separate reactions on a ViiA7 thermocycler (Applied Biosystems, Foster City, CA). One reaction amplied demethylated FoxP3 and the other amplified methylated FoxP3 using primers and probes directed against FoxP3 intron1 (Stockis et al. 2009). The reactions occurred in a total volume of 20 μl with 5 μl of bisulfite converted DNA. The thermal cycler conditions were as follows: 50 °C for 2 min, 95 °C for 10 min, 40 cycles at 95 °C for 15 s (denaturation) and 60 °C for 1 min (annealing and extension), and 25 °C for 2 min. The level of demethylation was calculated as published previously (Stockis et al. 2009) and values from female patients were doubled to account for 2 X chromosomes.

Flow Cytometry

For analysis of $CD4^+$ T cell population, cells were stained with CD3-APC-Cy7, CD4-PE-Cy7, and CD25-PE (BD Bioscience, San Jose, CA) and then fixed with Fixation Buffer (eBioscience, San Diego, CA) following their supplied protocol. After washing the cells with permiabilization buffer (eBioscience), FoxP3 antibody (236A/E7; eBioscience) was added to cells for the intracellular staining. Monoclonal isotype controls were used for each antibody and set as the negative control. Flow cytometric analysis was performed using a LSRII (BD Biosciences). All data were analyzed using FlowJo software (Tree Star, San Carlos, CA).

$CD4^+CD25^+$ T Cell Enrichment

PBMCs were thawed and then enriched for $CD4^+$ T cells using $CD4^+CD25^+$ Treg isolation kit (Miltenyi Biotec, Bergisch Gladbach, Germany). $CD4^+$ T cells were then labeled with CD25-biotin beads and separated on a column for isolation of $CD4^+CD25^+$cells and $CD4^+CD25^-$ cells. Purity was assessed by flow cytometry using an CD25-PE antibody (BD Biosciences clone M-A251). The results in this study on levels of FoxP3 TSDR demethylation was adjusted (normalized) to the purity of the $CD4^+CD25^+$ T cell bead isolation from each patient (that ranged from 50.7 to 90.6 % mean = 65.5 in HAM/TSP and 22.7–80.1 % mean = 53.03 in ND, p = NS).

Suppression Assays

Suppressive function of Tregs in ND and HAM/TSP patients was assessed by inhibitory effects of allogeneic cell proliferation. $CD4^+CD25^+$ T cells were magnetically isolated from 3 ND and 2 HAM/TSP patients. 2.5 μM CFSE (Invitrogen Life Technologies, Carlsbad, CA) was integrated into Teffs isolated from the same ND for each experiment. Teffs were added at 2×10^4 cells in 96 U-bottom microplates containing varying amounts of irradiated Tregs for final ratio of Treg:Teff of 0.25:1 to 1:1, 500 ng/mL anti-CD3 HIT3a (BD Biosciences) and 5×10^4 cells of autologous irradiated ND PBMCs (used as feeder cells) in 5 % Human AB serum in RPMI 1640 with 100 U/mL penicillin, 100 μg/mL streptomycin sulfate, and 2 mM L-glutamine. PBMC and Tregs were gamma irradiated to 3000 rad using a Cs irradiation source. After culture for 3 days, cells were stained with CD3-APC, CD4-Alexa700, and CD-25PE (BD Biosciences) and then analyzed on LSRII for proliferation. Cells stained with monoclonal isotype antibodies were used as negative controls.

Tax and HBZ mRNA Quantification

Total RNA was extracted from PBMCs using RNeasy Mini Kit (Qiagen) according to the manufacturer's instructions. 85 ng of total RNA was converted into cDNA and amplified in a one step reaction using TaqMan® RNA-to-CtTM 1-Step Kit (Applied Biosystems) according to the manufacturer's instructions. *Tax* primer and probe sequences (Oh et al. 2005) or *HBZ* primer probe (Enose-Akahata et al. 2013) were added to mRNA samples and amplified on a Viia7 (Applied Biosystems) thermocycler as follows: 48 °C for 15 min, 95 °C for 10 min, and 45 cycles at 95 °C for 15 s and 60 °C for 1 min. *HPRT* primers and probe were added to mRNA for an assessment of RNA quantity and quality on samples in each run. MT-2 was used as a calibrator sample and the level of *tax* and *HBZ* mRNA expression was then calculated using the comparative CT method on ViiA 7 software.

Tax Expression

6 HAM/TSP and 3 ND PBMCs were incubated at 37 °C in RPMI 10 %FBS for 24 h to allow for peak expression of HTLV-1 Tax (Rende et al. 2011). Cells were then stained with CD3-Pacific Blue, CD4-PECy7, CD25-PE, CD8-PerCp5.5 (BD Biosciences) for cell surface staining. FoxP3-APC (eBioscience), and Lt-4-Alexa Flour® 488 were added for intracellular staining according to the manufacturer's protocol. Cells were also stained with monoclonal isotype control antibodies as negative controls and analyzed on LSRII for staining intensity. PBMCs were collected before and after culture to extract total DNA and then analyze FoxP3 TSDR demethylation.

Proviral Load

Proviral load was determined from DNA using the same *tax* primers and probes mentioned previously (Oh et al. 2005) and amplified as a standard curve against TARL2 DNA standards. Relative proviral load was determined against *actin* quantity in the samples and run on a ViiA7 thermocycler as noted for quantitative PCR.

Statistical Analysis

TSDR demethylation, frequency of $CD4^+CD25^+$T cells and FoxP3 expression in NDs and HAM/TSP patients were analyzed by the Student's unpaired *t*-test. Suppression assays were grouped and analyzed by Two-way Anova. Intersample and intrasample comparisons of Treg:Teff ratios were analyzed by the Student's unpaired *t*-test. A linear regression was performed to determine correlation between TSDR demethylation and %suppression and between the change in TSDR demehtylation and Tax expression in $CD4^+CD25^+$ T cells after culture. All statistical analyses were performed using Prism (GraphPad software). p-values <0.05 % were considered significant.

Results

FoxP3 TSDR Demethylation in HAM/TSP Patients

To examine TSDR demethylation in HAM/TSP primary T cells, DNA from whole PBMCs, $CD4^+$ T cells, and $CD4^+CD25^+$T cells was isolated and compared to NDs for FoxP3 TSDR methylation status. TSDR demethylation was calculated as the percentage of DNA in FoxP3 intron 1 that amplified with primers directed against demethylated CpG islands in FoxP3 Intron 1 versus DNA that amplified with primers against methylated CpG islands in FoxP3 Intron 1 (Materials and Methods; (Toker and Huehn 2011; Sahin et al. 2013). In NDs, 2.066 % (s.d.+/− 0.154 %) of FoxP3 TSDR demethylation was detected in whole PBMCs (Fig. 1a). A significant increase in demethylation was detected in the total $CD4^+$ T cell (8.097 %) population and even higher in the isolated $CD4^+$ $CD25^+$ T cell subset (60.15 %) compared to whole PBMCs ($p=0.0004$ and $p<0.0001$, respectively; Fig. 1b). Similarly to ND, whole HAM/TSP PBMCs showed 3.022 % (s.d.+/− 0.552) of FoxP3 TSDR demethylation with a statistically significant increase in demethylation in $CD4^+$ T cell (10.11 %) and $CD4^+$ $CD25^+$ T cell subsets (48.43 %)

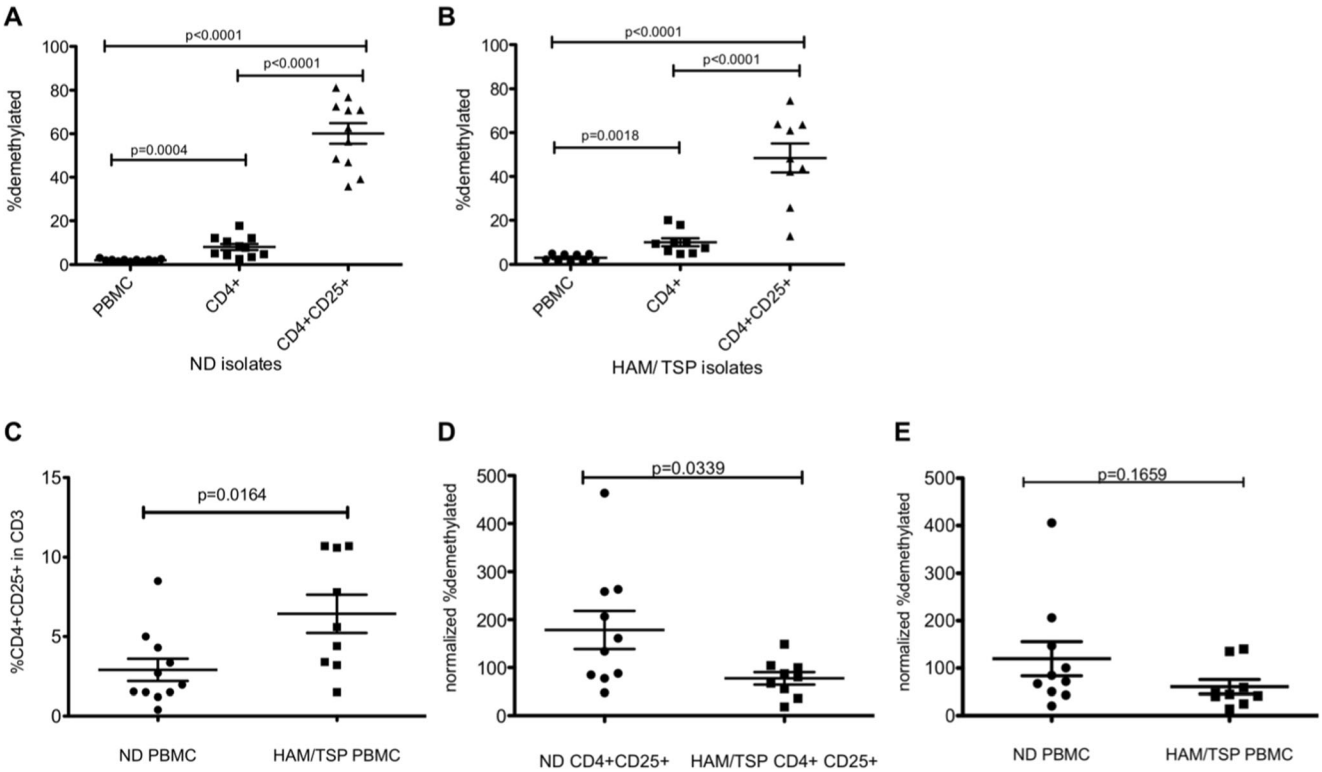

Fig. 1 **a** % FoxP3 TSDR demethylation in ND PBMC ($n=10$), isolated $CD4^+$ T cells, and isolated $CD4^+CD25^+$ T cells. **b** % FoxP3 TSDR demethylation in HAM/TSP PBMC ($n=9$), isolated $CD4^+$ T cells, and isolated $CD4^+CD25^+$ T cells. The *long horizontal bars* represent the mean for each group while the *shorter bars* represent the standard deviation. **c** A comparison of the % $CD4^+CD25^+$ in $CD3^+$ T cells of ND and HAM/TSP PBMC. **d** Normalized % FoxP3 TSDR demethylation in isolated $CD4^+CD25^+$ T cells of ND and HAM/TSP patients. % FoxP3 TSDR demethylation was normalized to the % $CD4^+CD25^+$. **e** Normalized % FoxP3 TSDR demethylation in PBMC of ND and HAM/TSP patients. % FoxP3 TSDR demethylation was normalized to the % $CD4^+CD25^+$

compared to whole PBMCs (p=0.0018 and p<0.0001, respectively; Fig. 1b). Thus, the enrichment of $CD4^+CD25^+$ T cells from whole PBMC significantly increases the percentage of FoxP3 TSDR demethylation and is consistent with previous studies (Liu et al. 2010).

Since the frequency of $CD4^+CD25^+$ T cells is known to be elevated in HAM/TSP patients compared to NDs (Mukae et al. 1994), it was important to incorporate this when measuring FoxP3 TSDR methylation. As shown in Fig. 1c, indeed the frequency of $CD4^+CD25^+$ T cells was significantly higher in HAM/TSP patients than NDs (p=0.0164). There was no significant difference in the percentage of $CD4^+$ T cells between the two groups (unpublished observations). Therefore, after normalization to the frequency of $CD4^+CD25^+$ T cells, HAM/TSP patients were found to have a statistically significant decreased demethylated percentage in isolated $CD4^+$ $CD25^+$ T cells as compared to NDs (p=0.0339; Fig. 1d). A similar trend was also observed in whole PBMCs although this relationship did not reach statistical significance (p= 0.1659; Fig. 1e) probably due to the low frequency of $CD4^+CD25^+$ cells in PBMCs (Fig. 1c).

No Correlation Between the Percent $FoxP3^+$ Cells and FoxP3 Demethylation

Many investigators have relied upon FoxP3 by flow cytometry for characterization of Tregs (Miyara et al. 2009). Although in NDs it appears to be a reliable marker, FoxP3 can also be increased upon T cell activation (Wang et al. 2007). FoxP3 mRNA and protein has been demonstrated to be decreased in HAM/TSP patients, although this was demonstrated in isolated T cell subsets (Oh et al. 2006). Interestingly, when the percentage of $FoxP3^+$ cells in HAM/TSP PBMCs were compared by flow cytometry, $CD4^+CD25^+$ cells were shown to have equivalent FoxP3 percentage compared to NDs (p=0.4676; Fig. 2a). In particular, the percent $FoxP3^+$ cells in PBMCs and the level of FoxP3 TSDR demethylation did not correlate in our experiments (p=0.2765, r^2=0.0692; Fig. 2b). These results are likely due to transient expression of FoxP3 in activated T cells, which are increased in HAM/TSP patients compared to NDs (Yamano et al. 2009). Therefore, the percent of $FoxP3^+$ cells by flow analysis does not correlate with FoxP3 TSDR demethylation in human PBMCs.

Correlation of FoxP3 TSDR Demethylation with Treg Suppressive Function

The level of FoxP3 TSDR demethylation in isolated $CD4^+CD25^+$ T cells varied widely between the HAM/TSP patients included in our study. To determine if there was a correlation between methylation status of the FoxP3 TSDR and functional suppression of isolated $CD4^+CD25^+$ T cells, allogeneic Treg suppression assays were performed. NDs with previously confirmed demethylated TSDRs were compared with HAM/TSP patients with confirmed methylated TSDRs. As a control, ND $CD4^+CD25^+$ T cells were able to suppress allogeneic activated ND Teffs and this suppressive capacity increased depending on Treg:Teff ratio (Fig. 3a–c). In contrast, HAM/TSP patients $CD4^+$ $CD25^+$ T cells suppressed to a significantly lesser extent, especially at high Treg:Teff (1:1) (p =0.0041; Fig. 3c). A two-way ANOVA analysis demonstrated a significant difference in suppression when assessing both patient type (HAM/TSP vs. ND) and Treg:Teff ratio. In addition, there was a trend (with 2 NDs and 2 HAM/TSP patients) for the level of demethylation in the FoxP3 TSDR to positively associate with the level of suppression. These results demonstrated that the decrease of Treg suppressive function in HAM/TSP patients may be associated with the demethylation status of FoxP3 TSDR.

FoxP3 Demethylation in HTLV-1 $CD4^+$ T Cell Lines

Initially, HTLV-1-infected and uninfected cell lines were characterized for expression of virus specific gene products, Treg markers (CD25 and FoxP3) and the demethylation levels of the FoxP3 TSDR.

Both HTLV-1-infected cell lines MT2 and HUT102 express CD25 (95.7, 96.5 % respectively) (Fig. 4a) while the HTLV-1-uninfected cell lines Jurkat and MOLT-3 were CD25 negative (Fig. 4a). Only MT2 expressed a high percentage of

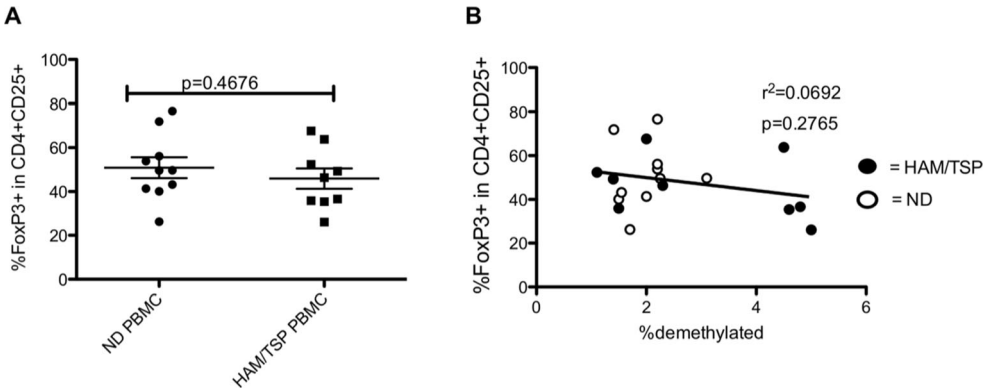

Fig. 2 **a** % $FoxP3^+$ cells in $CD4^+CD25^+$ T cells of ND and HAM/TSP patients. The *long horizontal bars* represent the mean for each group while the *shorter bars* represent the standard deviation. **b** No correlation of the %FoxP3 TSDR demethylation in PBMCs with the % $FoxP3^+$ cells in $CD4^+CD25^+$ T cells of ND (*opened circles*) and HAM/TSP patients (*closed circles*)

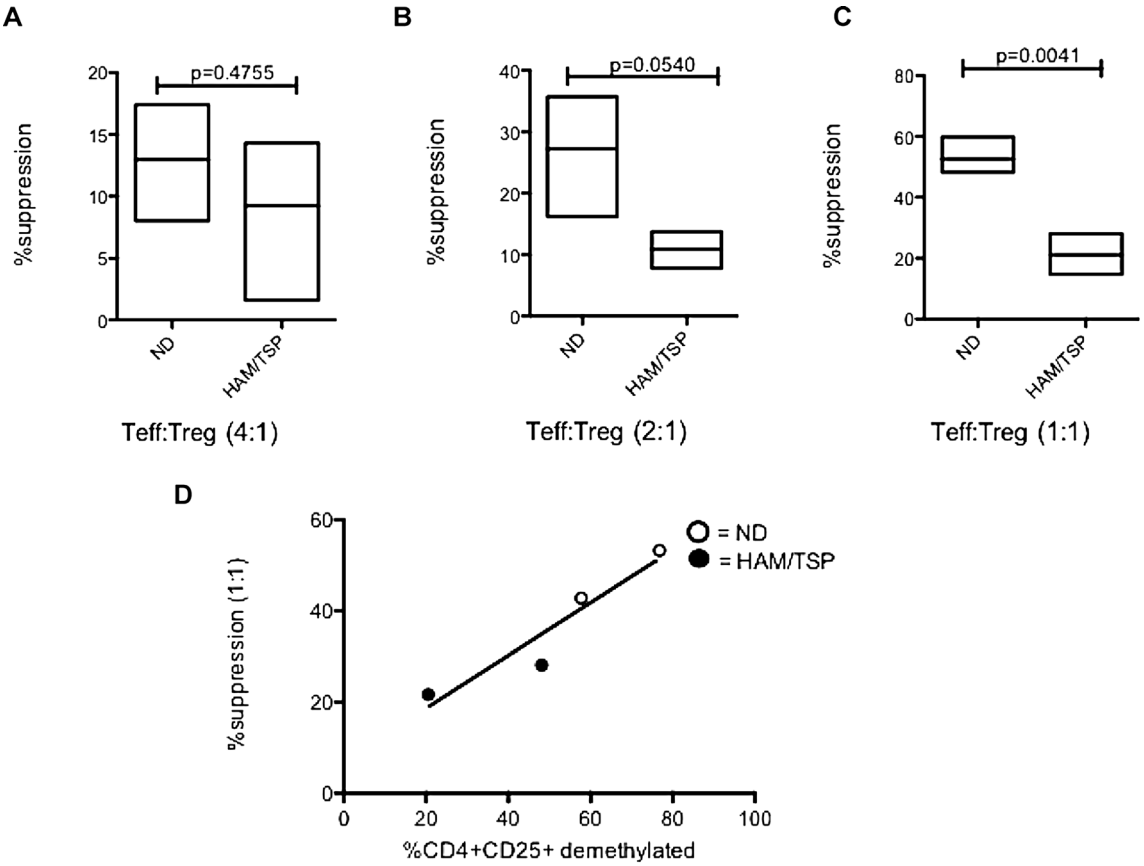

Fig. 3 Lymphoproliferation suppression assays were set up and ND (n=3) or HAM/TSP (n=2) $CD4^+CD25^+$ T cells were added at different ratios of Treg:Teff = 0.25:1 (**a**), 0.5:1 (**b**) and 1:1 (**c**). The % suppressions of Treg were normalized to Teff proliferation without Treg. **d** Correlation between $CD4^+CD25^+$ TSDR % demethylation and suppressive capacity as determined in lymphoproliferation suppression assays at Treg:Teff ratio of 1:1

$FoxP3^+$ cells in the $CD25^+$ T cell population (97.6 %) (Fig. 4a). In contrast, HUT102 had very few $CD25^+$ $FoxP3^+$cells (1.3 %) (Fig. 4a). The two uninfected $CD25^-$ T cell lines had low levels of FoxP3 positivity (Fig. 4a) consistent with previous reports (Yagi et al. 2004).

Given the variation of CD25 and the percent FoxP3 positivity in these cell lines, the level of FoxP3 TSDR demethylation was determined in each. The MT2 cell line, which had the highest percentage of FoxP3 by flow cytometry, had a FoxP3 TSDR that was completely demethylated, displaying similar levels of demethylation to that reported in natural thymus-derived Tregs from healthy donors (95–99.98 %) (Fig. 4b) (Janson et al. 2008). By contrast, HUT102 was completely methylated (Fig. 4b). Similarly, the two uninfected T cell lines that had low FoxP3 positivity by flow cytometry also displayed complete methylation.

Since HTLV-1 gene products including Tax and HTLV-1 basic leucine zipper factor (HBZ) have previously been suggested to interact with FoxP3 (Grant et al. 2008; Satou et al. 2011), we next determined if FoxP3 methylation status was associated with expression of these viral proteins. Since MT-2 expressed both *tax* and *HBZ* mRNA, all the data was normalized to *tax* and *HBZ* mRNA expressions in MT-2 as 1.00. When compared to MT-2, HUT102 expressed more *tax* mRNA (12.24 times) but had lower *HBZ* mRNA levels (Fig. 4c and d), as previously reported (Satou et al. 2006). As expected, *tax* and *HBZ* mRNA were not detected in Jurkat and MOLT3, the two HTLV-1-uninfected cell lines. Thus, *tax* mRNA expression levels were elevated in the HTLV-1-infected cell line that had complete FoxP3 TSDR methylation (HUT 102, Fig. 4b). By contrast, the MT2 cell line which had lower levels of *tax* expression had a completely demethylated FoxP3 TSDR. Since both HTLV-1 infected T cell lines expressed HTLV-1 *HBZ*, there appeared to be no relationship with FoxP3 TSDR methylation.

Negative Correlation of FoxP3 TSDR Demethylation with HTLV-1 Tax Expression

HTLV-1 Tax is a pleiotropic viral protein that transactivates a number of cellular pathways, directly regulates interleukin production, promotes IL-2 independent growth in infected T cells, and impacts gene expression through chromatin remodeling (Currer et al. 2012). HAM/TSP patients are known to

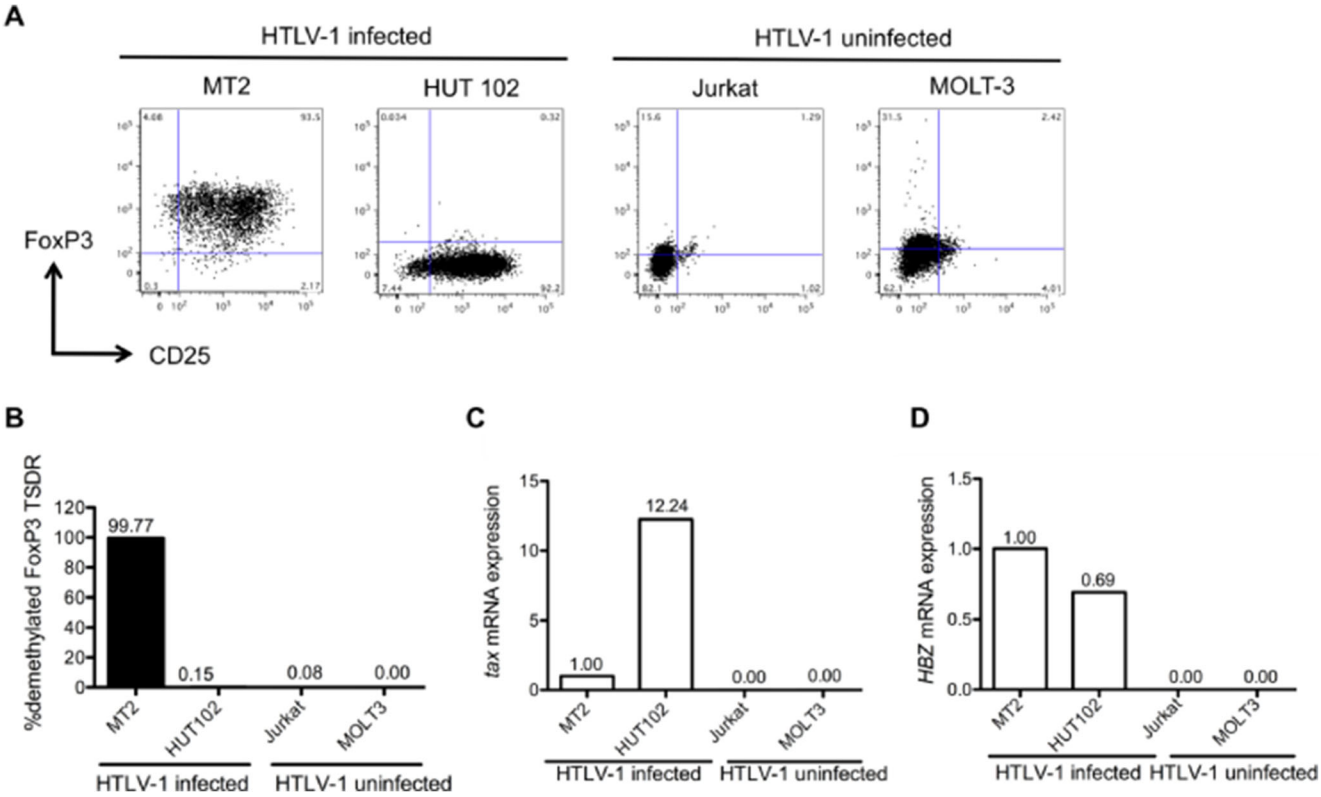

Fig. 4 HTLV-1-infected and HTLV-1-uninfected cell line profiles. **a** Flow cytometry profiles of HTLV-1-infected and HTLV-1-uninfected cell lines. The x-axis denotes CD25 expression and the y-axis denotes FoxP3 expression. **b** FoxP3 TSDR demethylation analysis of HTLV-1-infected and HTLV-1-uninfected cell lines. **c** *Tax* mRNA expression in the cell lines by RT-PCR. The data were calculated as relative amount to MT2 (1.00). **d** *HBZ* mRNA expression in the cell lines by RT-PCR. The data were calculated as relative amount to MT2 (1.00)

express more of this viral gene than asymptomatic carriers (AC) (Nagai et al. 1998). Moreover, Tax has previously been shown to decrease FoxP3 levels after transfection into ND $CD4^+CD25^+$ T cells (Yamano et al. 2005). We therefore asked if there was also a correlation with increased HTLV-1 Tax expression in HAM/TSP $CD4^+CD25^+$ T cells and decreased FoxP3 TSDR demethylation.

Freshly thawed PBMCs do not express HTLV-1 Tax at baseline by flow cytometry (Fig. 5a), however, after short-term culture (24 h), variable levels of Tax expression were observed, particularly in the $CD4^+CD25^+$ T cell subset (Fig. 5a). Proof of concept was performed by observing FoxP3 demethylation before and after culture in isolated $CD4^+$T cells from 2 HAM/TSP patients. Both showed a significant decline in FoxP3 TSDR demethylation after culture. Increasing levels of HTLV-1 Tax in $CD4^+CD25^+$ HAM/TSP T cells had a strong linear correlation (Coefficient of determination $r^2=0.7736$, $p=0.0145$; Fig. 5b) with a decline in the FoxP3 TSDR demethylation from HAM/TSP PBMC. This decreased FoxP3 TSDR demethylation in HAM/TSP also correlated with the levels of HTLV-1 *tax* mRNA expression in PBMC after 24 h culture (unpublished observations). As controls, there were no changes in FoxP3 TSDR demethylation in short-term cultures of ND PBMCs that were HTLV-1 Tax negative (Fig. 5b, circled points). To assess for the possibility that the decline in FoxP3 TSDR demethylation may be attributed to Treg death via $CD8^+$ cytotoxic T cell killing, two of our patient samples were depleted of $CD8^+$ T cells by bead isolation. As shown in Fig. 5c, in the absence of $CD8^+$ T cells, both patients still demonstrated a large decline in FoxP3 TSDR demethylation post-culture that mirrored a concomitant increase in *tax* mRNA expression (Fig. 5c).

Discussion

Immune dysregulation is a prominent feature in HTLV-1-associated disorders, although how the virus contributes to this outcome remains incompletely understood. Of particular interest, HAM/TSP patients display an activated inflammatory immune response associated with a decreased suppressive capacity in Treg cells (Nishiura et al. 1996). In contrast, it has been demonstrated that the immunocompromised state seen in ATLL patients may be a result of clonal expansion of a Treg precursor, suppressing anti-tumor immunity (Yano et al. 2007). Flow cytometry, has been used to characterize these Tregs, based on a number of cell surface markers and

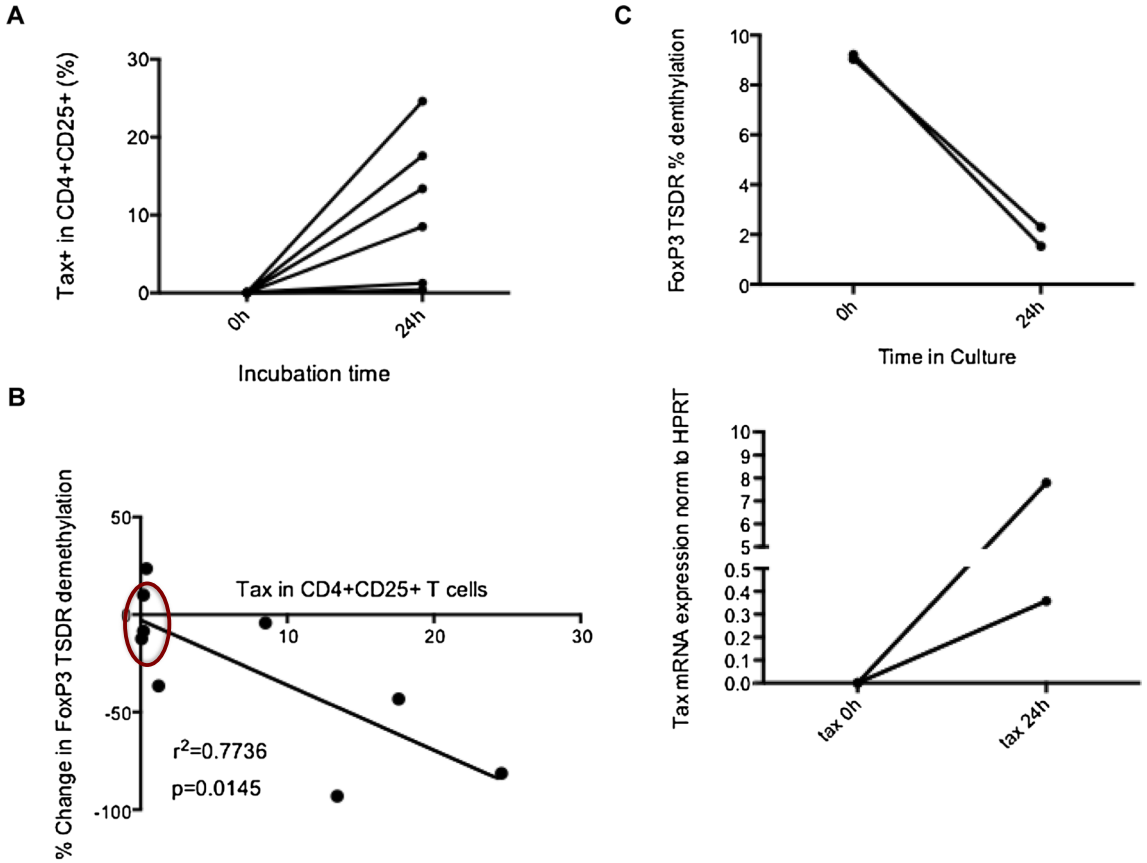

Fig. 5 Increased Tax expression correlates with reduced FoxP3 TSDR demethylation. **a** Tax protein expression in $CD4^+CD25^+$ T cells of HAM/TSP patients before and after culture. PBMCs of HAM/TSP patients (n= 6) were cultured for 24 h. **b** Correlation of the Tax protein expression in $CD4^+CD25^+$ T cells of HAM/TSP patients with the change in FoxP3 TSDR demethylation before and after culture for 24 h. ND samples are circled in red. Coefficient of determination r^2=0. 7736 (**c**) %FoxP3 TSDR demethylation and *tax* mRNA expression in isolated HAM/TSP $CD4^+$ T cells ex vivo

intracellular expression of FoxP3. However many of these same markers, including FoxP3, are also seen on activated T cells (Wang et al. 2007). Furthermore, the use of FoxP3 as a Treg lineage specific marker has been difficult due to the heterogeneity in phenotype and function within the human FoxP3 subset (d'Hennezel et al. 2011).

FoxP3 TSDR methylation status has been suggested to be a better indicator of sustained Treg suppressive function, particularly in inflammatory environments (Polansky et al. 2008). Recently, it has been demonstrated that FoxP3 TSDR demethylation can be characterized from whole blood PBMCs if used in conjunction with normalization to a specific T cell population (Barzaghi et al. 2012). We took a similar approach by enumerating demethylation of the FoxP3 TSDR in i) PBMCs; ii) $CD4^+$ T cells; iii) $CD4^+$ $CD25^+$ T cells of HAM/TSP patients normalized to the activated $CD4^+$ T cell population as determined by flow cytometry. Since HAM/TSP patients have a higher percentage of $CD4^+CD25^+$ T cells (Fig. 1c) reflective of the activated T cell population known to be elevated in this disease (Mukae et al. 1994; Yamano et al. 2009), it is informative to normalize the levels of FoxP3 TSDR demethylation to the percentage of $CD4^+$ $CD25^+$ T cells. After normalization, there was, a significant decrease in the percentage of FoxP3 TSDR demethylation observed in HAM/TSP patient $CD4^+CD25^+$ T cells compared to ND. In addition, attempts to more stringently select Treg cells and eliminate activated T cells by using $CD4^+CD25^+CD127^-$ bead isolation did not increase the FoxP3 TSDR demethylation of isolated cells compared with the Foxp3 TSDR demethylation calculated from cells isolated with $CD4^+CD25^+$ beads (unpublished observation). This suggested that levels of TSDR demethylation in purified CD^+CD25^+ T cells and normalization to CD25 expression is a reasonable method to purify Tregs.

The ultimate indicator of Treg function is the suppressive capacity of Tregs as determined by an in vitro functional assay such as lymphoproliferation (Ukena et al. 2011). Indeed, in HAM/TSP $CD4^+CD25^+$ T cells with lower levels of FoxP3 TSDR demethylation we observed substantially reduced Treg suppression compared to ND $CD4^+CD25^+$ T cells with higher levels of FoxP3 TSDR demethylation (Fig. 4) and a trend of an association with the level of FoxP3 TSDR demethylation with Treg suppression (Fig. 3). While additional patients and

controls will be required to confirm this observation, these results suggest that FoxP3 TSDR demethylation may be a good surrogate for Treg functional suppressive capacity. In addition, it would be of interest to compare FoxP3 levels, as assessed by FoxP3 protein expression or MFI analysis by flow, with Treg suppression. This dysregulation of Tregs may foster a proinflammatory environment that contributes to the pathogenesis of HAM/TSP (Grant et al. 2008).

The results in this study are consistent with previous reports demonstrating decreased Treg function in HAM/TSP (Yamano et al. 2005) though it had been unclear if this is due to a decreased Treg population, Treg function or both. Since it had been shown that the expression of an HTLV-1 *tax* was associated with a decrease in FoxP3 expression (Yamano et al. 2005) and that HTLV-1 Tax increases after short-term in vitro culture of HAM/TSP PBMC (Rende et al. 2011), we asked if there was also a correlation between the HTLV-1 proviral load and the observed decrease in FoxP3 TSDR demethylation. The observation of decreased FoxP3 demethylation in vitro concurrently with increasing Tax expression led us to believe that these changes in demethylation are a direct consequence of HTLV-1 protein expression since Tax expression did not affect the population of $CD4^+CD25^+$ T cells after culture (unpublished observation). Furthermore, the reduction of FoxP3 demethylation in isolated $CD4^+$ T cells (Fig. 5c) in the absence of cytotoxic T cells suggests a direct effect of Tax on FoxP3 expression rather than cytotoxic T cell mediated lysis of the Treg population. We conclude that the observed dysregulation of Tregs in HAM/TSP is associated with a decrease in Treg function rather than Treg numbers and suggest that this inhibition of Treg function is mediated by the trans-activating properties of the HTLV-1 *tax* gene.

HAM/TSP patients are known to express higher levels of *tax* mRNA compared to asymptomatic carriers (Nagai et al. 1998). Additionally, we have shown that the HUT102 cell line that had higher levels of *tax* expression compared to MT2 was associated with a completely methylated TSDR (Fig. 4). Collectively, these observations on the ex vivo association of reduced Fox P3 TSDR demethylation and high HTLV-1 *tax* expression coupled with the in vitro correlates of Tax expression with decreased demethylation supports the potential role for HTLV-1 *tax* in the dysregulation of the FoxP3 TSDR methylation in HAM/TSP.

Since we have shown that increased virus protein expression was associated with decreased FoxP3 TSDR demethylation, we asked if this also correlated with clinical outcome measures in HAM/TSP. Of the three patients with the largest decrease in FoxP3 TSDR demethylation (patients 1–3 in Table 1) two had high clinical disability scores (IPEC >13). Patients 1 and 2 also had rapid clinical deterioration and shorter duration of disease. Patient 3 had multiple brain lesions on MRI that have progressed since disease onset. Although proviral load correlated with HTLV-1 Tax expression after short-term culture (unpublished observation), it did not correlate with FoxP3 TSDR demethylation. This may be due to measurement of proviral load in whole PBMCs rather than in the main HTLV-1 peripheral reservoir, $CD4^+CD25^+$ T cells. However, if decreased FoxP3 TSDR demethylation is confirmed to be associated with poorer clinical outcome measures in larger cohorts of HAM/TSP patients, this would not only support dysregulation of Tregs as an immunopathological mechanisms in HTLV-1 neurologic disease (Yamano et al. 2005; Grant et al. 2008) but would also introduce potential therapeutic strategies that target epigenetic modification of Treg cells. Many studies have utilized demethylating agents such as 5-aza-2′-deoxycytydine (DAC) and procainamide to demethylate the TSDR in Teffs, thereby transforming them into functionally suppressive Tregs (Zheng et al. 2009; Blanco et al. 2009). Similar agents such as 5-azacytidine and valproate have been explored in HTLV-1 infection but only for their

Table 1 HAM/TSP patient clinical assessment

HAM/TSP patient	Onset of symptoms	Peripheral inflammatory involvement	IPEC disability scale	EDSS	AI	Progression	Tax expression in $CD4^+CD25^+$ after culture (%)	PVL (%)
1	6Y prior to sample collection	None	15	4	4	initial rapid decline, then slow	17.6	3.70
2	4Y prior to sample collection	Multiple: bilateral uveitis, dermatitis.	13	UN	12	rapid progression, ongoing	24.6	40.0
3	2Y prior to sample collection	None	1, multiple MRI lesions	1	0	Relatively stable, cognitive decline	13.4	25.2
4	2Y prior to sample collection	None	12	6	4	initial rapid decline, then slow progression	1.23	14.0
5	Insidious course, unclear date of onset	None	UN	4	2	insidious, slow progression	8.52	10.0
6	13Y prior to sample collection	Uveitis, eczema	7	3.5	UN	insidious, slow progression	0.39	6.32

UN unknown, *EDSS* Expanded disability status score, *IPEC* Instituta de Psquisa Clinica Evandro Chagas, *AI* Ambulatory Index, *PVL* proviral load

potential anti-retroviral and anti-leukemic properties (Belrose et al. 2011; Diamantopoulos et al. 2012). To date, no one has explored their use in restoring Treg function in HAM/TSP.

In summary, the results in this study support the observation that HAM/TSP patients have decreased demethylation in the FoxP3 TSDR that associated with reduced Treg function. These changes in the TSDR appear to be related to HTLV-1 Tax expression in vitro and might inform clinical status in HAM/TSP patients. FoxP3 TSDR methylation status may also serve as a good surrogate biomarker for Treg function in conjunction with other disease parameters in HTLV-1 infected patients. Moreover, these observations provide for a new avenue of therapeutic interventional strategies that may be beneficial to patients with HAM/TSP.

Acknowledgments Special thanks to Mr. Matt McCormick for his contributions to the demethylation protocols developed for this study.

Conflict of Interest The authors declare that they have no conflicts of interest.

References

Baecher-Allan C, Brown JA, Freeman GJ, Hafler DA (2001) CD4+ CD25high regulatory cells in human peripheral blood. J Immunol 167:1245–1253

Balandina A, Lecart S, Dartevelle P, Saoudi A, Berrih-Aknin S (2005) Functional defect of regulatory CD4(+)CD25+ T cells in the thymus of patients with autoimmune myasthenia gravis. Blood 105:735–741

Barmak K, Harhaj EW, Wigdahl B (2003) Mediators of central nervous system damage during the progression of human T-cell leukemia type I-associated myelopathy/tropical spastic paraparesis. J Neurovirol 9:522–529

Baron U, Floess S, Wieczorek G, Baumann K, Grutzkau A, Dong J, Thiel A, Boeld TJ, Hoffmann P, Edinger M, Turbachova I, Hamann A, Olek S, Huehn J (2007) DNA demethylation in the human FOXP3 locus discriminates regulatory T cells from activated FOXP3(+) conventional T cells. Eur J Immunol 37:2378–2389

Barzaghi F, Passerini L, Gambineri E, Ciullini Mannurita S, Cornu T, Kang ES, Choe YH, Cancrini C, Corrente S, Ciccocioppo R, Cecconi M, Zuin G, Discepolo V, Sartirana C, Schmidtko J, Ikinciogullari A, Ambrosi A, Roncarolo MG, Olek S, Bacchetta R (2012) Demethylation analysis of the FOXP3 locus shows quantitative defects of regulatory T cells in IPEX-like syndrome. J Autoimmun 38:49–58

Belrose G, Gross A, Olindo S, Lezin A, Dueymes M, Komla-Soukha I, Smadja D, Tanaka Y, Willems L, Mesnard JM, Peloponese JM Jr, Cesaire R (2011) Effects of valproate on Tax and HBZ expression in HTLV-1 and HAM/TSP T lymphocytes. Blood 118:2483–2491

Bettini ML, Pan F, Bettini M, Finkelstein D, Rehg JE, Floess S, Bell BD, Ziegler SF, Huehn J, Pardoll DM, Vignali DA (2012) Loss of epigenetic modification driven by the Foxp3 transcription factor leads to regulatory T cell insufficiency. Immunity 36:717–730

Blanco B, Perez-Simon JA, Sanchez-Abarca LI, Caballero-Velazquez T, Gutierrez-Cossio S, Hernandez-Campo P, Diez-Campelo M, Herrero-Sanchez C, Rodriguez-Serrano C, Santamaria C, Sanchez-Guijo FM, Del Canizo C, San Miguel JF (2009) Treatment with bortezomib of human CD4+ T cells preserves natural regulatory T cells and allows the emergence of a distinct suppressor T-cell population. Haematologica 94:975–983

Chen X, Zhou B, Li M, Deng Q, Wu X, Le X, Wu C, Larmonier N, Zhang W, Zhang H, Wang H, Katsanis E (2007) CD4(+)CD25(+)FoxP3(+) regulatory T cells suppress Mycobacterium tuberculosis immunity in patients with active disease. Clin Immunol 123:50–59

Currer R, Van Duyne R, Jaworski E, Guendel I, Sampey G, Das R, Narayanan A, Kashanchi F (2012) HTLV tax: a fascinating multifunctional co-regulator of viral and cellular pathways. Front Microbiol 3:406

d'Hennezel E, Yurchenko E, Sgouroudis E, Hay V, Piccirillo CA (2011) Single-cell analysis of the human T regulatory population uncovers functional heterogeneity and instability within FOXP3+ cells. J Immunol 186:6788–6797

Diamantopoulos PT, Michael M, Benopoulou O, Bazanis E, Tzeletas G, Meletis J, Vayopoulos G, Viniou NA (2012) Antiretroviral activity of 5-azacytidine during treatment of a HTLV-1 positive myelodysplastic syndrome with autoimmune manifestations. Virol J 9:1

Enose-Akahata Y, Abrams A, Massoud R, Bialuk I, Johnson KR, Green PL, Maloney EM, Jacobson S (2013) Humoral immune response to HTLV-1 basic leucine zipper factor (HBZ) in HTLV-1-infected individuals. Retrovirology 10:19

Evangelou IE, Oh U, Massoud R, Jacobson S (2012) HTLV-I-associated myelopathy/tropical spastic paraparesis: semiautomatic quantification of spinal cord atrophy from 3-dimensional MR images. J Neuroimaging: Off J Am Soc Neuroimaging 4(1):74–78

Grant C, Oh U, Yao K, Yamano Y, Jacobson S (2008) Dysregulation of TGF-beta signaling and regulatory and effector T-cell function in virus-induced neuroinflammatory disease. Blood 111:5601–5609

Gregg R, Smith CM, Clark FJ, Dunnion D, Khan N, Chakraverty R, Nayak L, Moss PA (2005) The number of human peripheral blood CD4+ CD25 high regulatory T cells increases with age. Clin Exp Immunol 140:540–546

Izumo S (2010) Neuropathology of HTLV-1-associated myelopathy (HAM/TSP). Neuropathol: Off J Jpn Soc Neuropathol

Janson PC, Winerdal ME, Marits P, Thorn M, Ohlsson R, Winqvist O (2008) FOXP3 promoter demethylation reveals the committed Treg population in humans. PLoS ONE 3:e1612

Lal G, Bromberg JS (2009) Epigenetic mechanisms of regulation of Foxp3 expression. Blood 114:3727–3735

Liu J, Lluis A, Illi S, Layland L, Olek S, von Mutius E, Schaub B (2010) T regulatory cells in cord blood–FOXP3 demethylation as reliable quantitative marker. PLoS ONE 5:e13267

Loser K, Hansen W, Apelt J, Balkow S, Buer J, Beissert S (2005) In vitro-generated regulatory T cells induced by Foxp3-retrovirus infection control murine contact allergy and systemic autoimmunity. Gene Ther 12:1294–1304

Michaelsson J, Barbosa HM, Jordan KA, Chapman JM, Brunialti MK, Neto WK, Nukui Y, Sabino EC, Chieia MA, Oliveira AS, Nixon DF, Kallas EG (2008) The frequency of CD127low expressing CD4+ CD25high T regulatory cells is inversely correlated with human T lymphotrophic virus type-1 (HTLV-1) proviral load in HTLV-1-infection and HTLV-1-associated myelopathy/tropical spastic paraparesis. BMC Immunol 9:41

Miyara M, Yoshioka Y, Kitoh A, Shima T, Wing K, Niwa A, Parizot C, Taflin C, Heike T, Valeyre D, Mathian A, Nakahata T, Yamaguchi T, Nomura T, Ono M, Amoura Z, Gorochov G, Sakaguchi S (2009) Functional delineation and differentiation dynamics of human CD4 + T cells expressing the FoxP3 transcription factor. Immunity 30: 899–911

Mukae H, Kohno S, Morikawa N, Kadota J, Matsukura S, Hara K (1994) Increase in T-cells bearing CD25 in bronchoalveolar lavage fluid from HAM/TSP patients and HTLV-I carriers. Microbiol Immunol 38:55–62

Nagai M, Usuku K, Matsumoto W, Kodama D, Takenouchi N, Moritoyo T, Hashiguchi S, Ichinose M, Bangham CR, Izumo S, Osame M (1998) Analysis of HTLV-I proviral load in 202 HAM/TSP patients

and 243 asymptomatic HTLV-I carriers: high proviral load strongly predisposes to HAM/TSP. J Neurovirol 4:586–593

Nishiura Y, Nakamura T, Ichinose K, Shirabe S, Tsujino A, Goto H, Furuya T, Nagataki S (1996) Increased production of inflammatory cytokines in cultured CD4+ cells from patients with HTLV-I-associated myelopathy. Tohoku J Exp Med 179:227–233

Oh U, Yamano Y, Mora CA, Ohayon J, Bagnato F, Butman JA, Dambrosia J, Leist TP, McFarland H, Jacobson S (2005) Interferon-beta1a therapy in human T-lymphotropic virus type I-associated neurologic disease. Ann Neurol 57:526–534

Oh U, Grant C, Griffith C, Fugo K, Takenouchi N, Jacobson S (2006) Reduced Foxp3 protein expression is associated with inflammatory disease during human t lymphotropic virus type 1 Infection. J Infect Dis 193:1557–1566

Osame M, Usuku K, Izumo S, Ijichi N, Amitani H, Igata A, Matsumoto M, Tara M (1986) HTLV-I associated myelopathy, a new clinical entity. Lancet 1:1031–1032

Poiesz BJ, Ruscetti FW, Gazdar AF, Bunn PA, Minna JD, Gallo RC (1980) Detection and isolation of type C retrovirus particles from fresh and cultured lymphocytes of a patient with cutaneous T-cell lymphoma. Proc Natl Acad Sci U S A 77:7415–7419

Polansky JK, Kretschmer K, Freyer J, Floess S, Garbe A, Baron U, Olek S, Hamann A, von Boehmer H, Huehn J (2008) DNA methylation controls Foxp3 gene expression. Eur J Immunol 38:1654–1663

Polansky JK, Schreiber L, Thelemann C, Ludwig L, Kruger M, Baumgrass R, Cording S, Floess S, Hamann A, Huehn J (2010) Methylation matters: binding of Ets-1 to the demethylated Foxp3 gene contributes to the stabilization of Foxp3 expression in regulatory T cells. J Mol Med (Berl) 88:1029–1040

Proietti FA, Carneiro-Proietti AB, Catalan-Soares BC, Murphy EL (2005) Global epidemiology of HTLV-I infection and associated diseases. Oncogene 24:6058–6068

Ramirez E, Cartier L, Rodriguez L, Alberti C, Valenzuela MA (2010) In vivo fluctuation of Tax, Foxp3, CTLA-4, and GITR mRNA expression in CD4(+)CD25(+) T cells of patients with human T-lymphotropic virus type 1-associated myelopathy. Braz J Med Biol Res = Rev Bras Pesquisas Med Biol/Soc Bras Biofisica … [et al] 43: 1109–1115

Rende F, Cavallari I, Corradin A, Silic-Benussi M, Toulza F, Toffolo GM, Tanaka Y, Jacobson S, Taylor GP, D'Agostino DM, Bangham CR, Ciminale V (2011) Kinetics and intracellular compartmentalization of HTLV-1 gene expression: nuclear retention of HBZ mRNAs. Blood 117:4855–4859

Sahin M, Sahin E, Koksoy S (2013) Regulatory T cells in cancer: an overview and perspectives on cyclooxygenase-2 and Foxp3 DNA methylation. Hum Immunol 74:1061–1068

Sakaguchi S (2005) Naturally arising Foxp3-expressing CD25+ CD4+ regulatory T cells in immunological tolerance to self and non-self. Nat Immunol 6:345–352

Satou Y, Yasunaga J, Yoshida M, Matsuoka M (2006) HTLV-I basic leucine zipper factor gene mRNA supports proliferation of adult T cell leukemia cells. Proc Natl Acad Sci U S A 103:720–725

Satou Y, Yasunaga J, Zhao T, Yoshida M, Miyazato P, Takai K, Shimizu K, Ohshima K, Green PL, Ohkura N, Yamaguchi T, Ono M, Sakaguchi S, Matsuoka M (2011) HTLV-1 bZIP factor induces T-cell lymphoma and systemic inflammation in vivo. PLoS Pathog 7: e1001274

Stockis J, Fink W, Francois V, Connerotte T, de Smet C, Knoops L, van der Bruggen P, Boon T, Coulie PG, Lucas S (2009) Comparison of stable human Treg and Th clones by transcriptional profiling. Eur J Immunol 39:869–882

Toker A, Huehn J (2011) To be or not to be a Treg cell: lineage decisions controlled by epigenetic mechanisms. Sci Signal 4(158):pe4

Ukena SN, Hopting M, Velaga S, Ivanyi P, Grosse J, Baron U, Ganser A, Franzke A (2011) Isolation strategies of regulatory T cells for clinical trials: phenotype, function, stability, and expansion capacity. Exp Hematol 39:1152–1160

van der Vliet HJ, Nieuwenhuis EE (2007) IPEX as a result of mutations in FOXP3. Clin Dev Immunol 2007:89017

Wang J, Ioan-Facsinay A, van der Voort EI, Huizinga TW, Toes RE (2007) Transient expression of FOXP3 in human activated nonregulatory CD4+ T cells. Eur J Immunol 37:129–138

Weiss VL, Lee TH, Jaffee EM, Armstrong TD (2012) Targeting the right regulatory T-cell population for tumor immunotherapy. Oncoimmunology 1:1191–1193

Wildin RS, Ramsdell F, Peake J, Faravelli F, Casanova JL, Buist N, Levy-Lahad E, Mazzella M, Goulet O, Perroni L, Bricarelli FD, Byrne G, McEuen M, Proll S, Appleby M, Brunkow ME (2001) X-linked neonatal diabetes mellitus, enteropathy and endocrinopathy syndrome is the human equivalent of mouse scurfy. Nat Genet 27: 18–20

Yagi H, Nomura T, Nakamura K, Yamazaki S, Kitawaki T, Hori S, Maeda M, Onodera M, Uchiyama T, Fujii S, Sakaguchi S (2004) Crucial role of FOXP3 in the development and function of human CD25+ CD4+ regulatory T cells. Int Immunol 16:1643–1656

Yamano Y, Cohen CJ, Takenouchi N, Yao K, Tomaru U, Li HC, Reiter Y, Jacobson S (2004) Increased expression of human T lymphocyte virus type I (HTLV-I) Tax11-19 peptide-human histocompatibility leukocyte antigen A*201 complexes on CD4+ CD25+ T Cells detected by peptide-specific, major histocompatibility complex-restricted antibodies in patients with HTLV-I-associated neurologic disease. J Exp Med 199:1367–1377

Yamano Y, Takenouchi N, Li HC, Tomaru U, Yao K, Grant CW, Maric DA, Jacobson S (2005) Virus-induced dysfunction of CD4+CD25+ T cells in patients with HTLV-I-associated neuroimmunological disease. J Clin Invest 115:1361–1368

Yamano Y, Araya N, Sato T, Utsunomiya A, Azakami K, Hasegawa D, Izumi T, Fujita H, Aratani S, Yagishita N, Fujii R, Nishioka K, Jacobson S, Nakajima T (2009) Abnormally high levels of virus-infected IFN-gamma+ CCR4+CD4+CD25+ T cells in a retrovirus-associated neuroinflammatory disorder. PLoS ONE 4:e6517

Yano H, Ishida T, Inagaki A, Ishii T, Kusumoto S, Komatsu H, Iida S, Utsunomiya A, Ueda R (2007) Regulatory T-cell function of adult T-cell leukemia/lymphoma cells. Int J Cancer J Int Cancer 120:2052–2057

Zheng Q, Xu Y, Liu Y, Zhang B, Li X, Guo F, Zhao Y (2009) Induction of Foxp3 demethylation increases regulatory CD4+ CD25+ T cells and prevents the occurrence of diabetes in mice. J Mol Med (Berl) 87: 1191–1205

Neurotherapeutics (2016) 13:535–546
DOI 10.1007/s13311-016-0450-6

REVIEW

Exosomes in Viral Disease

Monique R. Anderson[1,2] · **Fatah Kashanchi**[3] · **Steven Jacobson**[1]

Published online: 20 June 2016

Abstract Viruses have evolved many mechanisms by which to evade and subvert the immune system to ensure survival and persistence. However, for each method undertaken by the immune system for pathogen removal, there is a counteracting mechanism utilized by pathogens. The new and emerging role of microvesicles in immune intercellular communication and function is no different. Viruses across many different families have evolved to insert viral components in exosomes, a subtype of microvesicle, with many varying downstream effects. When assessed cumulatively, viral antigens in exosomes increase persistence through cloaking viral genomes, decoying the immune system, and even by increasing viral infection in uninfected cells. Exosomes therefore represent a source of viral antigen that can be used as a biomarker for disease and targeted for therapy in the control and eradication of these disorders. With the rise in the persistence of new and reemerging viruses like Ebola and Zika, exploring the role of exosomes become more important than ever.

Electronic supplementary material The online version of this article (doi:10.1007/s13311-016-0450-6) contains supplementary material, which is available to authorized users.

✉ Monique R. Anderson
andersonmr2@mail.nih.gov

[1] National Institutes of Health, National Institute of Neurological Disorders and Stroke, Neuroimmunology Branch, Viral Immunology Section, Bethesda, MD 20892, USA

[2] Department of Pathology Molecular and Cellular Basis of Disease Graduate Program, University of Virginia School of Medicine, Charlottesville, VA 22903, USA

[3] George Mason University, National Center for Biodefense and Infectious Disease, Laboratory of Molecular Virology, Manassas, VA 20110, USA

Key Words Exosomes · microvesicles · multivesicular bodies · "back fusion" · ESCRT

Introduction

In the struggle to maintain health, the immune system has evolved several mechanisms to protect the host from pathogens. Foremost is the ability to differentiate self from pathogen, but tools are also required to mobilize components of the immune system in response to threats. Therefore, intercellular communication is key in this process. Until 30 years ago, cell-to-cell signaling was encompassed by transfer of chemokines, cytokines, and direct cell contact. The discovery of vesicles being shed from the surface of reticulocytes as a mechanism for iron transfer forever changed how the field of immunology understood cellular communication [1, 2]. Since then, the understanding of how microvesicles (MVs) contribute to immunity and pathogenicity has exploded. However, pathogens have evolved in concert with the immune system and have developed methods to subvert and co-opt this form of intercellular communication to evade the immune system and aid spread. The cross-over and interaction between MVs, and specifically exosomes, and viruses will be the subject of this review.

The term "microvesicles" (MVs) has undergone an evolution despite there being overwhelming evidence that their secretion is conserved across all kingdoms [3]. In preferred terminology, MVs include vesicles ranging in size from 100 to 1000 nm that are shed from the plasma membrane, as well as exosomes, which range in size from 30 to 100 nm and originate within microvesicular bodies (MVBs) [4, 5]. For the purposes of this review, we will focus our discussion on exosomes; however, there are several excellent reviews in the literature that address

extracellular vesicles as a whole [6–11]. In appearance, exosomes are unilamellar vesicles composed of a lipid bilayer that have a homogenous cup-shaped appearance on scanning electromicroscopy [3, 12]. To date, they can be shown to originate from almost every cell type studied, including, but not limited to, T cells [13], B cells [14, 15], dendritic cells [16], neurons [17], astrocytes [18, 19], endothelial cells [20], smooth muscle cells [21], oligodendrocytes [22], and reticulocytes [2, 23]. The wide variety of cells that can excrete exosomes also dictates the wide array of materials in which they can be isolated: saliva, plasma, urine, cerebrospinal fluid, bronchial alveolar lavage, and serum [24]. The contents of exosomes are just as varied and depend heavily on the cells from which they originate but can be considered broadly to include proteins, mRNAs, microRNAs (miRNAs), lipids, and carbohydrates. Once released, the components within exosomes can influence the local microenvironment or spread through circulation to locations far removed from their origin. Indeed, exosomes have been shown to cross the blood–brain barrier [25], perhaps pointing to their role in allowing coordination with the immune system in even immune-privileged sites [26]. This aspect of exosome biology is especially important, as there are many instances in which viral proteins can be isolated, but the virus itself is difficult to detect. The presence of viral antigens in the absence of viral detection may be better understood through an understanding of exosome biogenesis and uptake.

Exosome Biogenesis

As aforementioned, exosomes originate in MVBs (late endosomes), which are a component of the endocytic pathway. MVBs contain intraluminal vesicles (ILVs) that range in size from 30 to 100 nm and can be targeted for 2 separate fates: lysosomal degradation or fusion with the plasma membrane, after which release of ILVs to the extracellular environment occurs and at which point they are termed exosomes [4, 27]. In a process called “back fusion”, ILVs deliver plasma membrane invaginations (through clathrin-mediated and clathrin-independent endocytosis) to the endosomal network, making them (and therefore exosomes) capable of carrying both intracellular and extracellular materials [8, 28, 29]. Indeed, exosomes are seen as an exciting avenue for their capability in giving snapshots of the microenvironment, and serving as a good source of biomarkers. Part of this advantage is owing to the large cross-over between exosome biogenesis and egress, pathogen entry, and normal macromolecule entry and cycling within the cell [23, 27, 28].

The exact intracellular signals that direct ILVs to the plasma membrane for release are still under investigation and will be discussed briefly here. Endosomal sorting complexes required for transport (ESCRT) machinery has been studied in its role for directing ubiquitin-labeled proteins into endosomes for delivery into MVBs, and, as such, ESCRT proteins, like Alix and TSG101, are enriched in exosomes [30, 31]. Lipid raft-associated proteins such as transferrin and caveolins, and other proteins involved in membrane trafficking, like the tetraspanins CD9, CD63, and CD81, which have been shown to bind to ESCRT machinery, are also enriched in exosomes [32–34]. There are now several databases that exist that list the assortment of materials that can be found in exosomes (Vesiclepedia, EVPedia, and Exocarta) [7, 35, 36].

However, ESCRT is not the only method by which exosome formation can occur as there are also ESCRT-independent methods by which proteins, lipids, and RNA can enter the endosomal pathway. For example, oligodendrocytes direct exosome formation via the ceramide pathway [37], while other cell types rely on oligomerization of tetraspanin complexes [8, 38, 39]. Furthermore, while knockdown of some ESCRT components may abrogate exosome production, it does not completely knock it out [40, 41]. Indeed, Rab GTPases, a known family of conserved proteins that regulate vesicular trafficking and membrane fusion events, are also involved in exosome formation as denoted by their high abundance in isolated exosomes [23, 42]. Several are implicated in the release of exosomes, including Rab11, Rab27, Rab5, Rab35, and Rab7, depending on cell type [8, 23]. Rab 27a, in particular, regulates the fusion of MVBs at the plasma membrane to release ILVs [8, 23, 43]. Knockdown of Rab 27a inhibits exosome secretion from tumor cell lines [4, 43]. There are several other Rabs that have also proven essential through a diminution in exosome levels after their knockdown, including Rab 2B, Rab9A, Rab5A, and Rab27b [4]. Being GTPases, the activation of each Rab is dependent on an influx of calcium, as is the case for Rab 11 in the K562 cell line, which may involve SNARE complexes [44–46]. Altogether, there are clearly several players within the cell that contribute to the endosomal compartment and, ultimately, to the release of exosomes, further emphasizing the importance of this pathway in normal biology. As such, it is not at all surprising that intracellular pathogens like viruses have also evolved mechanisms to incorporate their viral content at each stage of exosome formation.

Fate of Exosomes

Once in the extracellular space, exosomes can bind to neighboring cells, bind locally, travel passively through the bloodstream for a more paracrine destination, or be taken up by marginal zone phagocytes in the spleen and liver [4, 47].

Once released, they can have several fates, all of which dictate their downstream function. This can best be exemplified when analyzing the immune system and cancer cell biology, both of which have been extensively studied in the field of exosome biology. Importantly, the contents of exosomes have been shown to have activity in recipient cells [48], and are not just a means for removal of cellular waste material, as was first hypothesized, although this is still an important function [49]. First, exosomes can either be internalized or captured at the cell surface where they remain [4]. Both of these outcomes have been observed in dendritic cells [50]. Segura et al. [51] observed $CD8^+$ dendritic cells capture exosomes via dendritic cell (DC) lymphocyte function-associated antigen 1 (LFA-1) at the surface for presentation of exosome-borne major histocompatibility complex (MHC)–peptide complexes to $CD4^+$ T cells. These T cells could then be activated by exosomal antigens [52], a process that is much more efficient in the presence of DCs [4, 53, 54]. This process was dependent on intracellular adhesion molecule 1 (ICAM-1) expression on exosomes and is termed "cross-dressing" [55]. Another method by which DCs could capture exosomal antigens is through internalization, processing, and repackaging of endocytosed exosomal antigens into the endosomal pathway for representation on DC MHC II to naïve $CD4^+$ T cells [50]. This process was documented in elegant experiments by Morelli et al. [50]. Activation of $CD8^+$ T cells is also possible but requires the presence of DCs capable of "cross-presentation", that is, internalization of exosomal antigens followed by processing and representation on MHC I. This has been documented for the activation of tumor-specific cytotoxic T lymphocytes with tumor-derived exosomes [56]. Additionally, exosomes can be taken up by phagocytosis or pinocytosis where the contents can have direct consequences on gene expression of the recipient cells [57]. For example, regulatory T cells produce exosomes with miRNA profiles that directly downregulate inflammation in recipient cells [58]. Indeed, phagocytic uptake of exosomes can occur via phosphatidylserine on the surface of the vesicles via interaction with T-cell immunoglobulin and mucin domain-containing molecule (TIM)-4 on phagocytic cells [59, 60]. It has been shown that phagocytosis of exosomes from MT4, a human T-cell lymphotropic virus type I (HTLV-1) infected cell line, was reduced with the addition of TIM-4, but not TIM-1, antibodies [61]. This is intriguing as both TIM-1 and TIM-4 are known to serve has viral entry receptors for hepatitis A virus (HAV), Ebola, and several enveloped viruses [62, 63].

Viral manipulation of Exosomal Pathway

Remembering that exosomes originate in the endosomal compartment, viruses that enter via endocytosis are likely to co-opt exosomal communication; indeed, this proves to be the case. Members of the Flaviviridae family, including important human pathogens like Dengue, West Nile virus (WNV), hepatitis C virus (HCV), and the recently pandemic Zika virus, all enter via receptor-mediated or clathrin-mediated endocytosis [31, 64, 65]. HCV, Dengue, WNV and Zika virus then enter late endosomes after "back-fusion" of ILVs with this compartment, at which point the viral genome is dumped into the cytoplasm [66, 67]. However, in the case of HCV, it is known that the viral genome can remain in ILVs and be secreted within exosomes, where they can operate as infectious particles [68, 69]. As noted in Table 1, there is very little difference in size between viruses and exosomes, making observations of infectivity from exosomes difficult to substantiate. Thus, to remove the possibility of viruses accounting for observed infections, Longatti et al. [69] utilized exosomes isolated from an HCV subgenomic replicon cell line, which lacks viral structural proteins and therefore cannot produce virions. By using a transwell assay, they showed that they were able to infect Hu7 cells after exposure to these shed exosomes without the need for direct cell–cell contact. Further, this infection was inhibited by an exosomal release inhibitor, a sphingomyelinase inhibitor. Thus far, HCV is the only member of the Flaviviridae family, known to incorporate genomic RNA into exosomes. Only hepatitis A virus (HAV), a nonenveloped picornavirus, is believed to use this mode of transmission as well [70]. However, it raises the possibility of other, yet unstudied, viruses utilizing the endosomal/exosomal system as a means for delivery of viral message to uninfected cells. Indeed, this possibility was discussed in a review by Izquierdo et al. [71] of HIV and exosomes, and first dubbed the "Trojan Horse" hypothesis by Gould et al. in 2003 [72]. Gould et al. [72] hypothesize that with the similarities between HIV assembly and egress and exosome biogenesis, HIV has evolved to co-opt the exosome system and infect cells through packaging of the viral genome [72]. It is a theory supported by observations that HIV virions are released with exosomes and have enhanced infectivity in the presence of these vesicles [73]. However, this mechanism occurred via uptake of DCs, which subsequently transferred endocytosed HIV to closely associated uninfected T cells [74]. Specifically, HIV is endocytosed via DC sign into the endocytic pathway and trafficked back to the cell surface in intact DCs for presentation to T cells. However, direct packaging of HIV genome into exosomes has not been observed. Indeed, most

Table 1 Basic differences between exosomes and viruses

	Exosomes	Viruses
Size	30–100 nm	2 = 0400 nm (depending on virus)
Shape	Uniform, cup-shaped	Variable
Charge	Usually lacking charge	Uniform, charged

research suggests that HIV budding is from the plasma membrane and not from the endosomal pathway [75, 76].

As mentioned, several viruses enter via the endocytic pathway. While some, like the flaviviruses, proceed through ILVs, some, like HIV, completely subvert this process and instead are closely associated with the ESCRT, lipid raft domains, and Rab GTPases that are involved in exosome trafficking [8]. For example, HIV Gag has been shown to interact with tetraspanins, especially CD63 and CD81, to aid in virion egress [77]. Human herpes virus (HHV)-6 virions have been visualized by electron microscopy in MVBs and egress by the exosomal release pathway [78]. The viral glycoprotein gB was shown to colocalize with CD63, although whether this relationship is necessary for association of HHV-6 virions and ILVs was unclear. However, HHV-6 infection dramatically increased MVB formation, indicating the endosomal/exosomal pathway as important for HHV-6 infection and assembly [78]. Although the authors did not propose a mechanism by which viral components were incorporated in exosomes, the close association of the virus with exosomes in the endosomal pathway begs the question of whether HHV-6 components are also packaged in exosomes, and requires further investigation.

Beyond interactions with tetraspanins, there are still other viruses that are capable of hitching onto the ESCRT complex to facilitate transportation of virus particles to the plasma membrane. For example, influenza A virus, respiratory syncytial virus (RSV), and certain Bunyaviruses attach to Rab11a vesicles to get to the plasma membrane for egress [8, 79–81]. Human cytomegalovirus (HCMV) is known to increase Rab27a, which, as noted earlier, is essential for MVB fusion with the plasma membrane [82]. The mechanism and ultimate change to exosome production is as yet unknown, but Rab27a could be found in association with its viral envelope [82]. HIV also interacts with Rab27a, and increases its levels, as well as those of several other components of the ESCRT machinery [8, 83–85]. This is to be expected considering the aforementioned importance of ESCRT and exosome formation in HIV assembly and egress. Herpes simplex virus 1 (HSV1) is yet another virus that interacts with Rab27a. The interaction occurred through GSSHV-UL46, a viral tegument protein, in oligodendrocytes [86]. Viral glycoproteins gH and gD also interacted with Rab27a, and the importance of this association with Rab27a was proven in this paper by a decrease in viral production with Rab27a knockdown [86]. Whether this involved a decrease in exosome production, and how important this was for the lifecycle of HSV1, was not discussed at that time.

The movement of vesicles in the endosomal pathway as they track to and from the plasma membrane provides several opportunities for viral sabotage. Thus far, we have noted that viruses can enter the endosomal pathway just by viral fusion and entry into the cell. It was also noted that some viruses can hijack members of the ESCRT and vesicular trafficking machinery, and thereby integrate viral components into exosomes, owing to both close proximity and opportunity. This is important as endosomal trafficking allows for cellular contents, such as MHC II and tetraspanins to recycle through the cell and potentially incorporate other cellular proteins for representation at the plasma membrane. Thus, this process of "back fusion" may allow the entry of viral proteins that are being processed within the cell or even are targeted for the endosomal compartment. Additionally, viruses that require proximity to the nucleus and/or endoplasmic reticulum, such as herpesviruses and other DNA viruses, will also follow this route and thereby potentially have components incorporated into exosomes at this step [31, 87]. As stated, whether this process is natural happenstance due to proximity *versus* direct targeting is still under investigation but will be explored via the various examples mentioned herein.

HIV

HIV, which has been noted to take advantage of several steps in exosome biogenesis, has been shown to incorporate transactivating response (TAR) RNA into exosomes [88, 89]. The uptake of exosomal TAR in recipient cells can downregulate apoptosis and is postulated to have a role in supporting HIV infection. Importantly, TAR RNA was still able to be detected in exosomes isolated from the serum of HIV-positive patients on highly active antiretroviral therapy, indicating that even with antiretroviral therapy, short transcripts remain present in these exosomes [90]. Indeed, the same group later went on to find that exosomal TAR RNA could stimulate proinflammatory cytokines in recipient cells through activation of the nuclear factor kappa b pathway [89]. In a separate study, the HIV Nef protein was found in released exosomes [91]. Later uptake of these Nef^+ exosomes led to increased susceptibility of naïve T cells to HIV infection [91, 92]. Indeed, another report found that exosomes from HIV-infected cells could reactivate HIV in latently infected cells [93]. Exosomal Nef has also been shown to increase T-cell apoptosis *in vitro*, which may contribute to the $CD4^+$ T-cell depletion in AIDS pathogenesis [85]. Interestingly, Nef expression in $CD4^+$ T cells was also noted to decrease CD4 and MHC I export to released exosomes [94]. The authors postulated that this decreases the ability of $CD4^+$ T cells to inhibit HIV infection in uninfected cells by using exosomes as decoys to soak up HIV virions. This would further explain how Nef^+ exosomes enhance HIV infectivity. More recently, Luo et al. [95] dispute the incorporation of Nef into exosomes at all, despite several reports finding motifs within Nef that are necessary for exosomal incorporation [96, 97]. It is a subject that requires further investigation. Nevertheless, it is clear that HIV has

evolved mechanisms to alter the cellular microenvironment to its advantage through exosomal cellular communication.

HTLV

Like HIV, there are several other viruses that also seemingly target viral RNAs and proteins for exosomal export. HTLV-1, another human retrovirus and the cause of adult T-cell leukemia and HTLV-1-associated myelopathy/tropical spastic paraparesis (HAM/TSP), has also been shown to incorporate viral proteins into shed exosomes. Jaworski et al. [98] found that HTLV-1-infected cell lines shed exosomes containing Tax, a pleiotropic transactivating protein implicated in the immune dysregulation associated with infection [99, 100]. Tax appears to be targeted for exosome entry by ubiquitination [98, 101], which was noted earlier to be an important target for ESCRT machinery. Indeed, prior studies have shown Tax colocalization with organelles undergoing exocytosis [102, 103].

Exosomes shed from HTLV-1$^+$ cell lines were found to also contain viral mRNA and miRNAs such as *tax* and *hbz* [98]. Additionally, exosomes shed from HTLV-1-infected cell lines showed a different cell miRNA profile, as well as a unique set of host proteins and lipids, than was seen in those shed by uninfected cell lines. In as-yet-unpublished work from our laboratory in collaboration with Dr. Kashanchi, it was further demonstrated that HTLV-1 Tax could be found in exosomes isolated from the cerebrospinal fluid of some patients with HAM/TSP, while exosomes from uninfected controls were completely negative. Additionally, cultured, unstimulated peripheral blood mononuclear cells from patients with HAM/TSP were shown to shed exosomes that contained Tax protein, as well as Tax mRNA. Unlike the cell lines, however, no detectable HBZ mRNA could be isolated from exosomes (unpublished data). This may have functional consequences as HTLV-1 is a cell-associated virus and shedding of viral antigens may contribute to the inflammatory immune response. Indeed, it has previously been shown that extracellular Tax can have damaging consequences for neurons [102, 104], although neither study specifically implicated exosomes. Once Tax protein or *tax* mRNA enter recipient cells, it can stimulate the production of proinflammatory cytokines, like interleukin (IL)-6 and tumor necrosis factor-α [105]. Importantly, initial results from our laboratory indicate that cells that take up these exosomes can become targets for lysis by HTLV-1-specific cytotoxic T cells.

Of interest in the pathogenesis of HAM/TSP is the lack of documented infection of resident neuronal cells. While astrocytes and microglia can be infected *in vitro*, they have not been shown to be infected *in vivo* [106]. Moreover, the loss of oligodendrocytes that occurs with disease progression cannot be explained by active infection. One postulation is that the proinflamatory environment contributes to their eventual breakdown, while others have proposed direct targeting of oligodendrocytes due to a mechanism of molecular mimicry of Tax to a neuronal protein [107–109]. Exosomal Tax may therefore ultimately explain both possibilities by contributing to the inflammatory cytokine production through packaging of these cytokines, as well as induction in recipient cells (Fig. 1). Additionally, exosomal Tax uptake in uninfected cells could explain targeting by HTLV-1-specific T cells in the presence of aseptic resident neuronal cells. Clearly, further research must be undertaken to further elucidate the role of exosomes in the disease progression of HAM/TSP and potential targeting of therapeutics.

HSV1

As mentioned, HSV1 is also known to interact with the ESCRT complex through viral tegument proteins and glycoproteins. Though this relationship with Rab27a has not yielded an observed consequence to exosomal production or content, viral proteins can also be found in exosomes shed from infected cells. HSV infection results in the release of a variety of MVs from the cell, most prominent of which are L particles, which are composed of virus envelope and tegument but lack viral genome and capsid proteins [110, 111]. They are noninfectious on their own but have been shown to increase infectivity overall possibly through the transference of factors that increase susceptibility in uninfected cells [112, 113].

In contrast, exosomes shed from HSV1-infected cells express the tetraspanins known to be enriched on exosomes, CD9, CD63, and CD81 [114]. In addition to viral transcripts, HSV1 appears to direct the incorporation of certain host products into examples. An example of this is the Stimulator of INF genes (STING) protein. It was found not only to be upregulated with HSV infection in Vero cells, but also found to be shuttled out of cells in association with CD9 [115]. The authors demonstrated that STING was packaged in exosomes and delivered to uninfected cells. It was postulated that in addition to viral miRNAs also packaged in exosomes, such as miR-H5, miR-H3, and miR-H6, these exosomes could exert a negative effect on viral spread and potentially host–host infection by increasing host survival [114]. Conversely, immediate early transcripts such as ICP27 and late transcripts like VP16 can also be found in exosomes, thereby promoting spread and latency [115]. Additionally, HSV gB has been shown to colocalize with human leukocyte antigen-DR in exosomes shed from cells [3, 116]. Shuttling of this MHC to exosomes reduced the ability of cells to present peptide to the immune system and was postulated to serve as important mechanism promoting viral latency. There is more work to be done in terms of characterizing the effects of packaging host and viral products into exosomes. More importantly, it would be of interest to

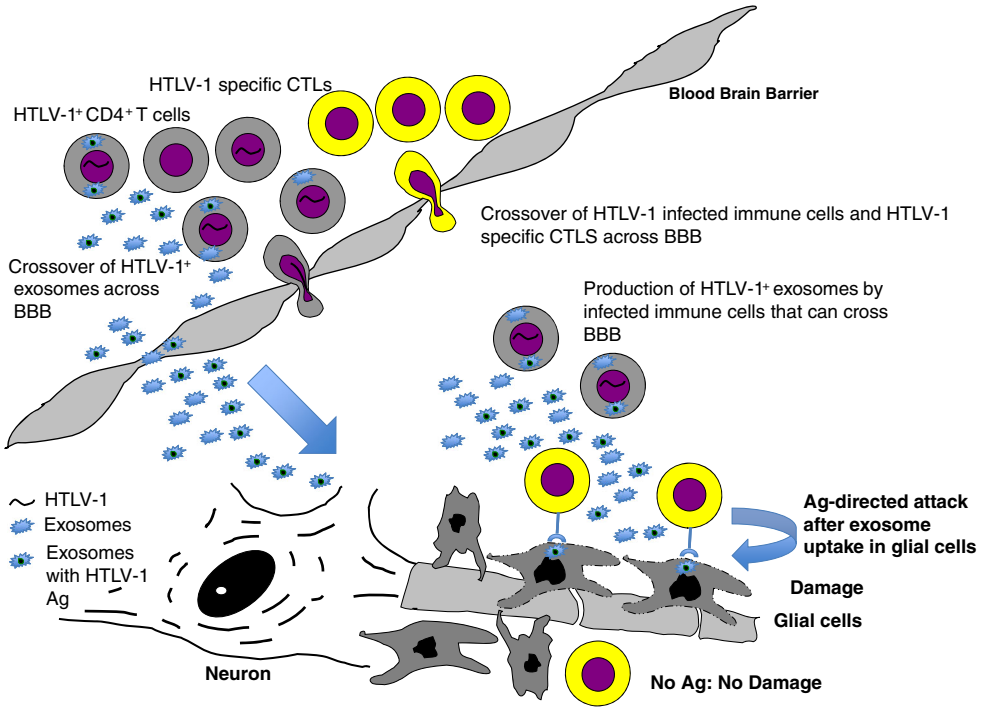

Fig. 1 HTLV-1 Immunopathogenesis

determine if patients that progress to central nervous system (CNS) disease or reactivation in the CNS have different exosome profiles compared with patients that remain latently infected. Of note, a literature search did not yield research on the association of exosomes with varicella zoster virus pathogenesis, although the role of exosomes in HSV1 pathogenesis suggests that additional research into this area would be warranted.

Epstein–Barr Virus

In addition to HSV1, several other herpesviruses also influence exosomal content. As mentioned, this may be owing to the proximity of herpes virus transcription with the ESCRT pathway as other cellular products enter via "back fusion" [31, 117]. Epstein–Barr virus (EBV) and Kaposi's sarcoma herpes virus (KSHV) have been the most studied, owing to the role of exosomes in the propogation of EBV- and KSHV-associated cancers, including nasopharyngeal sarcomas and Kaposi's sarcoma, respectively.

Latent membrane protein 1 (LMP1) was first discovered to be exported in exosomes isolated from EBV^+ cancer cells [118]. As a signal transduction protein, uptake of $LMP1^+$ exosomes was found to inhibit natural killer cell activity and T-cell activation and proliferation [32, 119, 120]. Additionally, similar to HSV1, EBV is able to promote the incorporation of host proteins into exosomes. Galectin-9 can be found in exosomes released from EBV^+ cells and can induce the apoptosis of EBV-specific T cells, signifying a method by which EBV actively avoids detection by the immune system through exosomes [23, 121]. Furthermore, epidermal growth factor and fibroblast growth factor-2, both activated in association with LMP-1-mediated transformation, are shuttled into exosomes in $LMP\text{-}1^+$ cells [10, 122]. This may represent a mechanism by which EBV cancers alter the microenvironment to increase propagation and survival of transformed cells. Still further evidence exists for EBV promoting packaging of viral miRNAs. These miRNAs are then able to decrease target genes like *CXCL11*, which is an immunoregulatory gene important for antiviral activity [23]. EBV further evades immune detection by the shuttling of important immune effectors like IL-1β, IL-18, and IL-33, into exosomes and out of the cell [123]. In this way, EBV also targets exosomes as a "trash receptacle". Taken together, all of these modulations to the exosomal pathway increase the survival and transformative abilities of EBV. Indeed, the transfer of viral antigens in the absence of active viral infection may lead to other consequences. A recent report by Baglio et al. [124] found that EBV EBER1, a viral small RNA, could be found in exosomes and that these exosomes, in turn, aberrantly activated DCs that were found in EBV-negative skin lesions of patients with lupus patients. This indicates a new potential mode of pathogenesis in autoimmune disease and other diseases where viral infection has been implicated, but a causal link has been difficult to verify. Furthermore, exosomes may serve as a potential tool for screening these affected individuals.

Another gamma herpes virus, KSHV or HHV-8, was also found to modulate the microenvironment through

the packaging of viral factors in exosomes. Exosomes produced by infected cells were demonstrated to carry both KSHV and host-derived miRNA. Exposure to patient-derived exosomes increased cell migration and IL-6 production in recipient endothelial cells [125]. Additionally, like EBV, KSHV reprogrammed the cell profile of infected B cells [126]. Infection promoted a switch to glycolytic metabolism, and glycolysis by-products like pyruvate kinase and lactate dehydrogenase were packaged into exosomes [7, 127].

CMV

HHV-5, or CMV, is a betaherpesvirus. Like all of the herpes viruses, it is able to infect cells and establish latency. It is an especially important pathogen considered in transplant medicine, as CMV infection or CMV discordance between donor and recipient can lead to increased rates of organ rejection [128–130]. Previous reports have shown that infected epithelial cells can produce exosomes that stimulate allogeneic donor memory $CD4^+$ T cells [20]. The authors proposed that this was a potential contributor to allograft rejection in transplant recipients. In addition to promoting an activated immune response, CMV infection can also increase the release of DC-SIGN on exosomes in complex with the viral glycoprotein gB [131]. DC-SIGN is a C-type lectin family member that is necessary for virus uptake [132]. It was shown that this release mediated infection of myeloid DCs by CMV and increased overall CMV infectivity [131].

HHV-6, another betaherpesvirus, has already been discussed in terms of the viral association with the endosomal pathway and MVBs. Additionally, HHV-6 was later detected to increase MHC I transfer to released exosomes in addition to viral particles [133]. MHC I downregulation is a well-known mechanism for immunoevasion employed by many classes of pathogens. This insight, gained by studying HHV-6, may point to shuttling of MHC I and MHC II to exosomes as an evolutionarily conserved mechanism that is used by many viruses.

Human Papilloma Virus

Exosome biology plays a large role in tumor pathogenesis. Thus, it is not surprising that so many oncogenic viruses have been shown to subjugate exosomal communication. Human papilloma virus (HPV) has several different serotypes, some of which are more associated with cervical cancer-like HPV type 16 and 18. In investigating patients with tumorigenic *versus* benign subtypes, differential miRNA content in exosomes was noted. Indeed, the miRNA profile of exosomes isolated from cells infected with pathogenic HPV strains were enriched for miRNA that controlled cell proliferation and apoptosis [134]. Although there was no evidence for the incorporation of viral oncogenes E6/E7 in released exosomes, the levels of E6/E7 were important in dictating the miRNA profile of released exosomes [8, 135]. Owing to this discrepancy in the profile of exosomes shed from oncogenic *versus* benign strains, there is a clinical trial currently underway at the National Institutes of Health to investigate the utility of screening salivary exosomes in patients at risk for HPV oropharyngeal carcinoma (https://clinicaltrials.gov/ct2/show/NCT02147418). Indeed, the importance of exosomes has been reinforced by a recent study in which normal cells were immortalized after incubation with exosomes derived from breast cancer cells [136].

HAV

HAV is a nonenveloped picorna virus that usually causes a mild gastrointestinal illness but which can, at times, lead to hepatitis with full clearance of the virus after infection. Interestingly, HAV has been shown to hijack endosomal membranes for encapsulation upon release [137]. These enveloped viruses are fully infectious and aid HAV in immunoevasion as they are protected from antibody neutralization [138]. Although envelopment of previously naked virus particles is different to the strategy taken by HCV, which incorporates naked viral genome into exosomes, both HAV and HCV co-opt the exosomal system for evasion from the adaptive arm of the immune system. Indeed, hepatitis B virus, which is a hepadnavirus, also hijacks exosomal communication. On HBV infection, cellular release of MVs is dramatically increased. However, these MVs are characterized as subviral particles and contain viral surface antigens but no viral genome and are therefore noninfectious [139]. The subviral particles can, however, serve as decoys to the immune system as they are able to absorb antibodies that might otherwise inhibit viral particles [32].

Bunyaviruses

Bunyaviridae is a family of enveloped, negative-stranded viruses that includes the hantavirus, nairovirus, orthobunyavirus, phlebovirus, and tospovirus genera. Of these, hantavirus and phlebovirus have clinical significance as human pathogens, including hanta pulmonary virus and Rift Valley fever virus (RVFV), respectively. Interestingly, recent reports suggest that the phlebovirus family can modulate the immune system via exosomes. Exosomes isolated from cells infected with RVFV not only contained viral RNA and proteins, but also immune cells exposed to these exosomes underwent apoptosis [140]. This suggests a mechanism for immune persistence early in the disease, as exosomes were detected prior to virion release [140].

Another phelebovirus, a newly recognized virus called severe fever with thrombocytopenia syndrome virus, also utilizes exosomes. Severe fever with thrombocytopenia syndrome virus was found to package virions within $CD63^+$ extracellular vesicles (exosomes), which allowed for efficient receptor-independent uptake by neighboring cells [141]. Of note, pheleboviruses also have DC-SIGN as a receptor [142] , which has been shown to be packaged into exosomes for uptake in uninfected cells by CMV [131]. Further investigation should be undertaken to observe if a similar mechanism for viral spread is employed by phleboviruses and bunyaviruses in general. There is currently no literature describing hantaviruses and exosomes, although this topic obviously warrants further investigation for the role of extracellular vesicles in Hanta pulmonary virus syndrome.

Discussion

As can be seen by the wide variety of viruses discussed in this review, there are several different viruses spread across different genera that take advantage of exosomal communication. While some cloak viral antigens to aid in viral spread, others increase shuttling of disadvantageous host products that would hinder viral infection into exosomes. Others utilize exosomes as decoys to the immune system and, counterintuitively, some viruses also seem to prime a directed immune response to inhibit spread. The examples presented by these viruses illustrate the many ways exosomal communication is important for immune function and maintenance of the cellular microenvironment. The one unifying factor is that all of the viruses present, except for HAV and the phleboviruses, are able to establish latency in the host. Thus, the question becomes: Does their ability to manipulate exosomal contents allow these viruses to establish latency, or does long-term infection favor the ability to isolate exosomes while transient infections have been largely ignored due to the belief that immune clearance negates the risk of exosomes? Indeed, the example of RVFV indicates that exosomes may play an early role in the viral spread of transient infections. Of note, the line between latency and transient infection is becoming blurred in the cases of Zika and Ebola, which have shown a remarkable ability to reappear in previously convalescent patients. Furthermore, the examples in this review highlight the ability of exosomes to increase not only viral spread, but also the type of cells that can be infected. This becomes an important consideration as we attempt to understand how viruses are able to establish and maintain viral reservoirs and "pockets of infection" in cells not normally believed to be permissive.

Ebola, chikungunya virus, avian flu, and Zika virus are just a few of the new and re-emerging viruses that are characterized by transient infection. However, in the cases of Ebola and Zika virus, scientists are discovering that virus and viral proteins can still be isolated months after the initial infection from immune privileged sites like the eye and semen [143–145]. All of these viruses pose serious health threats to the human population, and both Zika and Ebola have been of concern owing to increasing evidence of CNS disease [146–148]. Thus, an understanding of how these agents persist in these spaces and cause damage is imperative. As noted in this review, exosomes are a potential source of antigen that can easily cross the endothelial barriers protecting immune privileged sites. Additionally, in the case of Zika virus, which is a flavivirus, there is already precedence for other members of this virus family altering exosomal contents. Therefore, there is a high likelihood that this ability to incorporate viral contents into exosomes is a shared mechanism for immune evasion amongst the entire family, and warrants investigation. Considering the troubling consequences of Zika infection in pregnancy, screening for exosomes in prospective mothers might be a useful tool for evaluation of risks to the fetus. This is an attractive prospect as the ability to detect Zika virus by reverse transcription polymerase chain reaction is optimal 5–7 days after symptom onset and while the patient is still viremic (http://www.cdc.gov/zika/hc-providers/qa-pregnant-women.html). Additional testing involves detection of IgM; however, there is cross-reactivity with other flaviviruses like Dengue virus and WNV, and therefore it is not specific. A method that targets particles, such as exosomes, that can cross the placenta and that could still be detected after the window of viremia would be useful. Exosomes represent a potential biomarker that can be used in this way. Furthermore, exosome analysis may prove to be important in understanding Ebola pathophysiology as Alix, the ESCRT protein important in directing proteins to endosomes, is necessary for viral budding [149].

Overall, exosomes represent an exciting new avenue with which to explore in viral pathology, one that current evidence suggests plays a role in both transient and latent virus infection. The possibility of screening exosomes in viral disease presents a noninvasive technique for the management and treatment of patients.

Required Author Forms Disclosure forms provided by the authors are available with the online version of this article.

References

1. Trams EG, Lauter CJ, Salem N, Jr., Heine U. Exfoliation of membrane ecto-enzymes in the form of micro-vesicles. Biochim Biophys Acta 1981;645(1):63-70.
2. Johnstone RM, Bianchini A, Teng K. Reticulocyte maturation and exosome release: transferrin receptor containing exosomes shows multiple plasma membrane functions. Blood 1989;74(5):1844-1851.

3. Lai FW, Lichty BD, Bowdish DM. Microvesicles: ubiquitous contributors to infection and immunity. J Leukoc Biol 2015;97(2):237-245.
4. Robbins PD, Morelli AE. Regulation of immune responses by extracellular vesicles. Nat Rev Immunol 2014;14(3):195-208.
5. van der Pol E, Boing AN, Harrison P, Sturk A, Nieuwland R. Classification, functions, and clinical relevance of extracellular vesicles. Pharmacol Rev 2012;64(3):676-705.
6. van Dongen HM, Masoumi N, Witwer KW, Pegtel DM. Extracellular vesicles exploit viral entry routes for cargo delivery. Microbiol Mol Biol Rev 2016;80(2):369-386.
7. Schwab A, Meyering SS, Lepene B, et al. Extracellular vesicles from infected cells: potential for direct pathogenesis. Front Microbiol 2015;6:1132.
8. Alenquer M, Amorim MJ. Exosome biogenesis, regulation, and function in viral infection. Viruses 2015;7(9):5066-5083.
9. Chahar HS, Bao X, Casola A. Exosomes and their role in the life cycle and pathogenesis of RNA viruses. Viruses 2015;7(6):3204-3225.
10. Meckes DG, Jr. Exosomal communication goes viral. J Virol 2015;89(10):5200-5203.
11. Wurdinger T, Gatson NN, Balaj L, Kaur B, Breakefield XO, Pegtel DM. Extracellular vesicles and their convergence with viral pathways. Adv Virol 2012;2012:767694.
12. Li XB, Zhang ZR, Schluesener HJ, Xu SQ. Role of exosomes in immune regulation. J Cell Mol Med 2006;10(2):364-375.
13. Blanchard N, Lankar D, Faure F, et al. TCR activation of human T cells induces the production of exosomes bearing the TCR/CD3/zeta complex. J Immunol 2002;168(7):3235-3241.
14. Raposo G, Nijman HW, Stoorvogel W, et al. B lymphocytes secrete antigen-presenting vesicles. J Exp Med 1996;183(3):1161-1172.
15. Escola JM, Kleijmeer MJ, Stoorvogel W, Griffith JM, Yoshie O, Geuze HJ. Selective enrichment of tetraspan proteins on the internal vesicles of multivesicular endosomes and on exosomes secreted by human B-lymphocytes. J Biol Chem 1998;273(32):20121-20127.
16. Thery C, Regnault A, Garin J, P et al. Molecular characterization of dendritic cell-derived exosomes. Selective accumulation of the heat shock protein hsc73. J Cell Biol 1999;147(3):599-610.
17. Faure J, Lachenal G, Court M, et al. Exosomes are released by cultured cortical neurones. Mol Cell Neurosci 2006;31(4):642-648.
18. Basso M, Bonetto V. Extracellular vesicles and a novel form of communication in the brain. Front Neurosci 2016;10:127.
19. Wang G, Dinkins M, He Q, et al. Astrocytes secrete exosomes enriched with proapoptotic ceramide and prostate apoptosis response 4 (PAR-4): potential mechanism of apoptosis induction in Alzheimer disease (AD). J Biol Chem 2012;287(25):21384-21395.
20. Walker JD, Maier CL, Pober JS. Cytomegalovirus-infected human endothelial cells can stimulate allogeneic CD4+ memory T cells by releasing antigenic exosomes. J Immunol 2009;182(3):1548-1559.
21. Comelli L, Rocchiccioli S, Smirni S, et al. Characterization of secreted vesicles from vascular smooth muscle cells. Mol Biosyst 2014;10(5):1146-1152.
22. Kramer-Albers EM, Bretz N, Tenzer S, et al. Oligodendrocytes secrete exosomes containing major myelin and stress-protective proteins: Trophic support for axons? Proteomics Clin Appl 2007;1(11):1446-1461.
23. Schorey JS, Cheng Y, Singh PP, Smith VL. Exosomes and other extracellular vesicles in host-pathogen interactions. EMBO Rep 2015;16(1):24-43.
24. Boukouris S, Mathivanan S. Exosomes in bodily fluids are a highly stable resource of disease biomarkers. Proteomics Clin Appl 2015;9(3-4):358-367.
25. Yang T, Martin P, Fogarty B, et al. Exosome delivered anticancer drugs across the blood-brain barrier for brain cancer therapy in Danio rerio. Pharm Res 2015;32(6):2003-2014.
26. El Andaloussi S, Lakhal S, Mager I, Wood MJ. Exosomes for targeted siRNA delivery across biological barriers. Adv Drug Deliv Rev 2013;65(3):391-397.
27. Murk JL, Stoorvogel W, Kleijmeer MJ, Geuze HJ. The plasticity of multivesicular bodies and the regulation of antigen presentation. Semin Cell Develop Biol 2002;13(4):303-311.
28. Bissig C, Gruenberg J. ALIX and the multivesicular endosome: ALIX in Wonderland. Trends Cell Biol 2014;24(1):19-25.
29. Pegtel DM, van de Garde MD, Middeldorp JM. Viral miRNAs exploiting the endosomal-exosomal pathway for intercellular cross-talk and immune evasion. Biochim Biophys Acta 2011;1809(11-12):715-721.
30. Matsuo H, Chevallier J, Mayran N, et al. Role of LBPA and Alix in multivesicular liposome formation and endosome organization. Science 2004;303(5657):531-534.
31. Nour AM, Modis Y. Endosomal vesicles as vehicles for viral genomes. Trends Cell Biol 2014;24(8):449-454.
32. Meckes DG, Jr., Raab-Traub N. Microvesicles and viral infection. J Virol 2011;85(24):12844-12854.
33. Gan X, Gould SJ. Identification of an inhibitory budding signal that blocks the release of HIV particles and exosome/microvesicle proteins. Mol Biol Cell 2011;22(6):817-830.
34. Sampey GC, Meyering SS, Asad Zadeh M, Saifuddin M, Hakami RM, Kashanchi F. Exosomes and their role in CNS viral infections. J Neurovirol 2014;20(3):199-208.
35. Kalra H, Simpson RJ, Ji H, et al. Vesiclepedia: a compendium for extracellular vesicles with continuous community annotation. PLoS Biol 2012;10(12):e1001450.
36. Kim DK, Kang B, Kim OY, et al. EVpedia: an integrated database of high-throughput data for systemic analyses of extracellular vesicles. J Extracell Vesicles 2013;2.
37. Trajkovic K, Hsu C, Chiantia S, et al. Ceramide triggers budding of exosome vesicles into multivesicular endosomes. Science 2008;319(5867):1244-1247.
38. van Niel G, Charrin S, Simoes S, et al. The tetraspanin CD63 regulates ESCRT-independent and -dependent endosomal sorting during melanogenesis. Develop Cell 2011;21(4):708-721.
39. Perez-Hernandez D, Gutierrez-Vazquez C, Jorge I, et al. The intracellular interactome of tetraspanin-enriched microdomains reveals their function as sorting machineries toward exosomes. J Biol Chem 2013;288(17):11649-11661.
40. Stuffers S, Sem Wegner C, Stenmark H, Brech A. Multivesicular endosome biogenesis in the absence of ESCRTs. Traffic 2009;10(7):925-937.
41. Tamai K, Tanaka N, Nakano T, et al. Exosome secretion of dendritic cells is regulated by Hrs, an ESCRT-0 protein. Biochem Biophys Res Commun 2010;399(3):384-390.
42. Schwartz SL, Cao C, Pylypenko O, Rak A, Wandinger-Ness A. Rab GTPases at a glance. J Cell Sci 2007;120(Pt 22):3905-3910.
43. Ostrowski M, Carmo NB, Krumeich S, et al. Rab27a and Rab27b control different steps of the exosome secretion pathway. Nat Cell Biol 2010;12(1):19-30.
44. Savina A, Fader CM, Damiani MT, Colombo MI. Rab11 promotes docking and fusion of multivesicular bodies in a calcium-dependent manner. Traffic 2005;6(2):131-143.
45. Colombo M, Raposo G, Thery C. Biogenesis, secretion, and intercellular interactions of exosomes and other extracellular vesicles. Annu Rev Cell Develop Biol 2014;30:255-289.
46. Fader CM, Sanchez DG, Mestre MB, Colombo MI. TI-VAMP/VAMP7 and VAMP3/cellubrevin: two v-SNARE proteins

involved in specific steps of the autophagy/multivesicular body pathways. Biochim Biophys Acta 2009;1793(12):1901-1916.
47. Montecalvo A, Shufesky WJ, Stolz DB, et al. Exosomes as a short-range mechanism to spread alloantigen between dendritic cells during T cell allorecognition. J Immunol 2008;180(5): 3081-3090.
48. Lagana A, Russo F, Veneziano D, et al. Extracellular circulating viral microRNAs: current knowledge and perspectives. Front Genet 2013;4:120.
49. Thebaud B, Stewart DJ. Exosomes: cell garbage can, therapeutic carrier, or trojan horse? Circulation 2012;126(22):2553-2555.
50. Morelli AE, Larregina AT, Shufesky WJ, et al. Endocytosis, intracellular sorting, and processing of exosomes by dendritic cells. Blood 2004;104(10):3257-3266.
51. Segura E, Guerin C, Hogg N, Amigorena S, Thery C. CD8+ dendritic cells use LFA-1 to capture MHC-peptide complexes from exosomes in vivo. J Immunol 2007;179(3):1489-1496.
52. Thery C, Duban L, Segura E, Veron P, Lantz O, Amigorena S. Indirect activation of naive CD4+ T cells by dendritic cell-derived exosomes. Nat Immunol 2002;3(12):1156-1162.
53. Vincent-Schneider H, Stumptner-Cuvelette P, Lankar D, et al. Exosomes bearing HLA-DR1 molecules need dendritic cells to efficiently stimulate specific T cells. Int Immunol 2002;14(7): 713-722.
54. Admyre C, Johansson SM, Paulie S, Gabrielsson S. Direct exosome stimulation of peripheral human T cells detected by ELISPOT. Eur J Immunol 2006;36(7):1772-1781.
55. Segura E, Nicco C, Lombard B, et al. ICAM-1 on exosomes from mature dendritic cells is critical for efficient naive T-cell priming. Blood 2005;106(1):216-223.
56. Wolfers J, Lozier A, Raposo G, et al. Tumor-derived exosomes are a source of shared tumor rejection antigens for CTL cross-priming. Nat Med 2001;7(3):297-303.
57. Mulcahy LA, Pink RC, Carter DR. Routes and mechanisms of extracellular vesicle uptake. J Extracell Vesicles 2014;3.
58. Okoye IS, Coomes SM, Pelly VS, et al. MicroRNA-containing T-regulatory-cell-derived exosomes suppress pathogenic T helper 1 cells. Immunity 2014;41(1):89-103.
59. Zakharova L, Svetlova M, Fomina AF. T cell exosomes induce cholesterol accumulation in human monocytes via phosphatidylserine receptor. J Cell Physiol 2007;212(1):174-181.
60. Miyanishi M, Tada K, Koike M, Uchiyama Y, Kitamura T, Nagata S. Identification of Tim4 as a phosphatidylserine receptor. Nature 2007;450(7168):435-439.
61. Feng D, Zhao WL, Ye YY, et al. Cellular internalization of exosomes occurs through phagocytosis. Traffic 2010;11(5):675-687.
62. Moller-Tank S, Maury W. Phosphatidylserine receptors: enhancers of enveloped virus entry and infection. Virology 2014;468-470:565-80.
63. Rhein BA, Brouillette RB, Schaack GA, Chiorini JA, Maury W. Characterization of human and murine T-cell immunoglobulin mucin domain 4 (TIM-4) IgV domain residues critical for Ebola virus entry. J Virol 2016 Apr 27.
64. Smit JM, Moesker B, Rodenhuis-Zybert I, Wilschut J. Flavivirus cell entry and membrane fusion. Viruses 2011;3(2):160-171.
65. Hamel R, Dejarnac O, Wichit S, et al. Biology of Zika virus infection in human skin cells. J Virol 2015;89(17):8880-8896.
66. Nour AM, Li Y, Wolenski J, Modis Y. Viral membrane fusion and nucleocapsid delivery into the cytoplasm are distinct events in some flaviviruses. PLoS Pathog 2013;9(9):e1003585.
67. Cohen FS. How viruses invade cells. Biophys J 2016;110(5): 1028-1032.
68. Ramakrishnaiah V, Thumann C, Fofana I, et al. Exosome-mediated transmission of hepatitis C virus between human hepatoma Huh7.5 cells. Proc Natl Acad Sci U S A 2013;110(32):13109-13113.
69. Longatti A, Boyd B, Chisari FV. Virion-independent transfer of replication-competent hepatitis C virus RNA between permissive cells. J Virol 2015;89(5):2956-2961.
70. Longatti A. The dual role of exosomes in hepatitis A and C virus transmission and viral immune activation. Viruses 2015;7(12): 6707-6715.
71. Izquierdo-Useros N, Naranjo-Gomez M, Erkizia I, et al. HIV and mature dendritic cells: Trojan exosomes riding the Trojan horse? PLoS Pathog 2010;6(3):e1000740.
72. Gould SJ, Booth AM, Hildreth JE. The Trojan exosome hypothesis. Proc Natl Acad Sci U S A 2003;100(19):10592-10597.
73. Wiley RD, Gummuluru S. Immature dendritic cell-derived exosomes can mediate HIV-1 trans infection. Proc Natl Acad Sci U S A 2006;103(3):738-743.
74. Piguet V, Steinman RM. The interaction of HIV with dendritic cells: outcomes and pathways. Trends Immunol 2007;28(11): 503-510.
75. Yandrapalli N, Muriaux D, Favard C. Lipid domains in HIV-1 assembly. Front Microbiol 2014;5:220.
76. Woodward CL, Cheng SN, Jensen GJ. Electron cryotomography studies of maturing HIV-1 particles reveal the assembly pathway of the viral core. J Virol 2015;89(2):1267-1277.
77. Madison MN, Okeoma CM. Exosomes: implications in HIV-1 pathogenesis. Viruses 2015;7(7):4093-4118.
78. Mori Y, Koike M, Moriishi E, et al. Human herpesvirus-6 induces MVB formation, and virus egress occurs by an exosomal release pathway. Traffic 2008;9(10):1728-1742.
79. Bruce EA, Digard P, Stuart AD. The Rab11 pathway is required for influenza A virus budding and filament formation. J Virol 2010;84(12):5848-5859.
80. Rowe RK, Suszko JW, Pekosz A. Roles for the recycling endosome, Rab8, and Rab11 in hantavirus release from epithelial cells. Virology 2008;382(2):239-249.
81. Utley TJ, Ducharme NA, Varthakavi V, et al. Respiratory syncytial virus uses a Vps4-independent budding mechanism controlled by Rab11-FIP2. Proc Natl Acad Sci U S A 2008;105(29):10209-10214.
82. Fraile-Ramos A, Cepeda V, Elstak E, van der Sluijs P. Rab27a is required for human cytomegalovirus assembly. PLoS One 2010;5(12):e15318.
83. Gerber PP, Cabrini M, Jancic C, et al. Rab27a controls HIV-1 assembly by regulating plasma membrane levels of phosphatidylinositol 4,5-bisphosphate. J Cell Biol 2015;209(3): 435-452.
84. Meng B, Ip NC, Prestwood LJ, Abbink TE, Lever AM. Evidence that the endosomal sorting complex required for transport-II (ESCRT-II) is required for efficient human immunodeficiency virus-1 (HIV-1) production. Retrovirology 2015;12:72.
85. Lenassi M, Cagney G, Liao M, et al. HIV Nef is secreted in exosomes and triggers apoptosis in bystander CD4+ T cells. Traffic 2010;11(1):110-122.
86. Bello-Morales R, Crespillo AJ, Fraile-Ramos A, Tabares E, Alcina A, Lopez-Guerrero JA. Role of the small GTPase Rab27a during herpes simplex virus infection of oligodendrocytic cells. BMC Microbiol 2012;12:265.
87. Krummenacher C, Carfi A, Eisenberg RJ, Cohen GH. Entry of herpesviruses into cells: the enigma variations. Adv Exp Med Biol 2013;790:178-195.
88. Narayanan A, Iordanskiy S, Das R, et al. Exosomes derived from HIV-1-infected cells contain trans-activation response element RNA. J Biol Chem 2013;288(27):20014-20033.
89. Sampey GC, Saifuddin M, Schwab A, et al. Exosomes from HIV-1-infected cells stimulate production of pro-inflammatory

cytokines through trans-activating response (TAR) RNA. J Biol Chem 2016;291(3):1251-1266.
90. Jaworski E, Saifuddin M, Sampey G, et al. The use of Nanotrap particles technology in capturing HIV-1 virions and viral proteins from infected cells. PLoS One 2014;9(5):e96778.
91. Campbell TD, Khan M, Huang MB, Bond VC, Powell MD. HIV-1 Nef protein is secreted into vesicles that can fuse with target cells and virions. Ethn Dis 2008;18(2 Suppl. 2):S2-14-9.
92. Arenaccio C, Chiozzini C, Columba-Cabezas S, et al. Exosomes from human immunodeficiency virus type 1 (HIV-1)-infected cells license quiescent CD4+ T lymphocytes to replicate HIV-1 through a Nef- and ADAM17-dependent mechanism. J Virol 2014;88(19):11529-11539.
93. Arenaccio C, Anticoli S, Manfredi F, Chiozzini C, Olivetta E, Federico M. Latent HIV-1 is activated by exosomes from cells infected with either replication-competent or defective HIV-1. Retrovirology 2015;12:87.
94. de Carvalho JV, de Castro RO, da Silva EZ, et al. Nef neutralizes the ability of exosomes from CD4+ T cells to act as decoys during HIV-1 infection. PLoS One 2014;9(11):e113691.
95. Luo X, Fan Y, Park IW, He JJ. Exosomes are unlikely involved in intercellular Nef transfer. PLoS One 2015;10(4):e0124436.
96. Ali SA, Huang MB, Campbell PE, et al. Genetic characterization of HIV type 1 Nef-induced vesicle secretion. AIDS Res Hum Retroviruses 2010;26(2):173-192.
97. Campbell PE, Isayev O, Ali SA, et al. Validation of a novel secretion modification region (SMR) of HIV-1 Nef using cohort sequence analysis and molecular modeling. J Mol Model 2012;18(10):4603-4613.
98. Jaworski E, Narayanan A, Van Duyne R, et al. Human T-lymphotropic virus type 1-infected cells secrete exosomes that contain Tax protein. J Biol Chem 2014;289(32):22284-22305.
99. Romanelli MG, Diani E, Bergamo E, et al. Highlights on distinctive structural and functional properties of HTLV Tax proteins. Front Microbiol 2013;4:271.
100. Currer R, Van Duyne R, Jaworski E, et al. HTLV tax: a fascinating multifunctional co-regulator of viral and cellular pathways. Front Microbiol 2012;3:406.
101. Shembade N, Harhaj EW. Role of post-translational modifications of HTLV-1 Tax in NF-kappaB activation. World J Biol Chem 2010;1(1):13-20.
102. Alefantis T, Mostoller K, Jain P, Harhaj E, Grant C, Wigdahl B. Secretion of the human T cell leukemia virus type I transactivator protein tax. J Biol Chem 2005;280(17):17353-17362.
103. Alefantis T, Jain P, Ahuja J, Mostoller K, Wigdahl B. HTLV-1 Tax nucleocytoplasmic shuttling, interaction with the secretory pathway, extracellular signaling, and implications for neurologic disease. J Biomed Sci 2005;12(6):961-974.
104. Cowan EP, Alexander RK, Daniel S, Kashanchi F, Brady JN. Induction of tumor necrosis factor alpha in human neuronal cells by extracellular human T-cell lymphotropic virus type 1 Tax. J Virol 1997;71(9):6982-6989.
105. Dhib-Jalbut S, Hoffman PM, Yamabe T, et al. Extracellular human T-cell lymphotropic virus type I Tax protein induces cytokine production in adult human microglial cells. Ann Neurol 1994;36(5):787-790.
106. Lepoutre V, Jain P, Quann K, Wigdahl B, Khan ZK. Role of resident CNS cell populations in HTLV-1-associated neuroinflammatory disease. Front Biosci 2009;14:1152-1168.
107. Kubota R, Nagai M, Kawanishi T, Osame M, Jacobson S. Increased HTLV type 1 tax specific CD8+ cells in HTLV type 1-asociated myelopathy/tropical spastic paraparesis: correlation with HTLV type 1 proviral load. AIDS Res Hum Retroviruses 2000;16(16):1705-1709.
108. Levin MC, Lee SM, Morcos Y, Brady J, Stuart J. Cross-reactivity between immunodominant human T lymphotropic virus type I tax and neurons: implications for molecular mimicry. J Infect Dis 2002;186(10):1514-1517.
109. Irish BP, Khan ZK, Jain P, et al. Molecular mechanisms of neurodegenerative diseases induced by human retroviruses: a review. Am J Infect Dis 2009;5(3):231-258.
110. Rixon FJ, Addison C, McLauchlan J. Assembly of enveloped tegument structures (L particles) can occur independently of virion maturation in herpes simplex virus type 1-infected cells. J Gen Virol 1992;73(Pt 2):277-284.
111. McLauchlan J, Rixon FJ. Characterization of enveloped tegument structures (L particles) produced by alphaherpesviruses: integrity of the tegument does not depend on the presence of capsid or envelope. J Gen Virol 1992;73(Pt 2):269-276.
112. McLauchlan J, Addison C, Craigie MC, Rixon FJ. Noninfectious L-particles supply functions which can facilitate infection by HSV-1. Virology 1992;190(2):682-688.
113. Heilingloh CS, Kummer M, Muhl-Zurbes P, et al. L particles transmit viral proteins from herpes simplex virus 1-infected mature dendritic cells to uninfected bystander cells, inducing CD83 downmodulation. J Virol 2015;89(21):11046-11055.
114. Kalamvoki M, Deschamps T. Extracellular vesicles during Herpes Simplex Virus type 1 infection: an inquire. Virol J 2016;13(1):63.
115. Kalamvoki M, Du T, Roizman B. Cells infected with herpes simplex virus 1 export to uninfected cells exosomes containing STING, viral mRNAs, and microRNAs. Proc Natl Acad Sci U S A 2014;111(46):E4991-E4996.
116. Temme S, Eis-Hubinger AM, McLellan AD, Koch N. The herpes simplex virus-1 encoded glycoprotein B diverts HLA-DR into the exosome pathway. J Immunol. 2010;184(1):236-243.
117. Lee CP, Liu PT, Kung HN, et al. The ESCRT machinery is recruited by the viral BFRF1 protein to the nucleus-associated membrane for the maturation of Epstein-Barr Virus. PLoS Pathog 2012;8(9):e1002904.
118. Flanagan J, Middeldorp J, Sculley T. Localization of the Epstein-Barr virus protein LMP 1 to exosomes. J Gen Virol 2003;84(Pt 7):1871-1879.
119. Dukers DF, Meij P, Vervoort MB, et al. Direct immunosuppressive effects of EBV-encoded latent membrane protein 1. J Immunol 2000;165(2):663-670.
120. Nanbo A, Kawanishi E, Yoshida R, Yoshiyama H. Exosomes derived from Epstein-Barr virus-infected cells are internalized via caveola-dependent endocytosis and promote phenotypic modulation in target cells. J Virol 2013;87(18):10334-10347.
121. Klibi J, Niki T, Riedel A, et al. Blood diffusion and Th1-suppressive effects of galectin-9-containing exosomes released by Epstein-Barr virus-infected nasopharyngeal carcinoma cells. Blood 2009;113(9):1957-1966.
122. Meckes DG, Jr., Shair KH, Marquitz AR, Kung CP, Edwards RH, Raab-Traub N. Human tumor virus utilizes exosomes for intercellular communication. Proc Natl Acad Sci U S A 2010;107(47):20370-20375.
123. Ansari MA, Singh VV, Dutta S, et al. Constitutive interferon-inducible protein 16-inflammasome activation during Epstein-Barr virus latency I, II, and III in B and epithelial cells. J Virol 2013;87(15):8606-8623.
124. Baglio SR, van Eijndhoven MA, Koppers-Lalic D, et al. Sensing of latent EBV infection through exosomal transfer of 5'pppRNA. Proc Natl Acad Sci U S A 2016;113(5):E587-E596.
125. Chugh PE, Sin SH, Ozgur S, et al. Systemically circulating viral and tumor-derived microRNAs in KSHV-associated malignancies. PLoS Pathog 2013;9(7):e1003484.
126. Naranatt PP, Krishnan HH, Svojanovsky SR, Bloomer C, Mathur S, Chandran B. Host gene induction and transcriptional reprogramming in Kaposi's sarcoma-associated herpesvirus

(KSHV/HHV-8)-infected endothelial, fibroblast, and B cells: insights into modulation events early during infection. Cancer Res 2004;64(1):72-84.
127. Meckes DG, Jr., Gunawardena HP, Dekroon RM, et al. Modulation of B-cell exosome proteins by gamma herpesvirus infection. Proc Natl Acad Sci U S A 2013;110(31): E2925-E2933.
128. Kuo HT, Ye X, Sampaio MS, Reddy P, Bunnapradist S. Cytomegalovirus serostatus pairing and deceased donor kidney transplant outcomes in adult recipients with antiviral prophylaxis. Transplantation 2010;90(10):1091-1098.
129. McDevitt LM. Etiology and impact of cytomegalovirus disease on solid organ transplant recipients. Am J Health Syst Pharm 2006;63(19 Suppl. 5):S3-S9.
130. Roux A, Mourin G, Fastenackels S, et al. CMV driven CD8(+) T-cell activation is associated with acute rejection in lung transplantation. Clin Immunol 2013;148(1):16-26.
131. Plazolles N, Humbert JM, Vachot L, Verrier B, Hocke C, Halary F. Pivotal advance: The promotion of soluble DC-SIGN release by inflammatory signals and its enhancement of cytomegalovirus-mediated cis-infection of myeloid dendritic cells. J Leukoc Biol 2011;89(3):329-342.
132. Halary F, Amara A, Lortat-Jacob H, et al. Human cytomegalovirus binding to DC-SIGN is required for dendritic cell infection and target cell trans-infection. Immunity 2002;17(5):653-664.
133. Ota M, Serada S, Naka T, Mori Y. Expression of MHC class I molecule in HHV-6B-infected cells. Microbiol Immunol 2014;58(2):Februarycover.
134. Wang X, Wang HK, Li Y, et al. microRNAs are biomarkers of oncogenic human papillomavirus infections. Proc Natl Acad Sci U S A 2014;111(11):4262-4267.
135. Honegger A, Schilling D, Bastian S, et al. Dependence of intracellular and exosomal microRNAs on viral E6/E7 oncogene expression in HPV-positive tumor cells. PLoS Pathog 2015;11(3): e1004712.
136. Melo SA, Sugimoto H, O'Connell JT, et al. Cancer exosomes perform cell-independent microRNA biogenesis and promote tumorigenesis. Cancer Cell 2014;26(5):707-721.
137. Feng Z, Hensley L, McKnight KL, et al. A pathogenic picornavirus acquires an envelope by hijacking cellular membranes. Nature 2013;496(7445):367-371.
138. Feng Z, Li Y, McKnight KL, et al. Human pDCs preferentially sense enveloped hepatitis A virions. J Clin Invest 2015;125(1): 169-176.
139. Chai N, Chang HE, Nicolas E, Han Z, Jarnik M, Taylor J. Properties of subviral particles of hepatitis B virus. J Virol 2008;82(16):7812-7817.
140. Ahsan NA, Sampey GC, Lepene B, et al. Presence of viral RNA and proteins in exosomes from cellular clones resistant to Rift Valley fever virus infection. Front Microbiol 2016;7:139.
141. Silvas JA, Popov VL, Paulucci-Holthauzen A, Aguilar PV. Extracellular vesicles mediate receptor-independent transmission of novel tick-borne Bunyavirus. J Virol 2016;90(2):873-886.
142. Lozach PY, Kuhbacher A, Meier R, et al. DC-SIGN as a receptor for phleboviruses. Cell Host Microbe 2011;10(1):75-88.
143. Varkey JB, Shantha JG, Crozier I, et al. Persistence of Ebola virus in ocular fluid during convalescence. N Engl J Med 2015;372(25): 2423-2427.
144. Uyeki TM, Erickson BR, Brown S, et al. Ebola virus persistence in semen of male survivors. Clin Infect Dis 2016;62: 1552-1555.
145. Atkinson B, Hearn P, Afrough B, et al. Detection of Zika virus in semen. Emerg Infect Dis 2016;22(5):940.
146. Malkki H. CNS infections: Zika virus infection could trigger Guillain-Barre syndrome. Nat Rev Neurol 2016;12(4):187.
147. Garcez PP, Loiola EC, Madeiro da Costa R, et al. Zika virus impairs growth in human neurospheres and brain organoids. Science 2016;352:816-818.
148. Williamson PR, Nash TE, Williamson KC, Nath A. CNS infections in 2015: emerging catastrophic infections and new insights into neuroimmunological host damage. Lancet Neurol 2016;15(1):17-19.
149. Han Z, Madara JJ, Liu Y, et al. ALIX rescues budding of a double PTAP/PPEY L-domain deletion mutant of Ebola VP40: a role for ALIX in Ebola virus egress. J Infect Dis 2015;212(Suppl. 2): S138-S145.